Application of Organic Solvent Nanofiltration for Multi-Purpose Production

Zur Erlangung des akademischen Grades eines

Dr.-Ing.

von der Fakultät Bio- und Chemieingenieurwesen
der Technischen Universität Dortmund
genehmigte Dissertation

vorgelegt von

Dipl.-Ing. Stefanie Blumenschein

aus

Seeheim-Jugenheim

Tag der mündlichen Prüfung: 27.06.2017

1. Gutachter/-in: Prof. Dr.-Ing. Andrzej Górak
2. Gutachter/-in: Prof. Dr.-Ing. Gerhard Schembecker

Dortmund 2017

Der Weg ist das Ziel

Konfuzius

Danksagung

Die vorliegende Dissertation entstand während meiner Tätigkeit bei der Merck KGaA in Zusammenarbeit mit dem Lehrstuhl für Fluidverfahrenstechnik der Fakultät für Bio- und Chemieingenieurwesen der Technischen Universität Dortmund.

Mein besonderer Dank gilt meinem Doktorvater Herrn Prof. Dr.-Ing. Andrzej Górak für die Möglichkeit der Durchführung dieser Arbeit und die fachliche Betreuung. Zudem möchte ich herzlich Prof. Dr.-Ing. Gerhard Schembecker für die Übernahme des Koreferats danken. Herrn Dr. Peter Kreis und Herrn Dr. Philip Lutze danke ich für die bereichernden Diskussionen und kompetenten Anregungen.

Ein grosses Dankeschön gilt Dr. Uwe Kätzel, der durch seine motivierende, tatkräftige Unterstützung, das entgegen gebrachte Vertrauen, die Denkanstöße und das offene Feedback maßgeblich zum Erfolg dieser Arbeit beigetragen hat.

Mein Dank gilt außerdem dem Abteilungsleiter von PM-OTE Dr. Dirk Schmalz, der mir die Möglichkeit und den nötigen Freiraum für die Erstellung der Arbeit gegeben hat. Ein großes Dankeschön gilt außerdem allen Studenten, die einen aktiven Beitrag zu dieser Arbeit geleistet haben. Insgesamt danke ich allen Mitarbeitern der Abteilung PM-OTE für die tolle Arbeitsatmosphäre und die Hilfsbereitschaft, insbesondere aber den Mitarbeitern des Bereichs Membrantechnik, Daniel, Andrea und Andrea, für ihre unermüdliche Hilfe und Unterstützung, sei es bei der Versuchsdurchführung oder bei der Betreuung der Studenten. Außerordentlich dankbar bin ich zudem Henry für das Korrekturlesen dieser Arbeit.

Danke auch an meine Fellnasen, die immer wieder entscheidend dazu beigetragen haben meinen Kopf durchzulüften und auf andere Gedanken zu kommen und sicherlich in der ein oder anderen Phase deutlich mehr Aufmerksamkeit verdient hatten.

Mein größter Dank aber gilt meinen Eltern, die mir das Studium ermöglicht haben und Fabian für die Unterstützung, das Zurückstecken und die unendliche Geduld womit er mir die Kraft gegeben hat durchzuhalten.

Abstract

Due to increasing competitive pressure and a growing focus on environmentally friendly and sustainable production processes, energy-efficient and resource-saving processes are becoming more and more important. Organic solvent nanofiltration (OSN) is a relatively young membrane-based separation technology offering a high potential in process intensification compared to usual fluid separations: OSN enables up to 90 % energy savings and is able to separate mixtures without thermal stress or the use of additives.
Despite these advantages application in industry still faces many challenges. The lack of predictability of separation performance of polymeric membranes currently requires time-consuming, experiment-based process development. Contrarily, the pressure for accelerated process development based on experience or simulations is increasing, particularly in the specialty chemicals industry. Ceramic membranes promise a better predictability of separation in addition to higher resistance in terms of chemical, thermal and mechanical stress in comparison to polymeric membranes, but their development for OSN is considerably less advanced. Data and experience is marginal, particularly in the region of low cut-offs (<600 g/mol).

In this work two different approaches are pursued to significantly accelerate the development of OSN processes. On the one hand, with regard to polymeric membranes a systematic investigation on the interactions between membrane, solvent and solute is carried out. From these results, an heuristic approach is developed which allows the identification of the best membrane for a given separation problem based on easily accessible or computable properties. Additionally, predictability and understanding of the complex separation performance is significantly improved.
On the other hand, the separation behavior and the influence of diverse properties of ceramic membranes are investigated, in parallel to the development of new, narrow-pore separation layers for ceramic membranes, which are particularly suited to organic solvents. A transport model

originally developed for aqueous nanofiltration is adapted and extended to an organic environment. The results of a permporometry measurement serve as the only input parameters for this new model. This measurement provides information about the mean pore size and the number of defect pores in the separation layer. The experimental results of rejection of the new membranes and the simulation are in very good accordance.

Finally, the economic potential of organic solvent nanofiltration in a multi-purpose process environment is evaluated for a real production facility. Special terms and conditions in producing the high value and high purity substances, such as the application of a plant for several products at the same time with high yields and a good cleanability, are considered.

Kurzzusammenfassung

Durch steigenden Wettbewerbsdruck und einem zunehmenden Fokus auf ressourcenschonende, nachhaltige Produktionsverfahren, werden flexible, energie- und rohstoffsparende Prozesse in der chemischen Industrie immer wichtiger. Die organophile Nanofiltration ist ein relativ junges, membranbasiertes Trennverfahren, welches gegenüber herkömmlichen thermischen Trennprozessen ein großes Potenzial zur Prozessintensivierung bietet. So können mit diesem Verfahren Stoffgemische mit bis zu 90 % weniger Energieaufwand, ohne Temperaturbelastung der enthaltenen Produkte und ohne den Einsatz von Additiven getrennt werden.

Trotz der genannten Vorteile steht der großtechnische Einsatz dieser Technologie immer noch vor vielen Herausforderungen. Die schlechte Vorhersagbarkeit des Trennverhaltens polymerer Membranen erfordert aktuell eine zeitaufwendige, auf Experimenten basierte Prozessentwicklung. Dem steht jedoch insbesondere in der Spezialchemieindustrie ein immer größer werdender Druck zur schnellen erfahrungs- oder modellbasierten Prozessentwicklung entgegen. Keramische Membranen versprechen gegenüber polymeren Membranen neben einer besseren Vorhersagbarkeit der Performance eine höhere Stabilität hinsichtlich chemischer, thermischer und abrasiver Belastung. Allerdings ist hier die Membranentwicklung deutlich weniger fortgeschritten, so dass die Daten- und Erfahrungslage vor allem im Bereich niedriger Trenngrenzen (<600 g/mol) noch sehr gering ist.

Um die Prozessentwicklung von Membranverfahren zukünftig deutlich beschleunigen zu können, werden im Rahmen dieser Arbeit zwei verschiedene Ansätze verfolgt. Für polymere Membranen wird eine umfassende Untersuchung der dreidimensionalen Wechselwirkungen zwischen Membran, Lösungsmittel und Komponenten durchgeführt. Aus den Ergebnissen wird eine Heuristik entwickelt, die es ermöglicht auf Basis von einfach zugänglichen oder berechenbaren Stoffparametern die geeignetste polymere Membran für ein gegebenes Trennproblem zu identifizieren. Dadurch kann das Verständnis und die Vorhersagbarkeit des komplexen Trennvorgangs deutlich verbessert werden.

Für keramische Membranen werden begleitend zu der Entwicklung von neuen, engporigeren Trennschichten für den Einsatz in organischen Lösungsmitteln das Trennverhalten und der Einfluss verschiedener Eigenschaften der neuen Membranen untersucht. Zudem wird ein ursprünglich für die wässrige Nanofiltration entwickeltes Transportmodell für die organische Umgebung angepasst und erweitert. Als Eingangsparameter für das neue Modell dienen lediglich Daten, die aus Permporometriemessungen gewonnen werden. Diese gibt Auskunft über die mittlere Porengröße und den Defektporenanteil. Der Rückhalt der neuen Membranen kann so mit sehr guten Übereinstimmungen zwischen Modell und Experiment simuliert werden.
Abschließend wird das wirtschaftliche Potenzial in einem Multi-Purpose-Prozessumfeld am Beispiel eines realen Produktionsbetriebes der Merck KGaA bewertet. Dafür werden die speziellen Bedingungen, die die Herstellung der hochwertigen und extrem reinen Substanzen wie die flexible Einsetzbarkeit der Anlage für verschiedene Produkte bei gleichzeitig zu realisierenden hohen Produktausbeuten und die Reinigbarkeit aller produktberührenden Anlagenteile, berücksichtigt.

Contents

Danksagung i

Abstract iii

Kurzzusammenfassung v

Contents vii

Nomenclature xi

1 Introduction 1

2 State of the Art 4

2.1 Multi-purpose process environment 4

2.1.1 Production of specialty chemicals 4

2.1.2 Fundamentals of multi-purpose plants 5

2.1.2.1 Modular multi-purpose plant 6

2.1.2.2 Multi-purpose plant with mobile transfer containers 6

2.2 Fundamentals of organic solvent nanofiltration 7

2.2.1 Principles of the technology 9

2.2.1.1 Operating modes 10

2.2.1.2 Driving force reducing effects 11

2.2.2 Applications and potentials of OSN 13

2.2.3 Membrane materials and module geometries 14

2.2.3.1 Polymeric membranes 14

2.2.3.2 Ceramic membranes 17

2.2.3.3 Comparison between polymeric and ceramic membranes . . 19

2.2.3.4 Characterization of OSN membranes 20

2.3 Transport mechanism in membrane separation 21
2.3.1 Membrane dependent models 21
2.3.1.1 Pore-flow models 22
2.3.1.2 Solution-diffusion models 25
2.3.2 Transport in organic solvent nanofiltration 27
2.3.2.1 Transport description by adopting existing models 27
2.3.2.2 Factors influencing separation behavior in OSN 30

3 Gap analysis and approach 34
3.1 Gap analysis 34
3.2 Approach and structure 37

4 Potential of OSN in a multi-purpose-process environment 38
4.1 General procedure of the assessment 38
4.2 Theoretical potential 40

5 Investigations on polymeric membranes in organic solvent nanofiltration 46
5.1 Materials and Methods 46
5.1.1 Polymeric membranes 47
5.1.2 Substances 48
5.1.2.1 Specialty chemicals 48
5.1.2.2 Solvents 52
5.1.3 Experimental set-up 53
5.1.4 Analytics 56
5.1.4.1 Gas chromatography 56
5.1.4.2 Rotary evaporator 56
5.2 Membrane-solvent interactions 56
5.3 Membrane-solvent-solute interactions 61
5.3.1 Experimental database 61
5.3.2 Influence of solute on the separation behavior 65
5.3.3 Influence of functional groups on the separation behavior 70
5.3.4 Separation behavior in solvent mixtures 77
5.4 Validation of the results 84

5.4.1 Verification of the influence of the membrane material on the separation mechanism . . . 84
5.4.2 Verification of the influence of the solvents on the separation mechanism 86
5.4.3 Verification of the influence of the solutes on the separation mechanism 91
5.5 Heuristic rules . . . 96
5.5.1 Rejection estimation . . . 96
5.5.2 Heuristic for membrane selection . . . 99

6 Investigations on ceramic membranes in organic solvent nanofiltration 102
6.1 Materials and methods . . . 102
6.1.1 Ceramic membranes . . . 102
6.1.2 Polystyrene oligomers . . . 104
6.1.3 Experimental set-up . . . 105
6.1.4 Analytics . . . 107
6.2 Experimental investigations on the separation behavior of ceramic membranes . 107
6.2.1 Investigations on the solvent flux through ceramic membranes . . . 107
6.2.2 Identification of parameters determining the suitability of a membrane for OSN . . . 108
6.2.3 Influence of solvent on rejection . . . 112
6.2.4 Rejection of specialty chemicals . . . 117
6.3 Rejection modeling of ceramic membranes . . . 119
6.3.1 Model structure . . . 119
6.3.2 Mass transfer model . . . 121
6.3.3 Results of modeling . . . 122
6.3.3.1 Influence of membrane parameters on the modeling results . 125
6.3.3.2 Variation of process parameters . . . 127
6.3.3.3 Influence of solvents on the modeling results . . . 129
6.3.3.4 Transferability of the modeling results to other solutes . . . 130
6.4 Conclusion . . . 130

7 Refined potential assessment 133
7.1 Technically realizable potential . . . 133
7.2 Economically realizable potential . . . 138

8 Conclusion and Outlook 141

References 146

List of Figures 164

List of Tables 173

A Additional information concerning the investigations on polymeric membranes 175

B Additional information concerning the investigations on ceramic membranes 185

C Additional information concerning the potential assessment 189

Publications 193

Supervised Theses 196

Curriculum Vitae 197

Nomenclature

Latin Variables

A	Area	$[\mathrm{m}^2]$
a	Activity	$[\mathrm{mol\,m}^{-3}]$
a	Fraction of solute passing by viscous flow in the model of Tarleton[1]	[-]
b	Dimensionless variable in the model of Bowen and Welfoot[2]	[-]
B_0	Specific permeability of the membrane	$[\mathrm{m}^2]$
c	Concentration	$[\mathrm{mol\,m}^{-3}]$
C_A	Amortization costs	$[\mathrm{MU\,a}^{-1}]$
c_p	Specific heat capacity at constant pressure	$[\mathrm{J\,kg}^{-1}\,\mathrm{K}^{-1}]$
C_{ED}	Costs for energy demand of distillation	$[\mathrm{MU\,a}^{-1}]$
C_{EO}	Costs for energy demand of OSN	$[\mathrm{MU\,a}^{-1}]$
C_{MH}	Costs due to reduction of machine hours	$[\mathrm{MU\,a}^{-1}]$
C_{OP}	Operating costs	$[\mathrm{MU\,a}^{-1}]$
C_{PL}	Costs due to product losses	$[\mathrm{MU\,a}^{-1}]$
C_{PS}	Costs due to process shortening	$[\mathrm{MU\,a}^{-1}]$
$cost$	Specific rate for various resources	$[\mathrm{MU\,(a.u.)}^{-1}]$
D	Diffusion coefficient	$[\mathrm{m}^2\,\mathrm{s}^{-1}]$
d_{SL}	Thickness of a solvent layer at a pore wall	[m]
E_{coh}	Cohesive energy	[J]
f_0	Parameter characteristic of mixture of solvents [3]	$[\mathrm{s\,m}^{-2}]$

f_1	Membrane parameter characteristic of the NF membrane layer [3]	$[\mathrm{m\,s^{-1}}]$
f_1	Membrane parameter characteristic of the UF membrane layer [3]	$[\mathrm{m^{-1}}]$
H	Enthalpy	$[\mathrm{J\,kg^{-1}}]$
HV_{gas}	Heating value of natural gas	$[\mathrm{J\,kg^{-1}}]$
I	Investment costs	[MU]
J	Membrane flux	[a.u.]
k	Mass transfer coefficient	$[\mathrm{m\,s^{-1}}]$
K_c	Uncharged solute hindrance factor for convection	[-]
K_d	Uncharged solute hindrance factor for diffusion	[-]
K_i	Sorption coefficent	[-]
L	Coefficient	[a.u.]
l	Membrane thickness	[m]
M	Molecular weight	$[\mathrm{kg\,mol^{-1}}]$
m	Mass	[kg]
m^F	Mass flow	$[\mathrm{kg\,h^{-1}}]$
N	Number per year (of)	$[\mathrm{a^{-1}}]$
n	Empirical exponent in the model of Bhanushali[4]	[-]
P	Membrane permeability	[a.u.]
P	Permeability of nitrogen in permporometry	$[\mathrm{mol\,h^{-1}\,Pa^{-1}\,m^{-2}}]$
P	Power	$[\mathrm{kg\,m^2\,s^{-3}}]$
p	Pressure	[Pa]
p_s	Saturated vapor pressure	[Pa]
Pe'	Modified peclet number	[-]
Pot_{te}	Technical potential	$[\mathrm{MU\,a^{-1}}]$
Pot_{th}	Theoretical potential	$[\mathrm{MU\,a^{-1}}]$
Pr	Profit	$[\mathrm{MU\,a^{-1}}]$
Q	Molar flow	$[\mathrm{mol\,h^{-1}}]$

$q'(r_p)$	Truncated probability density function	$[\mathrm{m}^{-1}]$
$q(r_p)$	Theoretical probability density function	$[\mathrm{m}^{-1}]$
R	Rejection	[-]
r_p	Pore radius	[m]
r_s	Solute radius	[m]
R_{int}	Intrinsic rejection	[-]
ROI	Return on investment	[-]
RV	Residual value	[MU]
S	Selectivity	[-]
S_V	Volume related specific surface	$[\mathrm{m}^2\,\mathrm{m}^{-3}]$
T	Temperature	[K]
t	Time	[h]
t_A	Payback period	[a]
v	Solvent velocity	$[\mathrm{m\,s}^{-1}]$
V^F	Volume flow	$[\mathrm{m}^3\,\mathrm{s}^{-1}]$
w	Mass fraction	[-]
$wacc$	Weighted average cost of capital	[-]
Y	Dimensionless variable in the model of Bowen and Welfoot[5]	[-]
z	Valence of ion	[-]

Greek Variables

χ	Interaction parameter	[-]
δ	Solubility parameter	$[\left(\mathrm{J\,m}^{-3}\right)^{0.5}]$
δ	Thickness of the boundary layer	[m]
ε	Porosity	[-]
η	Dynamic viscosity	$[\mathrm{kg\,m}^{-1}\,\mathrm{s}^{-1}]$
η_D	Efficiency factor distillation	[-]
γ	Activity coefficient	[-]

γ	Surface tension	$[\mathrm{kg\,s^{-2}}]$
γ_c	Critical membrane surface tension [3]	$[\mathrm{kg\,s^{-2}}]$
γ_{SV}	Solid-vapor surface tension in the model of Bhanushali[4]	$[\mathrm{kg\,s^{-2}}]$
λ	Ratio of solute radius to pore radius	[-]
μ	Chemical potential	$[\mathrm{J\,mol^{-1}}]$
ϕ	Contact angle	[rad]
ϕ	Solute steric partition coefficient	[-]
ϕ	Sorption value in the model of Bhanushali[4]	[-]
π	Osmotic pressure	[Pa]
ψ	Electric potential within the pore	[V]
ρ	Density	$[\mathrm{kg\,m^{-3}}]$
σ_p	Standard deviation of the pore size distribution	[m]
τ	Tortuosity	[-]
υ	Molar volume	$[\mathrm{m^3 mol^{-1}}]$
ξ	Association parameter	[-]

Constants

$\mathrm{k_B}$	Boltzmann constant	$[\mathrm{J\,K^{-1}}]$
R	Universal gas constant	$[\mathrm{Jmol^{-1}K^{-1}}]$
K	Carman-Kozeny constant	[-]

Common Indices

av	Average
B	Bulk
b	Batch
c	Conditioning of membranes
D	Distillation
el	Electricity
F	Feed

i	Species i
j	Species j
liq	Condensable gas in permporometry
M	Membrane
MH	Machine hour
OSN	Organic solvent nanofiltration
P	Permeate
PF	Pore-flow
R	Retentate
S	Solvent
s	Solute
SD	Solution-diffusion
UEL	useful economic life
V	Vaporization
W	Water

Abbreviations

BEP	Break-even point
DCM	Dichloromethane
DEA	Diethanol amine
DFT	Density functional theory
DMA	Dimethylacetamide
DMC	Dimethyl carbonate
DMF	Dimethylformamide
DMSO	Dimethyl sulfoxide
DoE	Design of Experiments
EtOH	Ethanol
GC	Gas chromatography

GPC	Gas permeation chromatography
IBC	Intermediate bulk container
IKTS	Fraunhofer-Institut für Keramische Technologien und Systeme (Institute for Ceramic Technologies and Systems)
IPA	Isopropyl alcohol
MeOH	Methanol
MF	Microfiltration
MTBE	Methyl tert-butyl ether
MU	Monetary unit
MW	Molecular weight
MWCO	Molecular weight cut off
NF	Nanofiltration
NMP	N-Methyl-2-pyrrolidone
OSN	Organic Solvent Nanofiltration
PA	Polyamide
PAN	Polyacrylonitrile
PDMS	Polydimethylsiloxane
PEG	Polyethylene glycol
PI	Polyimide
PIM	Polymers of intrinsic microporosity
PMP	Poly[4-methyl-2-pentyne]
PS	Polystyrene
PTMSP	Poly[1-(trimethylsilyl)-1-propyne]
RO	Reverse osmosis
ROI	Return on investment
STR	Stirred tank reactor
TFC	Thin film composite

THF	Tetrahydrofuran
UF	Ultrafiltration

1 Introduction

Currently, Industry 4.0 is on everyone's lips. The term originates from a high-tech strategy of the German government and includes the digitalization of industry. In other countries this topic is also known as "Advanced Manufacturing", "Smart Manufacturing" or "Factory of the Future" [6]. In this day and age, product life-cycles become shorter and shorter combined with an increasing price pressure whereas product variety increases and the demanded time-to-market decreases [7]. Continuous, robust, flexible and optimized processes, have been identified thus as the main aspects for Industry 4.0 with regard to chemical process industry [6] to foster these developments. Modularization within the process industry has been defined as a possible solution approach and thus it becomes one of the big mega trends. Modular plant design promises to enable fast, flexible and competitive reaction to market developments [7]. An intermediate stage to this concept constitutes production in multi-purpose plants. Here, the process units are modularly designed and either the units themselves or the connections between them are flexibly combinable. Contrary to the modularization concept, which predominately intends automated continuous manufacturing, these processes are mostly run step-by-step in batch mode.

A material class which has been manufactured in multi-purpose plants for several years are specialty chemicals. Their very dynamic production is caused by frequent changes in the product portfolio as well as an often low total production volume. Specialty chemicals make up the largest share in German chemical production with an increasing forecast and therefore make a decisive contribution to safeguarding Germany as an industrial location for the chemical industry [8].

Further mega trends in chemical process industry [9] are focussed on cost reduction and competitiveness such as process intensification and operational excellence or process analytical technology to increase the automation of chemical processes. Due to increasing energy and resource scarcity and the increasing awareness for sustainability, ecological and sustainable processing

becomes more and more important. Reduction of product carbon footprint, energy and raw material efficiency are thus heavily pursued as well.

Organic solvent nanofiltration (OSN) is a relatively new, emerging pressure-driven membrane technology for downstream processing with the potential to address most of the latter trends. Although the concept of membrane separation has been known since the eighteenth century, the first use only came up after World War II in the 1960s. Larger industrial applications emerged in the eighties in micro- and ultrafiltration technologies [10]. An application, however, was until recently only possible in aqueous environments due to the instability of the employed membrane materials against organic solvents. The development of solvent resistant membranes over the last twenty years enables entirely new possibilities for an application in the chemical industry. Now, membrane technology can be used for the separation and purification of compounds in a molecular weight range between 200 and 1000 g/mol in organic solvents. OSN has thus in principle the potential for energy and raw material efficient manufacturing. Energy savings up to 90 % compared to thermal separations are reported [11] and process integrated recycling of e.g. solvents [12–15] or catalysts [16–19] enables resource savings.

Consequently, OSN is a versatile tool for process intensification and an aid to design sustainable processes. The major question that shall be addressed in this thesis is whether the technology is also capable for a use in a modular process concept where no dedicated plants are used and the downstream unit has to be applicable to several products and different processes. This will be examined by using the example of the production of specialty chemicals in a multi-purpose production environment.

To answer this question there are some general challenges in OSN that will have to be pursued:

- Process development for OSN requires a tremendous effort because the most suitable membrane for each process has to be defined by experimental evaluation. The identification of the most suitable membrane has to be addressed to simplify and accelerate laboratory process development.
- Mass transport in OSN is not completely understood. An improvement of the understanding of factors influencing the transport mechanism in OSN is essential to estimation of the process parameters rejection and flux and thus the potential of an OSN process.

Furthermore, unnecessary, expensive trial-and-error experiments, which are often leading nowhere, could be reduced. Short-cut models that accelerate the process development and enable a fast estimation of process feasibility are, thus, the most important task to evolve OSN into a standard unit operation in process engineering.

- Ceramic membranes promise several advantages as compared to polymeric membranes, but there is a lack of data and membranes to evaluate whether these membranes are an alternative to the current state-of-the-art.
- Finally, the economic benefit of OSN in multi-purpose batch processes has to be questioned with regard to its most decisive process parameters.

An overview of the state-of-the-art of OSN and on the fundamentals of a multi-purpose production environment is given in chapter 2 to define the subjects of this thesis more precisely. In chapter 3, these subjects are elaborated and the consequential structure of this work is presented.

The results of this work shall provide a first approach to assess the technological and economic potential of an application of OSN in a multi-purpose process environment. As a prerequisite, different aspects will be investigated to ease the process development of OSN and improve the current understanding of the occurring transport phenomena, thus providing an enhanced predictability of OSN process feasibility. Due to the focus on industrial applications, this work will not consider the wide range of membranes in developmental stage or membrane development itself but only membranes which were commercially available at the beginning of this study.

2 State of the Art

2.1 Multi-purpose process environment

The present work focuses on the potential of organic solvent nanofiltration (OSN) in a multi-purpose production typical for specialty chemicals. The characteristics and requirements in such a production environment will be examined therefore first.

2.1.1 Production of specialty chemicals

Depending on the different process industries, manufacturing of the products has to fulfill different requirements and to handle with diverse necessities. Figure 2.1 depicts the production characteristics of the most typical chemical process industries in order to emphasise the distinctive features of specialty chemicals manufacturing.

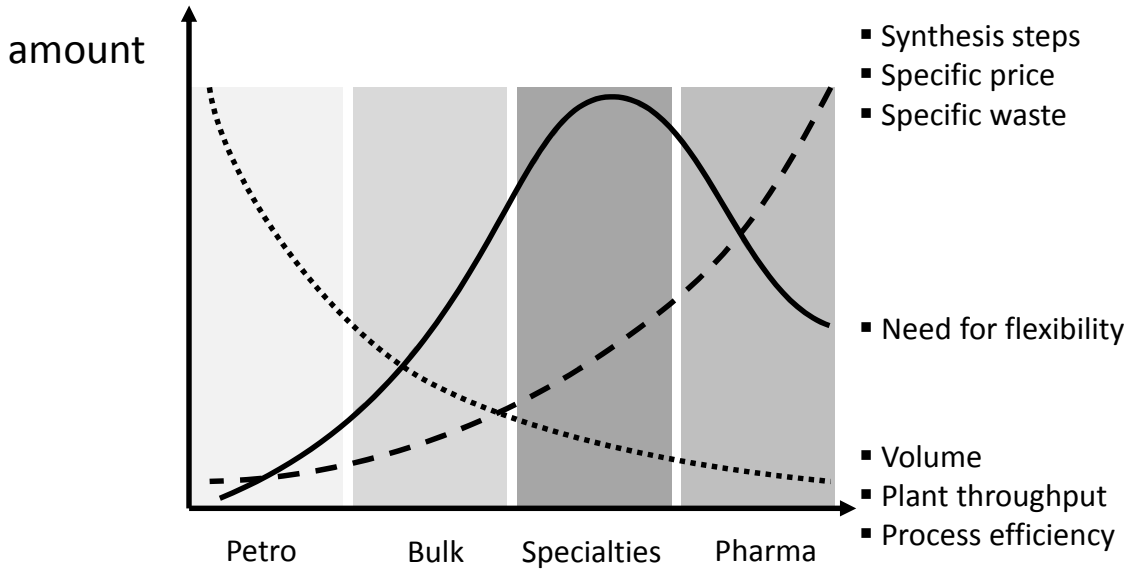

Figure 2.1: Characteristics of different chemical industries

The volume of the products declines from petrochemical industry, where huge quantities of mineral oil are continuously processed, to pharmaceutical industry. In conjugation with the produced volume, the plant throughput naturally declines as well. In continuous processes with long run-times, it is much easier to optimize the process. This is why the process efficiency decreases likewise from the petrochemical to the pharmaceutical industry, where typically batch production processes dominate. In contrast, the processes become more complex. The number of synthesis steps and thus the amount of specific waste and as a consequence the specific price increases. It is common, that a pharmaceutical compound is manufactured in twenty or more synthesis steps.

In principle two main characteristics of specialty chemicals are decisive for their production. These are the fact, that on the one hand specialty chemicals usually have very short life cycles, which causes in frequent changes in the production portfolio. On the other hand the volume demand is low and thus only small batch quantities need to be manufactured. In many cases several variants with different functionalities of a material class are produced and the number of synthesis steps results additionally in a large number of precursors and intermediates. For these reasons, dedicated plants are mostly not feasible. It is obvious that the production of specialty chemicals demands a highly flexible process environment. Multi-purpose plants fulfill these flexibility requirements.

2.1.2 Fundamentals of multi-purpose plants

Depending on the mobile parts and achieved flexibility of the units, five different types of multi-purpose plants are distinguished [20].

- standard multi-purpose plant
- modular multi-purpose plant
- multi-purpose plant with pipe distributors
- pipeless multi-purpose plant
- multi-purpose plant with mobile transfer containers [21]

Modular multi-purpose plants and multi-purpose plants with mobile transfer containers are the most common types in the production of specialty chemicals. For this reason, they will be explained in more detail in the following section.

2.1.2.1 Modular multi-purpose plant

A modular multi-purpose plant is characterized by an immovable stirred tank reactor (STR). The periphery around the reactor, like feed vessels, filters, dryers and storage vessels is modularly designed and thus the operating units are flexibly applicable allowing to adapt them to each specific process. Figure 2.2 schematically illustrates this type of multi-purpose plant.

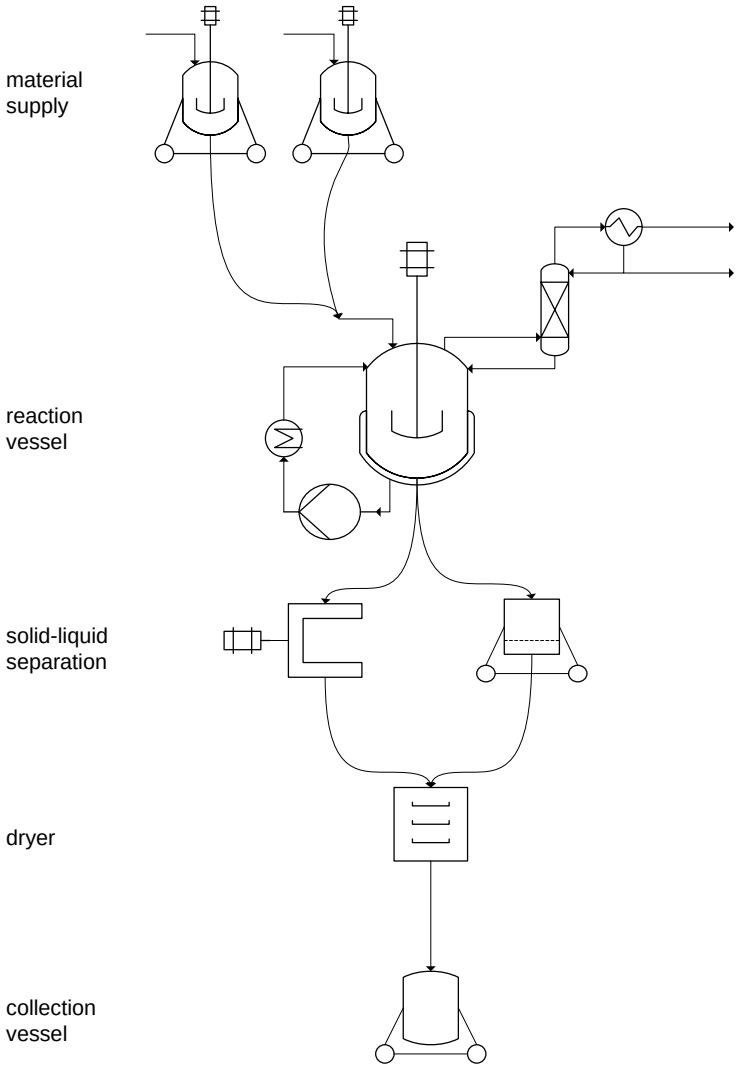

Figure 2.2: Modular multi-purpose plant [20]

2.1.2.2 Multi-purpose plant with mobile transfer containers

In this case, the operating units are all permanently installed. By using mobile transfer containers (IBC) with flexible hose couplings for the connection between the units, flexibility is

achieved. The basic design is given in Figure 2.3.

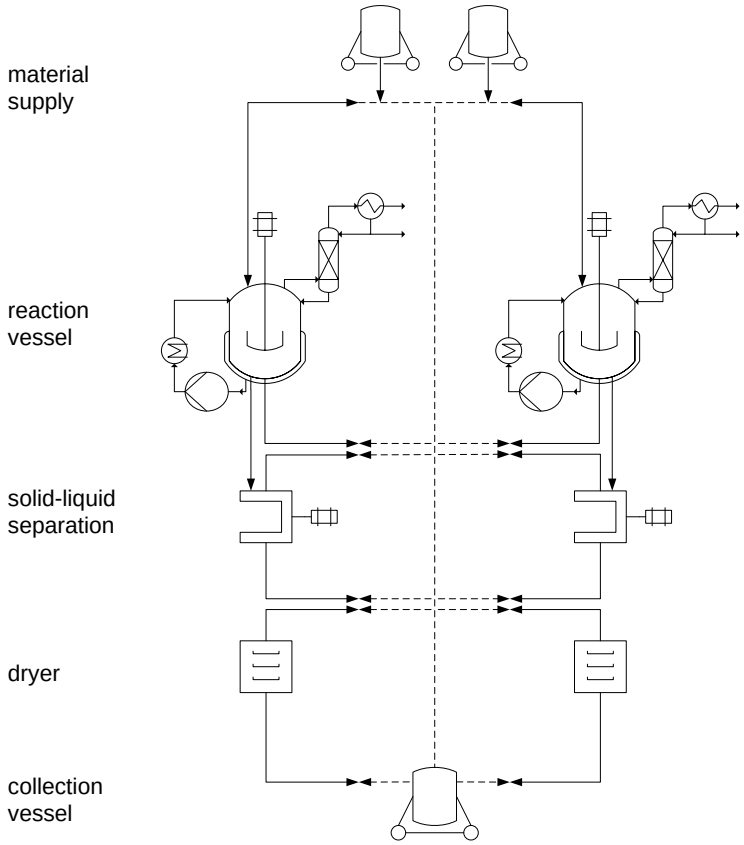

Figure 2.3: Multi-purpose plant with mobile transfer containers [21]

2.2 Fundamentals of organic solvent nanofiltration

A membrane describes a semipermeable system which serves as a selective barrier between two phases. A membrane is permeable for some species so that these can pass through the membrane when exposed to the action of a driving force. For other species the membrane remains impermeable whereupon these are concentrated. All the membrane processes have in common that this driving force is based on a difference in the electrochemical potential between the two phases at the membrane.

Nanofiltration (NF) is a pressure driven membrane process which means that pressure difference accounts for the largest part in electrochemical potential. It deals with the filtration of molecules in the range between 200 and 1000 g/mol at pressures from 3 to 60 bar. Figure 2.4 illustrates the

classification of nanofiltration within the other pressure driven membrane processes according to the compound size that is separated and the pressure demand. In the upper solute size range (> 1000 g/mol) nanofiltration is confined against ultrafiltration (UF) whereas for the separation of solutes smaller than 200 g/mol or monovalent salts typically the term reverse osmosis (RO) is used.

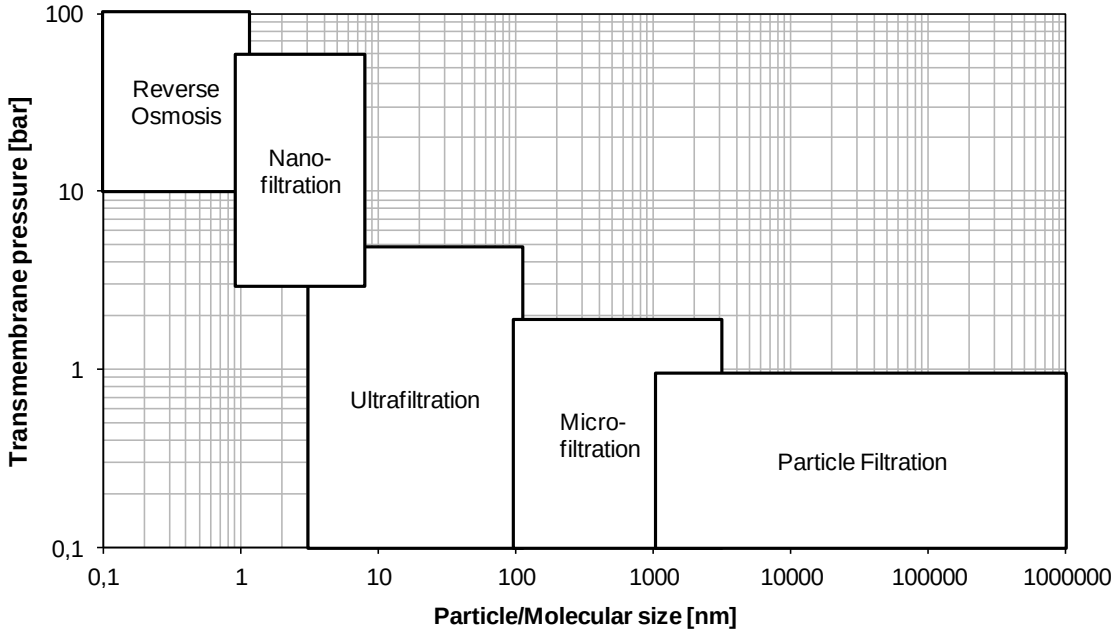

Figure 2.4: Overview pressure driven membrane processes [22]

Depending on whether membranes have microscopically identifiable pores or not, they are distinguished as porous or dense membranes [23]. With the decrease in particle/solute size from filtration to RO, the pore size decreases as well up to RO where the membranes are dense. Nanofiltration is in the transition region, i.e. there are both porous and dense membranes.
Most of the processes shown in Figure 2.4 are typically carried out in aqueous environments. In OSN, the largest differentiation from existing membrane processes is that it is used within organic solvents and hence enables the separation of dissolved molecules from organic solvents. As such, the technology offers high potential to replace or support conventional (thermal) separation techniques in the chemical process industry. OSN is, however, a relatively young technology. It has just emerged during the past 20 years with the development of stable solvent resistant nanofiltration membranes. Because of the availability of suitable membranes, the technology is still in its infancy with not all relevant questions for process description and layout being answered today as will be shown in the next sections.

2.2.1 Principles of the technology

In the process the membrane is housed in a membrane module. The part of the feed solution which is retained by the membrane is called retentate, the permeate is the part of the feed which passes through the membrane. A schematic illustration is shown in Figure 2.5.

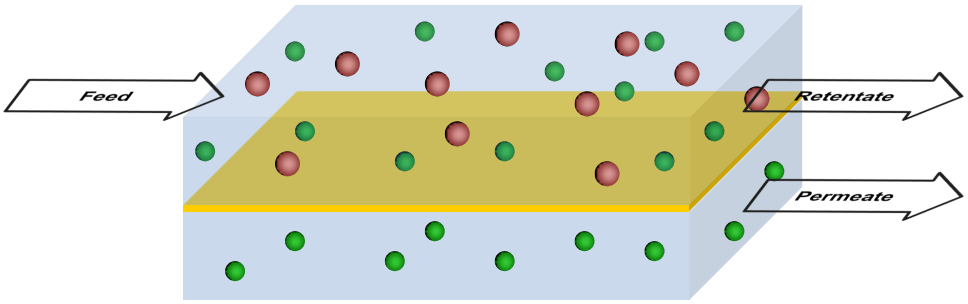

Figure 2.5: Principle of a membrane process [23]

To characterize a membrane process, basically two parameters are of central importance: The permeate flux through the membrane and the separation rate of the membrane described by the selectivity or the rejection. The selectivity S is the ability of the membrane to separate the compounds and can be calculated by the mass fractions w of permeate P and feed F as follows [23]:

$$S = \frac{\frac{w_{iP}}{w_{jP}}}{\frac{w_{iF}}{w_{jF}}} \tag{2.1}$$

Selectivities are often used e.g. in gas separations when all species of a system are able to pass. In fluid separations, a more common value to define the quality of a separation is the rejection R of a compound i [23].

$$R_i = 1 - \frac{w_{iP}}{w_{iF}} \tag{2.2}$$

Permeate flow referred to as flux J is described by the permeate volume flow V_P^F in relation to the active membrane area A_M.

$$J = \frac{V_P^F}{A_M} \tag{2.3}$$

In ultrafiltration and nanofiltration another value characterizing the separation behaviour of different membranes is often applied, the molecular weight cut off (MWCO). It is usually defined as the molecular weight of a molecule that is 90 % retained by the membrane and thus enables the differentiation of membranes in terms of molecular size selectivity. In aqueous applications

molecular standards of dextran or polyethylene glycol are usually used to determine the rejection of a species by molecular weight. The MWCO can then be readily obtained from such a rejection curve. This curve resembles the grade efficiency curve that is used in the classification of larger particles. It is in widespread use for OSN, however, there is no common standard method for its determination (see chapter 2.2.3.4).

2.2.1.1 Operating modes

In membrane technology two operating modes concerning the flow configurations are distinguished. These are the dead end mode, where the feed flow is vertical to the membrane and the cross-flow mode, where the feed flows tangential across the membrane. Figure 2.6 gives a schematic illustration.

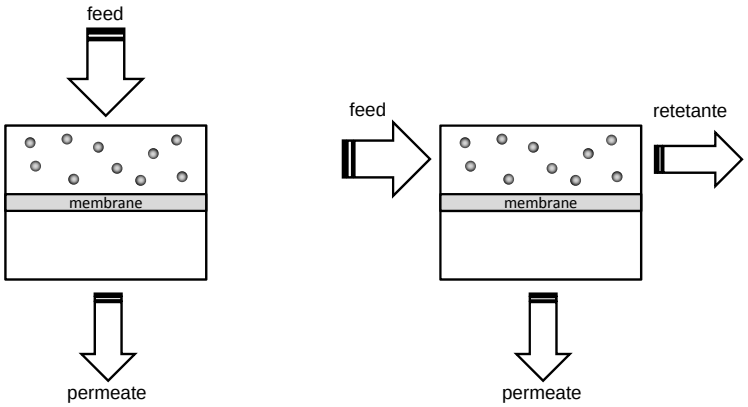

Figure 2.6: Different operating modes in membrane processes adapted from Mulder [10]
left: dead-end mode right: cross-flow mode

It is common practice to use the dead-end mode in microfiltration and filtration of larger particles. In OSN, it is usually only used for feasibility studies, membrane screenings or small and expensive product samples. Due to its simple set-up, the system is mostly pressurized by an inert gas, thus allowing for small feed volume. Based on the high concentration of compound on the membrane surface the transport resistance increases during the process. In larger scale, dead-end filtration is therefore only feasible for very dilute solutions.
In cross-flow mode, the flow on the feed side generates thorough mixing on the membrane surface, which induce a convective backhaul of retained species to the bulk flow. This reduces the concentration effect so that more highly concentrated solutions can be processed. For this reason, membrane applications are typically set up in cross-flow mode. This set-up has, however,

the disadvantage that a significantly higher feed volume is required because of the circulation pipes and a pump is needed to realize the cross-flow.

2.2.1.2 Driving force reducing effects

Starting from the basic approach

$$flux = \frac{driving force}{resistance} \tag{2.4}$$

there are different phenomena leading to reduced membrane performances due to an increase of the transport resistance.

Fouling

If a cover layer forms on the membrane which increases the resistance of the membrane, this effect is called fouling. The layer is mostly compressible and can be formed on the membrane surface as well as in the membrane pores. Reasons for the formation can be adsorption and accumulation/sedimentation of biological, chemical or colloidal substances or the precipitation of dissolved species when the solubility limit is exceeded (also known as scaling) [10]. The fouling layer acts as a filter cake introducing an additional transport resistance that increases when the layer grows over filtration time. Particularly, scaling and contained colloids in the process solutions may lead to problems in OSN, whereas e.g. biological fouling is almost absent.

Concentration polarization

Particularly during the start up of pressure driven membrane processes, solutes are transported convectively to the membrane surface. This leads to an increase of the concentration on the membrane surface, if the amount of the solutes transported convectively to the membrane is higher than the amount of solutes, which diffuse back to the bulk. This phenomenon is called concentration polarization. The corresponding concentration gradient at equilibrium is given in Figure 2.7.

Due to the increase of the concentration at the membrane surface, a boundary layer with thickness δ arises. At equilibrium, the permeate flux is the sum of the convective flow to the membrane and the diffusive back flow [10].

$$Jc_P = Jc + D\frac{dc}{dx} \tag{2.5}$$

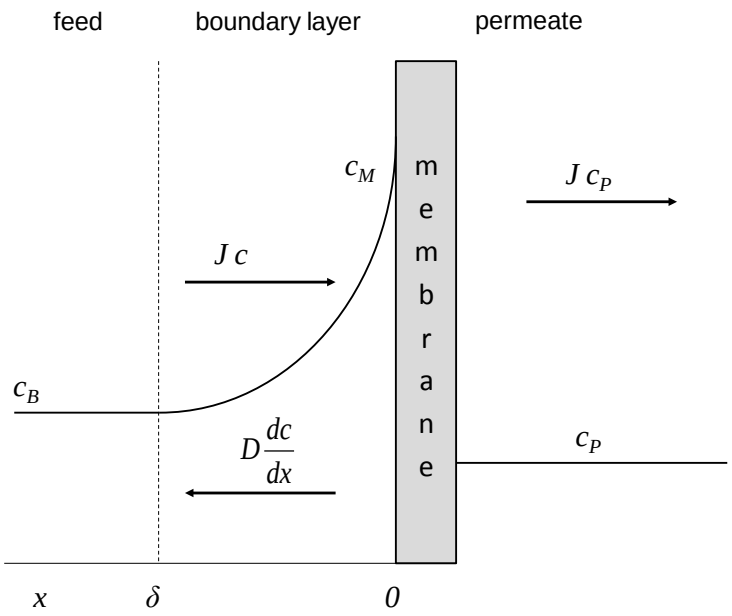

Figure 2.7: Concentration polarization: concentration gradient at equilibrium according to Mulder [10]

The mass transfer coefficient k describes the ratio of the diffusion coefficient D and the thickness of the boundary layer δ.

$$k = \frac{D}{\delta} \tag{2.6}$$

By integration of the equation under the assumption that the concentration of the solute at the permeate side c_P is zero (complete rejection), the following equation results:

$$\frac{c_M}{c_B} = \exp\frac{J}{k} \tag{2.7}$$

This indicates the two factors that are responsible for concentration polarization: the membrane flux (J) and the hydrodynamics (affecting the concentration profile at the feed side). A thorough mixing of the feed on the membrane surface is necessary to minimize the boundary layer and thus the effect of concentration polarization. This can be achieved by the use of feed spacers (geometrical fixtures in the feed channel that increase turbulence by sacrificing feed pressure drop), the selection of suitable membrane modules with good flow configuration and high cross flow rates.

As can be seen in Figure 2.7, with concentration polarization an observed rejection does not correspond with the actual rejection. In experiments only the concentration in the bulk can be determined. The real rejection R_{int} is dependent upon the maximal concentration c_M at the

membrane surface [10].

$$R_{int} = 1 - \frac{c_P}{c_M} \tag{2.8}$$

Osmotic pressure

If the concentration at the membrane c_M increases, the driving force is additionally reduced by the osmotic pressure. Osmotic pressure π rises with an increase of the concentration of solutes. Under the assumption of complete rejection, it can be calculated according to the following equation [10]:

$$\pi = -\frac{\mathrm{R}T}{\upsilon} \ln a_i \tag{2.9}$$

For dilute solutions the equation can be simplified to:

$$\pi = \mathrm{R}T \sum c_i \tag{2.10}$$

As solute concentration is requested in most membrane applications, the applied pressure has to be continuously enhanced during the process to keep the performance constant.

2.2.2 Applications and potentials of OSN

OSN is a versatile tool for process intensification and offers several advantages in comparison to conventional separation technologies. No thermal energy is usually required because separation is solely driven by a pressure difference. On the one hand these gentle process conditions may result in higher qualities especially of temperature-sensitive products. On the other hand OSN is less energy-intensive, because vaporization of the solvent is not required. For this reason high energy savings can be obtained by replacing distillation with OSN. Boam and Nozari [11] reported energy savings up to 90 % for product concentrations compared to distillation. Processing times can be reduced as well in many cases because membrane fluxes can be easily adjusted by the installed membrane area. This allows to increase the flow velocity of the separated fractions and free capacity of existing plants can be generated to increase production quantities. In comparison with separation technologies like extraction and adsorption, OSN has the advantage that no additional additives like solvents or adsorbents are necessary, which may be expensive, difficult to handle or may induce impurities. A scale-up of the technology is easily achieved just by a simple enlargement of membrane area (i.e. increasing the membrane modules for large processes). Separations with OSN are possible in a continuous set-up as well as in batch processing. A combination with other separation units, as e.g. a distillation column, is

also feasible allowing for the design of hybrid processes. Existing plants can be easily retrofitted with OSN due to the simple set-up which can then result in higher plant throughput [24]. Based on the energy savings and the possible recirculation or recycle of process streams, the application of OSN can help, moreover, to reduce the product carbon footprint significantly, which is more and more important for industries. For these reasons, the application of OSN in chemical industry is very promising for several separation tasks. Meanwhile, numerous successful feasibility studies and applications concerning product concentration [25, 26], separation of homogeneous catalysts [16–19], solvent recycle [12–15], product purification e.g. separation of intermediates, by-products or oligomeric products from reaction mixtures [27–32] and solvent exchange [33, 34] have been published in literature. Furthermore, there are already some studies on the integration of OSN in hybrid processes e.g. in combination with crystallization [35] and distillation [36–38].

2.2.3 Membrane materials and module geometries

2.2.3.1 Polymeric membranes

Materials and preparation

The key to high performances of an OSN membrane is a thin active layer minimizing the resistance against transport through the polymer. This requires a more porous support layer to stabilize the active layer against the high pressures why these membranes typically have an asymmetric structure. A distinction is made between integrally skinned and thin film composite (TFC) membranes [24]. The construction principle of these is schematically illustrated in Figure 2.8.

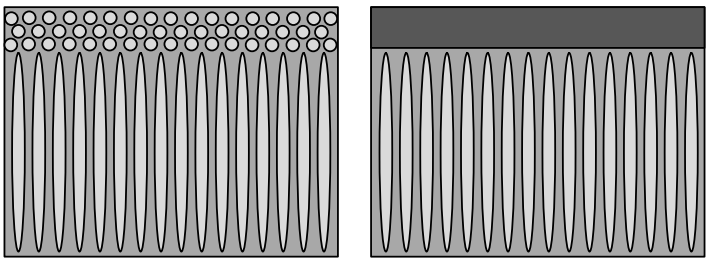

Figure 2.8: The two types of polymeric nanofiltration membranes left: integrally skinned membranes right: thin film composite membrane [24]

The differences in structure result from the differing preparation routes. Integrally skinned membranes are made via a phase inversion process for which the two layers are of the same composition. TFC membranes usually consist of different materials. Several techniques have been established for applying the thin layer on the support: dip coating, interfacial polymerization, spray coating, spin coating, in situ polymerization, plasma polymerization and grafting [39]. The advantage of the TFC type is that both active layer and support layer can be optimized independently in order to achieve the ideal membrane performance. Table 2.1 lists several polymers reported to be suitable for OSN membranes.

Commercially available

Despite the large number of publications concerning the development of new membranes for OSN, the number of commercialized membranes is rather limited. Koch Membrane Systems, Inc. (Wilmington, Massachusetts, USA) was the first company offering membranes suitable for organic solvents. Meanwhile, this membrane type is not offered anymore. The Starmem® membranes, consisting of non-cross linked polyimide P84® or Matrimid, have been widely used to investigate solvent fluxes, solute rejections and separation principles in OSN [62–70]. The Starmem® membranes were originally manufactured by W.R. Grace (Columbia, Maryland, USA) who later sold this business off to UOP (Des Plaines, Illinois, USA). Membrane Extraction Technology Inc. (MET) (London, UK) was the reseller for W.R. Grace and UOP in Europe. Additionally, this spin-off from the Imperial College of London commercialized the DuraMem® series membranes. These are cross-linked polyimide (PI) membranes that are able to withstand even harsh polar solvents as DMF or NMP. In 2010, MET was acquired by Evonik Industries AG (Essen, Germany) who developed the PuraMem® series membranes as replacement for StarMem. Both membrane types are made from P84® polyimide [42]. SolSep BV (Apeldoorn, The Netherlands) offers a UF membrane and five NF membranes suitable for organic solvents with diverging MWCOs [71]. The material of the membranes is not known, but the membranes seem to be hydrophilic, as they all work in alcohols. GMT Membrantechnik GmbH (Rheinfelden, Germany) is a subsidiary company of the BORSIG Group (Berlin, Germany) and offers three different membranes for applications in organic solvents. They are all composite membranes made of Polydimethylsiloxane (PDMS) on a Polyacrylonitrile (PAN) support.

Modules

In technical applications membranes have to be housed in a membrane module. These support

Table 2.1: Typical polymers used for preparation of OSN membranes

Name	Structure	Reference
Polydimethylsiloxane	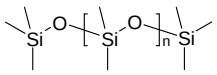	[40, 41], GMT
PI (Lenzig P84)	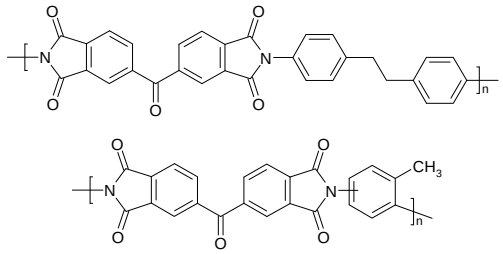	[42–46] Duramem®, Puramem®
PI (Matrimid 5218)	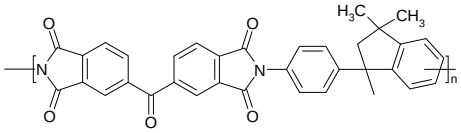	[47, 48]
PTMSP	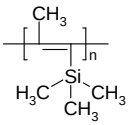	[49]
PIM-1	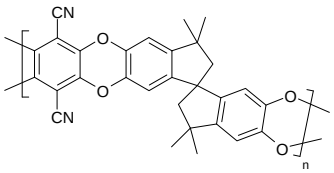	[50]
Polyphenylsulfone	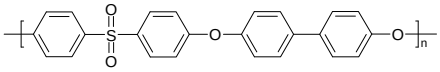	[51]
Polysulfone	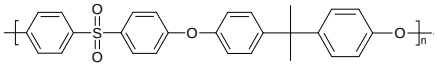	[52–54]
Polyaniline	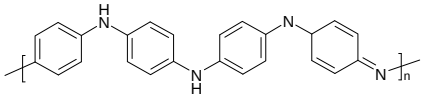	[55, 56]
Polyacrylonitrile	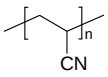	[57]
Polyether ether ketone	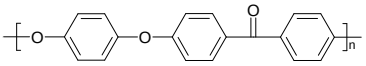	[58]
Polybenzimidazole	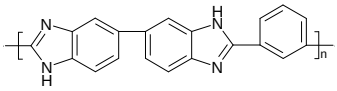	[59–61]

the membrane against the high pressures and determine the flow conditions over the membrane and thus driving force reducing effects. For feasibility studies and process development all

membranes are distributed as flat sheets. Mostly available in DIN A4 size, the individual shape of the lab module can be cut out of the sheet. In technical applications of nanofiltration, spiral wound modules are usually used. They offer a good pressure resistance and a compact assembly. In these modules flat envelopes are wound around a tube wherein the permeate is collected. The feed flows against the membrane package, disperses in the feed layers and passes along the length of the module. The permeate and the feed side contain spacers to enable the flow in the membrane package. A sliced spiral wound module is given in Figure 2.9 to show the composition of the different layers within the module.

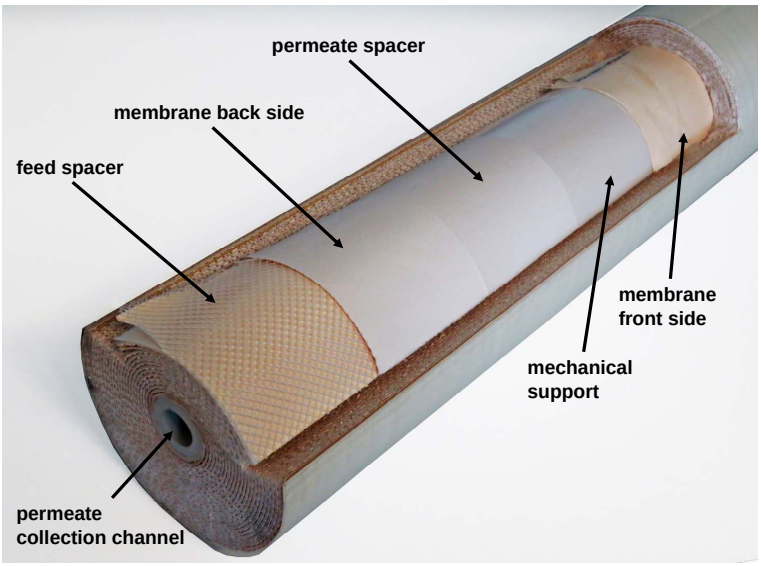

Figure 2.9: Sliced spiral wound module

Besides the standard modules, GMT Membrantechnik GmbH offers an envelope-type module. These modules distinguish oneself by the adhesive-free fabrication, short permeate distances, a spacer-free construction and an adjustable feed flow [72]. This special construction enables to exclude impurities caused by adhesives and even filtration of solutions with high viscosities becomes possible.

2.2.3.2 Ceramic membranes

Materials and preparation

The most common materials for the preparation of ceramic nanofiltration membranes are oxides of zirconium, aluminum, titanium and silicon or mixtures of them [10, 73–78]. They usually

have an asymmetric structure because they consist of multiple layers with decreasing pore sizes as illustrated in Figure 2.10.

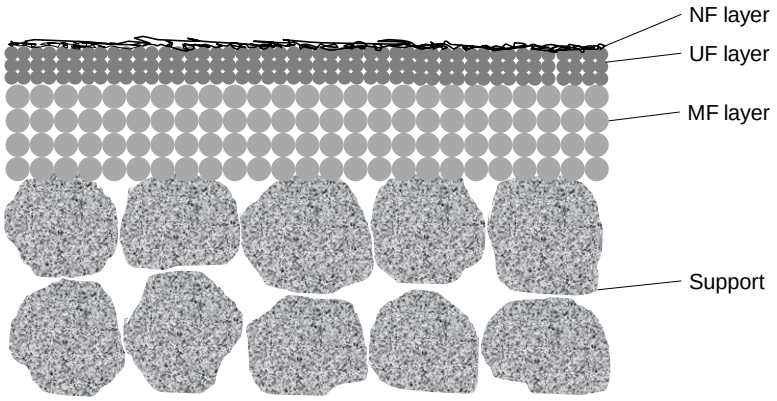

Figure 2.10: Structure of a ceramic nanofiltration membrane

The active nanofiltration layer is mostly prepared by sol-gel-techniques either by the 'colloidal gel' route or by the 'polymeric gel' route. In the former case, the metal alcoholates are mixed with an excess of water and due to full hydrolysis form colloidal oxide particles with a particle size in the range of 5 - 10 nm. After sintering, the particles adhere and the voids between the particles generate the pores which are limited by the particle size to a minimum of 3 - 5 nm. This technique is commonly used for the preparation of ultrafiltration membranes and the support layers of tighter membranes. In the second case, only a defined quantity of water is added to the alcoholates causing an incomplete hydrolysis and thus longchained polymers are formed. By addition of complexation agents, the incomplete hydrolysis can be additionally assisted [79]. Via this route nanofiltration layers with pore sizes smaller than 1 nm can be produced [74].

Commercially available

In the nanofiltration range (MWCO <1000 g/mol) there are only two membranes for aqueous and one for nonaqueous applications available to date. All are offered by Inopor GmbH (Veilsdorf, Germany), a subsidiary of the Rauschert Group (Judenbach, Germany). In Table 2.2, an overview of those membranes concerning their technical parameters is given.

Modules

The membranes described above are offered as monochannel or multichannel tubes with lengths of up to 1200 mm. The active membrane layer is always inside the channels and thus permeate is collected at the outside of the membranes. Figure 2.11 shows the different geometries of ceramic membrane tubular modules.

Table 2.2: Commercially available ceramic membranes in the nanofiltration range

Material	Mean pore size [nm]	MWCO [g/mol]	Porosity [%]	Type
SiO_2	1.0	600	30-40	hydrophobic
TiO_2	1.0	750	30-40	hydrophilic
TiO_2	0.9	450	30-40	hydrophilic

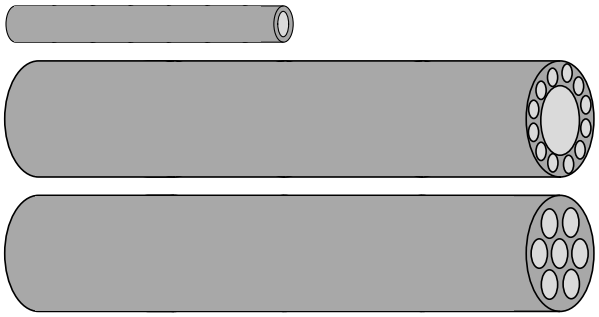

Figure 2.11: Different geometries of ceramic membrane modules

To realize high packing densities usually multiple multichannel membranes are arranged in a module for technical applications. Inopor offers modules for 1, 3, 7, 14, 19 and 37 membranes [80].

2.2.3.3 Comparison between polymeric and ceramic membranes

Every membrane material has its advantages. Currently, the cut-off of polymeric membranes is far less than that of ceramic membranes, whereas ceramic membranes promise higher chemical, mechanical (resistance against abrasion) and thermal stabilities. The storage and cleaning of ceramic membranes is much easier as those allow for steam sterilization and back flushing and they can be stored dry. For these reasons, the membranes have mostly a higher longevity than polymeric membranes. Ceramic membranes feature considerably lower packing densities compared to polymeric membranes which can be compensated by higher permeabilities. In Table 2.3 the direct comparison between polymeric and ceramic membranes for several properties is given. The given information are partially predicted characteristics adopted from other filtrations because the knowledge of the behaviour of ceramic membranes in organic solvent nanofiltration is still limited.

Table 2.3: Comparison between polymeric and ceramic membranes

	Polymeric	Ceramic
Solvent stability	depending on solvent	independent
Chemical stability	low	high
Mechanical stability	sensitive separation layer	higher resistivity
Thermical stability	up to 80 °C	up to 350 °C
Leaching	possible (pore fillers/polymer)	not reported
Compaction	yes	no
Swelling	yes	not expected
Minimal pore size	dense	unknown
Pressure range	up to 60 bar	up to 40 bar
Area per volume	high	low
Cleanability	difficult	back-flush possible, sterilizable
Storage	only wet	dry storage possible

2.2.3.4 Characterization of OSN membranes

Due to the interactions of the membrane materials with the solvents, the rejections (and thus the MWCO) of a membrane strongly depend on the specific solvent [81, 82] and therefore, it is difficult to find a consistent method for the determination of the MWCO in OSN. One proposed method is the filtration of a mixture of polystyrene oligomers with different molecular weights in toluene [83]. To consider the interactions between membranes and solvents, See-Toh et al. [84] extended the method to several solvents.

Because of their simple analysis, dyes are also widely used as model solutes. Several newly developed membranes, in particular at universities, are characterized by rejection measurements of dyes, for example Rose Bengal (MW: 1017 g/mol) [47, 48, 51, 85, 86], Safranin O (MW: 351 g/mol) [87], Brilliant Blue R (MW: 826 g/mol) [49, 87], Bromothymol Blue (MW: 624 g/mol) [86, 88], Methyl Orange (MW: 327 g/mol) [47, 48] and Crystal Violet (MW: 408 g/mol) [88]. Other authors use homologous series of e.g. polyolefins [89] or alkanes [43] to determine a rejection curve. In individual cases diverse linear and aromatic hydrocarbons [44, 50] are utilized. Only a few new OSN membranes are characterized according to the method of See-Toh et al. [43, 45, 50, 55, 56]. It must be stated that all these methods differ largely in their choice of solvents and filtration conditions. Up to now, no standard of testing OSN membranes has been agreed upon. This makes it rather difficult for the end user to judge between different

membranes and/or manufacturers. In addition, it is quite hard to compare the membrane performances with each other as there is no collective method within the membrane manufacturers as well.

2.3 Transport mechanism in membrane separation

Without a fundamental understanding of the occurring transport mechanism in membrane separation a tremendous experimental effort is necessary to identify the best membrane for a given separation problem and to specify a suitable process window. A thorough knowledge of the mechanism and mathematical models describing the transport enables the simulation of the separation over the membrane and thus the prediction of expected fluxes and rejections for a certain membrane. In addition, a flow-sheeting simulation of the whole process would be possible. This would facilitate detailed engineering and process optimization.
Despite extensive research and a growing number of publications during the last years, there is still debate on a universal transport model for OSN [65, 90, 91]. Different approaches have been published, which try to extend the known and accepted models of mostly aqueous membrane processes in ultrafiltration and reverse osmosis to organic solvent nanofiltration. In general, transport models are divided in membrane independent and dependent models [23]. Membrane independent models consider the membrane as a black box and are based on irreversible thermodynamics as the Kedem-Katchalsky-Model [92] and the Spiegler-Kedem-Model [93]. Membrane dependent approaches are based on an idea about the structure of the membrane and take membrane properties into account. These models are the solution-diffusion and pore-flow models which are described in the following section.

2.3.1 Membrane dependent models

Generally, there are two different models with respect to their assumptions on the fundamental membrane structure - the pore-flow model for porous membranes and the solution-diffusion model for dense membranes. Both models assume a phase equilibrium at the interface between the liquid and the membrane. Transport is driven by a gradient in the chemical potential μ; the first by a pressure gradient, the other by a gradient in the activity (c.f. Figure 2.12) and thus both

can be described by the simple equation:

$$J_i = L_i \frac{d\mu_i}{dx} \tag{2.11}$$

Wijmans and Baker [94] reviewed and compared both models.

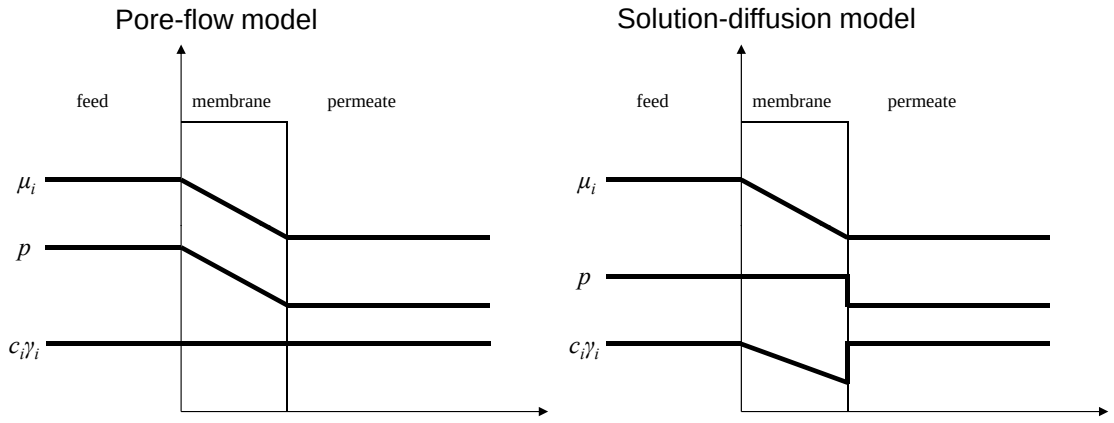

Figure 2.12: Gradient profiles of the chemical potential, the pressure and the activity assumed for the pore-flow and the solution-diffusion model adapated from Wijmans and Baker [94]

2.3.1.1 Pore-flow models

The pore flow mechanism assumes convective flow through the pores of a membrane. The concentration across the membrane is assumed to be constant. The driving force - the gradient of the chemical potential - is established only by the pressure gradient and can be expressed according to Darcys law with the membrane thickness l [94].

$$J_i = L_i \frac{p_0 - p_i}{l} \tag{2.12}$$

Due to the mostly negligible concentration gradient of the solvent between the feed and the permeate side, the solvent flux can generally be fitted either with the Hagen-Poiseuille equation (eqn 2.13) or the Carman-Kozeny equation (eqn 2.14). The distinction results from the assumed membrane structure. The different membrane types are illustrated in Figure 2.13.

The most common approach is the Hagen-Poiseuille equation assuming the membrane as a system of parallel cylindrical capillary tubes of equal diameter (see Figure 2.13 left). In this case, the flux is dependent on the porosity ε, the radius of the pores r_p, the dynamic viscosity

Figure 2.13: Possible pore structures adapted from Mulder[10]

η of the fluid and the tortuosity τ. Tortuosity describes the ratio between the real length of the capillary tubes and the membrane thickness [23].

$$J_i = \frac{\varepsilon r_p^2}{8\eta\tau}\frac{\Delta p}{l} \tag{2.13}$$

The Carman-Kozeny equation can be used if the structure of the membrane conforms to a packed bed of particles (see Figure 2.13 right) with the Carman-Kozeny constant K and the volume related specific surface S_V [10].

$$J_i = \frac{\varepsilon^3}{\mathrm{K}\eta S_V^2 (1-\varepsilon)^2}\frac{\Delta p}{l} \tag{2.14}$$

To calculate the rejection of solutes, and the solute fluxes respectively, several models [5, 95–98] have been developed. These models are based on the correlation between the hindrance factors for convection K_c and for diffusion K_d and the ratio λ of the solute radius r_s to the pore radius r_p [24] which is expressed in the solute steric partition coefficient ϕ.

$$\phi = \left(1 - \frac{r_s}{r_p}\right)^2 = (1-\lambda)^2 \tag{2.15}$$

Bowen and Welfoot [5] developed a model for the separation performance of porous nanofiltration membranes based on the extended Nernst-Planck equation.

$$J_s = K_c c_i v - c_i K_d D\frac{d(ln\gamma_i)}{dx} - \frac{c_i K_d D}{\mathrm{R}T}\upsilon_i\frac{dp}{dx} - K_d D\frac{dc_i}{dx} - \frac{z_i c_i K_d D}{\mathrm{R}T}F\frac{d\psi}{dx} \tag{2.16}$$

where D is the solute bulk diffusion coefficient and ψ is the electric potential within the pore. The equation can be used for ionic and uncharged solutes. In the case of uncharged components, the last term equals zero. The second term can also be neglected based on the assumption that the concentrations within the pores are small or the concentration gradient in the membrane is small. The model differs, therefore, from the widely adopted hydrodynamic models by the inclusion of the pressure term [5]. Solute flux can be described as well as

$$J_s = c_P v \tag{2.17}$$

Since the pressure gradient is assumed to be constant within the pore, it can be replaced by the Hagen-Poiseuille relationship in equation 2.16.

Based on this, equation 2.16 can be rearranged resulting in the following expression for the concentration gradient:

$$\frac{dc}{dx} = \frac{v}{K_d D}\left[\left(K_c - \frac{K_d D}{\mathrm{R}T}\upsilon_s \frac{8\eta}{{r_p}^2}\right)c - c_P\right] \tag{2.18}$$

Neglecting concentration polarization, integration of the equation over the membrane thickness $0 < x < l$ with the boundary conditions

$$c_{x=0} = \phi c_F \tag{2.19}$$

and

$$c_{x=l} = \phi c_P \tag{2.20}$$

leads to the following expression for the rejection:

$$R = 1 - \frac{(K_c - Y)\,\phi}{1 - (1 - (K_c - Y)\,\phi)\exp(-Pe')} \tag{2.21}$$

with the modified Peclet number Pe'

$$Pe' = \frac{(K_c - Y)\,{r_p}^2}{8\eta K_d D}\Delta p \tag{2.22}$$

Under the assumption that υ_s and D are independent of concentration the following dimensionless variable Y is defined for simplicity [5].

$$Y = \frac{K_d D}{\mathrm{R}T}\upsilon_s \frac{8\eta}{{r_p}^2} \tag{2.23}$$

The equations for the calculation of the hindrance factors can e.g. be taken from Bowen and Mohammed [99].

$$K_c = (2 - \phi)\left(1 + 0.054\lambda - 0.988\lambda^2 + 0.441\lambda^3\right) \tag{2.24}$$

$$K_d = 1 - 2.3\lambda + 1.154\lambda^2 + 0.224\lambda^3 \tag{2.25}$$

As there is sufficient evidence for an increase of viscosity in narrow nanofiltration pores [100–104], Bowen and Welfoot [5] proposed a simplified approach for the pore viscosity

$$\eta = \eta_0\left[1 + 18\left(\frac{d_{SL}}{r_p}\right) - 9\left(\frac{d_{SL}}{r_p}\right)^2\right] \tag{2.26}$$

where η_0 is the bulk viscosity and d_{SL} the thickness of a solvent layer at the pore wall. However, Bowen and Welfoot showed that there is just a marginal effect of the pore viscosity on the solute rejection.

Furthermore, the above model can be extended to integrate the effects of concentration polarization or pore size distribution. Bowen and Welfoot [2] proposed the log-normal distribution to take different pore sizes into account, expressed in a probability density function $q(r_p)$

$$q(r_p) = \frac{1}{r_p\sqrt{2\pi b}} \exp\left[-\frac{\left(\log\left(\frac{r_p}{\bar{r}_p}\right) + \frac{b}{2}\right)^2}{2b}\right] \tag{2.27}$$

including

$$b = \log\left[1 + \left(\frac{\sigma_p}{\bar{r}_p}\right)^2\right] \tag{2.28}$$

where $\bar{r}_p$ is a mean pore size and σ_p is the standard deviation. The theoretical probability density function considers pore sizes between 0 and ∞. As this is unlikely in reality, Bowen and Welfoot [2] suggested the truncation of the distribution. The new distribution function is restricted to pore radii $0 < r_p < r_{max}$.

$$q'(r_p) = \frac{q(r_p)}{\int_0^{r_{max}} q(r_p)\, dr_p} \tag{2.29}$$

They suggest to use an upper limit for the maximum pore radius of twice the mean pore radius. As a consequence of the pore size distribution all values dependent of r_p now have to be calculated for pores between 0 and r_{max}. Thus, the overall rejection for all possible pores is defined as

$$R = \frac{\int_0^{r_{max}} \left(q'(r_p)\, {r_p}^4 \frac{R(r_p)}{\eta(r_p)}\right) dr_p}{\int_0^{r_{max}} \left(\frac{q'(r_p){r_p}^4}{\eta(r_p)}\right) dr_p} \tag{2.30}$$

.

2.3.1.2 Solution-diffusion models

Lonsdale et al. [105] originally introduced the solution-diffusion model in 1965 for desalination with cellulose acetate membranes. It is based on the assumption of a dense membrane without any defects. Permeating components are assumed to be sorbed by the membrane material, to diffuse through the membrane and to be desorbed afterwards on the permeate side meaning separation is caused by different diffusion and sorption behavior of the compounds [90].

Due to the fact that no pressure gradient exists within the membrane, the flux through the membrane driven by a gradient of the chemical potential can be written as

$$J_i = -\frac{\mathrm{R}TL_i}{c_i}\frac{dc_i}{dx} \tag{2.31}$$

where the term $\frac{\mathrm{R}TL_i}{c_i}$ can be replaced by the diffusion coefficient D_i according to Ficks law. Integration over the membrane thickness then leads to

$$J_i = D_i\frac{c_{i0} - c_{il}}{l} \tag{2.32}$$

Equation 2.33 describes the sorption equilibrium at the feed side interface of the membrane:

$$c_{i,x=0} = \frac{\gamma_{iF}}{\gamma_{ix=0}}c_{iF} \tag{2.33}$$

For the ratio of the activity coefficients the sorption coefficient K_i can be introduced.

$$c_{i,x=0} = K_i c_{iF} \tag{2.34}$$

At the permeate side, the pressure difference between p_0 and p_l has to be taken into account. Rearranging and substituting for the sorption coefficient results in the following expression

$$c_{i,x=l} = K_i c_{iP}\exp\left(\frac{-\upsilon_i\,(p_0 - p_l)}{\mathrm{R}T}\right) \tag{2.35}$$

By substituting the concentrations in Ficks law 2.32 with equation 2.34 and 2.35 the following equation for the membrane flux can be obtained:

$$J_i = \frac{D_i K_i}{l}\left[c_{iF} - c_{iP}\exp\left(\frac{-\upsilon_i\,(p_0 - p_l)}{\mathrm{R}T}\right)\right] \tag{2.36}$$

The rejection can be calculated by insertion of the concentrations in equation 2.2.

To consider defects in the membrane or free volumes due to swelling, Mason and Lonsdale [106] developed the solution-diffusion model with imperfections in 1990, which assumes an additional viscous flow through pores. Consequently, they extended the equation for the membrane flux through solution-diffusion J_{SD} by a convective term J_{PF}:

$$J_i = J_{i,SD} + J_{i,PF} \tag{2.37}$$

$$J_{i,PF} = \frac{c_i B_0}{\eta l}\Delta p \tag{2.38}$$

where B_0 is the specific permeability of the membrane.

Paul [107] extended the solution-diffusion model by the Maxwell-Stefan multicomponent diffusion to take solute-solvent coupling and interactions between solvent and solute into account.

2.3.2 Transport in organic solvent nanofiltration

2.3.2.1 Transport description by adopting existing models

As mentioned above, there is still debate among researchers about the transport mechanism in OSN. Mainly, it is tried to adopt the models which are established e.g. in UF and RO processes because they are close to NF. The solution-diffusion model has been extensively used by several research groups to describe solvent permeation in OSN with polyimide membranes [44, 108] as well as with PDMS membranes [109]. However, especially with PDMS membranes good correlations were also found with the pore-flow model [90, 110].

Silva et al. [65] compared the pore-flow model and the solution-diffusion model for the permeation of mixtures of toluene with methanol and ethyl acetate through a StarMem® 122 membrane and found better agreement for solution-diffusion. Dijkstra et al. [90] modeled the permeation of pentane/decane and pentane/dodecane mixtures through PDMS membranes successfully with both the solution-diffusion model with imperfections and the Maxwell-Stefan equation. However, the values of the estimated parameters (membrane thickness l and specific permeability of the membrane B_0) were more realistic using the Maxwell-Stefan transport. Hesse et al. [69] were able to predict the fluxes of ethyl acetate, toluene, i-propanol and ethanol through a StarMem® 240 polyimide membrane with their newly developed model based on the Maxwell-Stefan approach. They determined the model parameters to describe sorption and diffusion in the polymer network of the active layer of the membrane from independent measurements [111, 112]. The modeled solvent fluxes showed an excellent agreement with the experimentally determined fluxes. Postel et al. [113] investigated transport behavior of a PDMS-based composite membrane on a polyimide support. They were able to predict the rejection of n-alkanes in toluene, isopropyl alcohol and methanol using the generalized Maxwell-Stefan equation, but the single solvent based fitting data were insufficient to predict solute rejection in binary solvent mixtures.

Marchetti and Livingston [114] conducted a comprehensive study on the accuracy of different transport models. They compared irreversible thermodynamics models [92, 93], simple solution-diffusion [94], classical solution diffusion [94], solution-diffusion based on Maxwell-Stefan equation [107], Donnan steric pore-flow [5], modified surface force pore-flow [115] and the solution-diffusion with imperfections model [116, 117] in terms of regression performance and the experimental effort required to fit the unknown model parameters. They

tested systematically commercial integrally skinned asymmetric cross-linked (DuraMem®) and non cross-linked (PuraMem® 280) membranes and commercial thin film composite silicone-coated PI membranes (PuraMem® S600) all from Evonik with polystyrene and Safranin-O dye in different solvents in their study. Non-commercial polymeric membranes were also taken into account by taking data from literature (PTMSP (Poly[1-(trimethylsilyl)-1-propyne]), PMP (Poly[4-methyl-2-pentyne]) membranes [118] and thin film composite silicone-coated PI membranes [119]). The best performing model for the PI membranes was the Maxwell-Stefan model whereas the classical solution-diffusion model could describe the performance very good as well while fewer experimental data are necessary. Only the performance of the glassy PTMSP and PMP membranes were better represented by the modified surface force pore-flow approach.

Others tried to find semi empirical approaches to describe the solvent permeability in OSN. Mostly, those provide efficient results for a certain set of compounds, though they cannot be readily transferred to other systems. Bhanushali et al. [4] conducted solvent permeation studies with different solvents as well as different membrane materials (hydrophobic and hydrophilic). A reasonable correlation for the solvent flux through hydrophobic membranes has been obtained for the following relation which is based on the solution-diffusion theory:

$$J \sim \frac{\upsilon_S}{\eta} \tag{2.39}$$

An incorporation of surface free energy of the membrane γ_{SV} and sorption values ϕ was proposed to predict the flux through various membranes.

$$J \sim \frac{\upsilon_S}{\eta} \frac{1}{\phi^n \gamma_{SV}} \tag{2.40}$$

Later, it has been shown in other studies that this approach is not universally applicable to describe solvent permeation [120, 121].

A semi-empirical approach adapted from the Hagen-Poiseuille equation was proposed by Machado et al. [3] that uses a series of coupled transport resistances through the membrane.

$$J = \frac{\Delta p}{f_0 [(\gamma_c - \gamma_S) + f_1 \eta] + f_2 \eta} \tag{2.41}$$

Transport is affected by a solvent parameter f_0, the critical membrane surface tension γ_c, the surface tension of the solvent γ_S and solvent independent intrinsic membrane parameters f_1 and f_2 characterizing the NF layer and the support layer, respectively. The model showed a good agreement for their permeation measurements of mixtures of acetone with water, paraffins and

alcohols through an uncharged silicone polymer membrane (Koch MPF-50). Again, this model was also disproven [82].

Geens et al. [122] carried out a series of permeability measurements with water-methanol, water-ethanol and methanol-ethanol mixtures and seven membranes of different materials. They compared the Hagen-Poiseuille equation, the Machado [3] and the Bhanushali [4] model in terms of their obtained results. They introduced a correction of the Bhanushali model by the difference in surface tensions between the membrane and the solvent $\Delta\gamma$ to consider solvent-membrane interactions.

$$J \sim \frac{v_S}{\eta \Delta\gamma} \tag{2.42}$$

However, they concede that the model is only suitable for polar solvents and NF-membranes and particularly useful for hydrophobic membranes.

Dobrak et al. [91] measured the permeance of alcohols, tetrahydrofuran (THF) and mixtures of toluene with isopropyl alcohol and THF with N-Methyl-2-pyrrolidone (NMP) / Dimethylformamide (DMF) / Dimethylacetamide (DMA) / Dimethyl sulfoxide (DMSO) through a PDMS and a PI membrane. They checked the agreement of the determined fluxes with the viscous flow model, the Bhanushali approach [4], the Geens approach [122], swelling, and the quotient of swelling and the solvent viscosity [40]. They found the best agreement for the latter.

For ceramic membranes there are considerably fewer publications concerning solvent permeation. Darvishmanesh et al. [123] adopted the idea of Machado et al. [3] to develop a coupled series-parallel resistance model for solvent permeation through ceramic nanofiltration membranes. According to them the solvent flux results from the resistances (1) against the transport from the bulk to the active layer of the membrane, (2) against convection through the pores and (3) against diffusion through the membrane material. This model seems to work well for ceramic NF membranes whereas it fails for UF membranes. The converse holds true for the Hagen-Poiseuille equation. Marchetti et al. [124] developed, thus, a semi empirical model bridging between nanofiltration and ultrafiltration. Buekenhoudt et al. [125] analyzed the solvent flux behavior of water and 11 different organic solvents through different ceramic membranes with pore sizes ranging from 0.9 nm to 100 nm. They observed a simple linear relationship between the product of permeate flux and viscosity of the solvent and the Hansen solubility parameter of the solvent independent of the membrane material and the pore size.

All the models introduced so far refer to the prediction of solvent permeation. If solute rejection

is considered research is even less advanced.

Van der Bruggen et al. [126] modeled the rejection of diverse organic molecules in aqueous nanofiltration by using the Spiegler-Kedem model and compared different approaches to calculate the reflection coefficient. They identified the log normal model to be the most useful one to predict the reflection coefficient in practical applications, because it consists of only two parameters. Later the same model was applied to explain the transport of organic compounds in organic solvents: Geens et al. [127] conducted measurements with several polymeric membranes as well as ceramic membranes and six dyes as reference substances dissolved in methanol, ethanol, acetone, ethyl acetate and n-hexane. By calculating the reflection coefficient according to different models (Steric hindrance pore model [128, 129], Ferry [98], Verniory [130] and log normal [126]), they found high correlations between the experimental data and the predicted values. Gibbins et al. [131] published a similar study. They used the Ferry, the SHP and the Verniory model to determine the pore size of polymer membranes from measured rejections and obtained reasonable results.
Tarleton et al. [1] suggested a semi-empirical model for solute rejection which considers a combination of convective and diffusive fluxes for solutes whereas solvent flux is assumed to be viscous. The solute flux is given by equation 2.43 where a is the fraction of solute passing by viscous flow and P the membrane permeability.

$$J_i = a\frac{c_F P \Delta p}{l} + (1-a)\frac{D\,(c_F - c_P)}{l} \tag{2.43}$$

D and a are fitting parameters which they obtained from their experiments with xylene, cyclohexane and n-heptane as solvents and iron(III)acetylacetonate and 9,10-diphenylanthracene as solutes by using a PDMS membrane.

2.3.2.2 Factors influencing separation behavior in OSN

An alternative approach found in literature is the investigation of parameters influencing the separation behavior in OSN to gain a better understanding of the occurring phenomena. Knowing the determining parameters an inference on the transport mechanism and particularly a prediction of the separation behavior is possible based on experience.

Bhanushali et al. [132] claimed that coupling effects of solvent and solute flux cannot be neglected. Geens et al. [133] concluded from their investigations with six compounds dissolved in ethanol and methanol, that solute transport is affected by (1) solute-solvent interactions due

to changing effective solute diameters, (2) membrane-solvent interactions determining the effective pore size due to swelling and pore wall solvation and (3) membrane-solute interactions based on polarity differences. From the measurements of rejections of several dyes (314 - 1017 g/mol) dissolved in alcohols with a PDMS membrane, Gevers et al. [134] observed a significant influence of the solute charge on the rejection especially for small molecules and a negligible role of solute size.

Zheng et al. [135] investigated the influence of molecular shape on the rejection in OSN with a PDMS and a polyimide membrane. They used small, neutral molecules in the range between 120 - 230 g/mol with similar solubility parameters, but different configurations (linear, branched and with aliphatic rings). They found an increase of rejection with increasing molecular weight for molecules with similar shape. However, the transport of linear molecules was preferred by all membranes followed by molecules with cyclic groups and the branched ones. In order to better account for the molecular size instead of its weight, they compared various molecular size parameters as the Stokes diameter, the equivalent molar diameter, the empirical effective diameter, the molecular length, the radius of gyration and the calculated mean size. It was concluded that the calculated mean size which is defined as the smallest molecular volume taken up by the solute provides the most characteristic size parameter.

Several authors [110, 136] pointed out the dependence of solvent fluxes through a polymer membrane from the Hildebrand solubility parameter. Apart from this, investigations concerning differences in rejections based on the solubility parameter of the solutes have been carried out by Bhanushali et al. [132] and Darvishmanesh et al. [70, 137]. The solubility parameter δ is a numerical value describing the relative solvency of a material, derived from the cohesive energy density [138].

$$\delta = \sqrt{\frac{\sum E_{coh}}{\sum \upsilon}} \tag{2.44}$$

It indicates whether substances are likely to be miscible, which is the case if the solubility parameters of the substances are similar. With the help of solubility parameters, the degree of swelling can be expressed by the polymer-solvent interaction parameter χ. It is considered to be the sum of the enthalpic component of polymer-solvent interactions χ_H and the entropic component or free-volume dissimilarity χ_S [139].

$$\chi = \chi_S + \chi_H = \chi_S + \frac{\upsilon_S}{\mathrm{R}T}(\delta_1 - \delta_2) \tag{2.45}$$

The Hildebrand solubility parameter has been successfully used for the prediction of polymer

swelling [139, 140] and therefore seems to be appropriate to cover the interactions between membrane and solvent.
Hansen [141] developed a three dimensional solubility parameter approach. This parameter considers dispersion, dipole-dipole and hydrogen-bonding forces. Methods for calculation by group contribution were proposed e.g. by Hoy [142, 143] or Van Krevelen [139].

Darvishmanesh et al. [137] studied the mechanisms of solute rejection with three marker substances of the same family and a polyimide membrane (StarMem® 122) over the whole range of solvents. By molecular modeling they investigated the effect of the solvent on the solute size. As a result a correlation between the employed solvent and the solute molecular size was given. However, the effect of the solvents on the membrane superposes this solute size effect in different solvents. Solute-solvent interactions were analyzed by means of a solubility parameter which indicates the affinity among two materials. They reported lower rejections for higher solute-solvent affinities. Even these interactions are more pronounced in the comparison of solvents from similar chemical identity. Negative rejections were measured for n-hexane. This phenomenon was explained by the higher affinity of the solute to the membrane than between the solvent and the membrane.

In a subsequent publication [70] the influence of solute size, polarity, dipole moment and solubility parameter using azo dyes of similar molecular structure with approximately equal molecular weight (350 g/mol) was investigated. The rejection measurements were conducted in methanol and ethanol with two nanofiltration membranes for aqueous systems, which are nevertheless stable in these alcohols, and a DuraMem® 150 polyimide membrane. Here, they observed a good correlation between the rejection and the dipole moment of the solutes which is independent of the membrane characteristics. In this study no clear correlation between solubility parameter and rejection was found.

Schmidt et al. [68] presented a comprehensive study concerning rejections in multi-component mixtures of three different solvents (n-hexane, toluene, isopropyl alcohol). They used two commercial polyimide membranes (StarMem® 122, PuraMem® 280) and chose five marker substances of similar molecular weight but absolutely different structural characteristics. They highlighted the importance of Hildebrand solubility parameter, solute critical diameter and membrane swelling on rejection behavior.

Postel et al. [144] investigated swelling behavior of PDMS in pure solvents, binary solvent mixtures and solvent/solute mixtures. They found a clear correlation between the degree of

swelling and the Hansen solubility parameter. They observed high rejections if the degree of swelling of the solute/solvent mixture is lower compared to the pure solvent. In contrast, higher degrees of swelling using dissolved solutes compared to pure solvent leads to low or negative rejections.
However, a transfer to other component systems is not feasible, because all these studies do not cover the complete three-dimensional space of interactions of OSN.

Concerning ceramic OSN membranes less research could be conducted due to the only recent availability of ceramic OSN membranes. Marchetti et al. [145] studied the effect of solute-solvent competition with hydrophilic ceramic membranes in organic/water mixtures. The effect of the solute charge was identified to be important for rejection in water while it is less significant in the presence of organic solvents. They found the solute-solvent competition in terms of preferential solvation to affect the rejection of charged solutes. This effect has been identified to be more significant at low pore dimensions and become negligible in the UF range. The influence of the solvent type on the ion rejection could be explained by considering the Hansen solubility parameter of the ion, the solvent and the preferential solvation of the ions. Hosseinabadi et al. [146] compared the separation behavior of a hydrophilic unmodified membrane with their Grignard functionalized modification. They demonstrated clear effects of solute- and solvent-membrane affinity detected by the solubility parameters and contact angle measurements [147], respectively. They pointed out the Hansen solubility parameter as an efficient tool to quantify the affinities and the rejections.

3 Gap analysis and approach

As emphasized in chapter 2, organic solvent nanofiltration is a relatively new, highly promising downstream processing method. It enables the separation of mixtures without thermal stress and any additives combined with a high potential for energy and resource savings and is thus a suitable tool for process intensification. Despite those advantages, there are still some obstacles that need to be overcome before OSN based on polymeric as well as ceramic membranes can become a widespread standard downstream operation. Particularly, an implementation in a multi-purpose production of specialty chemicals offers some additional challenges.

3.1 Gap analysis

The dedicated application of OSN in continuous processes with high throughputs has already been implemented and the economic benefit is appraisable and attested [148]. Currently, it is unclear whether the advantages of OSN can be exploited as well in specialty chemical industry where multi-purpose production is typically applied. A multi-purpose production site (see chapter 2.1) distinguishes itself by an extremely high demand for flexibility. Different unit operations are connected with one another as required depending on the process and are used for a huge number of products. An OSN plant in such a environment has to offer the same features to be used for multiple products and thus to achieve a sufficiently high occupancy and cost absorption. Additionally, for short life cycle products the effort for process development needs to be substantially eased. Summarizing, the following main challenges have to be solved:

- **Simplification of the identification of a suitable membrane for a separation task**
  As presented in detail in section 2.2.3.4, currently, there is no common standard method to characterize OSN membranes and therefore different membranes are not comparable in

terms of their separation performance. Additionally, from existent methods conclusions regarding real separation tasks and concerning other solvents cannot be drawn in general. A large time-consuming experimental effort of trial and error is thus inevitable to identify a suitable membrane for a given separation problem. Regarding the implementation of an OSN plant in a multi-purpose environment this implies that all imaginable processes have to be surveyed. This leads to extremely high cost for process development and a high risk of failure.

- **Predictability of relevant process parameters**

  The estimation of feasibility and efficiency of an OSN processes to reduce the risk is almost not possible since decisive technical information about the OSN process, like rejection and flux, cannot be estimated because no suitable short-cut methods for prediction of the separation behavior exist (see chapter 2.2.3.4). A substantiated theoretical potential assessment is not possible with the current state of knowledge and requires time-consuming and cost-intensive preliminarily investigations.

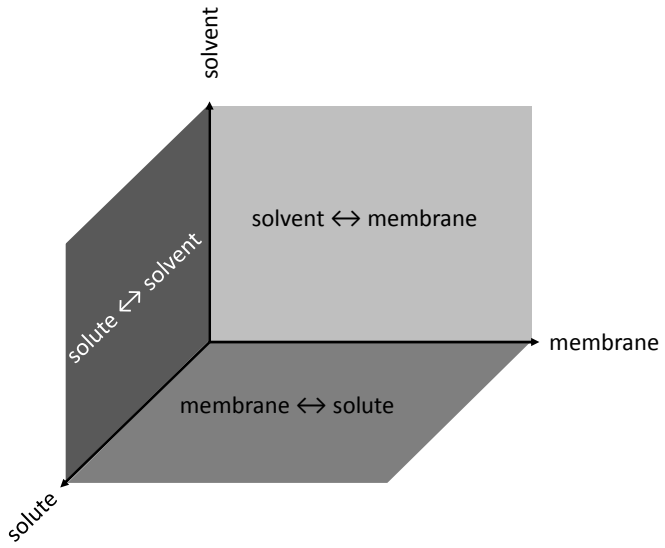

Figure 3.1: Three-dimensional interaction space of OSN

A lot of effort has been put into the description and prediction of transport phenomena in OSN (see chapter 2.3.2). Although in most of the published studies the measured data are described well with the therein used or developed models, still no consistency can be found when different membrane materials or solvents come into consideration. A unified transport model for polymeric membranes does not yet exist. However, the effort

of a detailed process modeling for a multitude of separation tasks in specialty chemicals processing would overshoot the benefit.

Besides modeling, several studies aimed at the identification of physicochemical parameters influencing the separation behavior in OSN (see chapter 2.3.2.2). None of these studies covered the complete three-dimensional space of possible interactions in OSN including different polymeric membrane materials, different solvents with varying properties such as e.g. polarity and a diversity in the used solutes (see Figure 3.1). Mostly, one of the factors was fixed and the investigations were only conducted in a two-dimensional space. These current findings cannot necessarily be transferred to systems involving other components, due to the aforementioned complex interactions.

- **Availability of data for the estimate of potential use of ceramic membranes in OSN**
  Ceramic membranes promise to overcome the aforementioned hurdles of polymeric membranes as e.g. the solvent independent separation performance and their possibility of dry storage and product interchange (see chapter 2.2.3.3). In particular the promised solvent independent separation performance makes ceramic membranes very interesting for an application in a multi-purpose environment. However, membranes with cut-offs in the lower nanofiltration range do not exist yet (see chapter 2.2.3.2). Today those advantages cannot yet be realized for organic solvent nanofiltration.

In conclusion, this thesis shall contribute an estimate for the potential of the technology in multi-purpose processing. Besides a thorough analysis of the specifics of the processes and their applicability for OSN, emphasis must be put into the acceleration of process development to enable a fast estimation of process feasibility. This can be facilitated by the development of short-cut models or heuristics for the membrane selection process. Furthermore, the promising properties of ceramic membranes need to be exploited in terms of their separation behavior in real process solutions as well as the governing transport behavior in OSN. Only with these deeper insights a reliable estimate of realization potential can be given that can help to pave the way for OSN to become a standard unit operation in process engineering.

3.2 Approach and structure

The theoretical potential of the implementation of OSN in a multi-purpose production is systematically assessed in chapter 4 using the example of a typical specialty chemicals production facility including a sensitivity analysis of the most relevant process parameters that need to be achieved for a reasonable economic potential.

In order to improve the predictability of an OSN process with polymeric membranes, a systematic experimental investigation covering the complete space of interactions of a typical class of specialty chemicals is carried out for the first time. These results are summarized in chapter 5 and consequently an heuristic is developed that enables to define the most suitable polymeric membrane for a given separation problem within that material class. These findings are meant to improve the understanding of the underlying transport mechanisms in polymeric OSN membranes and thus should allow for a rough estimate of the expected membrane rejection. The heuristic is tested for its ability to be extrapolated to substances not covered in the experimental assessment.

Chapter 6 aims to gain a deeper insight into the applicability of ceramic membranes in OSN. The separation behavior of new ceramic nanofiltration separation layers, which were developed by Fraunhofer Institute for Ceramic Technologies and Systems (IKTS) in parallel to this work, are experimentally investigated. The membranes are examined with regard to their application in a multi-purpose environment and on the assumed prerequisites given in chapter 2.2.3.3. Furthermore, their transport behavior is studied and a transport model originally developed for aqueous nanofiltration is extended for an organic environment to describe the measured membrane performances.

Finally, in chapter 7 the results of chapter 5 and 6 are applied in order to improve the potential assessment presented in chapter 4. The specifics of the process environment in terms of process and plant design are also included in the study to finally conclude on the realizable potential of the technology in specialty chemicals production.

4 Potential of OSN in a multi-purpose-process environment

As emphasized in chapter 2.1 the production of specialty chemicals is typically characterized by very small production volume, short product life-cycles and many different synthesis steps. The production plants demand for flexibility is very high because dedicated production lines are not feasible in general. This chapter focuses therefore on the question to what extent are the advantages of OSN economically exploitable in such a flexible production environment.

4.1 General procedure of the assessment

In chapter 2.2.2 the economic and technical advantages of OSN have been introduced. In order to estimate the potential of implementation of OSN within specialty chemicals production, a systematic assessment [149] of an OSN plant in a multi-purpose environment is conducted.

The assessment of potential is subdivided in three steps according to Figure 4.1. First of all, the theoretical potential which embraces the unrestricted, maximum savings is determined. It is estimated based on assumptions and experiences. Subsequently, technical limitations are considered to determine the technically realizable potential. In the last step, investments based on the requirements of a multi-purpose environment and necessities for success are taken into account to identify the economic potential. This method was applied to a typical multi-purpose production facility manufacturing specialty chemicals. Initially, the complete synthesis and downstream processing steps of the 39 substances with the highest production volume produced in this facility were collected. In order to understand the occupancy within the facility, the quantitative amount of the different production steps, e.g. reaction, distillation, chromatography,

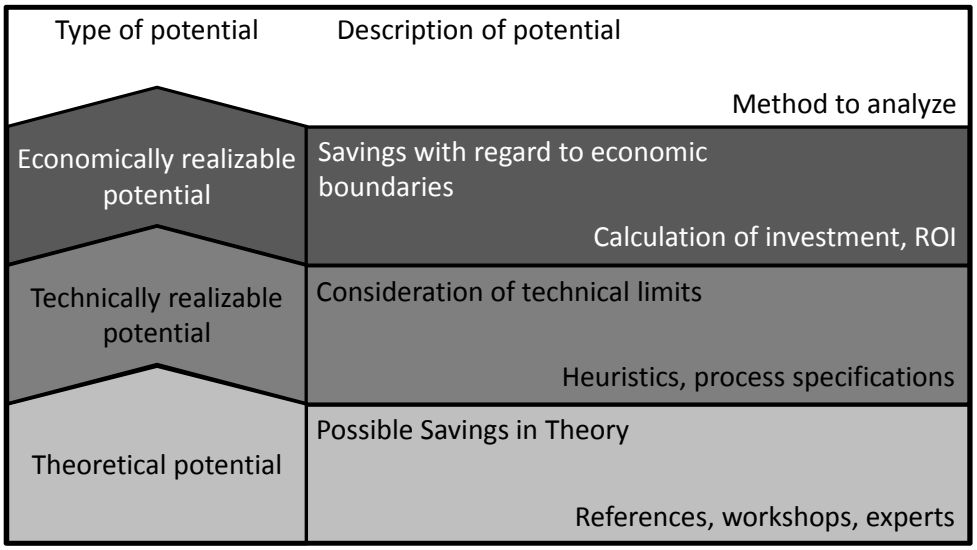

Figure 4.1: Assessment of technological potential of OSN adapted from [149]

crystallisation, etc. was determined. The 39 selected substances are produced in 336 steps, 248 of them are downstream processes. The breakdown in figure 4.2 clearly shows that distillation accounts for the highest share in terms of downstream processes. In general, distillation in a multi-purpose production is performed batchwise in stirred tank reactors. More than 80 % of the 75 distillations are intended for solvent exchange or product concentration.

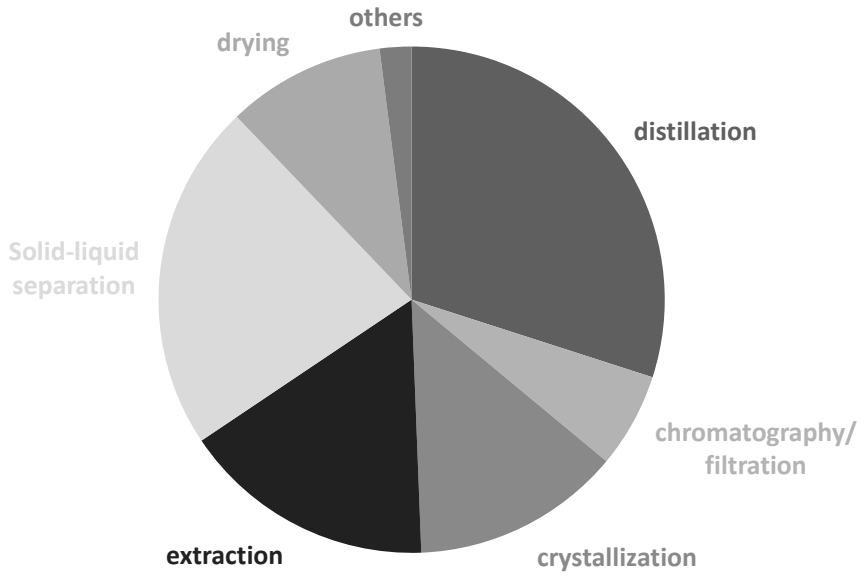

Figure 4.2: Distribution of different downstream process steps sorted according to their number in an exemplary multi-purpose production facility

Due to the long processing time of distillation and thus, a high plant allocation in addition to the highest percentage of processing steps, the distillation steps offer a high potential for

optimisation and process intensification. Fot this reason, this potential assessment is focused on the application of OSN to shorten distillation processes.

4.2 Theoretical potential

In order to get a rough overview of the potential, the savings which can be achieved by a combination of OSN and distillation compared to distillation alone are considered. The calculation is based on a two-stage filtration (filtration of the permeate in the second stage). The reduction of costs is based on shorter processing times and the difference in energy demand. Product losses to the permeate are considered as well as the energy demand of the pumps in an OSN plant. Product losses in distillation are assumed to be zero. The theoretical potential for savings Pot_{Th} of a product i is derived from the sum of the savings due to reduction of process time C_{PS}, machine hours C_{MH}, energy for distillation C_{ED}, the energy costs for OSN C_{EO} and the costs for product losses C_{PL} to the permeate.

$$Pot_{Th,i} = C_{PS,i} + C_{MH,i} + C_{ED,i} + C_{EO,i} + C_{PL,i} \tag{4.1}$$

The different items are calculated as follows:
C_{PS} describes the economic advantage of a reduction of the processing time. By reducing the process time, the tied capital of a company is available earlier for e.g. new investments. In measurable terms this advantage can be expressed by the weighted average cost of capital $wacc$ on the earlier available capital (market price of the products $cost_s$) for the respective period (process time for distillation t_D of the permeate m_P compared to the time required for OSN processing t_{OSN}).

$$C_{PS} = (t_D - t_{OSN}) N_b \cdot wacc \cdot N_b \cdot m_s \cdot cost_s \tag{4.2}$$

with

$$t_D = \frac{m_P}{m_D^F} \tag{4.3}$$

$$t_{OSN} = \frac{m_P}{\rho \cdot J \cdot A_M} \tag{4.4}$$

and

$$m_P = m_S - (1 - w_{R,max}) \cdot \frac{m_s}{w_{R,max}} \tag{4.5}$$

N_b is the number of batches produced per year. The mass of the total amount of solvent per batch and the quantity of product are represented by m_S and m_s, respectively. m_P describes

the mass of permeate which has to be removed to achieve the maximum concentration of the retentate $w_{R,max}$. It is that part of the solvent that does not need to be removed by distillation if OSN is applied.

Due to the reduction of the process time, the manufacturing costs are reduced as well. The manufacturing equipment is occupied less by the respective product and thus fewer machine hours are allocated to the products.

$$C_{MH} = (t_D - t_{OSN}) \cdot N_b \cdot cost_{MH} \tag{4.6}$$

For the estimation of the energy demand of distillation, solvent properties of the main solvent were assumed. Interactions and influences due to other solvents, the product or byproducts were neglected. Distillation temperatures were taken from the operation instructions for each product and each distillation. Energy losses because of heat transfer, etc. were taken into account by a fixed estimated efficiency factor η_D of 0.7.

$$C_{ED} = \frac{\frac{m_P \cdot c_{p,S} \cdot \Delta T + m_P \cdot \Delta H_V}{\eta_D} \cdot cost_{gas} \cdot N_b}{HV_{gas}} \tag{4.7}$$

The energy demand of the OSN process is determined by the electrical power of the pumps P_{Pumps}. The total runtime of the pumps including the membrane conditioning time t_c is considered.

$$C_{EO} = -P_{Pumps} \cdot cost_{el} \cdot (t_{OSN} + t_c) \cdot N_b \tag{4.8}$$

Product losses to the permeate were calculated with the average product concentration w_{av}.

$$C_{PL} = -\frac{m_P \cdot w_{av}}{1 - w_{av}} \cdot cost_s \cdot N_b \tag{4.9}$$

The overall theoretical potential of an implementation of OSN in the multi-purpose production facility is the sum of every theoretical potential in case the savings amount for >7000 MU per batch. The limit of savings was set to 7000 MU per batch to consider the additional expense for an extra process unit.

$$Pot_{Th,total} = \sum_{i=1}^{n} \left(Pot_{Th,i} \cdot \begin{cases} 1, & \text{if } Pot_{Th,i,b} > 7000 \\ 0, & \text{else} \end{cases} \right) \tag{4.10}$$

Processes in which e.g. the product losses exceed the savings due to processing time and energy demand are not incorporated. All assumptions made for the calculation are summarized in Table 4.1. Variations in the weighted average cost of capital *wacc* and product prices $cost_s$ are

considered by a multiplication factor. All *cost* values and the interest rate are taken from Merck KGaA database whereas m_D^F is based on the experiences of the respective production facility.

Table 4.1: Assumptions for the parameters necessary for the assessment of the theoretical potential

	Parameter	Assumption	Sensitivity analysis lower boundary	Sensitivity analysis upper boundary
R	rejection [-]	0.9	0.8	1
J	flux $[l/m^2h]$	30	1	100
A_M	membrane area $[m^2]$	100	50	150
m_D^F	distillate flow $[kg/h]$	100	80	300
$w_{R,max}$	maximum retentate concentration	0.5	0.2	0.6
t_c	conditioning $[h]$	2	1	4
f_{wacc}	changes in wacc [-]	1	0.6	1.2
f_{cost_s}	changes in product price [-]	1	0.5	1.5
$cost_{MH}$	costs machine hours $[\mathrm{MU}/h]$	1855	1686	2811
$cost_{el}$	costs electricity $[\mathrm{MU}/kWh]$	1.4	0.7	2.1
$cost_{gas}$	costs gas $[\mathrm{MU}/m^3]$	5.5	4.9	6.3
η_D	energy efficiency distillation [-]	0.7	0.8	0.5

With these assumptions, the theoretical potential calculated according to equation 4.1 for an implementation of a OSN plant in a multi-purpose production environment is 14m MU/a. The OSN process results in an additional benefit due to the reduced equipment occupancy of up to 10,000 h/a. This would enable to free one STR per year. However, concentration with OSN is only profitable for 11 of the 75 considered distillations. The others fail mostly due to too high costs for product losses or already too high concentrations.

Figure 4.3 indicates the distribution of the costs affecting the potential of OSN by means of two exemplary products out of the considered portfolio. The bars show the percentage of the respective cost term based on the overall potential. It clarifies that in the special case of a multi-purpose environment, the energy demand does not have a significant impact on the production costs and thus, contrary to large scale chemicals production energy savings are not the most beneficial advantage of OSN.

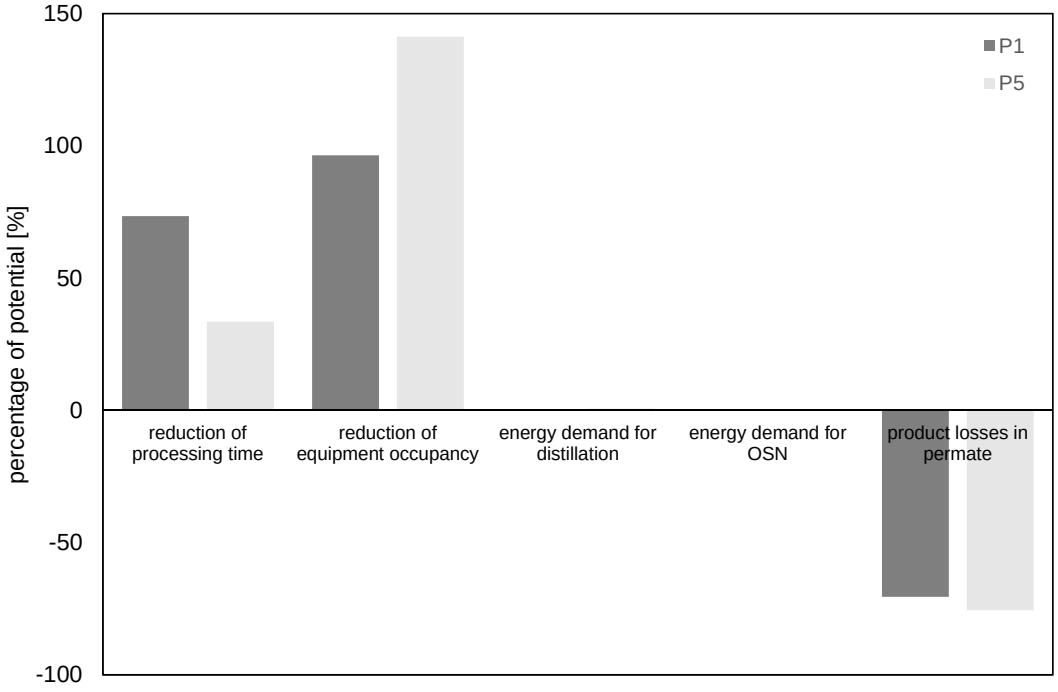

Figure 4.3: Percentage of the costs contributing to the theoretical potential using the example of two selected products manufactured in the multi-purpose facility

The influence of the two fundamental process parameters of OSN, namely rejection and flux, on the theoretical potential are shown in Figure 4.4 and 4.5. The potential rises steeply with an increasing rejection whereas the potential increase stagnates at fluxes above 20 l/m^2 h. The same behavior is observed for the number of economic processes that account for the theoretical potential, which are indicated by the line with the black numeric character. The number of processes can not be increased by higher membrane fluxes, whereas higher rejection minimizes the product losses of the high value products and thus more processes become feasible. Only 45 out of the 75 considered processes are economically viable assuming complete rejections and the estimated values given in Table 4.1. However, about half of the processes have to be implemented to save 90 % of the theoretical potential (indicated by the line with the white numeric characters). The potential of the six processes which are the main contributors to the potential stays nearly constant with increasing rejection, but with higher rejections more processes have promising potential.

In order to check the reliability of the potential assessment, a sensitivity analysis of the theoretical potential was conducted with a Monte-Carlo Simulation with varying process parameters. For this purpose, the software Oracle Crystal Ball (Oracle Corporation, Redwood Shores, Canada) was used. The influence of the different parameters and the stability of the potential against those factors was evaluated by a fluctuation of the parameters between the minimum and

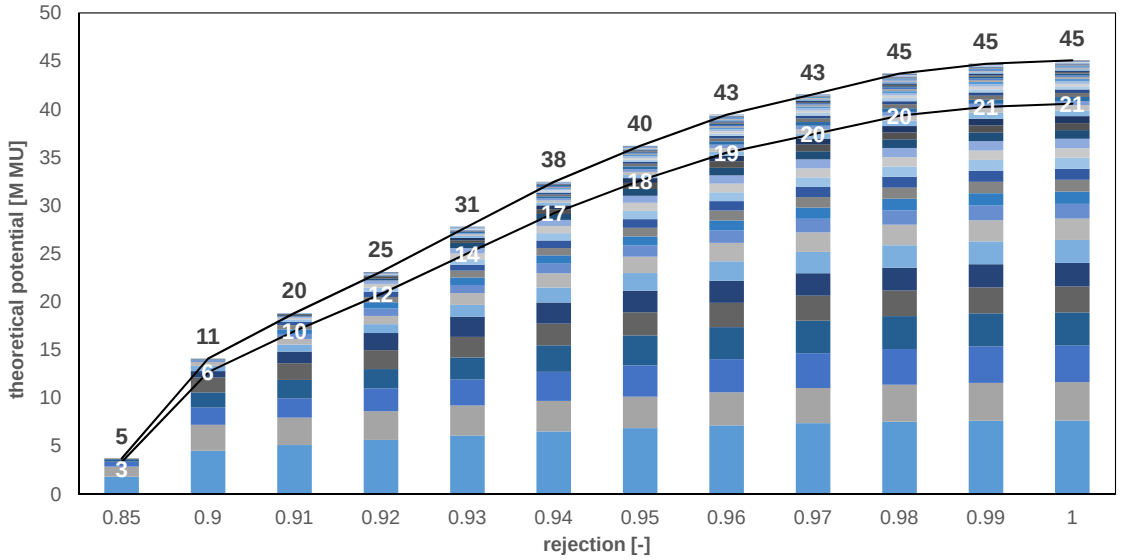

Figure 4.4: Influence of rejection of a membrane on the theoretical potential of a two-stage OSN plant in a multi-purpose environment (flux is fixed at 30 l/m^{2}h) and the number of economic processes (black numbers) as well as the minimal number of processes that amount to 90 % of the possible savings (white numbers)

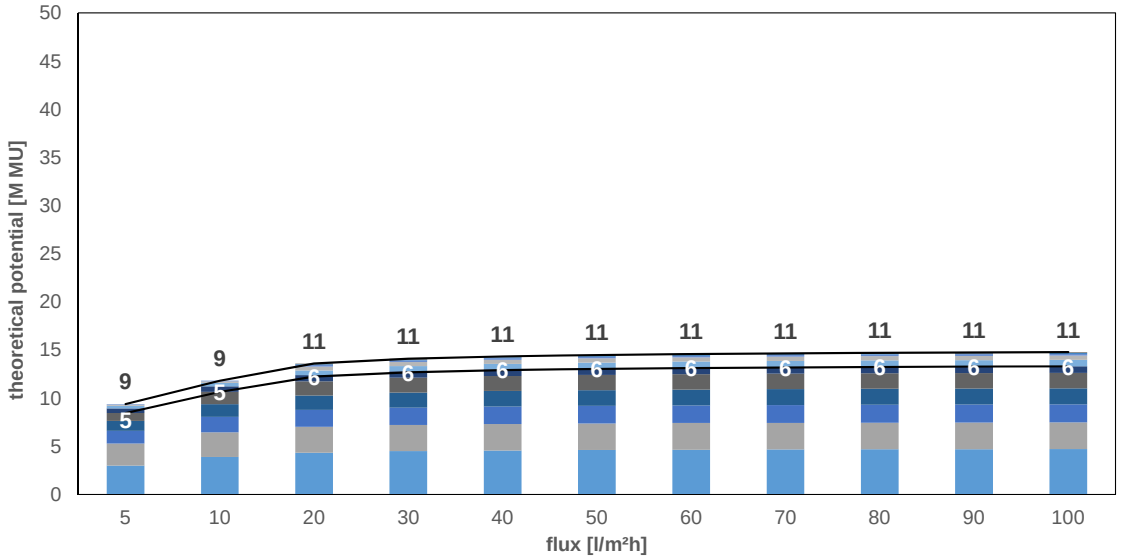

Figure 4.5: Influence of flux of a membrane on the theoretical potential of a two-stage OSN plant in a multi-purpose environment (rejection is fixed at 0.9) and the number of economic processes (black numbers) as well as the minimal number of processes that amount to 90 % of the possible savings (white numbers)

maximum limits given in Table 4.1. By varying the factors within this range, a huge amount of data points for the potential are generated and the most probable potential can be identified. This procedure enables to take economic uncertainties such as e.g. the product price or the weighted average cost of capital and process variations e.g. the maximum concentration or the conditioning time into account. The range of certainty of 95 % varies between 0 and 60m MU/a. The mean potential is 10m MU/a.

The sensitivities of the different factors on the theoretical potential $Pot_{th,total}$ are given in Figure 4.6. The diagram fortifies that rejection has the highest influence on the accessible savings when using OSN in a multi-purpose production for the acceleration of concentration steps. Other OSN process parameter such as membrane flux, membrane area and the maximum concentration of the retentate show almost no measurable effect on the potential. Another substantial influence is exerted by the distillate flow, since the savings are lower the faster the distillation is. Higher distillate flows cause lower processing time for distillation and reduce the benefit of OSN (lower C_{MH} and C_{PS}). Minor influence on the potential is given by the product price and the costs per machine hour and the weighted average cost of capital rate.

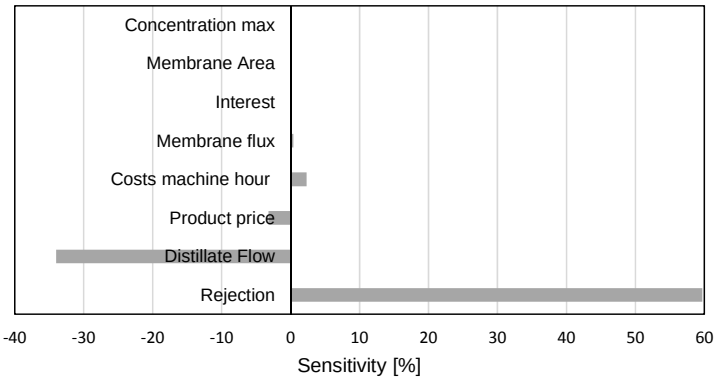

Figure 4.6: Sensitivity of different factors on the theoretical potential $Pot_{th,total}$

The results of the first rough potential assessment show the huge dependency of the potential of an OSN plant in a specialty chemicals production from the rejection of the membrane. To improve the potential assessment, the most important step is a reasonable prediction of the rejection. As aforementioned, there is no suitable tool for the prediction of membrane performance (chapter 2.2.3.4, 2.3.2, 3). A refinement of the potential estimation can only be done after a thorough analysis of the capabilities of polymeric (see chapter 5) and ceramic membranes (see chapter 6) and the development of a tool to predict membrane rejections in OSN. The results of the refined potential incorporating these analysis can be found in chapter 7.

5 Investigations on polymeric membranes in organic solvent nanofiltration

This chapter[1] presents the systematic investigations concerning the separation behaviour of polymeric membranes in OSN. They were conducted in order to gain a deeper insight into the underlying mechanisms and the interactions between membrane, solvent and solute and to develop a suitable tool to accelerate membrane selection for process development of OSN.

5.1 Materials and Methods

In order to identify the influencing parameters that impact membrane performance the following criteria for material selection have been defined for this thesis:

- Solvents must be of typical use in specialty chemicals production and cover the whole range of properties from polar to non-polar and from protic to aprotic.
- Membranes need to be commercially available in flat sheets as well as in spiral wound modules to obtain results of economic and industrial relevance. As highlighted in chapter 2.2.3.1, the number of commercially available membranes is limited. This limitation at

[1] The content of this chapter was partially adopted from: Zeidler, S.; Kätzel, U.; Kreis, P.: Systematic investigation on the influence of solutes on the separation behavior of a PDMS membrane in organic solvent nanofiltration. *Journal of Membrane Science 429* (2013), 295-303 and Blumenschein, S.; Kätzel, U.: An heuristic-based selection process for organic solvent nanofiltration membranes. *Separation and Purification Technology 183* (2017), 83-95

the beginning of this work led to the investigation of two different membrane materials, a hydrophobic and a hydrophilic one.

- Solutes have to cover a wide range of different sizes and properties. A typical material class produced at Merck KGaA (Darmstadt, Germany) was chosen because it offers molecules of different weights and with a similar core structure and diverse functional groups.

5.1.1 Polymeric membranes

As mentioned above, commercially available polymeric membranes should be applied in this work. In order to cover the widest possible range of membrane materials, the hydrophobic GMT-oNF membranes (GMT Membrantechnik GmbH, Rheinfelden, Germany) and the hydrophilic DuraMem® series (Evonik MET Ltd., Wembley, United Kingdom) were selected. Table 5.1 details the characteristics of the employed membranes. GMT Membrantechnik GmbH characterizes their membranes by a differing rejection experiment, summarized in Table 5.2.

Table 5.1: Commercially available polymeric membranes used in this work

Manufacturer	Name	Material	MWCO [g/mol]	Type
GMT Membrantechnik GmbH	GMT-oNF-1	PDMS/PAN support	- [2]	Composite
GMT Membrantechnik GmbH	GMT-oNF-2	PDMS/PAN support	- [3]	Composite
Evonik MET Ltd.	DuraMem 200	PI crosslinked with Polyamide (PA)	200 [4]	Integral asymmetric
Evonik MET Ltd.	DuraMem 300	PI crosslinked with PA	300 [5]	Integral asymmetric

[2,3]The manufacturer declaration is given in Table 5.2

[4,5]determined by rejection measurements of styrene oligomers in acetone [150]

As an indication for the hydrophobicity/hydrophilicity of the membrane, the solubility parameter of the material of the selective layer can be used. The solubility parameter for PDMS was taken from literature [153–155] where it is reported to be 15 $\left(\mathrm{J/cm^3}\right)^{1/2}$. Due to the unknown cross-linking of the selective layer of the DuraMem®, the use of literature values for polyimide is not reasonable. For the selective layer of the DuraMem®, a solubility parameter of

Table 5.2: Characterization of the GMT membranes given by the manufacturer [151, 152]

Membrane	Rejection [%]	
	GMT-oNF-1	GMT-oNF-2
Tetracosane (339 g/mol) in toluene	55	75
Hexatriacontane (507 g/mol) in toluene	96	98
Methyl Orange (327 g/mol) in isopropyl alcohol	88	93

28 $\left(\mathrm{J/cm^3}\right)^{1/2}$ was directly obtained from Evonik MET Ltd. [156].
A new membrane was used for each experiment. The GMT membranes were conditioned by storing them for at least 12 hours in the respective solvent prior to the rejection measurements.

The DuraMem® membranes contain a polyethylene glycol preservative that has to be flushed out by filtration with pure ethanol, acetone or THF prior the experiments. According to the manufacturers information, the membranes were first flushed with a permeate volume of 40 $\mathrm{l/m^2}$ at $20-30$ bar [150]. If possible, the membranes were washed with the respective pure solvent of the following experiment. In the case of experiments with other solvents e.g. n-heptane or MTBE, THF or acetone was used for flushing. Subsequently, the solvent was changed to the respective solvent to prepare the membrane and to wash out the flushing solvent by filtration.

5.1.2 Substances

5.1.2.1 Specialty chemicals

The present work focuses on a class of specialty chemicals with an elongated molecular structure. They consist of one to five ring-type core molecules (e.g. aromatic rings, cyclohexyl rings, etc.). The rings are either connected directly or via linking groups. Further functional groups as e.g. alkyl-, fluoro- or carboxyl may be attached. For the production portfolio of this material class at Merck KGaA, 15 two, three and four ring-type substances were selected in order to investigate their separation behavior in OSN. In Table 5.3 they are listed with their respective molecular weight and molecular structure. The molecular weight ranges from 220 to 480 g/mol. This range in molecular weight by keeping a similar structure allows to represent the measured rejections in terms of a rejection curve for the material class similar to the method of styrene oligomers (c.f. chapter 2.2.3.4). The explicit structure of the solutes cannot

be given for reasons of confidentiality. The functional group R symbolizes linear alkyl side chains with different length (R1<R2<R3<R4), X symbolizes a polar endgroup. Additionally, some of these molecules carry a fluorination. As the core structure of the molecules remains mostly unchanged, the influence of these functional groups on the OSN performance can be directly determined.

For the first rejection experiments solutions with 0.1 wt.-% of the respective solute (see Table 5.3) were prepared in the different solvents. Later, these results were compared to rejections measured with a mixture of the solutes in the respective solvent. Exemplarily, the comparison for the GMT-oNF-2 used with THF is given in Figure 5.1. The figure shows the average rejection during a three hours run and the standard deviation by the error bars. As there were no statistically significant deviations due to the solute-solute interactions observed, further experiments directly used the mixture approach to reduce the experimental effort.

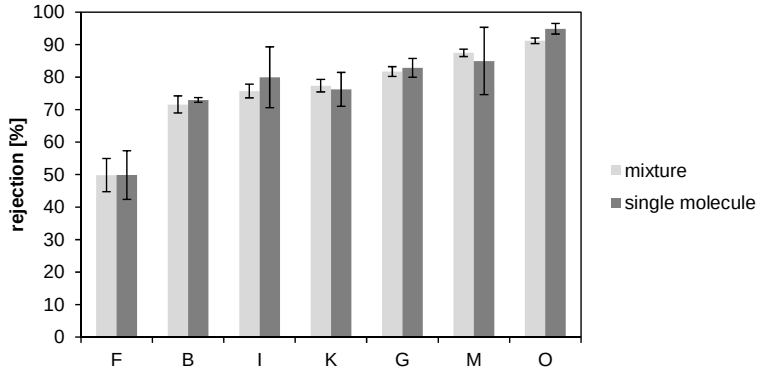

Figure 5.1: Comparison between the rejections measured with a mixture of the solutes and the single molecule (here GMT-oNF-2 in THF)

Two solute mixtures were prepared to ensure that during analysis with gas chromatography (GC) (see chapter 5.1.4.1) their peaks do not overlap in the chromatogram. In the mixture 0.1 wt.-% of each solute is dissolved in the respective solvent. The composition of the two mixtures is given in Table 5.4 together with the retention time of the gas chromatography analysis. Due to the low solubility of the four core molecules in polar solvents (e.g. ethanol), those tests were conducted without the four core molecules (L, M, N, O) in the mixtures.

The molecules are substances being not yet tested completely and having very short product life cycles, thus, only few physical properties of the substances are known. However, in order to develop a predictive model of the separation behavior of these molecules, several properties influencing the transport across the membrane have to be known. Because of the strong

Table 5.3: Specialty chemicals used for membrane characterization

Name	Structure	Molecular weight [g/mol]
A	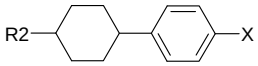	227
B	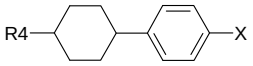	255
C	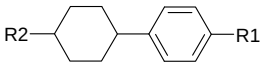	230
D	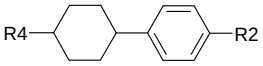	272
E	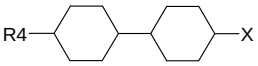	261
F	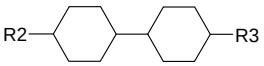	265
G	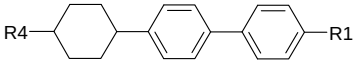	335
H	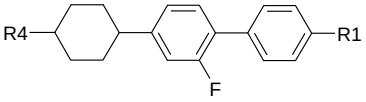	353
I	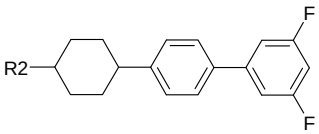	314
J	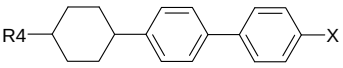	332
K		307
L	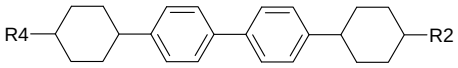	431
M	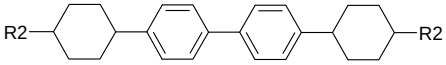	403
N	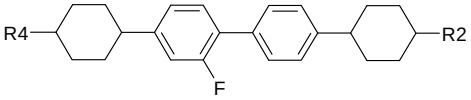	449
O	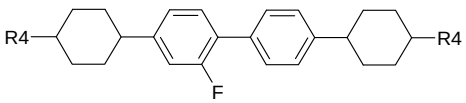	477

Table 5.4: Classification of the molecules of Table 5.3 in the two groups and their GC retention times

Group A		Group B	
Name	Retention time [min]	Name	Retention time [min]
B	21.1	A	16.0
F	16.3	C	12.3
G	34.8	D	19.5
I	25.5	E	21.2
K	30.4	H	34.4
M	45.8	J	37.4
N	48.9	L	49.5
O	52.4	-	-

interactions between membrane, solvent and solute in OSN, properties which describe those characteristics of the substances are required apart from such typical properties as molecular size and volume. These properties should be easily obtainable since costly experiments are not affordable for several hundreds of specialty chemicals the model shall be applicable to. Besides simple modeling of substance data, group contribution methods are particularly suited to determine properties of such molecules, because the values can be calculated only by the knowledge of the molecular structure without any further a priori known data.

One of these parameters which seems to be helpful in understanding the transport performance in OSN is the Hildebrand solubility parameter [68, 110, 136, 137, 157] (c.f. chapter 2.3.2). Diverse group contribution methods have been proposed [139, 158–161] to estimate this parameter. The solubility parameters of substances similar to the specialty chemicals were calculated with different methods in order to compare them with literature data [162]. The results are given in Table 5.5. The method of Stefanis et al. [161] provides the smallest deviation from the experimentally determined values in the literature [162] (c.f. Table 5.5). For this reason, this method was chosen to calculate the solubility parameter of the solutes.

The dimensions of the substances were determined by force field calculations via the software Spartan '08 (Wavefunction Inc., Irvine, USA). The dipole moments were calculated by density functional theory (DFT) with the M06 functional [163] via the software Gaussian 09 (Gaussian Inc., Wallingford, USA). The calculations were commissioned and performed at Merck KGaA.

Table 5.5: Substances of similar chemical structure to validate the calculation methods for the solubility parameter by means of the experimental values [162]

Name	Structure	Solubility parameter $\left[\left(\mathrm{J/cm^3}\right)^{1/2}\right]$			
		Daubert [162]	Van Krevelen [139]	Fedors [158]	Stefanis [161]
Bicyclohexyl	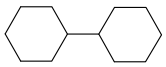	16.99	16.96	17.47	16.82
Biphenyl	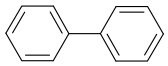	19.38	20.09	21.15	19.05
Cyclohexylbenzene	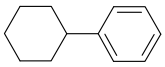	19.00	18.29	19.13	18.06
p-Terphenyl	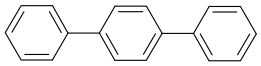	17.39	21.20	22.15	19.55
Diphenylmethane	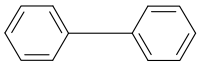	19.42	19.75	20.81	19.18
Diphenylethane	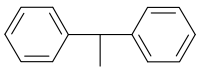	18.87	19.21	20.26	18.15
Diphenylether	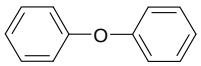	18.77	20.92	21.41	18.23
2-Cyclohexyl-cyclohexanone	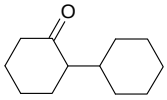	18.77	18.33	19.52	18.79
min. deviation	[%]		0.2	0.6	0.1
max. deviation	[%]		21.9	27.4	12.4

Due to the frequent notion of the molar volume of solutes as determining factor in the separation behavior of OSN [4, 122], the density was determined for five substances (A, F, G, I, L) to calculate the molar volume. The measurements were conducted at Siemens AG Prozess-Sicherheit in Frankfurt am Main, Germany with a Micromeritics MultiVolume Pycnometer 1305. The above mentioned data are summarized in Table A.1 in the appendix.

5.1.2.2 Solvents

All solvents used for the experiments were supplied by Merck KGaA, Darmstadt, Germany. Table A.2 lists the solvent grades used in this work. Ethanol was of absolute, undenatured quality to exclude interactions of the membrane or the solute with the denaturant.

To consider the influence of the solvents on the interactions in the separation behavior of OSN, their properties are of particular interest. Relevant properties of the solvents taken from Smallwood [164] are listed in Table A.3.

5.1.3 Experimental set-up

To investigate the transport behavior of the polymeric membranes, a modified METcell Cross-flow System (Evonik MET Ltd., Wembley, United Kingdom) was used. The feed vessel had a volume of 600 ml. The system was extended by a permeate recirculation in order to keep a largely constant feed concentration realized by a high pressure pump (Smartline Pump 100, Wissenschaftliche Gerätebau Dr. Ing. Herbert Knauer GmbH, Berlin, Germany). The set-up is shown schematically in Figure 5.2.

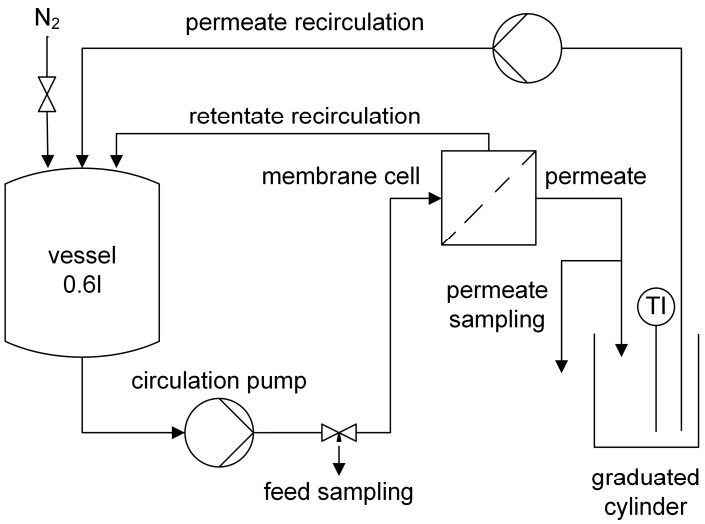

Figure 5.2: Schematical set-up of the experiments with the polymeric membranes

Two kinds of module were used in the lab experiments to house the flat sheet membranes. Predominantly, the METCell module was replaced by a rectangular membrane cell supplied by OSMO Membrane Systems GmbH, Korntal-Münchingen, Germany. The active membrane area in the rectangular cell is 80 cm^2. The feed channel is 47 mil high, 200 mm long and 40 mm wide. The cell was used with a feed spacer, thus, the hydrodynamic conditions resemble those in a spiral wound module. According to the manufacturer's specifications the cross-flow velocity is doubled when using a spacer. Figure 5.3 shows an illustration of the rectangular module.

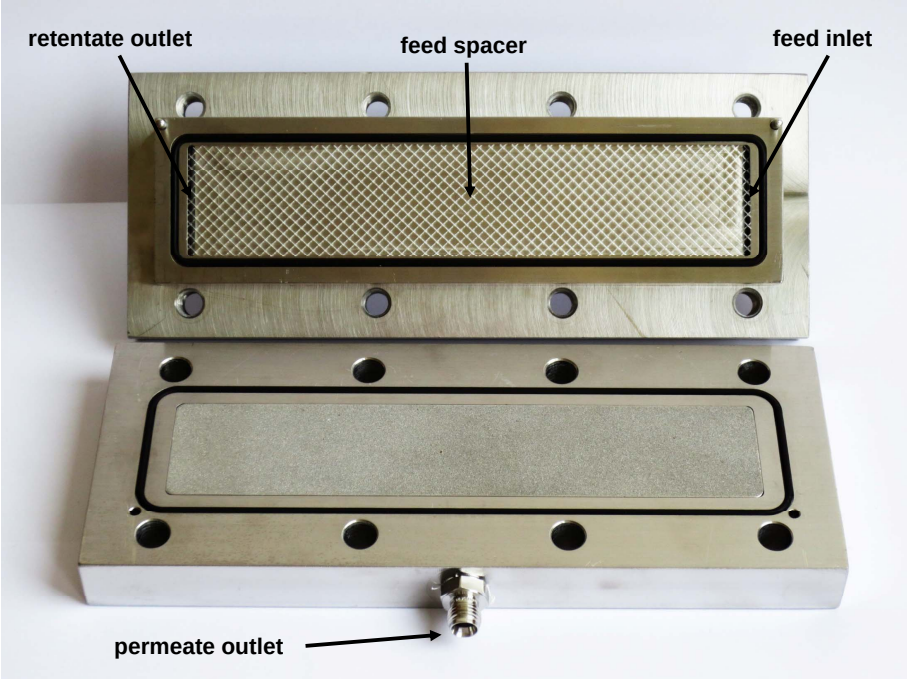

Figure 5.3: Rectangular membrane module

For some screening tests the radial 4" filtration cells (Evonik MET Ltd., Wembley, United Kingdom) were used because the experimental set-up system enables the connection of multiple radial cells in series and hence to test several membranes in one experiment. These cells have an active membrane area of 54 cm^2. Figure 5.4 shows the opened radial module.

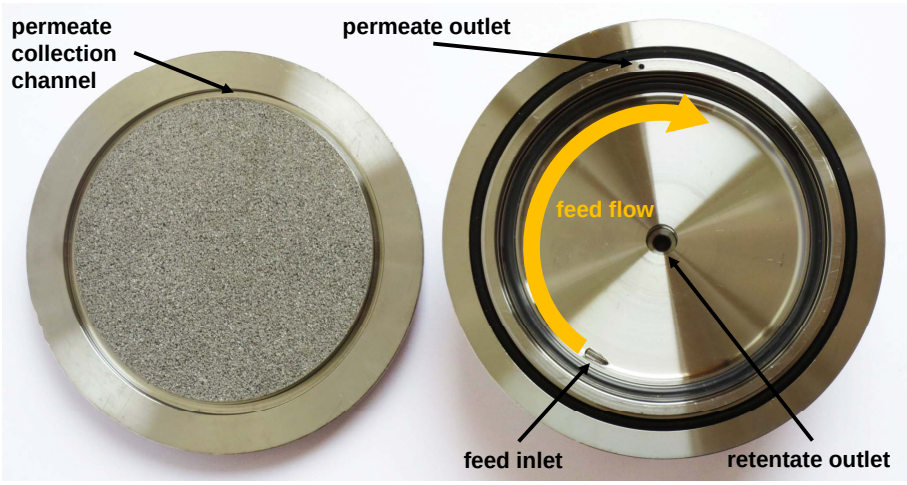

Figure 5.4: METCell 4" radial membrane module

Experiments were carried out at room temperature ($25 \pm 3\,°C$) and a fixed feed flow of 1 l/min resulting in a cross-flow velocity of 0.65 m/s in the rectangular cell when using a feed spacer. The system was pressurized with nitrogen to a constant transmembrane pressure of 30 bar. Permeate mass flow was determined by measuring the increase of permeate mass on an analytical

balance over time. Samples were taken after 30, 60, (90), 120, (150) and 180 min to observe the start-up and compaction behavior and the steady-state. A long-term experiment regarding pure solvent fluxes lasting for 8 h and 7 h for the GMT and the DuraMem® membranes, respectively, was carried out for each membrane to verify that steady-state is reached after 3 h. The results are shown in Figure 5.5a and Figure 5.5b. The diagrams show that the deviations of the fluxes are marginal (< 1 % for GMT-oNF-2 and < 3 % for DuraMem® 200) per hour after 3 h.

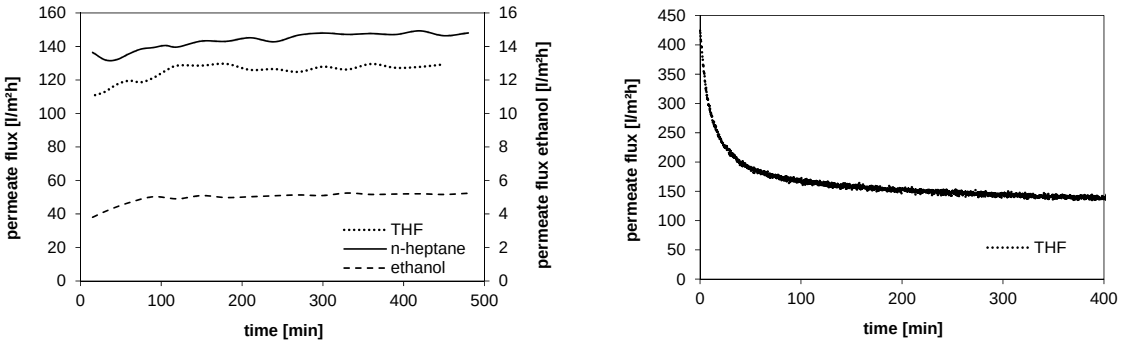

(a) (b)

Figure 5.5: Pure solvent flux measurement with a membrane housed in the rectangular cell measured at 30 bar, room temperature and 1 l/min feed-flow in a long-term experiment.

a) GMT-oNF-2 b) DuraMem® 200

The course of rejections was also investigated and is given in Figure 5.6 for both membranes in the different solvents for one solute.

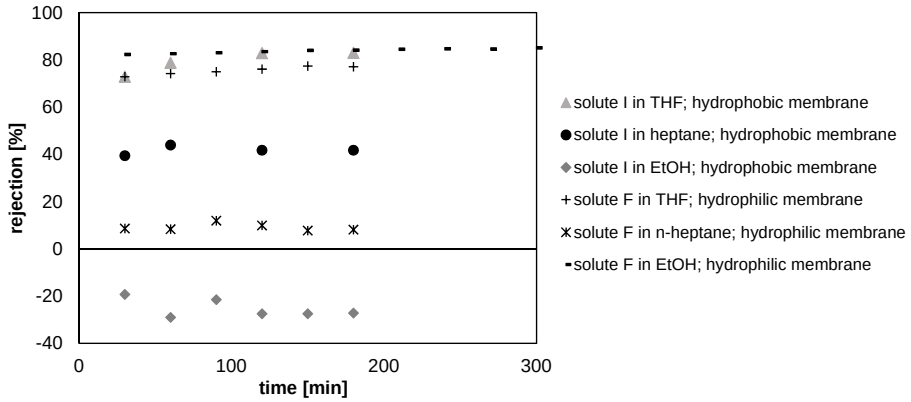

Figure 5.6: Rejection course of one solute in the three solvents THF, n-heptane and ethanol as a function of the time for both membranes

During the first two hours, some fluctuations and compaction effects can be detected. Constant rejections after two hours were verified in a long-term experiment. The slight changes in flux

are sufficient to start and run an OSN process because rejection is the more relevant separation parameter when investigating the potential of OSN in specialty chemicals production (c.f. chaper 4).

5.1.4 Analytics

5.1.4.1 Gas chromatography

Concentrations of the specialty chemicals (Table 5.3) in the permeate and retentate were analyzed by gas chromatography (AutosystemXL, Perkin Elmer, Massachusetts, USA). It was equipped with a flame-ionisation detector. Nitrogen was used as carrier gas with a flow rate of 3.2 ml/min. A polyphenylmethylsiloxane column (CP-Sil 8CB, Agilent, Böblingen, Germany) was used with a length of 50 m, a diameter of 0.32 mm and a film thickness of 0.012 mm. Calibration curves were obtained in advance to the rejection experiments for 10 solutes each in THF, n-heptane and ethanol to enable the computation of mass concentrations in the range of operation. A comparison of the calculated rejections via the calibration curves and the rejections calculated directly via the GC peak areas showed negligible differences. For this reason, the rejections of the other solvent-solute systems were directly calculated with the peak areas.

5.1.4.2 Rotary evaporator

To prove the developed model, rejection measurements with real production solutions were carried out. Here, the concentrations of the samples were determined via the dry residues. The mass of the solution samples was weighed on an analytical balance. The mass of the solutes was then weighed after evaporation of the solvents in a rotary evaporator (BÜCHI Labortechnik GmbH, Essen, Germany).

5.2 Membrane-solvent interactions

First of all, the pure solvent fluxes were measured in order to start with the two dimensional interaction level between different solvents and the membranes. The results of the flux measurements are illustrated in Table 5.6.

Table 5.6: Pure solvent flux measured at 30 bar and 25±3 °C

Solvent	Flux [l/m² h]	
	GMT-oNF-2	DuraMem® 200
THF	91.5	40.9
n-Heptane	121.2	52.9
Ethanol	4.5	31.0
Methanol	2.0	54.2
Ethyl acetate	68.4	38.5
Toluene	86.6	7.8
Isopropyl alcohol	11.5	6.8
Acetone	30.3	97.8
Water	0.0	

Swelling of the membrane is repeatedly mentioned to be a pivotal factor in the performance of polymeric OSN membranes [110, 137, 165]. In literature the equilibrium swelling of a polymer vs. the solubility parameter of different solvents is reported to be a bell-shaped curve with the maximum at the solubility parameter of the polymer [139]. According to several publications [110, 140], the degree of swelling of PDMS depends on the difference of its solubility parameter and that of the solvent. This correlation concerning the swelling could later also be confirmed for a composite PDMS/PAN membrane by Tarleton et al. [153]. If the difference approaches zero, high swelling is obtained and the dense thin film becomes looser. This behavior has also been proven by Tarleton [166] for a polyimide membrane by the expansion measurement of a StarMem® 122. The StarMem® 122 membrane is a integrally skinned membrane made of P84 as well as the DuraMem®. The highest expansion rate was measured in the range of 29 $\left(\mathrm{J/cm^3}\right)^{1/2}$. The difference in solubility parameter of a polymer and solvent should be thus also a suitable indicator for the amount of swelling of a membrane. The measured permeate fluxes of both membranes are illustrated therefore as a function of the solubility of the respective solvent in Figure 5.7 to check the influence of swelling on the performance of the membranes investigated in this work. The dashed line symbolizes the solubility parameter of the selective membrane layer.

Regarding the GMT-oNF-2 membrane, the figure demonstrates that the closer the solubility parameters of the membrane and solvents are the higher the solvent flux is. Keeping in mind that no solvents with a solubility parameter significantly lower than PDMS were used, even the

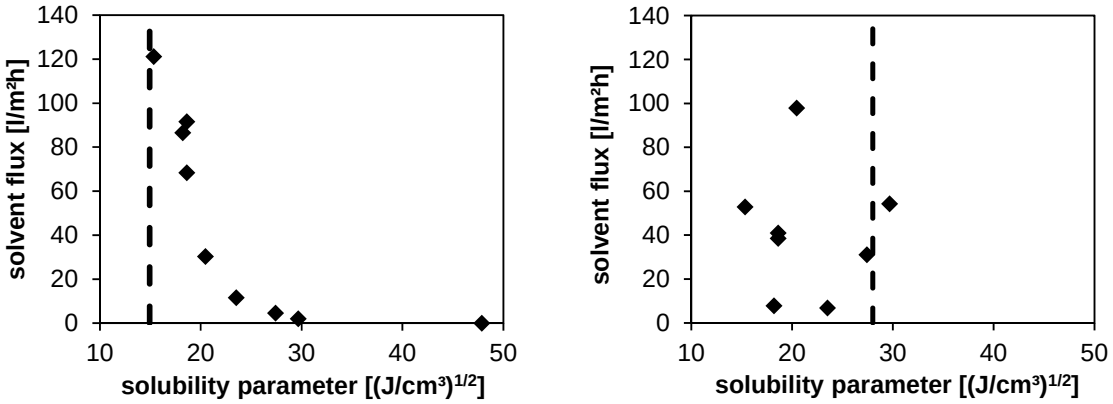

Figure 5.7: Pure solvent flux through the membranes as a function of the solubility parameter of the solvent and the solubility parameter of the membrane polymer (dashed line) a) GMT-oNF-2 b) DuraMem® 200

solvent fluxes follow in a way the bell-shaped curve just like the degree of swelling. The results in Figure 5.7 reveal thus that swelling of the selective layer of the PDMS composite membrane has the highest influence on solvent transport.

However, regarding the pure solvent fluxes through the DuraMem® membrane, there is no clear dependence of the solubility parameter of the solvents or of any other solvent parameter recognizable. This suggests that on the one hand swelling is not as decisive for the transport behavior of the DuraMem®. The comparison of literature data on the degree of swelling determined by gravimetric measurements of pure polymers confirm this presumption: Favre [140] measured mass uptakes of up to 80 % for PDMS (in toluene), whereas Hesse and Sadowski [111] gained a maximum mass uptake of 20 % for P84. On the other hand, the transport seems to be affected by a complex combination of different other factors.

Besides, the solvent fluxes of the GMT-oNF-2 correlate also with solvent properties like polarity index and dielectric constant (c.f. Figure A.1). Since those give a description of the polarity of a solvent it also gives a certain indication about the affinity to another component. These results show that swelling and the affinity between the components are essential for the transport through PDMS membranes and that the interactions between membrane and solvents can be simply described by a consideration of the solubility parameter of the selective layer material of the membrane and the solvents. Moreover, this suggests that even solute transport might be significantly regulated by the affinity between the membrane and the solute or in other words the solubility of the solute in the membrane material.

Several researchers have already found good correlations for solvent permeation especially through PDMS membranes according to the pore-flow model [90, 110], therefore, this should also be surveyed with the results of this work. According to the Hagen-Poiseuille equation (2.13), viscosity is the only variable factor at equal pressures when using the same membrane under the assumption that porosity, tortuosity, membrane thickness and pore radius are membrane specific constants. Considering this, the solvent fluxes versus the inverse of the viscosity should lie on a straight line [110]. To verify if transport through the membranes follows the pore-flow mechanism, the pure solvent fluxes (Table 5.6) are plotted against their inverse viscosity in Figure 5.8. Clearly, there is no proportional correlation between the inverse viscosity of the different solvents and the solvent flux. However, as became apparent above, the "pore radius" cannot be assumed to be constant in different solvents at least for the GMT-oNF-2 membrane, since swelling of the selective layer is the determining factor for the solvent transport.

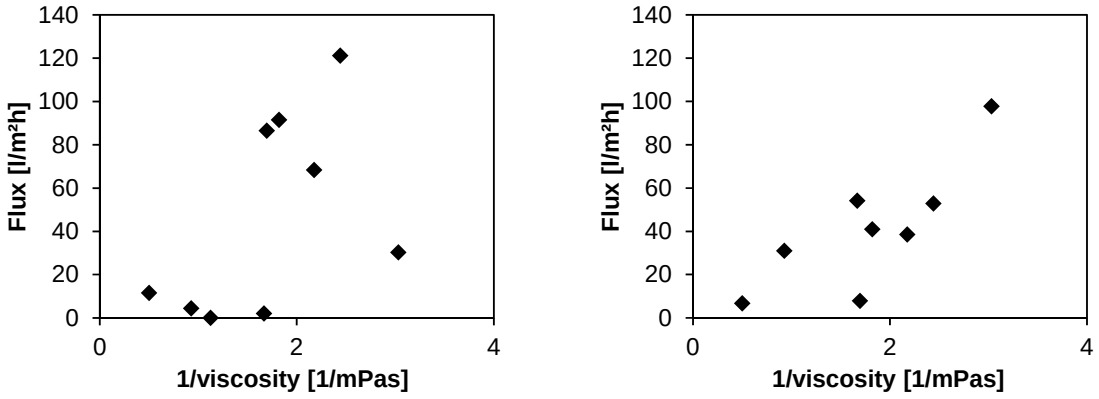

Figure 5.8: Pure solvent flux through the membranes as a function of the inverse viscosity of the solvent a) GMT-oNF-2 b) DuraMem® 200

To exclude the effect due to different amounts of swelling, the viscosity was varied by measuring pure solvent fluxes at different temperatures between 15 and 55 °C. The results of the GMT-oNF-2 membrane, given in Figure 5.9a, show a linear dependency for the fluxes of n-heptane and THF. This points to a convectively dominated transport in the measured range. In contrast, the fluxes of ethanol through the PDMS membrane show an exponential behavior on the inverse viscosity and illustrate a different transport mechanism. The solubility parameter of ethanol differs substantially from that of the membrane and hence there is almost no interaction between

the GMT-oNF-2 membrane and the solvent and the separation layer swells only marginally.

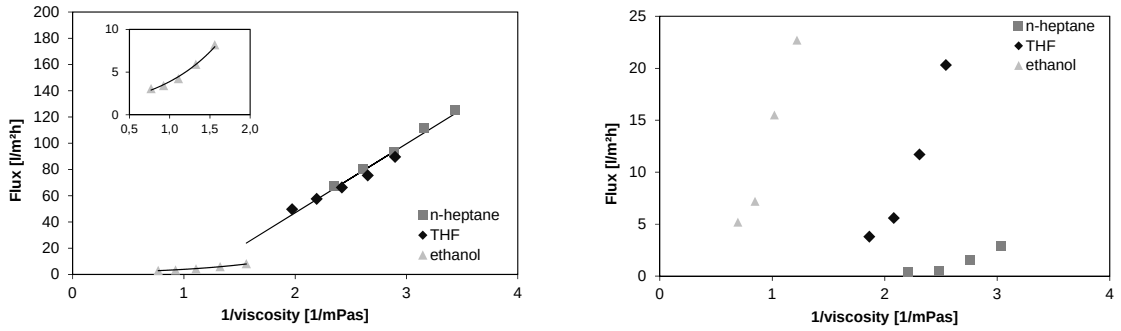

(a) (b)

Figure 5.9: Pure solvent fluxes of ethanol, n-heptane and THF as a function of their inverse viscosity a) GMT-oNF-2 b) DuraMem® 200

Plotting the solvent fluxes through the DuraMem® against the inverse viscosity (see Figure 5.9b) does not result in a straight line. The curves of each solvent rather show an exponential behavior. The diffusion coefficient in liquids as well as in solids shows a non-linear dependency on the temperature, therefore, this exponential course could give a hint on a solution-diffusion driven transport mechanism through the PI membrane (similar to what was shown already in literature [65, 69, 114]) as well as for ethanol through the PDMS membrane. Concluding, solvent flux is affected by parameters influencing solution and diffusion, which results in a complex interplay of the different phenomena.

From the long-term flux measurements (see Figure 5.5) the first differences between the two membrane materials or the membrane structure became apparent. Regarding the GMT-oNF-2, there is a slight increase of the permeate flux detectable in the first two hours whereas the permeate flux through the DuraMem® 200 decreases by more than 50 % in the first hour followed by a slight decrease of about 3 % per hour. This observation suggests that the thin dense PDMS layer of the composite membrane still swells marginally when starting the filtration process when the solvent is forced through the membrane material. Contrarily, the decrease of the permeate flux through the integrally skinned PI membrane might also be an effect of swelling. Solvents might swell the membrane causing a density increase of the more porous structure of the integrally skinned membrane. The solvent flux is thus a combination of the density increase of the membrane material by swelling and the affinity between solvent and the membrane when diffusing through the material. This would explain the somehow ambiguous dependencies of the permeate flux from the solvent properties. The fact that the PI membranes are not in contact

with the respective solvent prior to the experiments might be the reason why the change of flux is more distinctive compared to the PDMS membrane. Here, the swelling process just starts with the filtration experiment. Furthermore, the integrally skinned PI membrane might be more sensitive to a compaction of the selective layer due to the more porous membrane structure compared to the composite membrane which additionally reduces the permeate flux over filtration time. This would imply, that even for the rejection of the DuraMem® membrane, the solubility parameter of the solvent is of importance because swelling would be important for the rejection of solutes.

Basically, it has to be mentioned that the performance of the DuraMem® 200 changed significantly during this work. After the acquisition of MET by Evonik the membranes were reworked and optimized. This became particularly apparent when considering the n-heptane fluxes. At the beginning of this work, these fluxes were the highest despite the low affinity to the membrane material. A possible explanation could be found in the integrally skinned structure of the membrane. A certain degree of swelling might be necessary to densify the top layer of the membrane. Solvents like n-heptane, which do not swell the material, can thus pass through little pores where phase inversion e.g. stopped too early. After the optimization of the membrane, maybe by an increase of the top layer thickness (indicated by a general trend to lower fluxes regardless of the solvent), the membrane might have become denser and swelling lost importance. Moreover, to conduct the measurements in n-heptane, the membranes had to be flushed with acetone. If acetone swells the membrane, the n-heptane flux could additionally profit by this preparation.

5.3 Membrane-solvent-solute interactions

5.3.1 Experimental database

Firstly, the rejection of the two membranes GMT-oNF-2 and DuraMem® 200 for the chemicals listed in Table 5.3 were measured. The experiments were conducted with solutions containing only one solute. The obtained values are given in Table A.4. The rejections as a function of the molecular weight of the solutes are illustrated in Figure 5.10. As expected, the results vary widely between the different solvents and the molecular weight range.

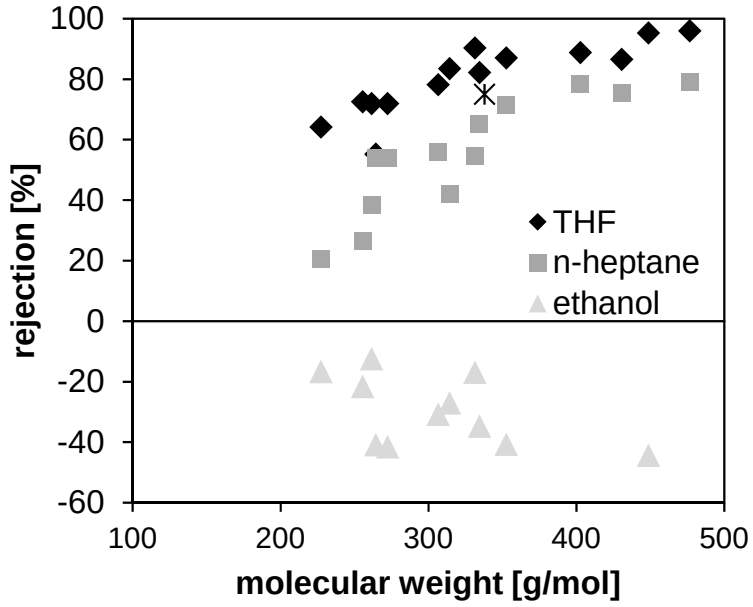

(a)

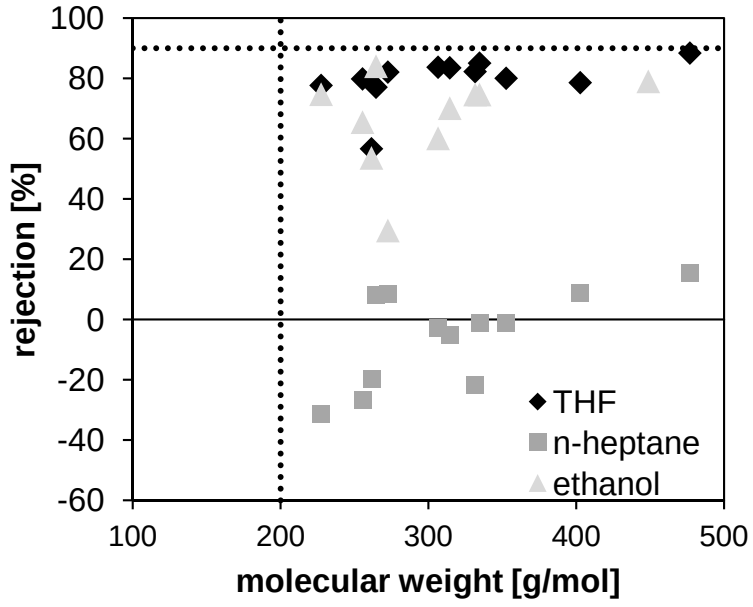

(b)

Figure 5.10: Rejections of specialty chemicals in ethanol, THF and n-heptane vs. their molecular weight. Values taken after 180 min at 30 bar transmembrane pressure.
a) GMT-oNF-2 membrane, star symbols the separation characterization given by the manufacturer determined by rejection measurements of alkanes in toluene.
b) DuraMem 200 membrane, dotted line symbols the MWCO given by the manufacturer determined by rejection measurements of styrene oligomers in acetone.

For both membranes, the highest rejections were measured in THF. With the GMT-oNF-2 the rejection generally increases with the molecular weight of the solutes and is between 55 and 95 %. The specification for toluene given by the membrane manufacturer is exceeded in THF. Molecules larger than 330 g/mol are retained by more than 90 %. The increase of the rejection with the molecular weight is significantly lower for the DuraMem® 200. Here, the rejections are between 77 and 88 % except for solute E which has a considerably lower rejection of 57 %. The specification of the manufacturer (MWCO: 200 g/mol measured with polystyrenes in acetone) could not be reached with any of the solutes.

The rejection in n-heptane differs radically between the two membrane materials. With the GMT-oNF-2 membrane rejection values are within a range of 20 and 80 % and are thus below the rejection level in toluene as given by the manufacturer. In particular at low molecular weights, the rejections in n-heptane were significantly lower than in THF. These results can be explained by the high swelling of the PDMS layer in n-heptane because they show similar solubility parameters as reported e.g. by Van Krevelen [139]. If the structure of the active layer becomes looser due to swelling, solute permeation is eased. The DuraMem® shows negative rejections for the majority of the solutes (-30 - -1 %), but rejection increases with the molecular weight resulting in low positive rejections (9 and 16 %) for the largest molecules. Negative rejection means that the concentration of the solute in the permeate is higher than the concentration in the retentate. Concentration polarization can be excluded as a root cause due to the very low concentrations applied in the experiments.

In Ethanol the behavior is the opposite. The rejection of every molecule measured with the GMT-oNF-2 is negative and ranges between -10 and -45 %, but there is no clear dependence of the rejection on the molecular weight. The rejection of the DuraMem® is in a range between 30 and 85 % and thereby lower than in THF. This is again explainable by the high affinity of the membrane to the solvent and thus swelling of the membrane material. However, the membrane seems to swell not to the same extent as the PDMS membrane because the difference to the rejections in THF is marginal.

The dependence of the separation performance from solvent demonstrates again that the MWCO is not a suitable measure to select an adequate membrane. In order to check the reproducibility, the experiments with substance G in ethanol was repeated three times. The value given in Table A.4 is the average of the measurements. The standard deviation in this case is 3.6 % for the hydrophobic membrane and 1.9 % for the hydrophilic membrane, respectively, indicating statistically significant results of the measurements.

Permeate fluxes of the above rejection measurements (see Table A.5) varied widely within one solvent, as for each experiment a new membrane sheet was used. It can be assumed that small irregularities in the layers have a significant impact on the membrane flux. The observation of the partial fluxes of the solutes given in Table 5.7 gives more reliable results. The partial fluxes were calculated by equation 5.1 and are only given for the solutes for which a GC calibration curve were determined and thus the solute concentration in the permeate exists.

$$J_s = \frac{m_P^F \cdot w_s}{M} \tag{5.1}$$

Table 5.7: Partial fluxes of the solutes in THF, n-heptane and ethanol

	GMT-oNF-2			DuraMem® 200		
Name	THF [mol/min]	n-heptane [mol/min]	ethanol [mol/min]	THF [mol/min]	n-heptane [mol/min]	ethanol [mol/min]
A	$1.91\ 10^{-3}$	$3.78\ 10^{-3}$	$0.18\ 10^{-3}$	$0.85\ 10^{-3}$	$0.89\ 10^{-3}$	$0.32\ 10^{-3}$
D	$1.52\ 10^{-3}$	$2.08\ 10^{-3}$		$0.55\ 10^{-3}$	$3.05\ 10^{-3}$	
E	$1.81\ 10^{-3}$	$1.73\ 10^{-3}$	$0.20\ 10^{-3}$	$1.65\ 10^{-3}$	$1.74\ 10^{-3}$	$0.97\ 10^{-3}$
F	$1.73\ 10^{-3}$	$2.19\ 10^{-3}$	$0.27\ 10^{-3}$	$0.78\ 10^{-3}$	$3.28\ 10^{-3}$	$0.25\ 10^{-3}$
G	$0.80\ 10^{-3}$	$1.11\ 10^{-3}$	$0.18\ 10^{-3}$	$0.38\ 10^{-3}$	$1.33\ 10^{-3}$	$0.56\ 10^{-3}$
I	$1.00\ 10^{-3}$	$1.35\ 10^{-3}$	$0.13\ 10^{-3}$	$0.30\ 10^{-3}$	$3.93\ 10^{-3}$	$0.39\ 10^{-3}$
J	$0.39\ 10^{-3}$	$1.62\ 10^{-3}$	$0.16\ 10^{-3}$	$0.45\ 10^{-3}$	$3.40\ 10^{-3}$	$0.41\ 10^{-3}$
M	$0.57\ 10^{-3}$	$0.53\ 10^{-3}$		$0.48\ 10^{-3}$	$0.93\ 10^{-3}$	
N			$0.16\ 10^{-3}$			$0.29\ 10^{-3}$
O	$0.14\ 10^{-3}$	$0.49\ 10^{-3}$		$0.14\ 10^{-3}$	$1.17\ 10^{-3}$	

Because of the high degree of swelling of the GMT-oNF-2 membrane in heptane, those fluxes are the highest decreasing with an increase of the molecular weight. The same behaviour occurs for THF but with lower fluxes compared to heptane. This is in accordance with the above mentioned theory of the solubility parameters (see chapter 5.2). The difference between the solubility parameter of the membrane and the solvent is higher for THF compared to n-heptane, therefore swelling in THF is lower and the partial fluxes are lower as well. The fluxes of the solutes in ethanol are all in the same range and show no significant dependence on the molecular size of the solute. The fluxes of the small molecules in ethanol are significantly lower than in THF and n-heptane. This suggests that due to the minimal swelling in ethanol, the transport mainly occurs by diffusion. It can be assumed that the dominating transport mechanism changes

when the size of the solute increases because the partial fluxes of the larger solutes J, M and especially O in THF become similar to the partial fluxes in ethanol. This assumption would also lead to the fact that a 100 % rejection will not be achievable in the nanofiltration range.

In contrast to the GMT-oNF-2 membrane, the fluxes through the DuraMem® membrane are the highest at negative rejections. This is in accordance with the theory, that the DuraMem® stays more open in solvents which do not swell the membrane. This allows the solutes and solvent to easily pass the membrane. The effect might be additionally intensified by the required flushing of the membrane with acetone or THF prior to the experiments. The partial fluxes of the solutes in THF and ethanol are in a similar range and comparable to the values of the GMT-oNF-2 membrane, where diffusion is assumed. After the acquisition of MET by Evonik, the DuraMem® type was reworked and quality standards were defined. During that initiative, the membrane seems to have been changed or modified over the time while this work was conducted (c.f. Figure A.2). Meanwhile, e.g. heptane fluxes are the lowest while rejection in n-heptane still stays negative. As already mentioned in the previous chapter, a possible explanation is that the structure of the integrally skinned membrane was optimized so the separation performance is less influenced by the swelling of the material. However, the general rejection behavior did not change with the differences in fluxes and thus, these changes do not affect the general goal of this work. Secondly as shown in chapter 4, for specialty chemicals rejection is the most important process property whereas flux changes are not as economically important.

To elucidate the partly extreme deviations between the rejections of the solutes, the next section addresses the membrane-solvent-solute interactions.

5.3.2 Influence of solute on the separation behavior

To investigate the influence of the solutes on the separation behavior, several solute properties were investigated and taken into consideration. As summarized in chapter 2.3.2.2, some properties related to transport behavior have already been identified in previous publications. These are e.g. the mean size [135], the dipole moment [70] or the solubility parameter [68, 137, 144] of the solute. However, none of the studies span the complete OSN range concerning different membrane materials, solvents over the whole polarity range and solutes of different sizes and properties. Nevertheless, these proposed solute properties were considered to prove their universal validity.

According to Zheng et al. [135], the molecular size of the molecule was represented best by the mean size which is defined as the smallest molecular volume. Because of the inflexible, linear structure of the molecules, here, the width was used to represent the minimum size of the molecules depending on the orientation towards the membrane. The rejection in dependency of the maximum width determined by force field calculations (c.f. Table A.1) is shown in Figure 5.11. Over the complete range of solutes, no relationship between the rejection and the size of the solutes can be detected, thus, other measures have to be taken into consideration.

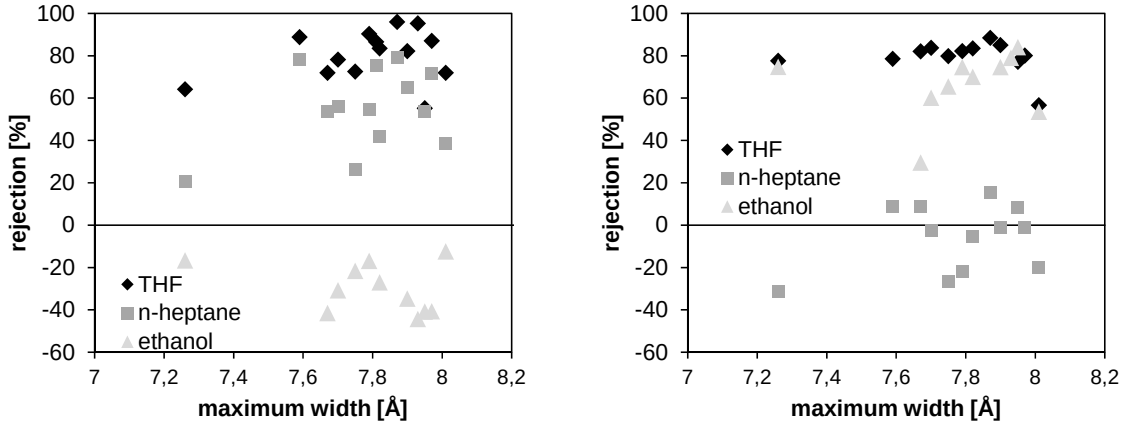

Figure 5.11: Rejection in dependence of the maximum width of the solutes determined by force field calculations a) GMT-oNF-2 b) DuraMem® 200

The dipole moment, which showed good correlation in the study of e.g. Darvishmanesh et al. [70], is considered in Figure 5.12. No dependence between rejection and dipole moment could be identified with the solutes-solvents-membranes system investigated in this work. Even when taking the dipole moments of the solvents (THF: 1.75; n-heptane: 0; ethanol: 1.7) into account, the picture does not become clearer.

The solubility parameter was already helpful to explain the pure solvent fluxes, therefore, the solubility parameters of the solutes are added to the considerations. The solubility parameter has furthermore the advantage that it allows for the incorporation of the other involved parties, namely membrane and solute. The difference in the solubility parameters of two components provides an insight about the affinity between them. Due to the very non polar nature of the solutes, the Hildebrand solubility parameter was chosen and calculated by the group contribution method of Stefanis [161]. The computed values are listed in Table A.1. The rejections vs. the solubility parameters including the values of PDMS and PI, respectively and the respective

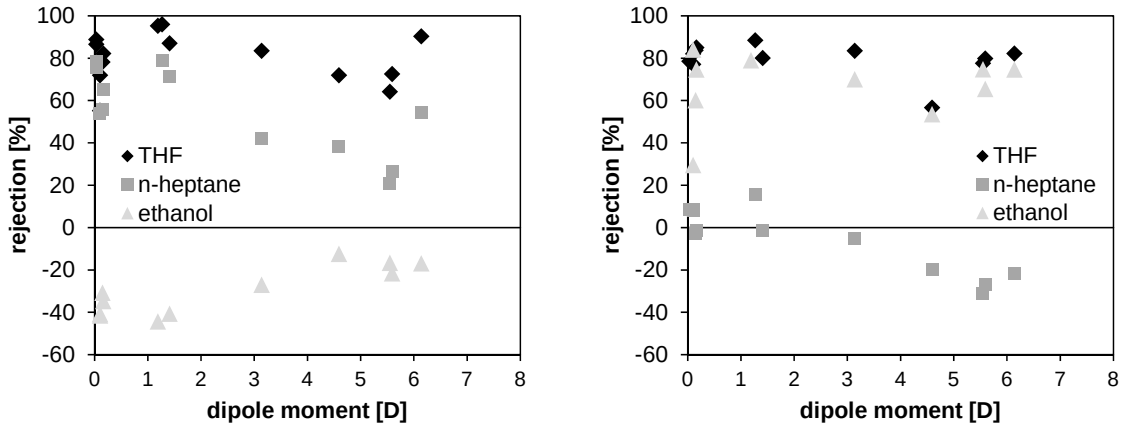

(a) (b)

Figure 5.12: Rejection in dependence of the dipole moment of the solutes calculated by density functional theory (DFT) a) GMT-oNF-2 b) DuraMem® 200

solvent are shown in the following Figures (Figure 5.13, 5.14 and 5.15). In order to exclude significant size effects of the solute on the rejection in the interpretation of the results, the presentation of the rejections of the solutes is divided in three groups by their amount of cyclic carbon rings named as 2-, 3- or 4-cores.

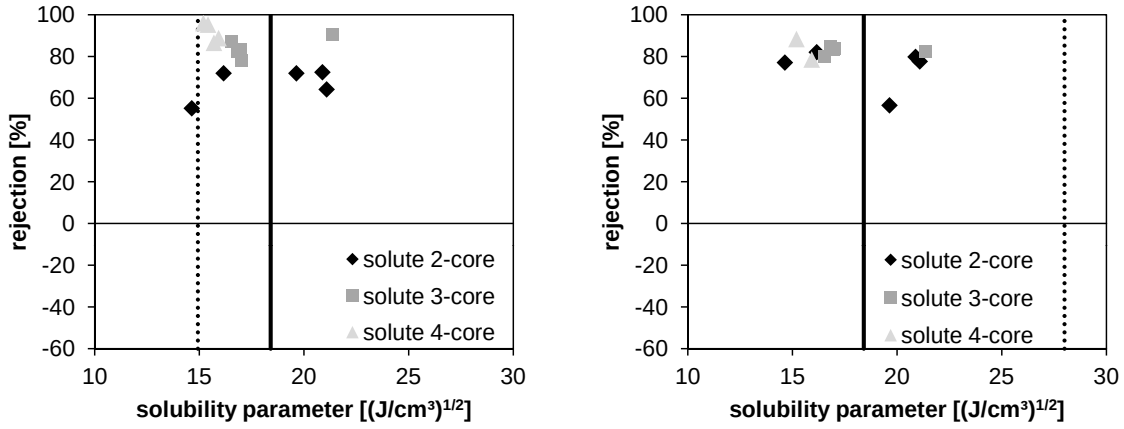

(a) (b)

Figure 5.13: Rejection in dependence of the solubility parameters of the solutes calculated by the method of Stefanis [161] and the solubility parameters of the membrane (dashed line) and THF (solid line) a) GMT-oNF-2 b) DuraMem® 200

First of all, Figure 5.13 illustrates the rejection in THF, where both membranes have a good performance. Comparing the solubility parameters of membrane material, solute and THF, the values of the solubility parameters of the solutes are close to THF ($|\delta_{\text{solute}} - \delta_{\text{solvent}}|_{\max} = \Delta\delta_{\max} = 4\left(\text{J/cm}^3\right)^{1/2}$). This indicates that the affinity of the solutes to THF is very high and

the interactions of both with the membrane are moderate. The driving force of dissolution and permeation of the solutes in and through the membrane is marginal, therefore, rejections in THF are highest.

Rejections of both membranes in n-heptane are shown in Figure 5.14. The solubility parameters of n-heptane and the membrane material PDMS are very similar, indicating high swelling of the membrane and similar affinities of the solutes to the membrane and to n-heptane and hence rejection in n-heptane is not as high as in THF. Furthermore, a decline in rejection can be observed with an increase of the solubility parameter, but a dependence of the molecular weight (symbolized by the number of cores) can still be observed.

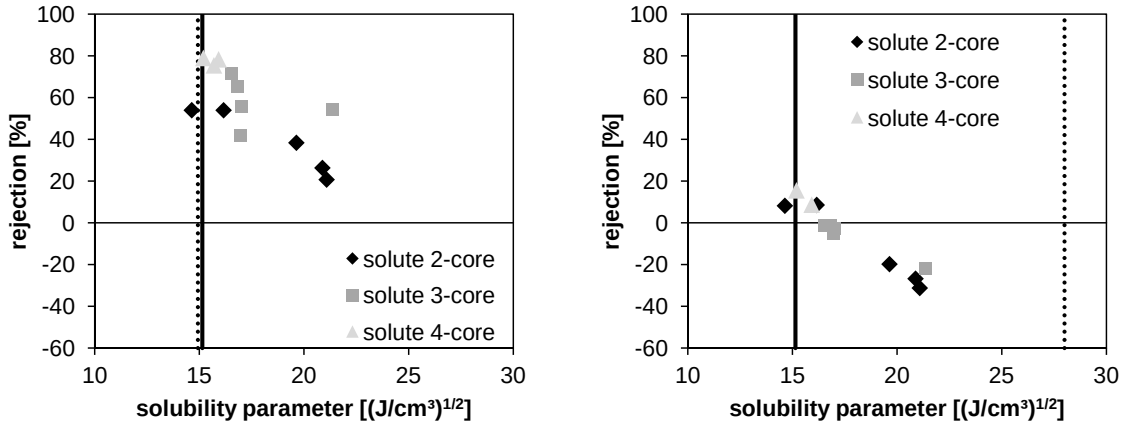

Figure 5.14: Rejection in dependence of the solubility parameters of the solutes calculated by the method of Stefanis [161] and the solubility parameters of the membrane (dashed line) and n-heptane (solid line) a) GMT-oNF-2 b) DuraMem® 200

In contrast, the rejection of the PI membrane is linearly dependant on the solubility parameter of the solutes without any influence of their molecular weights. The closer the solubility parameter of the solute to the membrane, the lower is the rejection. The difference between the solubility parameter of the membrane and n-heptane is very large ($\delta_{\text{solvent}} - \delta_{\text{membrane}} = \Delta\delta_{\text{S-M}} = 13\,\left(\text{J/cm}^3\right)^{1/2}$) indicating a low affinity of the solvent to the membrane. The solubility of the solutes in the membrane material is preferred to the solvent and therefore the flux of the solute through the membrane is higher in relation to that of the solvent causing negative rejections.

Rejections of the PDMS and the PI membrane in ethanol are illustrated in Figure 5.15. Here, the same rejection behavior is observed for the PDMS membrane as for the PI membrane in

n-heptane. The difference between the solubility parameter of PDMS and ethanol is very large ($\delta_{\text{solvent}} - \delta_{\text{membrane}} = \Delta\delta_{\text{S-M}} = 11.2\,\left(\text{J/cm}^3\right)^{1/2}$). Consequently, the affinity between solvent and the membrane and thus swelling of the selective layer is low. The solubility parameters of the solutes indicate a higher affinity to the membrane, therefore, the dissolution of the solutes in the membrane material is preferred compared to the solvent and rejection becomes negative. Rejection linearly increases when the solubility parameter of the solute approaches that of the solvent as well.

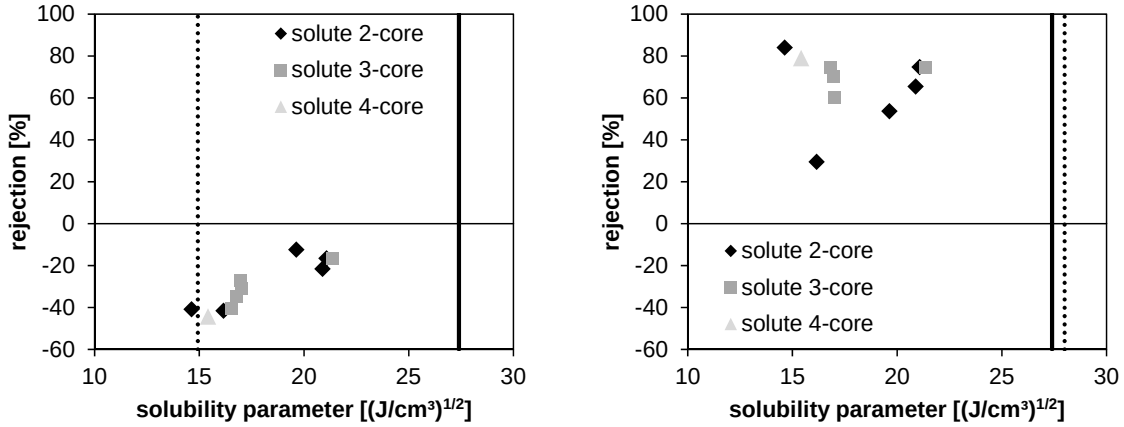

Figure 5.15: Rejection in dependence of the solubility parameters of the solutes calculated by the method of Stefanis [161] and the solubility parameters of the membrane (dashed line) and ethanol (solid line) a) GMT-oNF-2 b) DuraMem® 200

Rejections of the DuraMem® 200 in ethanol are lower than in THF, as indicated by the small difference between the solubility parameter of the membrane material and that of ethanol. The membrane swells thus to a higher extent compared to THF and the solutes can pass easier through the membrane. The same behavior was observed with the GMT-oNF-2 in n-heptane.

Although it is not possible to predict rejections exactly with this comparative examination, it easily allows an estimatation of the expected range of rejection. This is already of large importance because it facilitates membrane selection for a given solvent/solute mixture during process development. Of course, to conclude on general rules, the findings have to be extended to other membrane types.

5.3.3 Influence of functional groups on the separation behavior

The fact that solutes of similar molecular weights have significantly differing rejections in some cases clearly shows that even besides size exclusion other effects have to be considered. The comparison of the rejection of substance e.g. G and J or E and F (Δ molecular weight = 3 g/mol) indicates that functional groups can have a distinct influence on transport behavior. By incorporating the substances A-O (except B and C) into a complete Design of Experiments (DoE) [167, 168], the most important functional groups to be considered in the estimation of rejection could be defined with a manageable number of experiments. The DoE software Modde (Umetrics AB, Umeå, Sweden) was applied for the analysis. In Table 5.8 the varied functional groups that were used as factors in the DoE are listed. Figure 5.16 explains the notation of the functional groups.

Table 5.8: Functional groups used as factors in the DoE

Factor	Type	Value
number of cores	quantitative	2,3,4
endgroup	qualitative	polar/nonpolar
left side chain	quantitative	R2/R4
right side chain	quantitative	-/R1/R2/R3/R4
fluorination	qualitative	yes/no
right end core	qualitative	benzene/cyclohexane

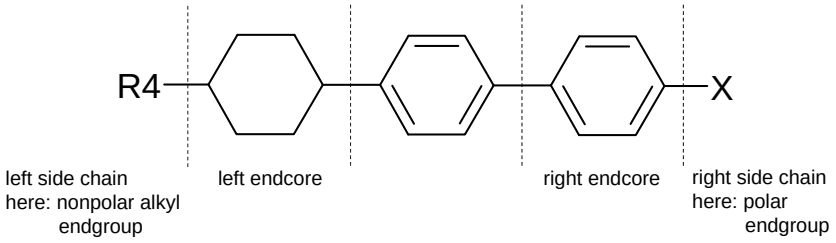

Figure 5.16: Example for the notation of the functional groups

Because of the restricted number of tests that can be performed due to the fixed structure of the molecules and the categorical factors (endgroup, fluorination and right end core), a D-optimal design of experiments was designed. A manual candidate set was generated which takes the limited combination of factor settings into account. Further background information about the general procedure of Design of Experiments can be found in [167, 168]. The fitted model is a

linear regression model without interactions. In its basic form it is described by the following equation (here for three factors A, B and C):

$$y = b_0 + b_A x_A + b_B x_B + b_C x_C \tag{5.2}$$

where y is the response value (here: rejection), b_0 a constant term, b_{A-C} the estimated coefficients of the different factors and x_{A-C} represent the settings of the factors in the experimental domain. The necessary extensions to handle higher-order terms and categorical factors in a regression model are described in [168]. The interpretation of the data was done individually for each solvent because the solvent itself would otherwise give the highest impact factor on the rejection and would suppress the other factors. The analysis of the DoE allows for a qualitative comparison of the factors influencing the measured result. Figures 5.17 and 5.18 illustrate the functional groups having a significant impact on the response value for the three solvents. The bars show the coefficients of the centered and scaled settings of the factors:

$$x_{centered\&scaled} = \frac{2(x - x_{center})}{(x_{max} - x_{min})} \tag{5.3}$$

By centering and scaling the influence of different factors with different scales can be compared [167]. Those are presented in the diagrams for the most significant functional groups. The error bars represent the confidence intervals of the respective coefficient with a confidence level of 95%.

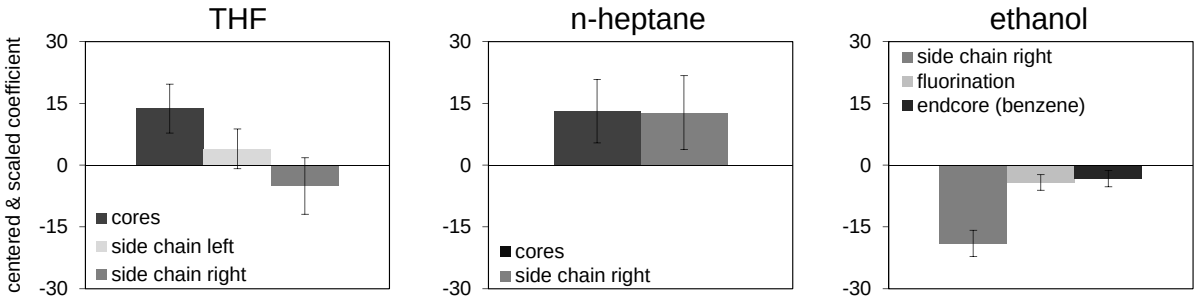

Figure 5.17: Functional groups influencing the rejection of the GMT-oNF-2 in different solvents

Concerning the GMT-oNF-2 membrane (see Figure 5.17), the molecular weight (represented by the number of cores) is a crucial factor in the analysis of the DoE as well, as already shown in Figure 5.10, especially for the solvents THF and n-heptane where size exclusion is the proposed separation mechanism. An elongation of the side chains causes an increase of the molecular weight and the size as well and therefore a positive impact on the rejection in n-heptane. Figure

5.10 already illustrated that the molecular weight has no influence on the rejection in ethanol. This result is also reflected by the results of the DoE where the number of cores does not show any impact on the rejection.

However, the effect of the right side chain in ethanol is very distinctive and significant. Here, an elongation of the right side chain has a negative effect on the rejection. In this case the reason is not the change in the molecular size but in the polarity of the solute. On the one hand polarity decreases slightly with an elongation of the side chain. On the other hand the molecule features a polar endgroup, if the length of the side chain on the right side is zero. With decreasing polarity of the solute the affinity to ethanol gets lower. Additionally, the affinity of the solute to the membrane rises and causes lower rejections. Fluorination and benzene as an endcore only show a small negative impact on rejection in ethanol.

As mentioned, the right side chain has a considerable influence on the polarity of the solute besides the impact on the molecular size. The mixture of effects in the factor right side chain probably causes the negative, less significant influence of this functional group in THF.

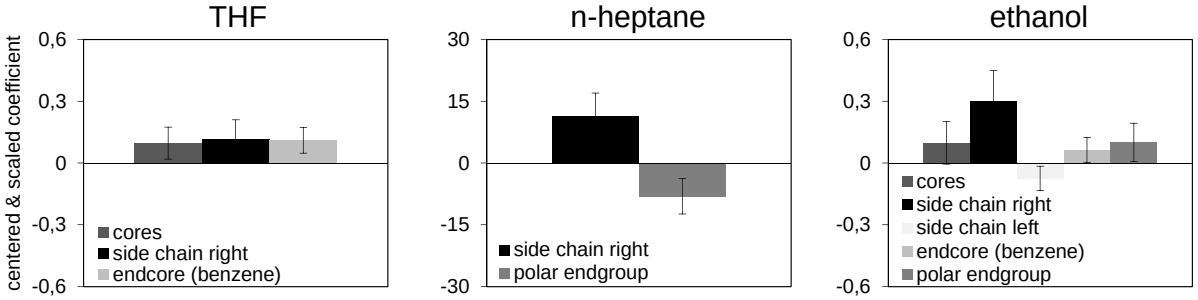

Figure 5.18: Functional groups influencing the rejection of the DuraMem® 200 in different solvents

The influence of the functional groups on the separation of the DuraMem® 200 membrane is illustrated in Figure 5.18. It has to be mentioned that the influence of the investigated factors on rejection in THF and ethanol is significantly lower (up to a factor of 50) compared to n-heptane as well as compared to the GMT-oNF-2 membrane. The cores show a positive effect on the rejection in THF and ethanol as well as for the PDMS membranes in THF and heptane. The very low dependence of rejection based on the molecular weight (represented here by the number of cores) compared to the GMT-oNF-2 has already been depicted in Figure 5.10. An elongation of the right side chain causes better rejections in each solvent as the polarity of the solute decreases and thus the affinity of the solute to the membrane. Due to the same reason, the polar endgroup has a negative effect on the rejection in heptane. According to the outcome of

the DoE, a benzene endcore influences the rejection in THF and ethanol positively. This effect might appear due to a distribution of the polarity of the polar endgroup by delocalized electrons of the aromatic ring. Partly, the functional groups factors are closely linked with each other like the right side chain with the polar endgroup (no right side chain = polar endgroup). For this reason, effects due to changes in molecular weight might be mixed with effects based on the polarity of the solute, therefore, some inaccuracies due to combined positive and negative effects on the rejection may occur. This might be the reason e.g. for the negative, less significant influence of the right side chain on the rejection in THF of the GMT-oNF-2. To assure the significant effects of the polarity of the solutes on the rejection behavior suggested by the DoE and to eliminate uncertainties due to averaging effects, the results were fortified by a direct comparison of two molecules which only differ in one functional group.

In the following section, the comparisons for the left side chain, the polarity of the endgroup, the endcore and the fluorination (for nomenclature of the substances see Table 5.3) are discussed. The figures show the average values of the rejection after 3 h and their standard deviation for the three solvents THF, n-heptane and ethanol.

Using the example of substance G and K, Figure 5.19 demonstrates the influence of different left side chain lengths (alkyl chains) on the rejection. The figure shows the rejections in the three solvents for the GMT-oNF-2 (Figure 5.19 left) and for the DuraMem® 200 (Figure 5.19 right). In all cases, except for the GMT-oNF-2 in ethanol, a longer left side chain (substance G) has a slightly positive influence on the rejection due to the higher molecular weight, as it has already become apparent from the results of the DoE. In contrast to the results of the DoE, the longer left side chain shows a clear improvement of the rejection of the GMT-oNF-2 in n-heptane. This is in accordance with the hypothesis that a convective transport mechanism and therefore size exclusion is dominant in THF and n-heptane. The higher polarity of a short side chain leads to a better rejection of the GMT-oNF-2 in ethanol and a worse rejection of the DuraMem® 200 in heptane due to lower affinity to the PDMS membrane and the higher affinity in the case of the PI membrane, respectively.

The comparison of the rejections of the two solutes (J and G) with a polar and a nonpolar endgroup, respectively, is contrasted in Figure 5.20 for both membranes. The results demonstrate that the polarity of a functional group has a significant impact on the membrane performance, although the influence of the polarity on the rejection of the DuraMem® is significantly lower

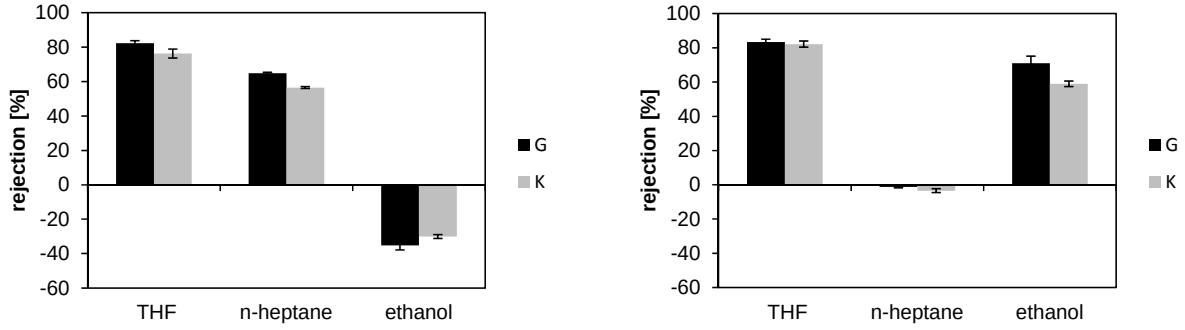

(a) (b)

Figure 5.19: Rejection of two molecules which differ only in their left side chain length ($R_G > R_K$) a) GMT-oNF-2 b) DuraMem® 200

than on the rejection of the GMT-oNF-2. For both membranes a general trend can be found that rejections are higher for solutes with a lower affinity to the membrane. This means that rejections of solutes with polar endgroups (here: J) are lower for the DuraMem® and higher for the GMT-oNF-2 compared to solutes with nonpolar endgroups (here: G). This is even true for the rejections in solvents where the membranes show negative rejections. The only exception occurs with the GMT-oNF-2 in n-heptane. Following the above interpretation the rejection should be better for solute J which has a lower affinity to the membrane. This behavior is also known and verified by molecules investigated within the scope of chapter 7. Contrarily, the rejection of solute J in n-heptane is significantly lower. In terms of the polar group analyzed within this chapter, the lower rejection of the more polar solute might be an effect of an interaction of the polar group with the very similar functional groups of the support layer of the membrane. Due to the high extent of swelling in heptane, this might come into effect and cause an additionally enhanced transport of the polar molecule. The results of the GMT-oNF-2 also demonstrate that despite the convectively dominated transport in non-polar solvents the polarity of a solute has, nevertheless, a significant influence on the rejection. Even though the molecular weight of substance J is slightly lower, the rejection in THF is higher due to the higher polarity of J and thus the lower affinity to the membrane.

The results reinforce the outcome of the DoE considering that the polar endgroup is linked to the factor 'right side chain' in the DoE. The comparison of solutes G and J shows the same results for the GMT-oNF-2 as the results of the DoE. With an elongation of the right side chain and an associated increase of the affinity to the membrane layer, the rejection in THF and ethanol decreases, while in n-heptane the rejection increases. The comparison for DuraMem® reflects

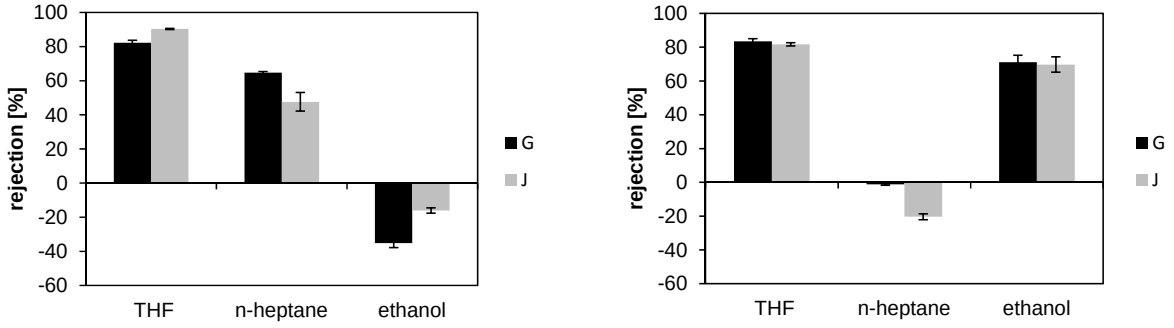

Figure 5.20: Rejection of two molecules which differ only in their endgroup (G: nonpolar; J: polar) a) GMT-oNF-2 b) DuraMem® 200

the results of the DoE as well, except for the predicted positive effect of a polar endgroup and the negative effect of an elongation of the left side chain on the rejection in ethanol. However, due to the minor differences in the rejections of the DuraMem® and the limited significance of the above mentioned factors, those results of the DoE have to be handled carefully.

Figure 5.21 compares the rejections of the two solutes E and B possessing a polar endgroup. The polar endgroup is either bound to a cyclohexane ring or to a benzene ring. The substances differ thus only by 6 g/mol in their molecular weight. The comparison confirms the hypothesis that a polar endgroup linked to a cyclohexane ring has a stronger influence on the rejection than a polar endgroup bound to an aromatic ring, particularly for the DuraMem® 200. The rejections of the GMT-oNF-2 measured in THF show no clear differences, but those of substance B with an aromatic endcore are worse in heptane and ethanol. In contrast, the rejections of the DuraMem® 200 in THF and ethanol are better for the solute with the benzene ring because the electrons are able to delocalize and the affinity to the membrane is lowered. This effect can be very well captured by comparison of the solubility parameters. As already shown in Figure 5.15b, negative rejection is more or less linearly dependent on the solubility parameter of the solute. The rejection decreases with minor differences between the solubility parameter of the solute and the membrane. Therefore, the rejection of the DuraMem® 200 of substance E ($\delta = 19.6\left(\mathrm{J/cm^3}\right)^{1/2}$) is better than B ($\delta = 20.8\left(\mathrm{J/cm^3}\right)^{1/2}$) and vice versa for the GMT-oNF-2 in ethanol.

The influence of a fluorination on the rejection is investigated in Figure 5.22 by the comparison

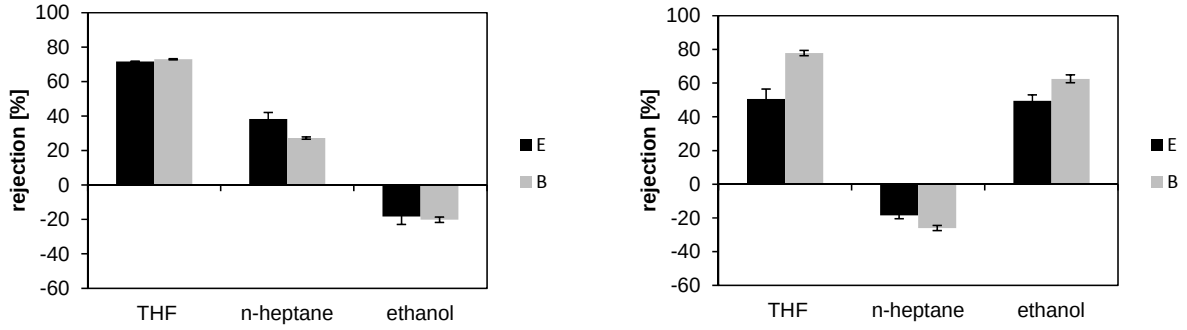

(a) (b)

Figure 5.21: Rejection of two molecules which differ only in their endcore (E: cyclohexane; B: benzene) a) GMT-oNF-2 b) DuraMem® 200

of a solute with a fluorine substituent (here: H) and a solute consisting only of hydrocarbons (here: G). Fluorination has an impact on the molecular weight as well as on the dipole moment of the solute. Both increase with fluorination (c.f. Table A.1). In accordance with the results of the DoE, where fluorination shows no significant influence on the rejection, the differences in the direct comparison are hardly measurable as well. A significant variation in the rejection can merely be observed for the GMT-oNF-2 in THF and n-heptane due to the slight increase of molecular weight and polarity caused by the fluorination.

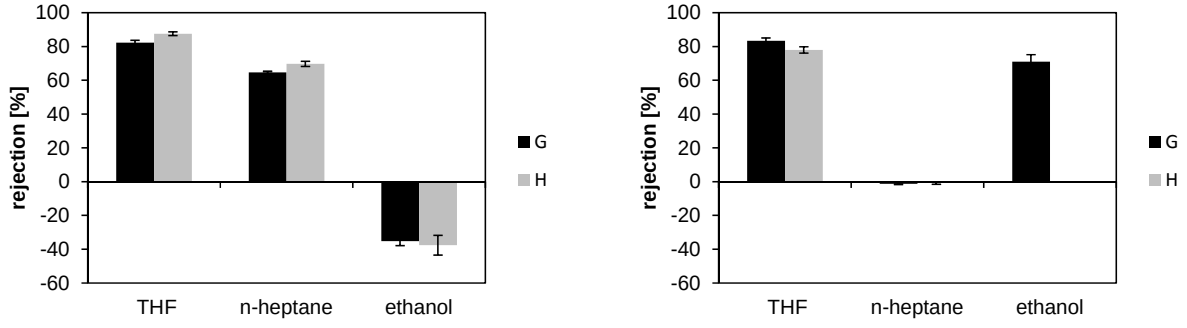

(a) (b)

Figure 5.22: Rejection of two molecules which differ only in the fluor substituent (G: no fluorination; H: fluorination) a) GMT-oNF-2 b) DuraMem® 200

Generally, the direct comparison of two molecules which differ only in the functional group reflects the results of the DoE. The polarity of a solute seems to have a minor effect on the rejection in THF, while the effects in n-heptane and ethanol are significantly higher. This implies that for a given solute/solvent system in process development the membrane selection process

must include the polarity of the solute to find suitable membranes.

5.3.4 Separation behavior in solvent mixtures

In industrial applications, products are not exclusively separated within pure solvents, but often in solvent mixtures. In order to enable the prediction of the separation behavior even in solvent mixtures, the experiments were conducted in binary solvent mixtures of different compositions as well. The rejections of the solutes of group A were measured at compositions of 25, 50 and 75 mol-% to visualize the influence of the relation of the solvent molecules to each other in the mixture. Rejections of the GMT-oNF-2 within pure solvents were taken from chapter 5.3.1. Rejections of the DuraMem® 200 in pure solvents were remeasured with the same membrane batch used for the solvent mixtures due to the changes of the DuraMem® performance.
In Figure 5.23 the rejections in a mixture of THF and ethanol vs. an increasing proportion of ethanol are illustrated. The rejections of the GMT-oNF-2 decrease from THF to ethanol to negative values because of the decreasing affinity of the solvent to the membrane. For compositions of 25 and 50 mol-% of ethanol the distribution of rejections for different solutes widens. Interestingly, the order of rejection changes in pure ethanol, e.g. solute O always shows the highest rejection in THF and in mixtures of THF and ethanol, whereas it shows least rejection in pure ethanol.

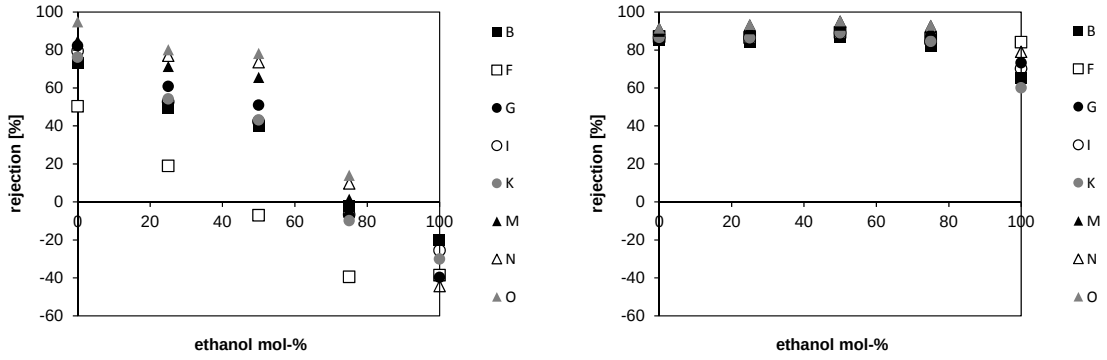

(a) (b)

Figure 5.23: Rejection progression of specialty chemicals (squares: 2-core solutes; circles: 3-core solutes; triangles: 4-core solutes) in a mixture of ethanol and THF of different composition a) GMT-oNF-2 b) DuraMem® 200

For the DuraMem®, the rejections decrease slightly in ethanol due to swelling of the membrane indicated by similar solubility parameters of ethanol and the membrane. The distribution of the

rejections is very narrow and the effect of swelling only becomes visible at very high ethanol concentrations. This demonstrates once more that rejection behavior of the DuraMem® is far less affected by swelling compared to the GMT-oNF-2.

Rejections in a mixture of THF and n-heptane are illustrated in Figure 5.24. Regarding the GMT-oNF-2, rejections increase with an increasing amount of THF and the differences in rejections become smaller. The increase in rejection of solutes with higher solubility parameters is more distinctive than for those with lower solubility parameters.

Rejections of the DuraMem® 200 behave linearly except for rejections in pure n-heptane. This behavior is equal to the course of rejections of the GMT-oNF-2 in a mixture of ethanol and THF. In both cases solvents with the best rejection and solvents causing negative rejections are used.

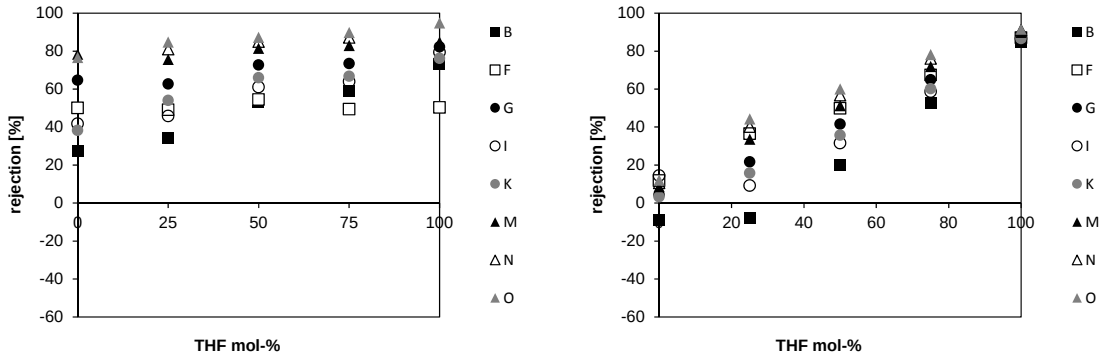

(a) (b)

Figure 5.24: Rejection progression of specialty chemicals (squares: 2-core solutes; circles: 3-core solutes; triangles: 4-core solutes) in a mixture of THF and heptane of different composition a) GMT-oNF-2 b) DuraMem® 200

In Figure 5.25 rejections in a mixture of n-heptane and ethanol are shown. In general the range of rejections of the GMT-oNF-2 is constant from pure heptane up to a 1:1 mixture similar to the behavior in THF/ethanol. Then, rejection drops sharply for higher proportions of ethanol. Ebert et al. [41] investigated the performance of polyethylene glycols (PEG) in mixtures of ethanol and n-alkanes and detected an increase of rejection with an increase of the alkane proportion as well for PEG in the lower molecular range.

For rejection of the DuraMem® there is no significant shift in the order of the rejections. However, the maximum at a 1:3 composition of n-heptane/ethanol attracts attention. The same behavior has been observed by Schmidt et al. [68] for the StarMem® 122 and the PuraMem®

280, which are PI based membranes as well, with different solutes in a mixture of n-hexane and isopropyl alcohol. It is likely that this is due to an effect of a reduced degree of swelling due to the lower proportion of ethanol. Figure 5.23 already demonstrated that the effect of swelling in ethanol can be easily suppressed by a small amount of a second solvent with a lower solubility parameter.

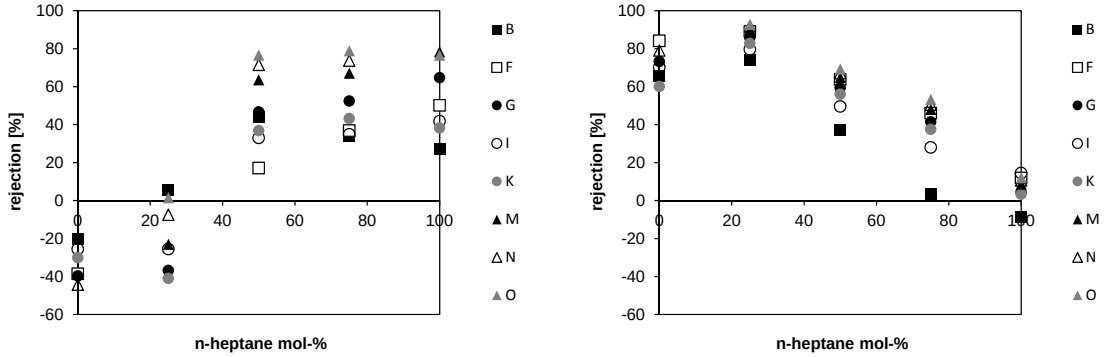

(a) (b)

Figure 5.25: Rejection progression of specialty chemicals (squares: 2-core solutes; circles: 3-core solutes; triangles: 4-core solutes) in a mixture of heptane and ethanol of different composition a) GMT-oNF-2 b) DuraMem® 200

In order to gain a deeper insight into the behavior of solute rejection in solvent mixtures, the solubility parameters of the involved components are now additionally taken into consideration. The solubility parameter of the solvent mixture is the arithmetic mean of the solubility parameters of the two solvents and was calculated by the volume fractions ϕ according to equation 5.4 [169]:

$$\delta_{S1S2} = \phi_{S1}\,\delta_{S1} + \phi_{S2}\,\delta_{S2} \tag{5.4}$$

It has been ensured that the two solvents are completely miscible in each other. The calculated solubility parameters for each solvent composition are given in Table 5.9.

Table 5.9: Solubility parameters of the solvent mixtures

Molar ratio	0:1	1:3	1:1	3:1	1:0
Ethanol/THF $\left[\left(\mathrm{J/cm^3}\right)^{1/2}\right]$	18.6	20.3	22.3	24.6	27.4
THF/n-heptane $\left[\left(\mathrm{J/cm^3}\right)^{1/2}\right]$	15.3	15.8	16.5	17.3	18.6
n-heptane/ethanol $\left[\left(\mathrm{J/cm^3}\right)^{1/2}\right]$	27.4	21.8	18.7	16.7	15.3

The membranes are now compared in terms of similar affinities to the solvents, e.g. mixture of the solvent which has a similar solubility parameter compared to the membrane and a solvent that causes negative rejections due to the large difference between the solubility parameter of the membrane and the solvent. The course of rejection will be discussed by the two core substances B and F, which have the largest difference in their solubility parameters ($\delta_B = 20.88\,\left(J/cm^3\right)^{1/2}$; $\delta_F = 14.63\,\left(J/cm^3\right)^{1/2}$). They show thus the most distinguishable changes. In the interest of clarity, their rejections are illustrated in a second diagram (Figures 5.26, 5.27, 5.28) together with their solubility parameter and those of the solvent mixture (taken from Table 5.9) and the membrane.

Firstly, rejections of the hydrophobic GMT-oNF-2 are contrasted with those of the hydrophilic DuraMem® 200 in Figure 5.26 in a mixture of a solvent in which the membrane swells significantly (ethanol for DuraMem® and n-heptane for GMT-oNF-2; $\Delta\delta_{S-M} < 1\,\left(J/cm^3\right)^{1/2}$) and a solvent that possesses high rejections (THF).

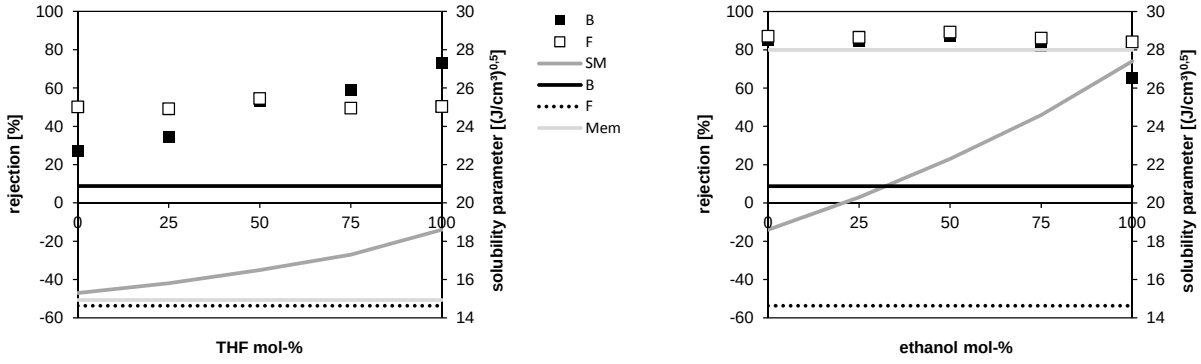

(a) (b)

Figure 5.26: Rejection of substances B and F (symbols) in solvent mixture of a solvent with high rejections and a solvent with a high affinity to the membrane. Additionally, the solubility parameter (lines) of the solutes B and F, the membranes (Mem) and the solvent mixture (SM) are given.
a) GMT-oNF-2 in n-heptane/THF b) DuraMem® 200 in THF/ethanol

Regarding the GMT-oNF-2, rejection of solute B increases linearly with the amount of THF in the mixture. The extreme difference of rejections can be attributed to the reduction of swelling and to the fact that solutes with polar endgroups like substance B have worse rejections in n-heptane and better rejections in THF than solutes with nonpolar endgroups (c.f. chapter 5.3.3). Rejection of solute F stays on a constant level at different compositions in the mixture. This might also be an effect of the inverse rejection behavior in n-heptane and THF concerning the

endgroups of the solute (c.f. Figure 5.20) and of the high affinity of the membrane to the solute ($\delta_{\mathrm{F-M}} = 0.37\left(\mathrm{J/cm^3}\right)^{1/2}$).

Rejection of the DuraMem® 200 for solute F remains nearly constant due to the very low affinity of the nonpolar solute to the membrane ($\delta_{\mathrm{F-M}} = 13.37\left(\mathrm{J/cm^3}\right)^{1/2}$). In contrast, rejection of solute B decreases by 20 % if the membrane structure gets looser due to swelling occurring at high concentrations of ethanol (> 75 mol-%), because the affinity of substance B to the membrane is higher ($\delta_{\mathrm{B-M}} = 7.12\left(\mathrm{J/cm^3}\right)^{1/2}$). The comparison again confirms that the separation performance of the DuraMem® 200 is far less affected by swelling.

Figure 5.27 compares the separation of solutes from the mixture of one solvent, for which rejections are very high (THF for both membranes) and one inducing negative rejections (ethanol for GMT-oNF-2 and n-heptane for DuraMem®). The membranes show the same rejection behavior with respect to their affinity to the solvents and the solutes.

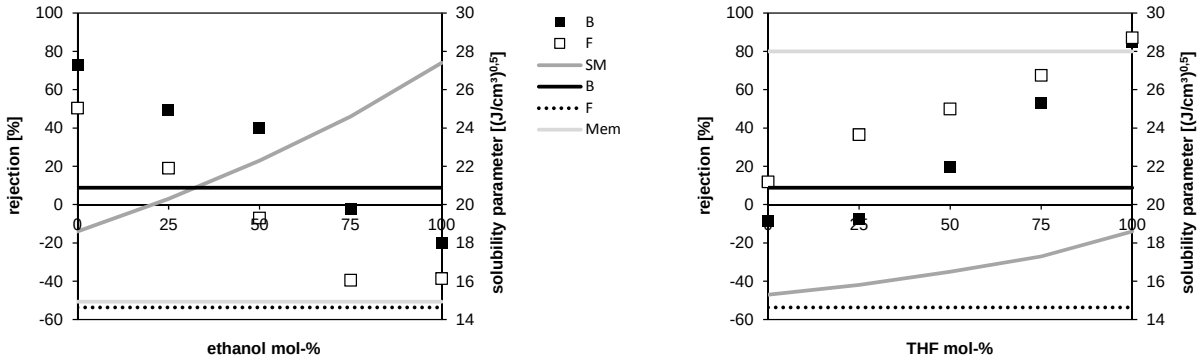

(a) (b)

Figure 5.27: Rejection of substances B and F (symbols) in solvent mixture of a solvent with high rejections and a solvent causing negative rejections. Additionally, the solubility parameter (lines) of the solutes B and F, the membranes (Mem) and the solvent mixture (SM) are given.
a) GMT-oNF-2 in THF/ethanol b) DuraMem® 200 in THF/n-heptane

Substance B, the solute with a polar endgroup and the higher solubility parameter, is retained well by the GMT-oNF-2 whereas the rejection for substance F is worse. For the DuraMem® 200, the effect is inverse. Rejection of the nonpolar solute F is higher and solute B is retained worse. This observation can be attributed to the lower affinity of solute B to the hydrophobic membrane and the higher affinity to the hydrophilic membrane, respectively, and vice versa

for the nonpolar solute. This effect has already been described in the previous chapter 5.3.3. Furthermore, rejections of the substance with lower affinity to the membrane decrease linearly to negative rejections whereas rejections of the solute with the higher affinity to the membrane decline faster and seem to stagnate at a minimum for both membranes. The constant minimal rejection of those molecules might be attributed to the fact that rejection within solvents of large differences in their solubility parameters to that of the membrane is predominantly a function of the solubility parameter of the substance (c.f. Figures 5.14b, 5.15a, 5.33b and 5.34a).

In Figure 5.28 rejections in a mixture of ethanol and heptane are compared. Those solvents cover the largest difference in the solubility parameter among the investigated solvents and lead to swelling of the membrane and negative rejections, respectively.

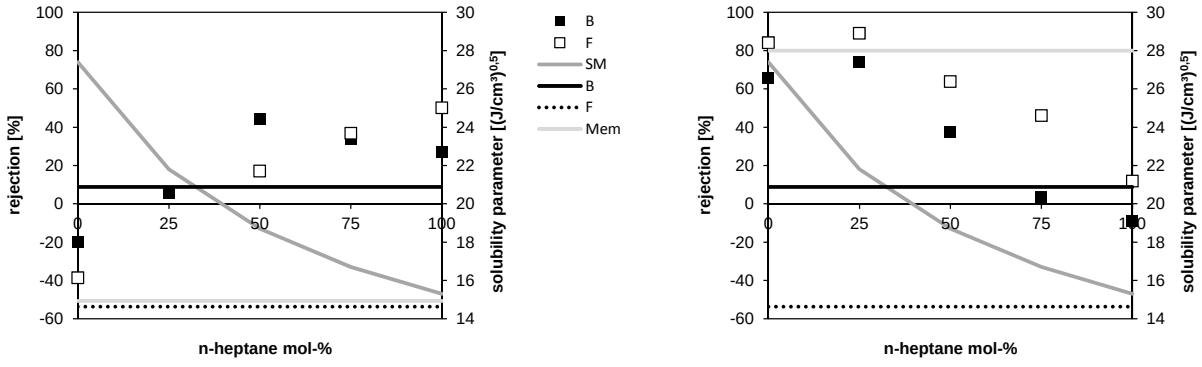

(a) (b)

Figure 5.28: Rejection of substances B and F (symbols) in mixture of n-heptane and ethanol. Additionally, the solubility parameter (lines) of the solutes B and F, the membranes (Mem) and the solvent mixture (SM) are given.
a) GMT-oNF-2 b) DuraMem® 200

For low concentrations of n-heptane the affinity of solute B to the GMT-oNF-2 membrane is higher than the affinity of the solvent mixture. At 25 mol-% n-heptane the affinity of the solute ($\delta_B = 20.88\,(J/cm^3)^{1/2}$) and the solvent mixture ($\delta_{SM} = 21.8\,(J/cm^3)^{1/2}$) to the membrane is similar and rejection is close to zero. Then, at concentrations of n-heptane > 50 mol-% the effect that substances with polar endgroups are retained more poorly in n-heptane is becoming relevant and rejection decreases again. Interestingly, solute F exhibits an extreme minimum at 1:3 composition of n-heptane and ethanol of -100 % (it is therefore not visible in the diagram). Solute F has nearly the same solubility parameter as the membrane and thus a very high affinity

to the membrane and a very poor affinity to ethanol. Adding n-heptane to this system, might swell the membrane to a certain extent and solute F could pass easier into the membrane material whereupon the low affinity to the solvent mixture additionally drives the solute into the polymer. This observation definitely gives a hint to non-ideal solubility effects.

The maximum in rejections of a DuraMem® 200 at a 1:3 composition of heptane and ethanol can be attributed to a decrease of swelling of the membrane due to the lower amount of ethanol and a decrease in the averaged solvent solubility parameter. The affinity of the solvent mixture to the membrane ($\delta_{\mathrm{SM-M}} = 6.2\left(\mathrm{J/cm^3}\right)^{1/2}$) is still higher than the affinity of the solute to the membrane ($\delta_{\mathrm{solutes-M}} > 7.12\left(\mathrm{J/cm^3}\right)^{1/2}$). If this relation is significantly reversed (> 75 mol-% n-heptane), rejection becomes negative.

In the majority of cases rejection in solvent mixtures can thus roughly be predicted by a linear combination of the rejections in pure solvents. However, the detected minima and maxima in the rejection course within solvent mixtures indicate some non-ideal effects of the solubility. Similar effects were found by Schmidt et al. [68] who measured the rejection in solvent-mixtures as well. These results show that solvent mixtures can not be taken into account solely by an ideally calculated solubility parameter to predict membrane performance (c.f. rejections in THF and in a 1:1 mixture of n-heptane and ethanol). Nevertheless, the relation of the solubility parameters helps to understand the course of rejection when keeping the general effect of the pure solvents (e.g. swelling) in mind. These investigations reinforce the statement of Schmidt et al. [170] that a membrane process can be optimized by adding an additional solvent.

Generally, as already described in chapter 5.3.2 rejections are high, if the affinity (indicated by the solubility parameter) of the solvent to the membrane is higher than the affinity of the solute to the membrane. If these affinities are contrary, rejections are very low or negative. However, there seems to be a range of tolerance $\Delta\delta_{\mathrm{S-M}} \approx 3\,(\mathrm{J/cm^3})^{1/2}$, i.e. the solubility parameter of a solute can be slightly closer to the membrane than the solvent and rejection still remains positive (c.f. rejections in THF in Figure 5.13).

The permeate fluxes of the above presented rejection experiments are given in Table A.9. It has already been mentioned (chapter 5.3.1) that permeate fluxes varied widely, especially for the DuraMem®. Evaluation of the fluxes is difficult because a new membrane sheet was used for every experiment. As a tendency, it can be stated that permeate fluxes of the solvent mixtures range between those of pure solvents. Despite those large differences, rejections are reproducible particularly in terms of their relation to each other. Most noticeably, the flux performance of the DuraMem® changed during the course of the work. Obviously, the membrane was

improved by the manufacturer. At the beginning especially n-heptane fluxes were conspicuous because they were the highest though there is a low affinity of the solvent to the membrane. For the experiments presented in this section the fluxes are lower than expected from the previous data. In order to verify this behavior the rejections of the DuraMem® were determined again. The measured fluxes are all significantly lower and the flux in n-heptane is the lowest among all tested solvents. Rejections in THF and ethanol are slightly better, whereas rejections in n-heptane are unchanged. For further details see Figure A.2. These results show that the rejection behavior is not necessarily correlated with the permeate flux.

5.4 Validation of the results

5.4.1 Verification of the influence of the membrane material on the separation mechanism

To ensure that the identified effects influencing the separation behavior in organic solvent nanofiltration can be attributed to the membrane material and that they are not specific to the applied membranes, the results were validated with higher cut-offs but the same membrane materials (see Table 5.1). These results are illustrated in Figure 5.29.

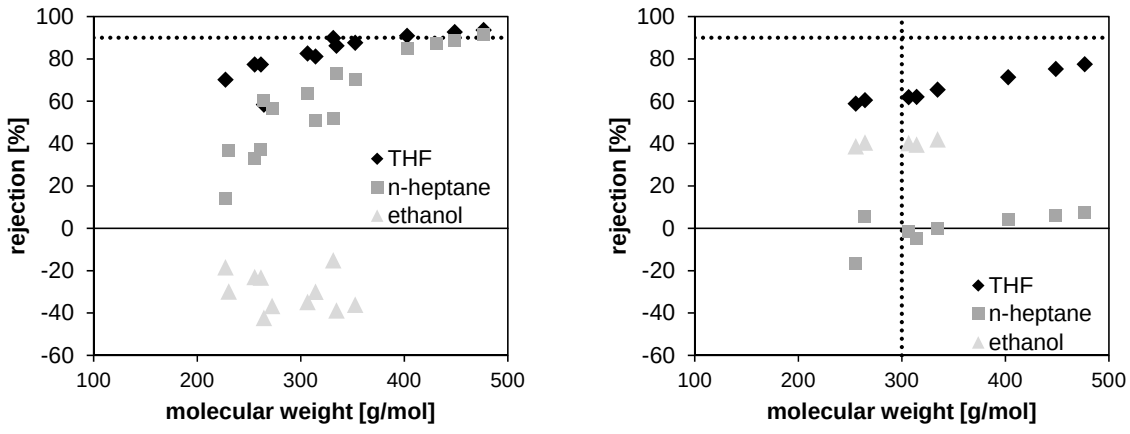

(a) (b)

Figure 5.29: Rejections of specialty chemicals in ethanol, THF and n-heptane vs. their molecular weight. Values taken after 180 min at 30 bar transmembrane pressure.
a) GMT-oNF-1 b) DuraMem® 300

Considering the lower separation limit, the results are exactly identical within the accuracy of

the measurement (see Figure 5.10). Rejection of the GMT-oNF membranes in THF is predominantly dependent on the molecular weight. Even putative outliers exhibit the same behavior e.g. in both cases the rejection of substance F, which has the lowest solubility parameter, is about 20 % lower than those of other substances of similar size. Furthermore, the unexpected fact that substances with the polar endgroup have lower rejections in heptane than those with nonpolar side chains (c.f. Table A.4 and Figure 5.20) has been proven. In Figure 5.30 the rejections are subdivided in those two classes. Within their classes the rejection follows the influence of the molecular weight, but there is a difference of approximately 20 % between the two trends.

The relations between the rejections of the DuraMem® 300 in the different solvents are identical, but rejections in THF and ethanol are significantly lower compared to those of the tighter DuraMem® 200 membrane. Moreover, rejections are in direct dependency of the molecular weight and the influence of other solute properties seems to decrease with increasing MWCO. Permeate fluxes are given in Table A.6. N-heptane fluxes through the DuraMem® are once more the highest, whereas the permeate fluxes of GMT-oNF-1 in ethanol are the lowest. Rejections of the GMT-oNF-1 in ethanol and of the DuraMem® 300 in n-heptane are also very low and negative, respectively, and once more in linear dependence of the solubility parameter.

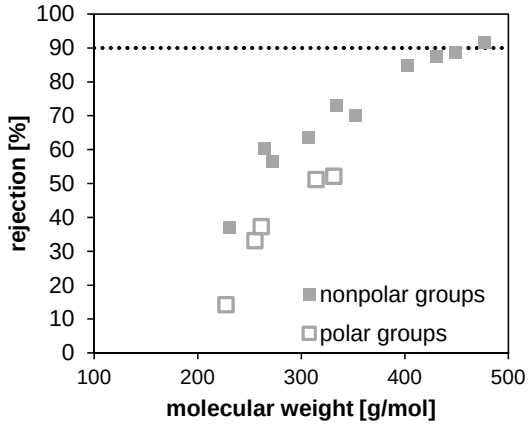

Figure 5.30: Rejections of GMT-oNF-1 in n-heptane subdivided in the specialty chemicals with polar endgroups (filled square) and without (unfilled square)

Summarizing, the general rejection behavior observed in the previous chapter was confirmed by membranes with higher separation limits. However, the effect of solute properties seems to become negligible with an increase of the separation limit if the affinity between solvent and membrane is higher than the affinity between solute and membrane because size exclusion becomes dominating. Solubility parameters of the solutes and polarity of functional groups seem to have a minor effect on the rejection of PI membranes compared to PDMS.

5.4.2 Verification of the influence of the solvents on the separation mechanism

In chapter 5.3.2 the solubility parameter has been identified as a suitable tool to predict the affinity between membrane, solvent and solute and thus the separation performance. In order to validate this theory and to exclude that this dependency is an effect of the structure of the selected solvents, the experiments were complemented with solvents of different structures but with similar solubility parameters. THF was replaced by ethyl acetate, n-heptane by methyl tert-butyl ether (MTBE) and ethanol by dimethyl sulfoxide (DMSO) and isopropyl alcohol (IPA), respectively. The corresponding solubility parameters are given in Table A.3 as well. Experiments in DMSO were carried out with the DuraMem® 200 T2, because the DuraMem® 200 T1 support is not stable in DMSO. The GMT-oNF-2 is not stable in DMSO as well. Due to a lack of alternatives, isopropyl alcohol had to be used for the validation. Unfortunately, there is a larger difference in the solubility parameters $\Delta\delta_{\text{ethanol}-\text{IPA}} = 3.9\left(\text{J/cm}^3\right)^{1/2}$. The experiments were conducted with mixtures of the solutes according to Table 5.4 (mixture A: solute B, F, G, I, K, M, N, O; mixture B: A, C, D, E, H, J, L). Rejections of the solutes (data given in Table A.7) vs. their molecular weight in the three validation solvents are illustrated in Figure 5.31. In principle the results follow the rules found in section 5.3.1 and are in the same order except for the rejection of the GMT-oNF-2 in ethyl acetate which replaces THF and is worse than the rejection in MTBE.

For a more detailed interpretation of the differences in separation behavior, rejections of the solutes in dependence of their solubility parameters are also considered. Firstly, rejections of the solutes in ethyl acetate vs. their solubility parameters are illustrated in Figure 5.32. The results are generally in accordance with THF (c.f. Figure 5.13). However, the performance of the GMT-oNF-2 is a bit worse in ethyl acetate compared to THF even though there is no significant discrepancy in the other solvent properties of THF and ethyl acetate. The general behavior is the same as in THF, but the range of rejections is more widespread and rejection of the largest molecules is about 20 % lower. Rejection in ethyl acetate seems to be more sensitive to the size (number of cores) and to the solubility parameters of the substances as e.g. the rejection of substance F which has a solubility parameter equal to those of the membrane $\Delta\delta_{\text{s}-\text{M}} = 0.37\left(\text{J/cm}^3\right)^{1/2}$ is zero.

Rejections of the DuraMem® 200 in ethyl acetate are identical to those in THF. Once more

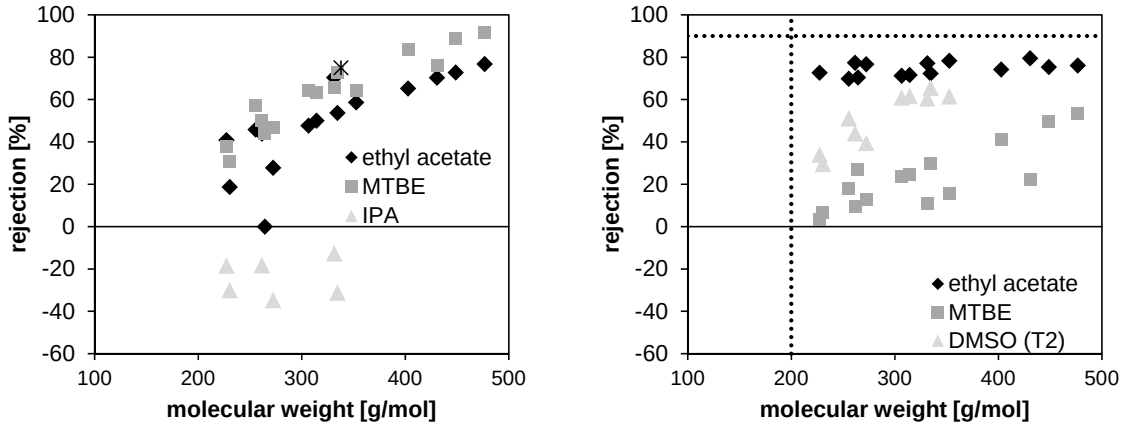

(a) (b)

Figure 5.31: Rejections of the substances in ethyl acetate, MTBE and isopropyl alcohol and DMSO, respectively vs. their molecular weight. Values taken after 3 h at 30 bar transmembrane pressure.

a) GMT-oNF-2 membrane, star symbols the separation characterization given by the manufacturer determined by rejection measurements of alkanes in toluene.

b) DuraMem 200 membrane, dotted line symbols the MWCO given by the manufacturer determined by rejection measurements of styrene oligomers in acetone.

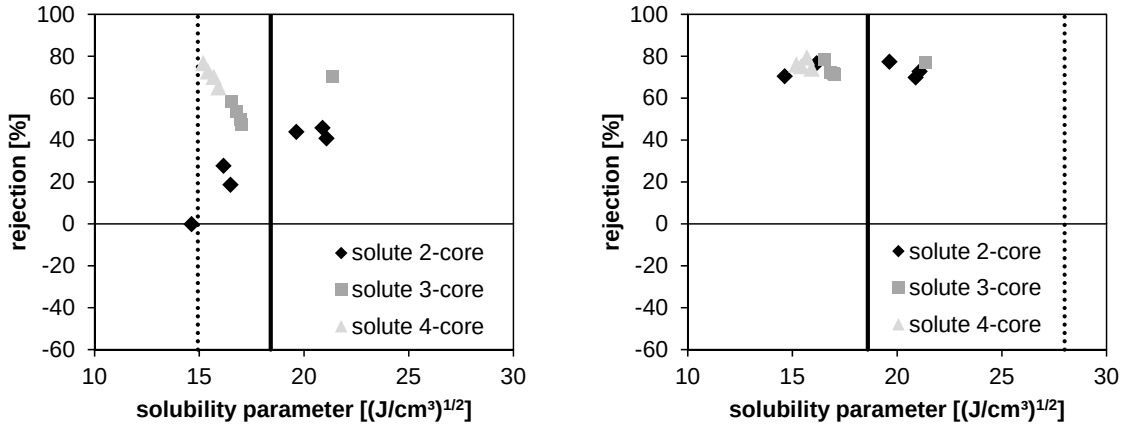

(a) (b)

Figure 5.32: Rejections of the substances in dependence of the solubility parameters of the solutes calculated by the method of Stefanis [161] and the solubility parameters of the membrane (dashed line) and ethyl acetate (solid line) a) GMT-oNF-2 b) DuraMem® 200

a nearly linear rejection curve, independent on the molecular weight was observed. In ethyl acetate and THF (except for solute E) neither a significant dependence on the molecular weight nor on the solubility parameter of the solute or any other property can be detected.

Figure 5.33 shows the rejections of the specialty chemicals in MTBE. The separation performance of the GMT-oNF-2 membrane is nearly the same as in n-heptane. It has to be noted that rejection is predominantly dependent on the molecular weight. Convective flow seems to dominate the transport through the membrane and to prevail over other interactions. However, slightly better rejections of the solutes with the polar endgroup can be observed in particular for the two core substances. This behavior contradicts the results obtained in n-heptane, but it emphasises the general behavior that polar solutes are retained better by the GMT-oNF-2 than nonpolar solutes. The reverse observation in n-heptane can be ascribed to an exception due to special interactions with this specific polar group.

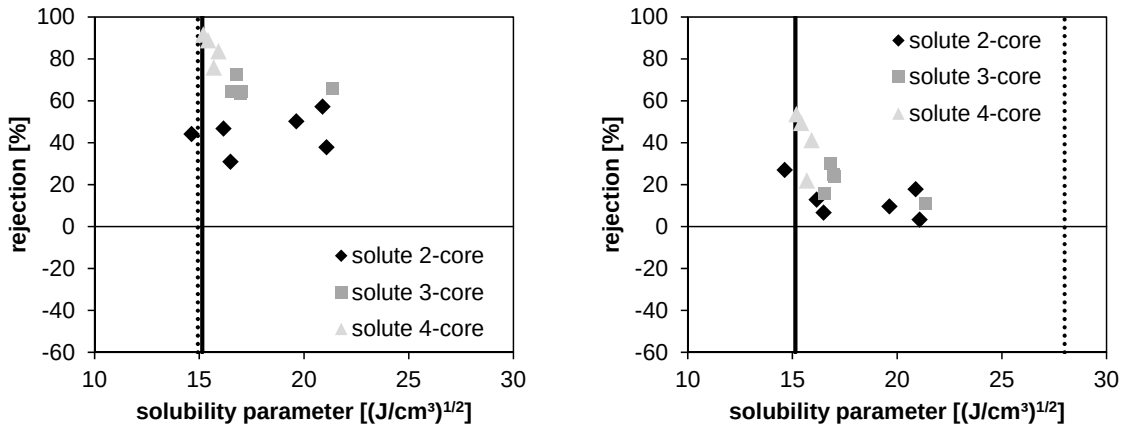

Figure 5.33: Rejection in dependence of the solubility parameters of the solutes calculated by the method of Stefanis [161] and the solubility parameters of the membrane (dashed line) and MTBE (solid line) a) GMT-oNF-2 b) DuraMem® 200

Rejections of the DuraMem® 200 are very low because the affinity of the solutes to the membrane is higher than the affinity of the solvent to the membrane. Even in the case of MTBE a slightly decreasing influence of the polar endgroups on the rejection can be detected. This is also reflected by the linear trend of the rejection just as in n-heptane. Rejections decrease, the closer the solubility parameter of the solute is to that of the membrane. However, rejections are about 30 % higher compared to n-heptane.

Rejections in DMSO or IPA, which are intended to validate the results in ethanol, are illustrated in Figure 5.34. Rejections of GMT-oNF-2 are nearly the same as in ethanol and show again a linear dependence of the rejection on the solubility parameter. Regarding DuraMem®, a significant dependency of the molecular size on the rejection can be detected which is contrary to the rejections in ethanol. Rejections are also in a medium positive range, but a bit lower than in ethanol, particularly for the two core substances. DMSO is a universally known solvent for polymer casting [24] because it possesses a very good solubility for many polymers [47]. Despite the stability of the DuraMem® 200 T2 in DMSO, a very high swelling occurs inducing the lower rejections and the high dependence on the molecular weight. This swelling can not be predicted solely by the comparison of the solubility parameters (c.f. $\delta_{ethanol}$ - δ_{DMSO} = $0.8\ \left(J/cm^3\right)^{1/2}$).

In summary, the general trend was confirmed by the validation. Both membranes show rejections in the medium range for solvents with almost equal solubility parameters which indicates significant swelling of the membrane. If the difference of the solubility parameters between the membrane and the solvent is moderate and the solubility parameters of the solutes are in the range of the solvent, the rejection is predominantly the highest. Rejection in solvents with a large difference in the solubility parameter of the solvent and the membrane are very low up to negative rejections.

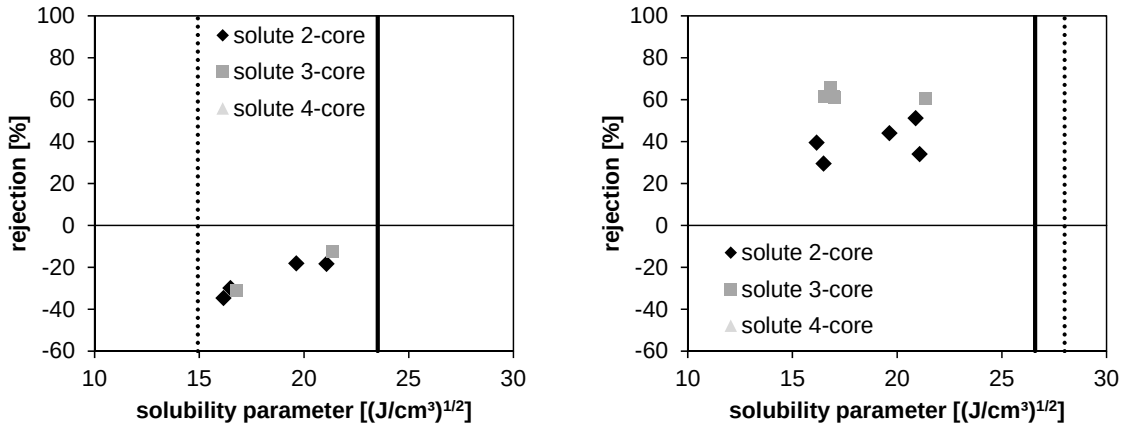

Figure 5.34: Rejection in dependence of the solubility parameters of the solutes calculated by the method of Stefanis [161] and the solubility parameters of the membrane (dashed line) and the solvent (solid line) a) GMT-oNF-2 measured in IPA b) DuraMem® 200 (T2) measured in DMSO

In order to verify the effect of the functional groups in these solvents, the results were incorporated into a DoE as well. The analysis of the influencing factors is given in Figure 5.35 for the GMT-oNF-2 and in Figure 5.36 for the DuraMem® 200. The results for the GMT-oNF-2 correlate with the results presented in chapter 5.3.2. In ethyl acetate the numbers of cores show the highest effect on the rejection just like in THF, but the amount of the effect is significantly lower than in THF. Besides the number of cores, here, the left side chain has a significant positive influence on rejection as well because of their impact on the molecular weight and size. The previously mentioned mixed effect of the right side chain and the polar endgroup (c.f. chapter 5.3.2) becomes apparent in the positive effect of the polar endgroup. A shortening of the right side chain results in a polar endgroup (except for substance I) and thus a higher polarity of the molecule which lowers the affinity to the membrane and causes higher rejections. Fluorination has here an additional positive effect on rejection due to its slight influence on the polarity and the molecular size. This effect was not distinctive in the analysis of the DoE for THF, but is significant when directly comparing the rejection of the two substances G and H.
The results in MTBE confirm the first impression that rejections are solely dependent on the molecular weight. Only functional groups with an exclusive impact on the molecular weight, namely the number of cores and the length of the left side chain, show a significant effect on the rejection. An analysis of the rejections in isopropyl alcohol by a DoE was not possible because of the small number of rejection data due to the low solubility of the substances in isopropyl alcohol. However, the rejections in IPA are very similar to those in ethanol and lie on a straight line as well when plotted vs. the solubilty parameter of the solutes (c.f. 5.15 and 5.34).

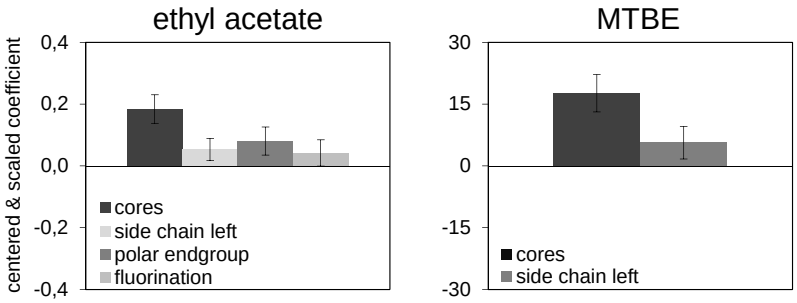

Figure 5.35: Functional groups influencing the rejection of the GMT-oNF-2 in varying solvents to validate the results of chapter 5.3.2

The effect of the functional groups on the rejection of the DuraMem® 200 in ethyl acetate is negligible and despite the influence of the left side chain, there is no significance for one of the factors. This result is not surprising because rejections are almost unchanged over the whole

range of molecular weights (c.f. Figure 5.31). A similar behavior was already observed for THF except for one solute (E, which is very polar). Rejections in MTBE depend strongly on the molecular weight (here: number of cores). Although the effect of the polar endgroup is not very significant, the strong effect of the polarity of the solute can be fortified by the direct comparison of e.g. substances G and J, and supports the results of the DoE for n-heptane. The rejection behavior in DMSO is somehow contrary to the behavior in ethanol. The number of cores and the left side chain have a distinctively higher and very significant positive effect on the rejection since the membrane seems to swell more in DMSO than in ethanol. According to the DoE, the influence of the polarity indicated by the right side chain is opposed to the results in ethanol. The same unexpected behavior occured for the influence of the polar endgroup on the rejection of the PDMS membrane in n-heptane which also caused high swelling.

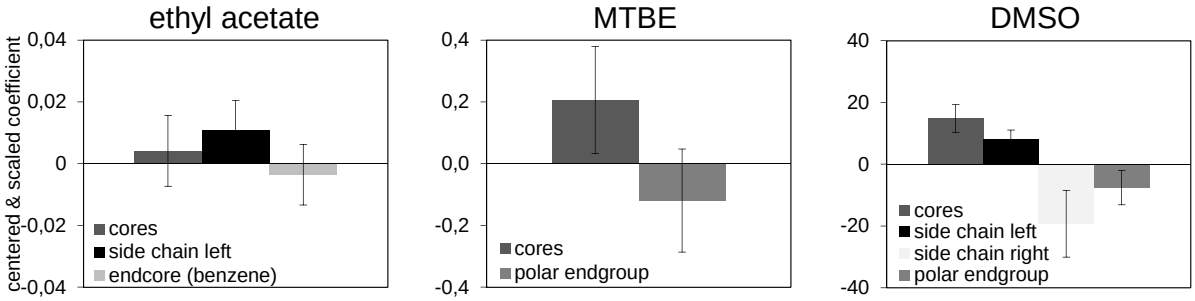

Figure 5.36: Functional groups influencing the rejection of the DuraMem® 200 in varying solvents to validate the results of chapter 5.3.2

In general, the rules identified with THF, n-heptane and ethanol were confirmed by the validation experiments and can thus now be treated as a general guideline for the development of an heuristic.

5.4.3 Verification of the influence of the solutes on the separation mechanism

In order to verify the transferability of the results to other solute classes, a short literature review is conducted. Schmidt et al. [68] investigated the rejection of five solutes (n-hexadecane, 2,2,4,4,6,8,8- heptamethylnonane, 1-phenyldodecane, 2,6-diisopropylnaphthalene and triphenylphosphine) with the two commercially available PI membranes StarMem® 122 and PuraMem® 280 in the three solvents toluene, n-hexane and isopropyl alcohol (IPA). In general, their results are in accordance with the findings of the present work. Besides the solubility parameters, the

authors additionally highlighted the importance of the critical diameter of the solutes which varied widely in their size. They found a good correlation of the critical solute diameter with rejection in high swelling solvents (IPA). In toluene and n-hexane, the solute solubility parameter dominated the rejection behavior. They also observed non ideal flux minima and maxima in solvent mixtures.

Micovic [37] performed membrane screening experiments for the rejection of hexacosane in decane. Three PDMS membranes (including GMT-oNF-2 and GMT-oNF-1), the polyimide membrane PuraMem® 280 and a silicon-coated polyimide membrane PuraMem® S380 were tested. In accordance with the findings in this work, rejections of the polyimide membrane are around zero (because of the large difference in solubility parameters) whereas the tight PDMS membranes and the silicon coated membrane retain hexacosane by 60-80 %. As the solubility parameter of decane and the membrane (15 $\left(\mathrm{J/cm^3}\right)^{1/2}$) is the same, the silicon membranes swell in the solvent and rejections are moderate.

Postel et al. [119] investigated the separation behavior of a composite membrane consisting of a polyimide support and a thin film of silicone acrylates as active layer (15.5 $\left(\mathrm{J/cm^3}\right)^{1/2}$). They measured the rejection of n-alkanes, polystyrenes (PS), polyethylene glycols (PEG) and carboxylic acids in methanol, isopropyl alcohol, toluene and n-hexane. The values of the solubility parameters are given in Table A.10. In toluene, the rejection of all solutes are positive and increase with their molecular weight as well as in n-hexane (except for polyethylene glycol which is not soluble in n-hexane). Rejections of carboxylic acids and n-alkanes in isopropyl alcohol and methanol are negative and thus they are in accordance to the observations with the PDMS membrane in ethanol and isopropyl alcohol in the present work. Rejections of both, n-alkanes and specialty chemicals in methanol, isopropyl alcohol and ethanol, respectively, decrease with an increase of molecular weight. Polyethylene glycols are retained by 40-80 % in both solvents. The separation behavior of polystyrenes was not determined for reasons of solubility. Postel et al. explain the rejections with the solubility parameter of the components and the affinity to each other as well. However, there are some inconsistencies compared to the present work. The result in methanol is somewhat surprising as the affinity of the polyethylene glycols to the membrane is higher than the affinity of the solvent to the membrane according to the given solubility parameter. Pursuant to the findings of this work, rejection should be low. The high rejections might be caused by the polar ether group due to the free valence electrons. The solubility parameters given in the cited work are compared with solubility parameters calculated by the methods [158, 161] used in the present work in Table A.10. The comparison between the

solubility parameter values shows significant differences which attracts attention. The results of Postel et al. [119] in dependence of the solubility parameter calculated by this method of Stefanis [161] are shown in Figure 5.37. Using those values, rejection in methanol follows the same rules as the rejection of the specialty chemicals in this work.

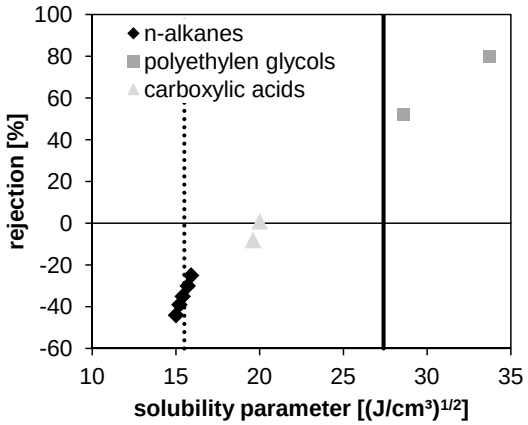

Figure 5.37: Rejections of a silicone acrylate composite membrane in methanol as a function of the solubility parameter of the solutes calculated by the method of Stefanis[161]. Data taken from Postel et al. [119]

In a following publication, Postel et al. [113] presented rejections of n-alkanes in binary solvent mixtures of toluene/isopropyl alcohol and toluene/methanol. They found minima in rejection at compositions between 50 and 75wt.-% of toluene and alcohol similar to the findings observed in this work (c.f. Figure 5.25). Rejections decline more strongly when adding methanol to toluene compared to the addition of isopropyl alcohol. Less methanol than isopropyl alcohol is necessary to reach the point where the transport of the bigger solutes through the membrane is preferred compared to solvent transport because the solubility parameter of methanol is higher and thus the affinity to the membrane is lower.

Darvishmanesh et al. [137] measured the rejection of Sudan II (276 g/mol), Sudan Black (457 g/mol) and Sudan 408 (465 g/mol) in methanol, ethanol, acetone, methyl ethyl ketone, toluene and n-hexane by the polyimide membrane StarMem® 122 (MWCO: 200 g/mol). Rejections in n-hexane are negative for all solutes. Rejections in methanol and ethanol are the highest whereas those in acetone and methyl ethyl ketone are in a range of 30 and 55 % and in toluene between 60 and 80 %. They calculated the solubility parameters of the solutes by the method of Fedors [158] (Sudan II (25.6 $\left(\mathrm{J/cm^3}\right)^{1/2}$), Sudan Black (25.4 $\left(\mathrm{J/cm^3}\right)^{1/2}$) and Sudan 408 (21.8 $\left(\mathrm{J/cm^3}\right)^{1/2}$)) and claimed a solubility parameter for the membrane of 23.2 $\left(\mathrm{J/cm^3}\right)^{1/2}$. However, according to several publications [68, 171], the solubility parameter of the membrane

material (Lenzing P84) is significantly higher: 26.8 $\left(\mathrm{J/cm^3}\right)^{1/2}$ and 27 $\left(\mathrm{J/cm^3}\right)^{1/2}$, respectively. Taking this solubility parameter into account, the measurement results (illustrated in Figure 5.38) follow the same correlation as identified in this work, except for the rejections measured in toluene which are higher than expected. The differences in rejection of the solutes of similar solubility parameters (around 25.5 $\left(\mathrm{J/cm^3}\right)^{1/2}$) can be attributed to the effect of the difference in the molecular weight (MW) of the solutes (ΔMW = 180 g/mol).

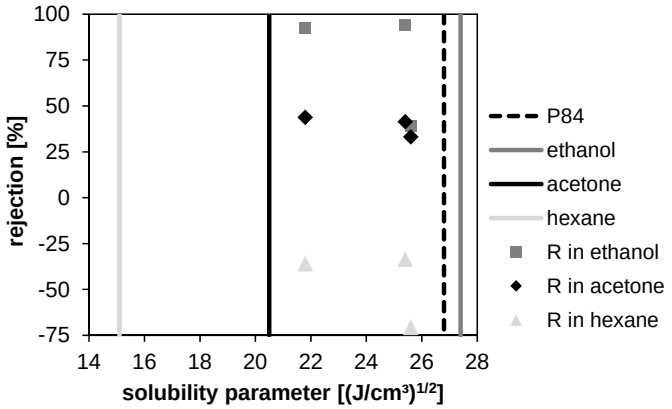

Figure 5.38: Rejections in different solvents in dependence of the solubility parameter of the solutes calculated by the method of Fedors [158]. Data taken from Darvishmanesh et al. [137]

Tsarkov et al. [118] investigated the rejections of membranes of glassy polymers with high free volume fraction (PTMSP, PMP and PIM-1) for different dyes (Safranine O (25.6 $\left(\mathrm{J/cm^3}\right)^{1/2}$), Solvent Blue 35 (23.7 $\left(\mathrm{J/cm^3}\right)^{1/2}$), Orange II (29.2 $\left(\mathrm{J/cm^3}\right)^{1/2}$), Remazol Brilliant Blue R (29.4 $\left(\mathrm{J/cm^3}\right)^{1/2}$)) in ethanol. Since the first three solutes all have a molecular weight of 350 g/mol, size exclusion effects can be neglected in the consideration. Except for solvent blue, the dyes are of ionic nature. Even for these completely new membrane polymers and the ionic solutes, the identified rules can be verified. In Figure 5.39 the rejections as a function of the solubility parameters are represented together with the solubility parameter of the solvent and the membrane materials. Rejections are the lowest for solvent blue, because the affinity of the solute to the membrane is higher than the affinity of the solvent to the membrane. With an increase of the solubility parameter, the rejections increase, because the affinity to the membrane decreases and thus the difference between the solvent-membrane and the solute-membrane affinity. Rejections are the highest, when the solvent-membrane affinity is higher than the solute-membrane affinity. The PTMSP membrane has the highest free volume fraction, therefore rejections for each solute are the lowest. PIM-1 was reported to have the lowest free volume fraction, but re-

jection of Safranine O is lower compared to PMP. This might be an effect of the higher affinity of Safranine O to the membrane material PIM-1.

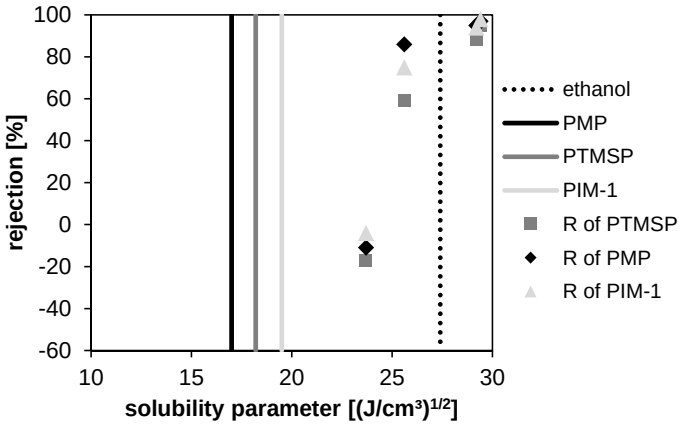

Figure 5.39: Rejections in dependence of the solubility parameter of the solutes calculated by the method of Van Krevelen [139] for high permeability glassy polymers in ethanol. Data taken from Tsarkov et al. [118]

Soltane et al. [172] analyzed the rejections of different dyes and alkanes with a PDMS pervaporation membrane in different solvents (e.g. toluene, DMC, ethanol). The used solutes and their rejections are summarized in Table A.11. Although it is not a membrane intended for OSN, even those results are in accordance with the identified governing rules (see Figure 5.40). However, a precise interpretation of the data is difficult as the rejections of the alkanes and of the dyes primarily increase with their molecular weight as well as with the solubility parameters. Furthermore, it has to be mentioned, that the authors used the Hansen solubility parameter, calculated with the HSPIP software and the Y-MB Group method. Thus, the values vary from the other calculation methods (c.f. Table A.10 for alkanes, Tsarkov [118] for Sudan Blue = Solvent Blue 35, Disperse Red 82 calculated by the method of Fedors [158] = 24.3 $(\mathrm{J/cm^3})^{1/2}$).

This literature review shows that the identified correlations can also be transferred to other solute types and even to other membrane materials. However, depending on the method used for calculation of the solubility parameter of the solute the interpretations vary significantly. For this reason, the method should be chosen carefully and preferably be verified by data of similar solutes or experimental measurements.

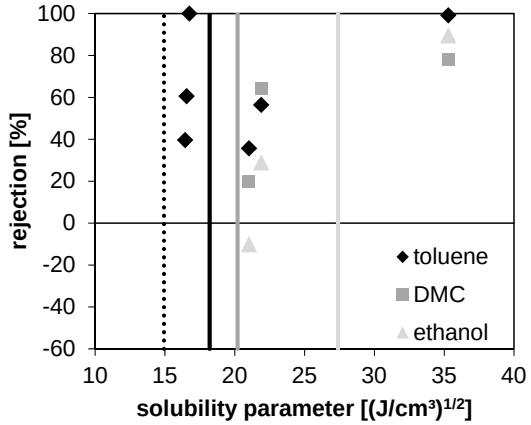

Figure 5.40: Rejections in dependence of the solubility parameter of the solutes for a PDMS membrane (PERVAP™ 4060)(symbolized by the dotted line) in toluene, DMC and ethanol. Data taken from Soltane et al. [172]

5.5 Heuristic rules

As emphasized in chapter 4.2 (see Figure 4.6) rejection is the crucial factor for the success of OSN in specialty chemicals industry. Due to the high value of the products, losses have to be minimized by high rejections. The heuristic is therefore solely based on rejection and not on permeate flux because this is of minor importance (c.f. Figure 4.4 and 4.5).
In this work rough rules to estimate the rejection of a separation problem have been generated on the one hand. These rules are summerized in chapter 5.5.1. On the other hand, based on these results, an heuristic for the identification of the best membrane for a given separation problem has been developed which is presented in chapter 5.5.2.

5.5.1 Rejection estimation

In general, three different cases could be identified by the investigation on the separation behavior of the specialty chemicals. Moreover, the literature review (c.f. 5.4.3) shows, that these rules can be widely used and are also transferable to other membrane materials or solute types.

First case

The difference between the solubility of the membrane and the solvent is very small.

$\delta_{Membrane} \approx \delta_{Solvent}$

This indicates that the membrane swells in the respective solvent to a high extent which leads to slightly lower rejections because the polymeric network becomes looser (in particular for dense

composite membranes).

Second case

The difference between the solubility parameters of the membrane and the solute is larger than the difference between the solubility parameters of the membrane and the solvent.

$$|\Delta\delta_{Membrane-Solute}| > |\Delta\delta_{Membrane-Solvent}|$$

In this case, transport of the solvent through the membrane is preferred to transport of the solute. If high rejections for the solute are required, this is the optimal case. Even within solvents in which negative rejections are observed (e.g. in isopropyl alcohol for the specialty chemicals), high rejections can be reached if the solute has a lower affinity to the membrane than the solvent (c.f. the specification for the GMT-oNF-2 given by the manufacturer for methyl orange in isopropyl alcohol (c.f. Table 5.2) or the results of Postel et al. [119] for PEGs in methanol).

In the first and second case, additionally the molecular weight of the solute has to be taken into account whereby it should be noted that this effect is more pronounced with the PDMS composite membranes. In terms of the latter case, the MWCO can give a hint on the molecular weight which is 90 % rejected. Rejections of separation tasks that fall under the first case are accordingly lower. The effect of functional groups has to be considered as well when estimating the expected rejection. Polar functional groups can increase the rejection of the PDMS membrane whereas they might slightly reduce the rejection of DuraMem® membranes.

Third case

The solubility parameters of the solutes range between the solubility parameter of the membrane and the solvent. The difference between the solubility parameters of the membrane and the solute is thus smaller than the difference between the solubility parameters of the membrane and the solvent.

$$|\Delta\delta_{Membrane-Solute}| < |\Delta\delta_{Membrane-Solvent}|$$

This relationship of the solubility parameters indicates a higher affinity between the solute and the membrane than between the solvent and the membrane. Solution of the solute in the membrane is preferred and rejections are low and very often negative. For the specialty chemicals used in this work, a linear dependence of the solubility parameter of the solute on the rejection was observed independently of the molecular weight of the substances.

This classification illustrates that the selection of a suitable membrane is in the first instance determined by the solvent of the given separation problem. If the solvent can be chosen freely, this enables the optimization of the OSN process.

These rules were used in chapter 7.1 to estimate the rejection of the separation tasks considered in the analysis of the technically realizable potential. Solvent mixtures were considered by the averaged solubility parameter according to equation 5.4.

Besides giving a first clue on the expected rejections and estimating the feasibility of a membrane for a specific separation task, the above described simple procedure could additionally give a hint about the dominating transport mechanism and the main influencing effects. Generally, the obtained results indicate that the separation behavior is dominated by different transport mechanisms depending on the solvent. If the solubility parameters of the GMT-oNF-2 membrane and the solvent are similar, the results suggest a contribution of convective flow for solute transport. The separation layer swells in the solvent, the structure becomes thus looser and the solutes are then mainly retained by size exclusion. This is in good agreement with the results of Robinson [110], who measured the flux through dense PDMS membranes. Robinson used several apolar solvents like n-heptane, i-octane, cyclohexane and xylene, which have solubility parameters in a range between 14 and 19 $\left(\mathrm{J/cm^3}\right)^{1/2}$. He could explain the fluxes successfully by using the Hagen-Poiseuille equation (eqn 2.13).

This is also supported by the solvent flux measurements presented in chapter 5.2 in particular by Figure 5.9 where the fluxes of THF and n-heptane follow a straight line in contrast to ethanol. Nonetheless, the affinity of the solute to the membrane may have a significant additional effect on the rejection, especially in n-heptane. From the results in this chapter it became clear, that transport is solely affinity driven when the solute-membrane affinity is higher than the solvent-membrane affinity. The same behavior was observed for the DuraMem®. However, indicated by the measured fluxes, the transport seems to be also convectively driven besides the affinity effect indicated by the linear dependency of the solubility parameter of the solute in solvents which do not swell the membrane very well like n-heptane. After the optimization of the membranes the convective part became negligible. The fact, that there is nearly no detectable solute size effect in the rejection of the DuraMem® in solvents with a high affinity to the membrane, leads to the conclusion that the transport here is dominated by solution-diffusion. The identified predominating transport effects are summarized in Table 5.10.

Table 5.10: Predominating transport mechanism in dependency of the respective solvent and membrane type

Membrane	low solvent solubility parameter	medium solvent solubility parameter	high solvent solubility parameter
GMT-oNF	size exclusion as well as affinity driven	mostly driven by size exclusion	affinity driven
DuraMem®	affinity driven	diffusive	diffusive

5.5.2 Heuristic for membrane selection

An heuristic was defined as the most suitable tool for simplification of OSN membrane selection for specialty chemicals which are produced in a multi-purpose production. This approach allows a fast decision for the high quantity of different products which have to be evaluated based on simple and easy accessible parameters. The later point is even more essential in the production of specialty chemicals where only few product properties are known.

In chapter 5.3.1 and in many further publications [82, 119, 137] the solvent has been identified as the main factor influencing the transport in organic solvent nanofiltration. The solubility parameter of the solvent has emerged as a helpful tool for the identification of interactions of the membrane material with the solvent. The solubility parameter of the solvent is thus the first step in the developed heuristic (see Figure 5.41) to select the most suitable membrane for a given separation problem. Differences in rejections of solutes in one solvent are based on differences in molecular weight, solubility parameter and polarity depending on the membrane and the solvent as pointed out in chapter 5.3.2 and 5.3.3. To consider these effects, specific solute properties are integrated into the heuristic in the following step in cases where the properties are relevant to separation behavior.

The final decision is driven by the presence of a second solvent. An additional solvent may drastically reduce rejection if the second solvent is unsuitable for the membrane or improves rejection e.g. due to reduced swelling of the membrane in the solvent mixture as investigated in chapter 5.3.4.

The estimated values in the heuristic in Figure 5.41 (like 350 g/mol) are based on the membranes investigated in this work. For the selection of membranes with higher cut-offs because of larger solutes or if higher fluxes are required, these values have to be adjusted. For the specialty

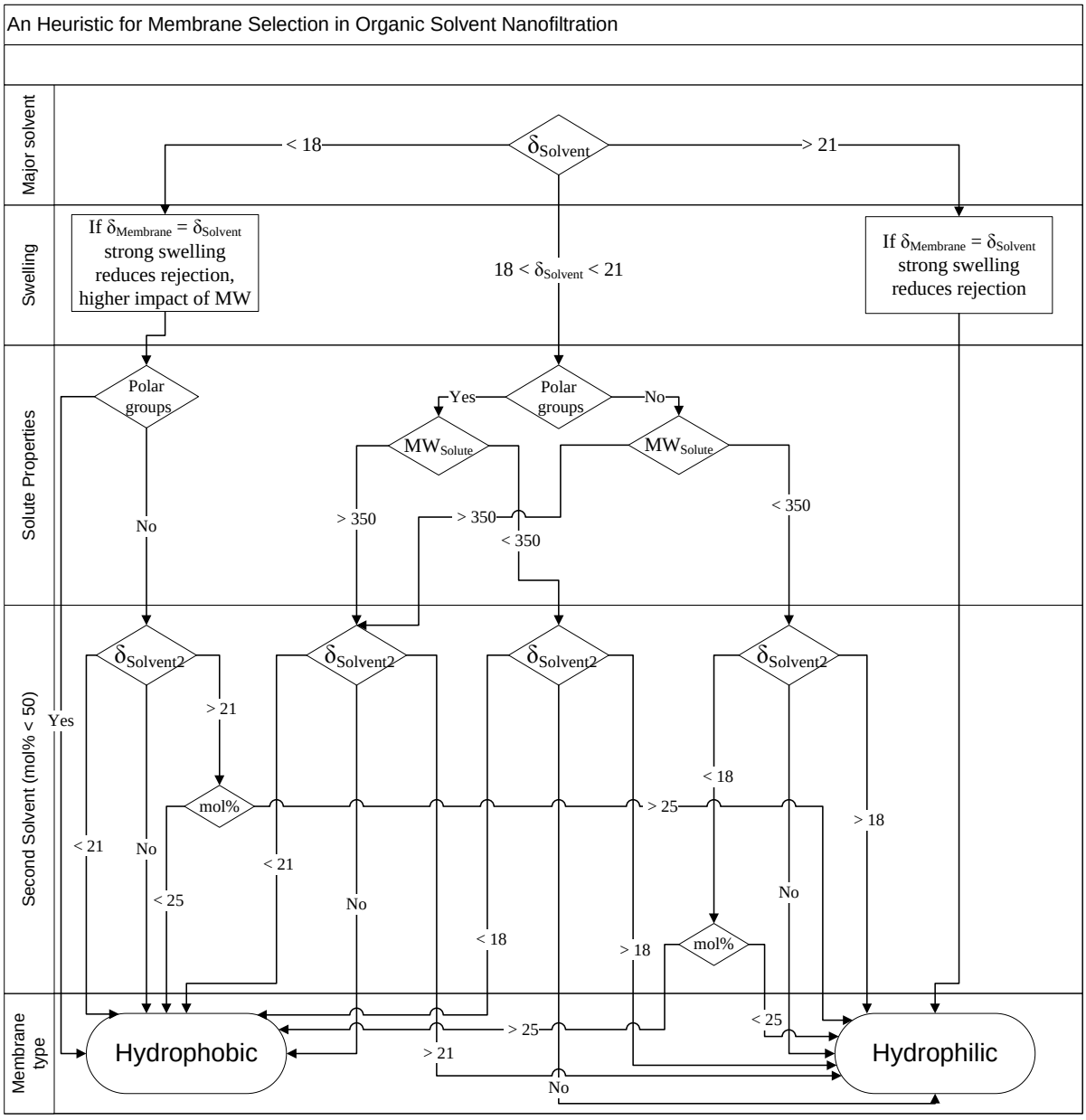

Figure 5.41: Heuristic for membrane selection

chemicals applied in this work, the flux performance of the membrane is of negligible interest whereas rejection is expected to be the highest possible. The comparison of the two tightest membranes of the individual membrane compositions is therefore the most practical approach. Successful verification of the heuristic by solutes which were not used for the development will be presented in chapter 7.

6 Investigations on ceramic membranes in organic solvent nanofiltration

This chapter [1] presents the investigations concerning the applicability of ceramic membranes in a multi-purpose-production environment.

6.1 Materials and methods

6.1.1 Ceramic membranes

As mentioned in chapter 2.2.3.2, there are hardly any ceramic membranes for organic solvent nanofiltration. Only one membrane in the upper nanofiltration range (MWCO: 600 g/mol) is commercially available. However, this membrane showed no rejections for the relevant specialty chemicals (chapter 5.1.2.1). The Fraunhofer Institute for Ceramic Technologies and Systems (IKTS), Hermsdorf, Germany developed new membranes focused on higher rejections in the lower nanofiltration range. These membranes are intended for aqueous as well as organic solvent environments. The separation layer was prepared by the polymeric sol-gel technique. By addition of complexation agents and sintering under inert conditions the pores of the membranes became narrower and more hydrophobic. Further details about the preparation procedure can be found elsewhere [173]. Results presented in this work were mostly obtained with the newly developed membranes concentrating on the fundamental understanding of the functionality of ceramic membranes for their use in organic solvents. An overview of the ceramic

[1] The content of this chapter was partially adopted from: Zeidler, S.; Puhlfürß, P.; Kätzel, U.; Voigt, I.: Preparation and characterization of new low MWCO ceramic nanofiltration membranes for organic solvents. *Journal of Membrane Science 470*, (2014), 421-430

membranes used within this work is given in Table 6.1. To prevent solvent residues and water vapor condensation in the pores the membranes were stored for at least 12 h under vacuum (100-250 mbar) at 80 °C in a drying cabinet before the rejection measurements.

Table 6.1: Ceramic membranes

Type	Material	Agent	Membrane No.
1	ZrO_2	silanisation	
2	TiO_2/ZrO_2	diethanol amine (DEA)	N0265 (less sublayers), N0328, N0330, N0353, N0354, N0403 - N0411
3	TiO_2/ZrO_2	phenolic resin	N0157, N0288
4	TiO_2/ZrO_2	-	N0346, N0426

The prototype membranes were provided as single channel tubes with a length of 250 mm, an outer diameter of 10 mm and an inner diameter of 7 mm [80]. The active membrane layer is located on the inner surface of the tube and amounts to approximately 4800 mm^2. Prior to the experiments, the membranes were characterized by permporometry at the Fraunhofer IKTS. Here, the permeation of a mixture of an incondensable and a condensable gas through the membrane is measured. The incondensable gas (here nitrogen) is loaded stepwise with the condensable gas. The decrease of the permeation due to pore blocking by the condensed gas is recorded for each composition. Cyclohexane was used as condensable gas because the wettability of the pores with a hydrophobic solvent is of interest here.

From the measurement of the molar flow rates Q, the transmembrane pressure Δp and the temperature T, the partial pressure of the condensable gas can be calculated

$$p_{liq} = \frac{Q_{liq}}{Q_{liq} + Q_{N_2}} (p_0 + \Delta p) \tag{6.1}$$

$$Q_{liq} = \frac{V_i^F \rho_i}{M_i} \tag{6.2}$$

with the feed flow rate V_i^F, the density ρ_i and the molecular weight of the condensable gas M_i [174]. The permeability of nitrogen P was then calculated from the permeate flow rate Q_P, the transmembrane pressure and the membrane area A_M as follows:

$$P = \frac{Q_P}{\Delta p A_M} \tag{6.3}$$

Using the Kelvin equation,

$$\ln\left(\frac{p}{p_s}\right) = \frac{\gamma\cos\phi}{r_p}\frac{2\upsilon}{RT} \tag{6.4}$$

the pore size distribution of the membrane can be calculated. The contact angle ϕ is set to zero because complete wetting is assumed. An example of a determined permporometry curve is given in Figure 6.1. The relative permeance related to the pure nitrogen permeance is plotted over the pore diameter of equation 6.4. Subsequently, the nominal pore radius was determined by the interpolation of the permeance curve at a relative permeance of 50 %.

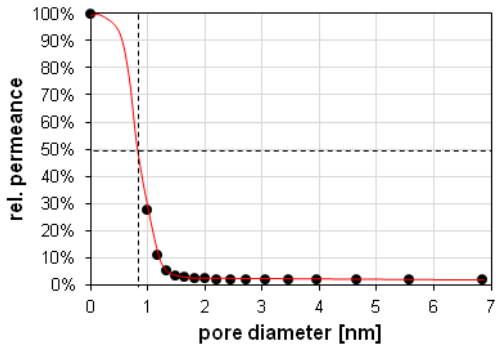

Figure 6.1: Permporometry measurement using the example of membrane N0328 (data kindly provided by Fraunhofer IKTS)

Permporometry was known as a tool for the characterization of ultrafiltration membranes [175]. During the development of the new membranes it was perceived that permporometry might also be a valuable tool for organic solvent nanofiltration membranes. In addition to the information obtained about the pore sizes, it was found helpful for quality control because defects in the membrane separation layer can be detected [173]. The results of the permporometry measurement of each membrane listed in Table 6.1 are presented in the Appendix in Figure B.1, B.2, B.3. The data concerning the mean pore size and the defect pores derived from the permporometry measurements are given in Table B.1.

6.1.2 Polystyrene oligomers

First of all, the functionality of the new ceramic membranes was tested according to the method proposed by See-Toh et al. [84]. A styrene oligomer mixture containing PSS-ps560, PSS-ps1.8k and PSS-ps5.6k (Polymer Standards Service GmbH, Mainz, Germany) was used. One

gram of each standard was dissolved in one liter of the respective solvent. It was thus possible to obtain a rejection curve from a single experiment due to the different molecular weights of the styrene standards.

6.1.3 Experimental set-up

Experiments with the ceramic membranes were carried out in a Multi-Purpose-Cross-Flow-Membrane Plant at Merck KGaA, Darmstadt, Germany. A schematic diagram of the part of the plant which was used for the experiments is shown in Figure 6.2.

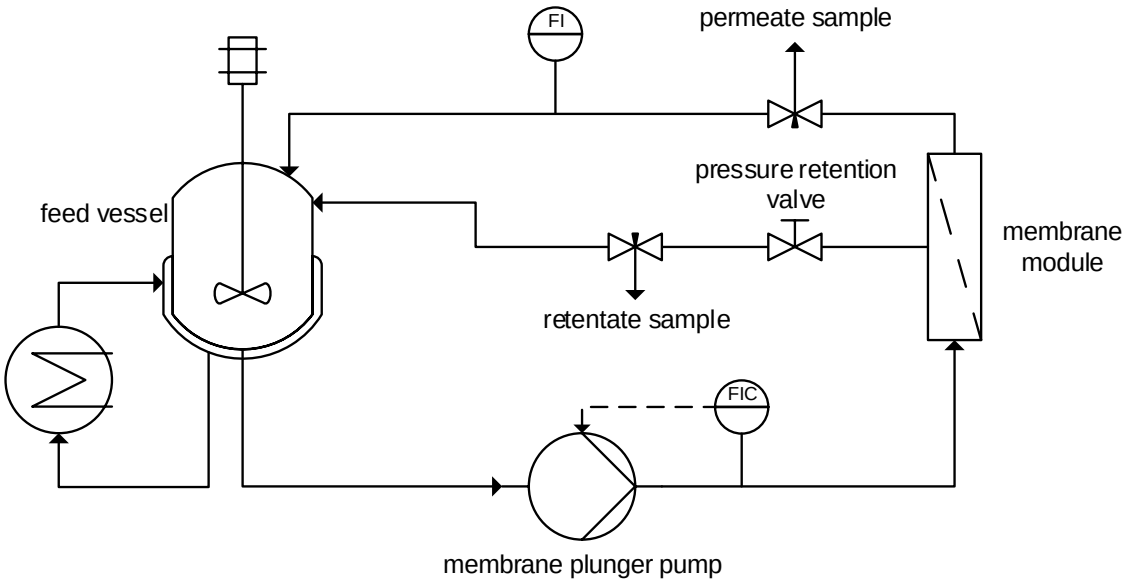

Figure 6.2: Multi-purpose cross-flow membrane plant

The stirred feed vessel had a volume of 2.8 l. The feed temperature could be controlled via the double jacket of the feed vessel, while the whole tubing was isolated to prevent temperature changes across the test set-up. The feed was circulated across the membrane by a membrane plunger pump (Hydracell G03, Wanner Engineering, Inc., Minneapolis, USA). The membranes were housed in a vertically fixed monochannel module (Andreas Junghans, Frankenberg, Germany). Figure 6.3 shows a picture of the module. The feed flow is axial through the membrane tube. The permeate drains off outside the membrane at the bottom of the module. At the top of the module the permeate channel can be vented.

By closing the pressure valve behind the membrane module, the system was pressurized. Both, the retentate and the permeate were recirculated into the feed vessel. A coriolis mass flow meter

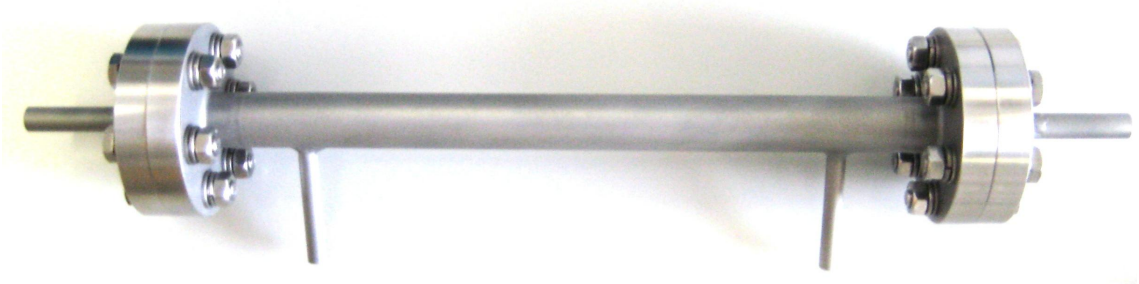

Figure 6.3: Lab scale ceramic module housing

was integrated in the permeate recirculation to determine permeate mass flow. If the permeate flow was below the detection limit, it was determined by measuring the increase of permeate mass on an analytical balance per time.

The characterization experiments were always carried out under the same standard process conditions, i.e. a transmembrane pressure of 20 bar, a temperature of 20 °C and a feed flow of 6 l/min, i.e. a cross-flow velocity of 3 m/s. In long-term experiments conducted exemplary for a type 1 and a type 4 membrane, the flux behavior over time was evaluated to secure constant conditions for sampling. The trends are shown in Figure 6.4. After 1 h the permeate flux deviates less than 0.5% per hour, therefore, membranes were always conditioned for 1 h after reaching equilibration of the process conditions in the system. Subsequently, retentate and permeate samples were taken to determine the rejection of the membrane.

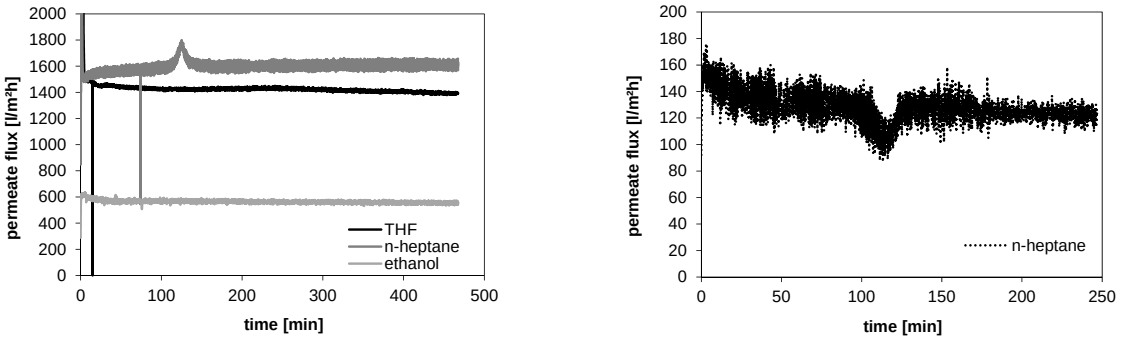

(a) (b)

Figure 6.4: Pure solvent flux measurement measured at 20 bar and 20°C in a long-term experiment. a) type 1 b) type 4

6.1.4 Analytics

The concentrations of the polystyrene fractions in the retentate and the permeate were determined by gel permeation chromatography (GPC) (Hitachi Elite LaChrom, Hitachi High Technologies America, Illinois, USA). The used colums Shodex GPC KF-801, KF-802 and KF-806M were supplied by Showa Denko K.K., Tokyo, Japan. The measurements were conducted at the chromatography lab of the central analytics department at Merck KGaA, Darmstadt, Germany.

6.2 Experimental investigations on the separation behavior of ceramic membranes

6.2.1 Investigations on the solvent flux through ceramic membranes

The separation of ceramic membranes is supposed to follow the pore-flow transport mechanism. In order to check the validity of the Hagen-Poiseuille equation, pure solvent fluxes were measured at a constant transmembrane pressure of 20 bar and different temperatures varied between 15 and 55 °C. The results of the commercially available hydrophobized 600 Da membrane and a newly developed membrane are illustrated in Figure 6.5.

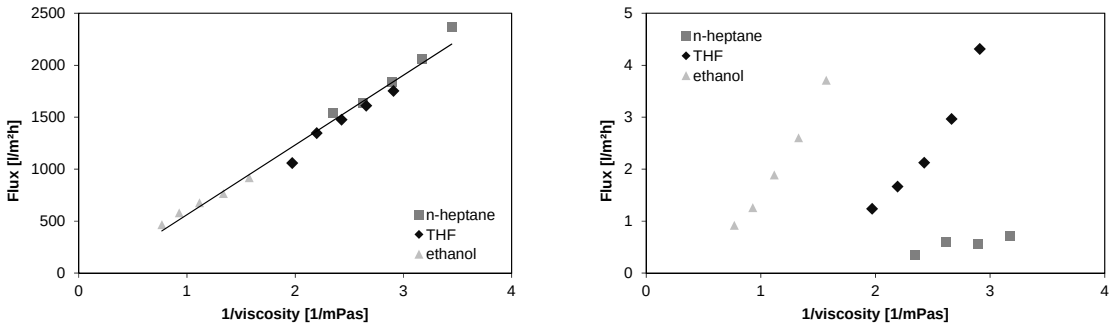

(a) (b)

Figure 6.5: Pure solvent fluxes of n-heptane, ethanol and THF
a) commercially available hydrophobized membrane
b) newly developed hydrophobic membrane

It can clearly be seen that the solvent fluxes through the commercial membrane are extremely high and are determined by the viscosity independent of the used solvents. Regarding the newly

developed membrane, there is no correlation detectable of the permeate flux with the viscosity and thus the pure solvent flux does not follow the pore-flow theory (Hagen-Poiseuille equation) anymore. This first observation indicates that with lower separation limits changes in transport mechanism occur and that further properties and effects influence the separation of narrow pore ceramic size membranes.

6.2.2 Identification of parameters determining the suitability of a membrane for OSN

In order to prove the applicability of the newly developed membranes for OSN, all membranes were characterized by rejection measurements of different polystyrene oligomers as proposed by See-Toh et al. [84] in THF. Those results are subsequently compared with the membrane properties provided by the permporometry measurements to investigate how the rejection behaves against the pore size or whether there is a hint on the suitability of these membranes for the use in organic solvents detectable.

In Figure 6.6 and 6.7 the permporometry measurements and the results of the MWCO determination according to See-Toh et al. [84] are illustrated. Despite the same mean pore size of the two membranes the rejection curves differ significantly.

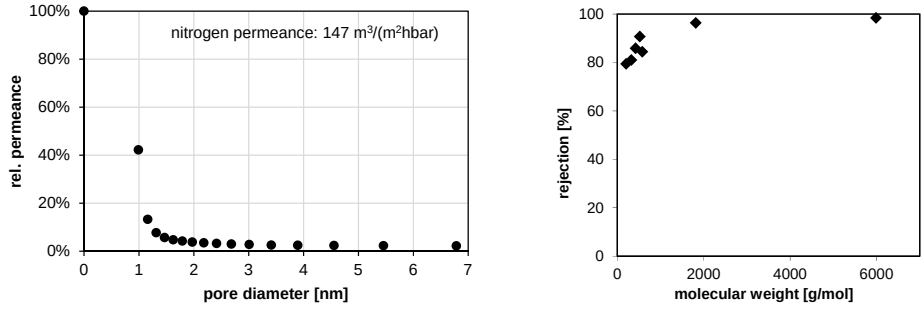

(a) (b)

Figure 6.6: Characterization of a new membrane (N0354)

a) Permporometry measurement by use of cyclohexane as condensable vapor (data kindly provided by Fraunhofer IKTS)

b) rejection curve determined with polystyrenes in THF at 20 bar

This can be attributed to the course of the permporometry curve at larger pore diameters. Membranes that have a constant relative permeance for larger pores (> 5 nm) in the permporometry

measurement like membrane N0353, show an incomplete rejection for higher molecular weight oligomers. The rejection curve often stagnates or even decreases. This implies that the larger molecules are able to pass through some larger pores, which is undesirable and therefore called defect pores.

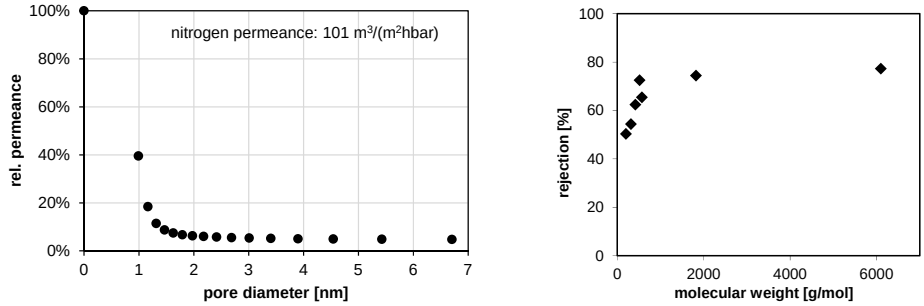

(a) (b)

Figure 6.7: Characterization of a new membrane (N0353)

a) Permporometry measurement by use of cyclohexane as condensable vapor (data kindly provided by Fraunhofer IKTS)

b) rejection curve determined with polystyrenes in THF at 20 bar

In aqueous applications this effect seems to be negligible. Rejection measurements of aqueous NF membranes (type 4 sintered under air) with a mixture of polyethylene glycols in water show excellent rejections despite a considerable portion of defect pores (see Figure 6.8).

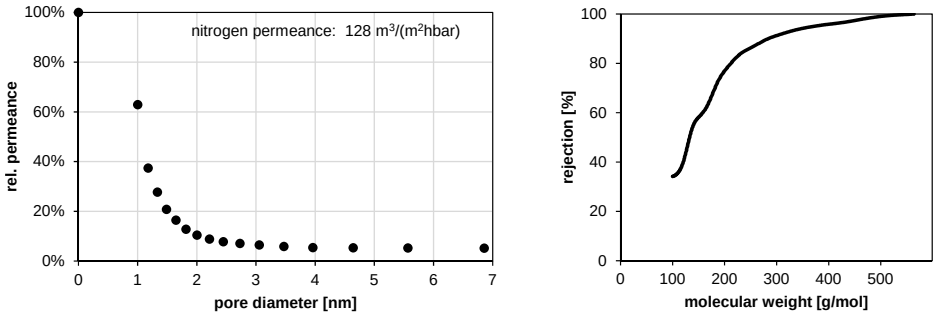

(a) (b)

Figure 6.8: Characterization of a new membrane type 4 (N0426) for aqueous nanofiltration

a) Permporometry measurement by use of cyclohexane as condensable vapor (data kindly provided by Fraunhofer IKTS)

b) rejection curve determined with polyethylene glycol in water at 10 bar (data kindly provided by Fraunhofer IKTS)

There are different explanations for the observed behavior. On the one hand the water molecules

are smaller than the solvent molecules and additionally show a better wettability of the membrane surface. For this reason, they can pass more easily through the very small pores and the relative transport through the defect pores becomes marginal. On the other hand, in water there are also electrostatic repulsion forces acting between the membrane surface and charged solutes (not the case for PEG) so that larger pores may also be masked by such an effect, which is not existent in organic solvents. Nevertheless, the results clearly show that if good OSN performance of ceramic membranes is sought, the reduction of the number of defect pores in the membranes active layer is essential.

If defect pores are reduced to a minimum, the performance of ceramic membranes is mostly determined by the mean pore size as expected. In Figures 6.9 and 6.10 the membranes with the lowest amount of defect pores are presented. Membrane N0157 (Figure 6.9), prepared with a phenolic resin (type 3), has a very good pore size distribution with a mean pore size of 1.55 nm and no pores bigger than 2.5 nm. It can be seen, that larger polystyrenes are almost completely retained. A MWCO of $\sim$ 1000 Da was determined at a permeate flux of 240 l/m^2h for this membrane. However, the pore size is still too large to achieve significant rejections in the nanofiltration range.

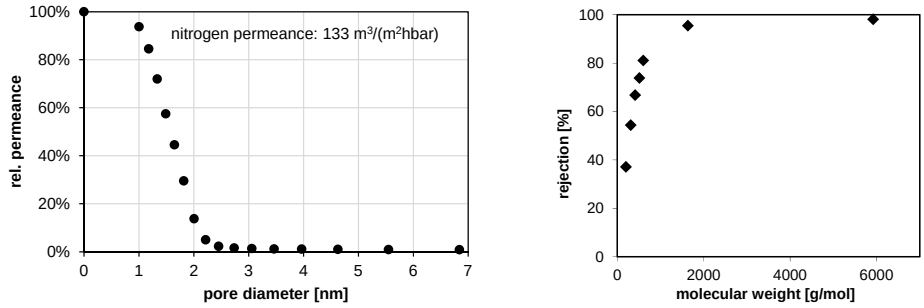

(a) (b)

Figure 6.9: Characterization of a new membrane (N0157) hydrophobized by a phenolic resin
a) Permporometry measurement by use of cyclohexane as condensable vapor (data kindly provided by Fraunhofer IKTS)
b) rejection curve determined with polystyrenes in THF at 20 bar

A type 2 membrane (N0328) is presented in Figure 6.10. The mean pore size is significantly reduced ($\sim$ 0.6 nm) compared to membrane N0157 and the number of pores > 2 nm is marginal. The rejection curve measured with polystyrene in THF is given in Figure 6.10b and provides a cut-off of 350 g/mol. Molecules larger than 1800 g/mol are completely retained. The permeate

flux at 20 bar transmembrane pressure was 70 l/m^2h. The MWCO has been clearly improved, but the reduction of the pore size entails a drastic decline in permeate flux.

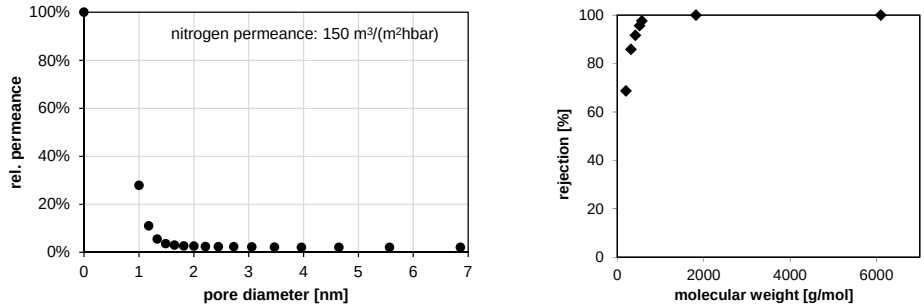

(a) (b)

Figure 6.10: Characterization of a new membrane (N0328) hydrophobized by DEA

a) Permporometry measurement by use of cyclohexane as condensable vapor (data kindly provided by Fraunhofer IKTS)

b) rejection curve determined with polystyrenes in THF at 20 bar

Those MWCO measurements revealed that a low mean pore size is not the most important property of a good OSN membrane. Defect pores have been identified having a strong negative impact on the performance in organic solvents. The permporometry measurement emerged as a helpful tool to detect those defects. However, it delivers no indication on the amount of pores in the module. Permeate flux is dependent on the amount of pores in a module and on their size. The pore size distribution provided by the permporometry measurements gives only an idea of the pore size and of the amount of defect pores which could induce higher fluxes. Besides, the dry nitrogen permeance measured prior to the loading with condensable gas in the permporometry measurements could help to indicate highly permeable membranes. Together with a low amount of defect pores a good performing membrane should be identifiable. Figure 6.11 depicts the maximum rejection of all characterized membranes determined with polystyrene in THF in dependency of the ratio of the dry nitrogen permeance and the amount of defect pores represented by the relative permeance at 5 nm pore size. It is noticeable, that maximum rejection increases with a higher ratio of permeance to defect pores. Furthermore, defect pores seem to limit the rejection to a greater extent the lower the nitrogen permeance is. Dry nitrogen permeance should therefore also be considered when characterising a ceramic OSN membrane.

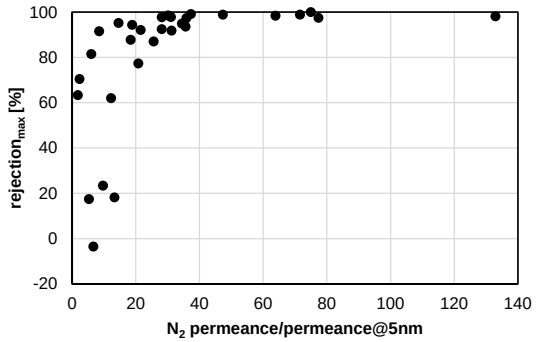

Figure 6.11: Maximum rejection of a membrane measured with polystyrenes in THF as a function of the ratio of dry nitrogen permeance and the permeance at a pore size of 5 nm (representing the number of defect pores in the membrane)

6.2.3 Influence of solvent on rejection

It is known from polymeric OSN membranes that considerable deviations in fluxes and rejections occur when different solvents are used for separations [68, 82, 119, 127, 157]. All known transport models for solvent permeation and solute transport through ceramic OSN membranes are more or less based on the pore-flow theory. Some authors extended the models by further influencing factors as the surface tension [121, 123, 124], dielectric constant [121, 123], dipole moment [124], effective molecular dimension [121, 124] or a solubility parameter [125]. However, with all the models and according to Darcy's law, only the viscosity, the applied pressure and the molecular size of the solvent should cause differences in permeations. Assuming the validity of the models also for the new nanofiltration membranes, MWCO should not change much when switching from THF to other solvents. In an experimental assessment the single layer DEA membrane (MWCO: 490 g/mol) was also characterized with polystyrenes in n-heptane and ethanol. The results are given in Figure 6.12. The experiments were conducted in the sequence THF, ethanol, n-heptane, n-heptane and ethanol again. As the results of the second measurements were comparable, only the results of the first run are given in the figure. The rejection curves clearly illustrate that similar to the investigations with polymeric membranes, substantial differences exist between the rejections in the different solvents. THF provides the highest rejections. The rejections in ethanol are about 40 % lower and polystyrene in n-heptane is not retained at all up to a solute size of 2000 g/mol. Those results contradict the expectations based on the pore flow theory. If rejections are solely dependent on the different viscosities of the solvents and the effective molecular solute size in the solvent, rejection curves should only be shifted along the x-axis. Even the polarity of the solvents cannot solely explain those

extreme differences in rejections. The polarity as well as the viscosity increases from n-heptane < THF < ethanol, whereas rejection increases from n-heptane to ethanol and THF.

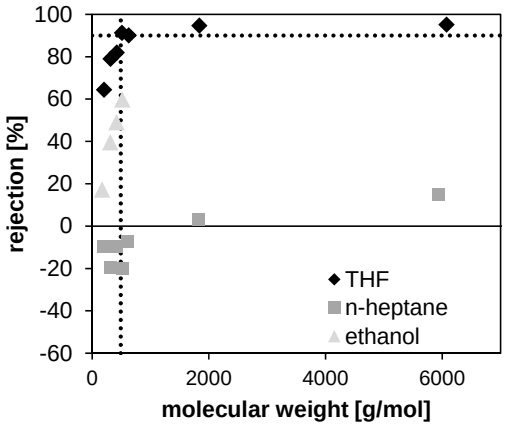

Figure 6.12: Rejection curves of the DEA membrane (N0265) determined with polystyrene in n-heptane, ethanol and THF

It has been proposed for solvent filtration, that the performance of a membrane is dependent on the first medium permeating the membrane [125]. As the rejections in THF (cyclic solvent) were always better than the rejections in other solvents, a similar effect due to cyclohexane used for permporometry could be assumed here. In order to check the influence of the precharacterization by permporometry on the performance of the membranes, nine membranes were produced via the same synthesis route as membrane N0328. Three of them were characterized by permporometry to ensure the quality of the membranes. Subsequently, the rejection curves of one precharacterized membrane and two membranes without a pretreatment were determined in THF, ethanol and n-heptane, respectively. The results are shown in Figures 6.13-6.15. Permporometry results of the membranes are given in Figure B.4.

Rejections in THF (Figure 6.13) seem to be better after preconditioning with cyclohexane by permporometry measurements. This may be due to the structural similarity between THF and cyclohexane which are both cyclic solvents. Cyclohexane could potentially adsorb at the pore walls whereby the THF could pass easier through the pores by reason of a higher affinity. However, a deteriorated performance based on defect pores cannot be excluded because the quality of the supports and the separation layer could not be verified beforehand.

If a permanent solvent layer is really formed at the first use of the membrane, the rejections in ethanol of a precharacterized membrane should be lower than the rejections of an untreated membrane because the affinity of the nonpolar cyclohexane to the small polar ethanol molecule

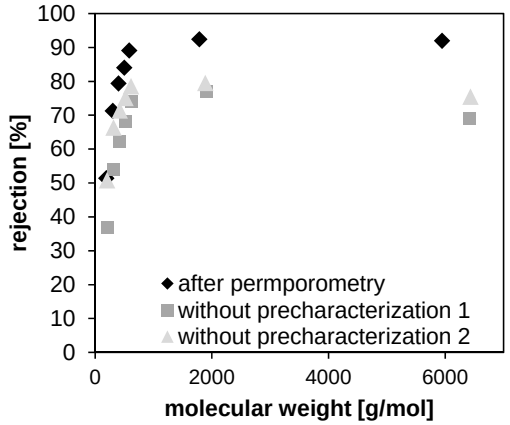

(a)

Figure 6.13: Rejection measurements of membranes containing DEA in THF. One membrane was characterized with permporometry prior to the rejection measurements (N0403), the other two membranes were measured untreated (N0406, N0407)

is very small. Figure 6.14 illustrates that the measured results substantiate this hypothesis. The rejections after the permporometry measurement are negative meaning that the solutes preferentially permeate instead of the solvent. Since the solute (polystyrene) is similar to the precharaterization solvent (cyclohexane), the affinity is higher than to ethanol and therefore permeation could be preferred. In particular the rejection of the smallest molecules is significantly worse than that observed with the untreated membrane. For the larger molecules this effect might be extenuated due to sterical hindrance.

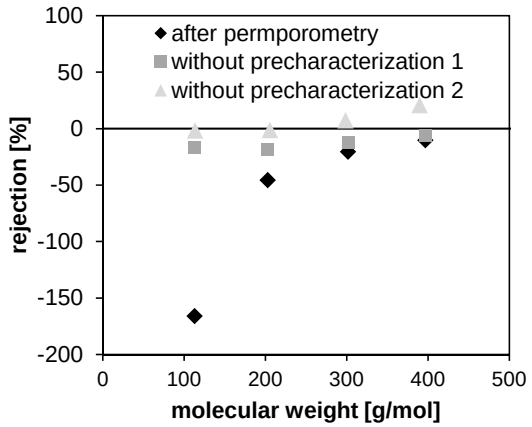

(a)

Figure 6.14: Rejection measurements of membranes containing DEA in ethanol. One membrane was characterized with permporometry prior to the rejection measurements (N0405), the other two membranes were measured untreated (N0410, N0411)

The significantly worse results of the rejection measurements compared to the results achieved with membrane N0265 (c.f. Figure 6.12) can be attributed to the high amount of defect pores (relative permeance at 5 nm = 8 %) and the higher mean pore size (c.f. Figure B.4c). Furthermore, the high rejections measured with membrane N0265 might be also an effect of the history of the membrane because THF was the first solvent in contact with the membrane after the permporometry measurement. Since THF is a more polar solvent than cyclohexane, this pretreatment could influence the rejection positively similar to the negative effect of the cyclohexane pretreatment.

Rejection curves in n-heptane are given in Figure 6.15. Here, no differences between the membranes could be identified. None of the molecules were retained by any of the membranes.

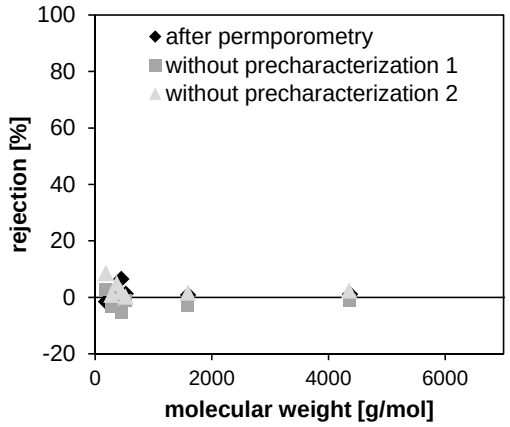

(a)

Figure 6.15: Rejection measurements of membranes containing DEA in n-heptane. One membrane was characterized with permporometry prior to the rejection measurements (N0404), the other two membranes were measured untreated (N0408, N0409)

The permeate fluxes of the measurements are given in Table 6.2. Following the above theory, one would expect significant differences in permeate flux particularly for ethanol. Here, no distinctive effects are identifiable. A high amount of measurements would be necessary to evaluate the results statistically since no characterization data are available for the untreated membranes.

Concluding, some differences due to the pretreatment of the membranes with cyclohexane in permporometry measurements could be identified. These, however, cannot solely explain the

Table 6.2: Permeate fluxes of THF, ethanol and n-heptane of type 2 membranes with and without precharacterization

	THF [l/m^{2}h]	Ethanol [l/m^{2}h]	n-Heptane [l/m^{2}h]
after permporometry	200	270	170
without pretreatment 1	350	400	230
without pretreatment 2	200	200	400

large change in rejections for different solvents in ceramic OSN membranes. For instance, the membranes show no rejection in n-heptane independent of the pretreatment. This discrepancy should be a topic of further research and is believed essential for a successful implementation of ceramic OSN membranes in industry.

In order to check the influence of different solvent properties on the rejection, further rejection measurements were conducted. The solvents THF, toluene, MTBE and ethyl acetate have been selected which are partially similar and partially differing in terms of their different properties (c.f. Table A.3). The rejection curves of the four solvents measured with polystyrene are illustrated in Figure 6.16. Rejections occur in the order THF $\geq$ ethyl acetate $\gg$ toluene $\geq$ MTBE.

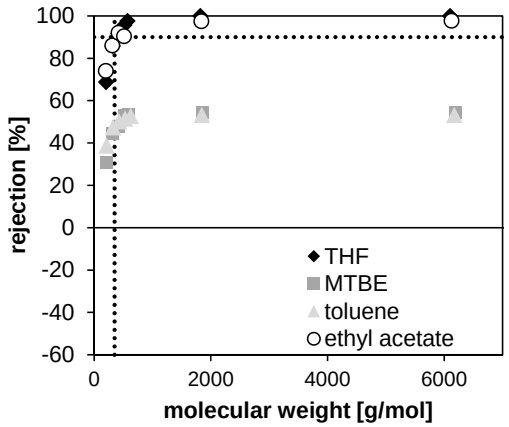

Figure 6.16: Rejection curves of the DEA membrane (N0328) determined with polystyrene in THF, MTBE, toluene and ethyl acetate

The order of the solvents concerning several solvent properties is given in Table 6.3. Comparing the order of the rejections and that of the properties, the main influence can be attributed to those properties related to the hydrophobicity. The order of the rejections correlate with the order of

the dipole moment and the polarity and roughly the trend of the solubility parameter.

Table 6.3: Order of THF, MTBE, toluene and ethyl acetate in terms of different solvent properties

Solvent property	Order of the solvents
Molecular weight	THF < MTBE = ethyl acetate < toluene
Molar volume	THF < ethyl acetate < toluene < MTBE
Viscosity	MTBE < ethyl acetate < THF ≈ toluene
Dipole moment	toluene < MTBE < ethylacetate ≈ THF
Polarity	toluene < MTBE < THF ≈ ethyl acetate
Solubility parameter	MTBE < toluene ≈ THF = ethyl acetate

Another explanation could be an adsorption of the solvent molecules at the pore wall. If the solvent molecules form a layer, the effective pore diameter is dependent on the molar volume of the respective solvents. This is in accordance with the order of the rejections and the reverse order of the molar volume of the solvents. THF, which has the smallest molar volume, forms the thinnest layer and allows for a flux of the solvent through the smaller pores. The larger the solvent, the more pores are blocked by the formed layer. Transport has to occur more and more through the larger defect pores where solutes are less retained. Since fewer pores are available for solvent permeation, the solvent fluxes decrease for solvents with higher molar volumes.

This theory is also confirmed by the permeate fluxes (see Table 6.4). The permeate fluxes are in the chronological order of the experiments. It is noticeable that the viscosity of the solvent seems to have no significant impact while this property plays the dominant role in the assumed pore flow models. However, it has to be mentioned that the measured values could also be influenced by pore blocking of the polystyrenes.

6.2.4 Rejection of specialty chemicals

The transferability of the results to the specialty chemicals and the applicability of ceramic membranes in a multi-purpose process environment has been verified by rejection measurements according to the experiments conducted to develop the heuristic (chapter 5). The rejections of the membrane N0265 in the solvents THF, n-heptane and ethanol for the substances presented in Table 5.3 were determined. The results are presented in Figure 6.17a.

Table 6.4: Permeate fluxes determined for membrane N0328 in the chronological order of the experiments

Solvent	Permeate flux $[l/m^2h]$
THF	45
ethyl acetate	45
MTBE	8
toluene	10

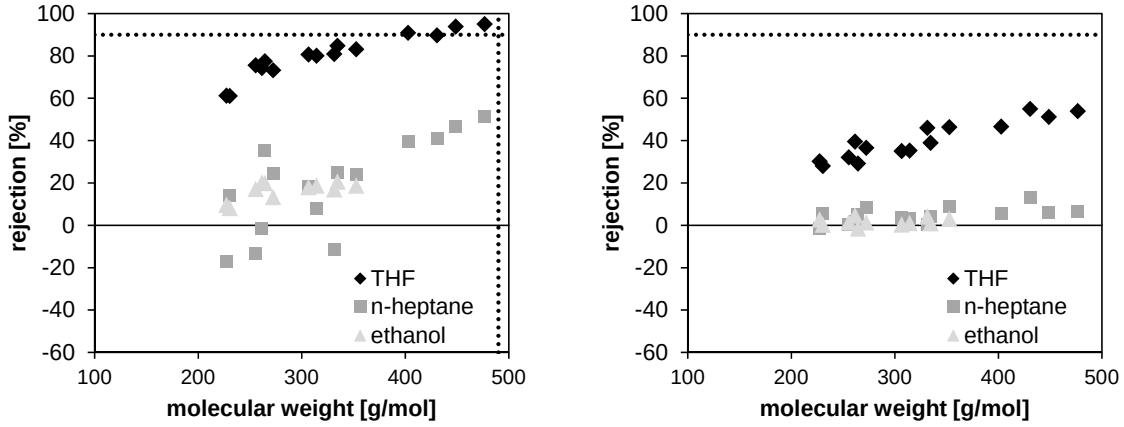

(a) (b)

Figure 6.17: Rejections of specialty chemicals in ethanol, THF and n-heptane vs. their molecular weight.

a) N0265 (Values taken after 180 min at 30 bar transmembrane pressure)

b) N0346 (Values taken after 60 min at 20 bar transmembrane pressure)

The MWCO of 490 g/mol determined with polystyrenes in THF is symbolized by the dotted line. The rejection of the specialty chemicals in THF substantiate the MWCO. The rejections in heptane and ethanol are significantly lower as well as with polystyrenes. This type of membrane shows once more a strong dependence of the rejection on the solvent. Interestingly, a similar picture emerges for the rejection of the ceramic membrane in heptane as for the DuraMem® 200 (c.f. Figure 5.10). Exactly the same substances deviate from the general trend. These are the nonpolar (no polar functional groups) substances C, D and F among the two core substances, which attract attention by higher rejections than the trend, and substance J having a significantly lower rejection. The latter is the only substance with a polar endgroup among the three core molecules. Ceramics are in general polar materials and despite the hydrophobization the mem-

brane is probably rather polar. Nonpolar molecules, especially those of low molecular weights, are therefore retained better. Solutes with polar functional groups are retained worse due to the higher affinity to the membrane. Possibly, molecules with polar endgroups might be oriented to the membrane and thus permeation through the pores is simplified for the elongated substances. Nevertheless, solute properties even seems to have an influence on the rejection of ceramic membranes at least in the range of narrow pores. In order to prove whether the behavior is influenced by the complexation agent, the rejections of the specialty chemicals were investigated with a membrane manufactured without DEA. These results are presented in Figure 6.17b. In comparison, there are no differences concerning the influence of the solvent, except for the lower rejections caused by the significantly higher MWCO. Differences in rejection due to different functional groups become marginal as it is the case with higher MWCO polymeric membranes as well. These results indicate interactions between ceramic membranes, solvent and solute to a similar extent compared to polymeric membranes.

6.3 Rejection modeling of ceramic membranes

This chapter [2] aims to identify a transport model for OSN with ceramic membranes that allow for acceleration of process development due to the prediction of the membrane process parameters as rejection and permeate flux. Furthermore, a suitable model would enable the simulation of the complete production process including the effects of a membrane module as well as preceding and subsequent downstream process steps.

6.3.1 Model structure

In order to describe the complex separation behavior of organic solvent nanofiltration, the simulation environment Aspen Custom Modeler^{TM} (Aspen Technology, Inc., Cambridge, Massachusetts, USA) was used. Aspen Custom Modeler^{TM} (ACM) enables the user to implement own models and features a freely self-designable model structure and thus, the model can be easily expanded and modified. The model structure used is illustrated in Figure 6.18.

[2] The content of this chapter was partially adopted from: Blumenschein, S.; Böcking , A.; Kätzel, U.; Postel, S.; Wessling, M.: Rejection modeling of membranes in organic solvent nanofiltration. *Journal of Membrane Science 510*, (2016), 191-200

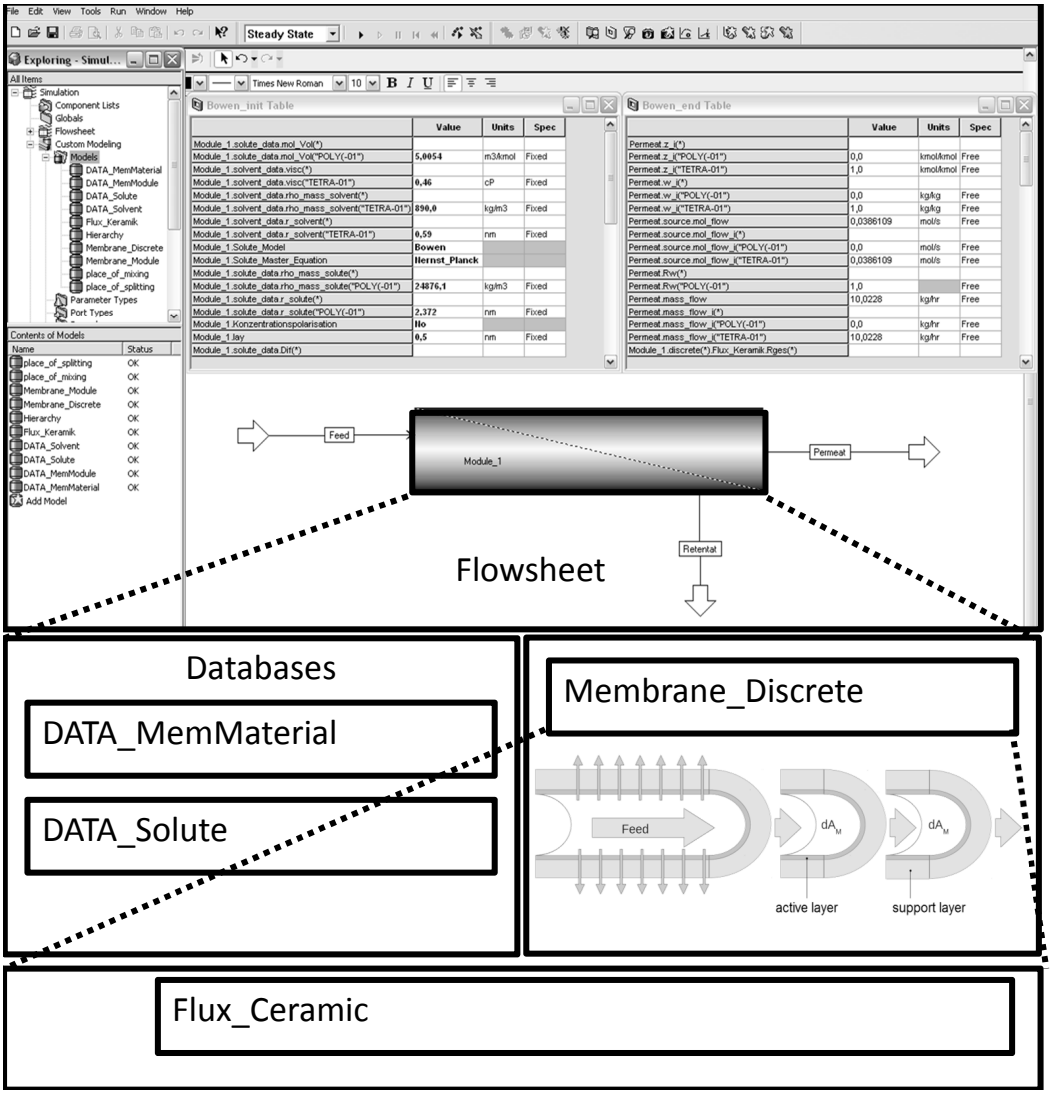

Figure 6.18: Model structure of the ACM simulation for mass transport through ceramic OSN membranes

The model Membrane_Module consists of the submodels Membrane_Discrete, which contains the submodel Flux_Ceramic, and the databases DATA_MemMaterial, DATA_MemModule, DATA_Solvent and DATA_Solute. The submodels DATA contain specific data concerning the membrane material, the geometry of the modules, solvent properties and properties of the solutes, respectively. Membrane_Module transfers the input parameter and required data to Membrane_Discrete. Here, the membrane can be split into discretes to enable the consideration of changes in pressure, concentration, velocity and temperature during the flow across the membrane. The way of discretization of the single channel membranes used in the present work are schematically illustrated in Figure 6.18 as well. The input parameters of every discrete element are passed to Flux_Ceramic where the output parameters are calculated by the actual transport model.

6.3.2 Mass transfer model

The transport model of Bowen and Welfoot [5], presented in chapter 2.3.1.1, has emerged advantageous compared to other transport models due to its flexibility and extensibility and was therefore implemented in the submodel Flux_Ceramic. To adapt the existing model to OSN applications, pore size dependent viscosity (see chapter 2.3.1.1, equation 2.26) and pore size distribution (see chapter 2.3.1.1, equation 2.29) of the ceramic membrane were implemented. Unknown solute parameters such as molar volume, solute radius and diffusion coefficient were estimated in dependency of the respective solvent. The values calculated for the polystyrenes are listed in Table B.2.

Molar volume

The molar volume of the respective solutes was estimated by the group contribution method of Fedors [158] assuming independence on the solvent. The solute molecules are split in several groups (CH_3, CH_2, e.g.) for which fractional values can be found in [158]. The sum of the individual contributions results in the total volume of the solute.

Solute radius

Assuming no interactions of the solute molecules due to the low concentrations, the radius of the

solutes in dependence of the solvent can be calculated by a combination of the Wilke-Chang-Equation (Equation 6.5) and the Stokes-Einstein-Equation (Equation 6.6). The association parameter ξ of the solvents has been taken from Baerns et al. [176].

$$D_{sS} = 7.4 \cdot 10^{-8} \frac{\sqrt{\xi M_S} T}{\eta_S v_s^{0.6}} \tag{6.5}$$

$$2r_s{}^S = \frac{k_B T}{3\pi \eta_S D_{sS}} \tag{6.6}$$

The ratio of two radii of the identical solute in different solvents is now given by:

$$\frac{r_s{}^{S2}}{r_s{}^{S1}} = \frac{\sqrt{\xi M_{S1}}}{\sqrt{\xi M_{S2}}} \tag{6.7}$$

An empirical relation between water and an organic solute was found by Van der Bruggen and Vandecasteele [177].

$$2r_s{}^W = 0.065 M_s^{0.438} \tag{6.8}$$

The combination of Equation 6.7 and 6.8 allows for the estimation of the solute radius.

Diffusion coefficient

The diffusion coefficient was calculated by equation 6.5 which implies that the molar volume of the solute is known.

6.3.3 Results of modeling

The rejections were initially simulated with the constant standard process parameters and the properties of THF, polystyrene and the membranes. Molar masses and densities of the mixtures of the polystyrenes were taken over from ASPEN Properties. Membrane specific data were obtained from the manufacturer and their permporometry measurements. According to the manufacturer the active separation layer has a thickness of $\sim$ 50 nm. The pore length was assumed to be twice the thickness. The porosity of the membranes is between 0.3 and 0.4 and was set to 0.35 as a standard in the simulation. Pore radii and the defect pores are an outcome of the permporometry measurements. The default for the maximum pore radius r_{max} was set to twice the mean pore radius r_p of the respective membrane. The MWCO was identified by rejection measurements of polystyrenes in THF (c.f. chapter 6.2.2). Table 6.5 gives an overview about the experimentally determined characteristics of the used membranes.

Table 6.5: Ceramic membranes used for the verification of the rejection modeling

Name	Hydrophobization by	MWCO [g/mol]	Mean pore radius [nm]	Defect pores
N0157	phenolic resin	1200	0.78	ca. 1% rel. permeance
N0265	DEA	490	0.55	ca. 6% rel. permeance
N0288	phenolic resin	2000	0.35	ca. 8% rel. permeance
N0328	DEA	350	0.3	ca. 2% rel. permeance
N0330	phenolic resin	650	0.43	ca. 4% rel. permeance

Due to the simple geometry of the modules radial parameter changes are assumed to be negligible, therefore, the membrane modules were split in one-dimensional discrete elements (Number of discretes was set to 5). Changes in concentrations and velocity are considered between the discretes. However, pressure and temperature differences are not expected because of the short and thermally insulated membrane module and are thus neglected. For the presented results, concentration polarization was not incorporated as the concentrations applied in the verification measurements were very low.

Rejections of the polystyrenes could thus be calculated without any fitting parameter. A selection of those simulation results for four membranes with different nominal pore sizes in comparison with the experimentally determined rejections are illustrated in Figure 6.19 and 6.20. The calculated rejections are shown without pore size distribution and with standard deviations of the pore size distribution of 0.1, 0.2 and 0.5.

As expected the calculated rejection curves for membranes with narrow pore sizes (< 0.5 nm) given in Figure 6.19 show a steeper slope than those with larger pores sizes. The rejection is lower for bigger standard deviations and nominal pore sizes. In total, the differences between the rejections gradually decrease by increasing the standard deviation. The simulated curves are generally in good agreement with the experimentally determined rejections of the polystyrenes. The simulated rejections of membrane N0328 exhibit the closest agreement with the experimental results which are represented excellently by the proposed model with a pore size distribution of 0.1. Overall, there is a recognizable tendency that membranes with mean pore sizes $r_p \leq 0.5$ nm (c.f. Figure 6.19) show the best match with higher standard deviations whereas membranes with mean pore sizes $r_p \geq 0.5$ nm (c.f. Figure 6.20) give the best fit with the experimental results without pore size distribution or with very low standard deviations.

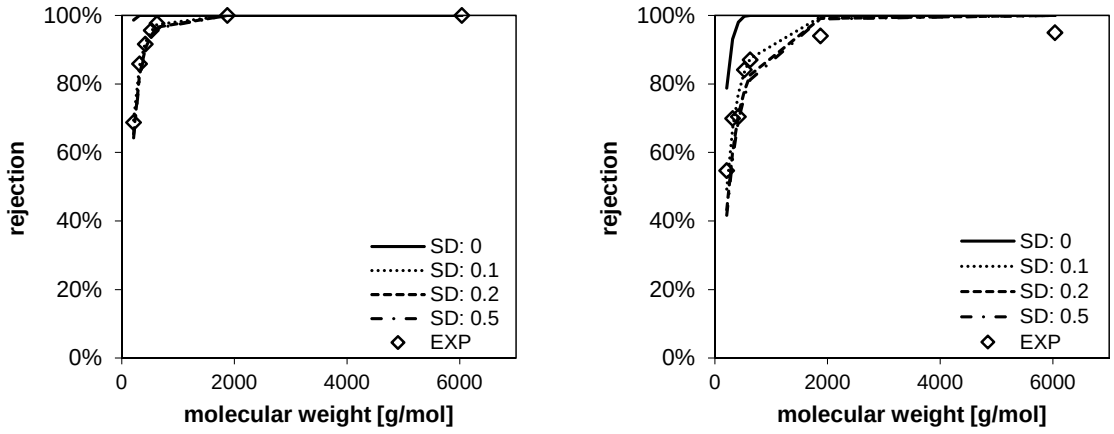

(a) (b)

Figure 6.19: Simulation results of rejection of polystyrene in THF with different standard deviations of the pore size distribution (σ_p =0; 0.1; 0.2; 0.5) and the experimental results

a) N0328 ($r_p = 0.3$) b) N0330 ($r_p = 0.43$)

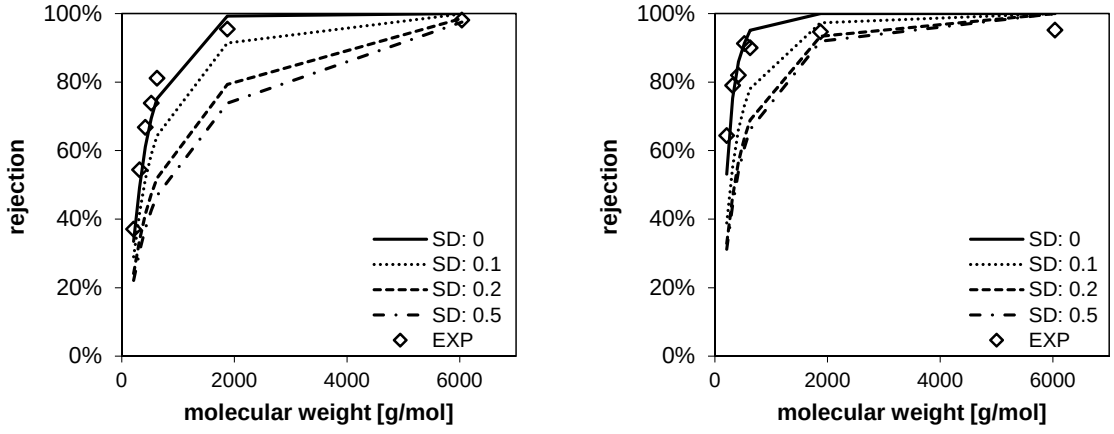

(a) (b)

Figure 6.20: Simulation results of rejection of polystyrene in THF with different standard deviations of the pore size distribution (σ_p =0; 0.1; 0.2; 0.5) and the experimental results

a) N0157 ($r_p = 0.78$) b) N0265 ($r_p = 0.55$)

This is in accordance with the observation that defect pores have higher impact the lower the pore size is (c.f. Table 6.5). Due to the higher portion of permeation of solvent and solute through the defect pores, rejections of membranes with very narrow pores are slightly lower than expected. This can be reflected by a higher standard deviation. However, the simulated results for solutes with high molecular weight are overestimated compared to the experimentally observed rejection. Those incomplete rejections due to the defect pores cannot be described by a variation of the standard deviation of the pore size (see Figure 6.19b). Pore flow models are based on the assumption that molecules with diameters larger than the pore size ($\lambda \geq 1$) are completely retained. Rejection will converge in any case to 100 % rejection and hence will not stagnate at lower rejections. Incorporation of concentration polarization would not improve the accordance of the rejection of larger molecules with the experimental results. Even by an adjustment of the maximum pore size, this effect cannot be represented (discussion in chapter 6.3.3.1). Another opportunity to reflect the influence of the defect pores would be the implementation of a bypass stream or a bimodal pore size distribution.

In Table 6.6 the experimental and simulated permeate fluxes according to equation 2.13 are given. It is obvious that measured fluxes are significantly lower than the calculated ones. This could be attributed to the fact that solvent molecules are larger than water molecules and thus the amount of pores, which are available for transport, is less. Furthermore, the solvent transport might be hindered by the lower affinity of solvents to the ceramic material compared to water. Another explanation is a lower porosity of this membrane type for example due to a higher complexation by DEA or phenolic resin and therefore tortuosity is higher than given. By a simple permeation experiment prior to the simulation, an effective porosity and tortuosity can be easily fitted to reflect the permeate fluxes as well, however, permeate flux prediction was not in the focus of this work since rejection turned out as the more relevant process parameter in the production of specialty chemicals.

6.3.3.1 Influence of membrane parameters on the modeling results

A sensitivity analysis for the membrane model was performed with respect to some membrane parameters in order to verify their influence on the simulated rejections and the opportunity to improve the reproduction of the experimental results by an adjustment for membranes, which show indications of defect pores in permporometry. First, the influence of the estimated value

Table 6.6: Calculated and measured permeate fluxes in $\left[\mathrm{l/m^2h}\right]$

Name	Permeate flux $\left[\mathrm{l/m^2h}\right]$ experimental	simulated	Faktor sim/exp
N0157	240	3966	16.5
N0265	110	1998	18.2
N0328	70	595	8.5
N0330	115	1192	10.4

of r_{max} was investigated. In Figure 6.21 it is shown that even an enlargement of the maximum pore size r_{max} would not reflect the incomplete rejection of membranes with defect pores since the largest polystyrenes are still larger than the maximum pore size. Higher limits of the pore size would also reduce the rejection of the smaller molecules. However, in case of high amounts of defect pores, it might be reasonable and helpful to increase the maximum pore size in order to improve the accordance with the actual rejections and implement a bimodal pore size distribution or a bypass stream.

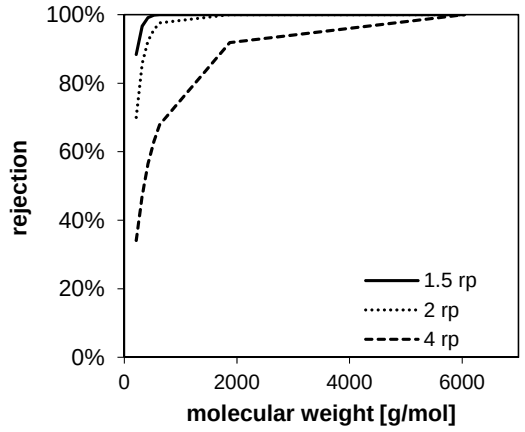

Figure 6.21: Influence of $r_{max}(= x \cdot r_p)$ on calculated rejections of polystyrene in THF (exemplarily shown for membrane N0328 with σ_p =0.15)

An example for the clear improvement of the results with a variation of the standard maximum pore size is given in Figure 6.22. Even the calculation with the highest standard deviation (0.95; $r_{max} = 2\, r_p$) could not reflect the experimental results, but an increase of r_{max} to 2.5 r_p enables the representation of the rejections of the small polystyrenes. As mentioned above, however, the incomplete rejection of large molecules cannot be reflected. The only possibility to represent the permeation through the defect pores is thus the implementation of a bypass for the permeation

through the membrane.

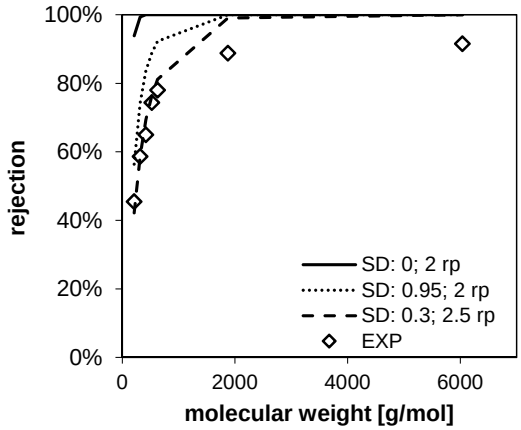

Figure 6.22: Improvement of calculated rejections of polystyrene in THF by enlargement of the maximum pore size r_{max} (exemplarily shown for membrane N0288)

Other membrane specific values like the pore length and the porosity have almost no influence on the calculated rejections because porosity and tortuosity have only an indirect influence on the rejection in the proposed model. Only the solvent permeability is changed by these parameters. An adaptation of those parameters can thus be used to represent the fluxes without a significant influence on the calculated rejections.

6.3.3.2 Variation of process parameters

In order to check the suitability of the model for process design, the representation of the influence of the process parameters was verified. Since membrane N0328 showed the best accordance of the simulated rejections with the experimental ones at standard conditions, this membrane was selected for further experimental investigations. To analyze the effect on the simulation the pressure value in the model was varied between 5, 20 and 30 bar. The rejection of the solutes increases with increasing pressure (see Figure 6.23). Due to the ratio of solute radius to pore radius, the effect is lower for bigger solutes than for smaller ones. There is no effect for solutes with ($\lambda \geq 1$). The pressure effect on rejection decreases with increasing pressures.

This result can be explained by the equation for the modified Peclet number (see equation 2.22). With increasing pressure this modified Peclet number increases and the subtrahend in the equation for the rejection (see equation 2.21) decreases. For high pressures, the influence of the modified Peclet number is smaller due to the exponential function.

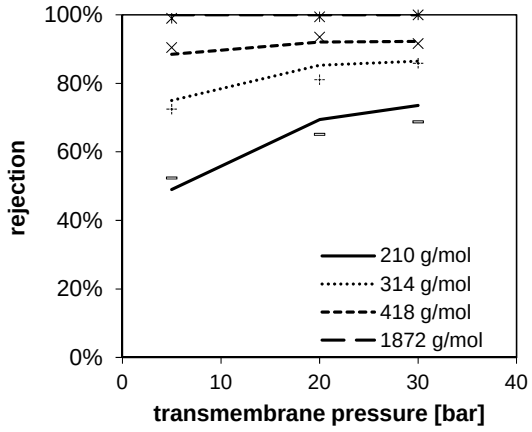

Figure 6.23: Influence of transmembrane pressure on the calculated (lines) (σ_p =0.1) and experimentally determined rejections of polystyrenes (symbols) in THF at 20 °C, 6 l/min of membrane N0328

The influence of temperature and feed velocity is presented in Figure 6.24. Variation of temperature shows only a marginal effect on the rejection which is in accordance with the experimental validation. Feed flow has no significant influence on rejection which was confirmed by the experimental measurements as well. As expected the transmembrane pressure emerged as the most crucial process parameter.

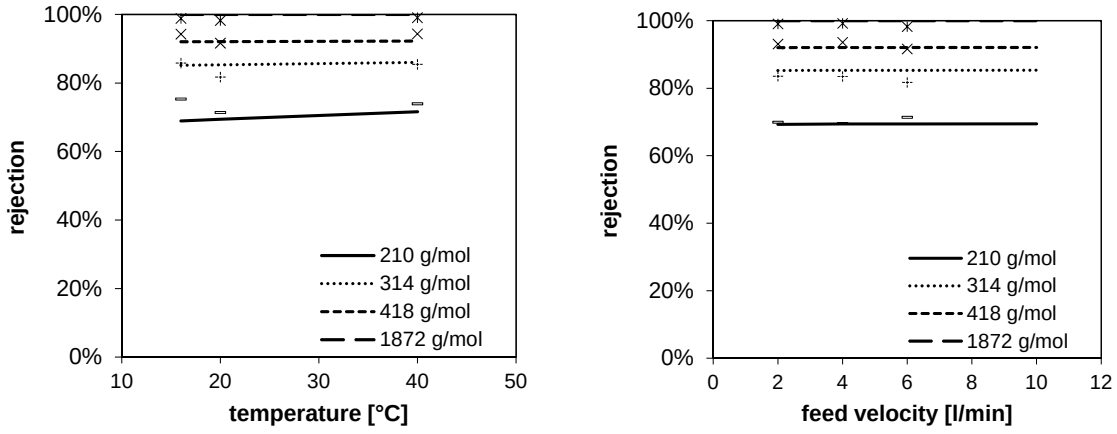

(a) (b)

Figure 6.24: Influence of

a) temperature at 6 l/min b) feed velocity at 20 °C

on the calculated (lines) (σ_p =0.1) and experimentally determined rejections of polystyrenes (symbols) in THF at 20 bar of membrane N0328

6.3.3.3 Influence of solvents on the modeling results

As presented in chapter 6.2.3 the use of some solvents leads to unexpected bad rejections. The influence of the solvent on the calculated rejection is investigated by changing the solvent to n-heptane and ethanol. Using solutions with ethanol the solute sizes are slightly increased while in n-heptane the sizes are decreased (see Table B.2). Because of the different solute sizes in the different solvents, the rejections differ as well in dependency of the solute sizes r_s and hence the calculated rejection decreases in n-heptane and increases in ethanol (c.f. Figure 6.25). However, these results do not reflect the experimental measurements. Although the calculated rejections in different solvents exhibit significant differences (presented in Figure 6.25), the drastic discrepancies determined in the measurements (c.f. Figure 6.12) could not be reflected by the simulation. In description of rejection in different solvents, the model fails. As already mentioned in chapter 6.2.3 the transport in ceramic OSN membranes is less investigated and these large differences in rejection in different solvents are up to now not sufficiently explained. A possible theory might be that different solvents create differing layers in the ceramic pores or even block them in dependence of the affinity between the solvents and the membrane material. With further insights into the root causes of this behavior, the model could be easily extended, e.g. by a solvent dependent pore size.

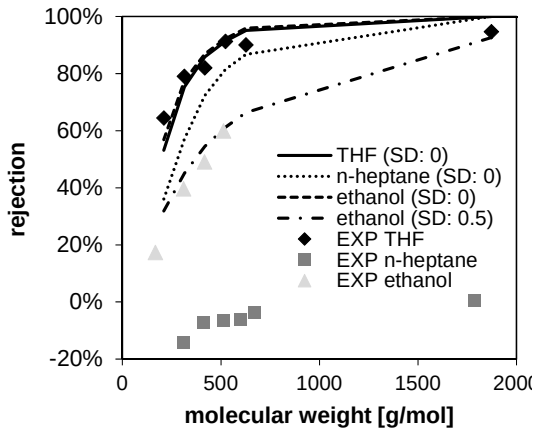

Figure 6.25: Calculated rejections (lines) of membrane N0265 in comparison to experimentally determined rejections of polystyrene in THF, n-heptane and ethanol (symbols)

The predicted effect of the solute size is thus superseded. However, by using different standard deviations for the pore size distribution for the different solvents these effects can be partially

compensated. This is shown in Figure 6.25 by the example of ethanol rejections, which are in good accordance with the simulated results using a standard deviation of 0.5 whereas the rejections in THF are reflected best without a standard deviation of the pore size.

6.3.3.4 Transferability of the modeling results to other solutes

In order to check the transferability to other solutes and the adaptability to real life applications, the rejections of the specialty chemicals (see Table 5.3) were measured with one of the membranes (N0265). Similar to the measurements with polystyrenes, the calculated rejections are in good agreement with the experimental results in THF (see Figure 6.26) whereas experimentally determined rejections in ethanol and heptane were significantly lower than predicted with the model.

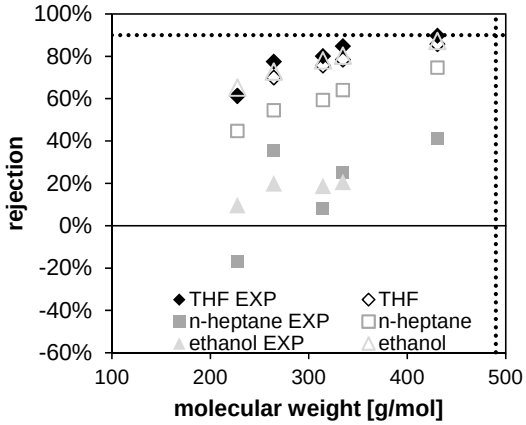

Figure 6.26: Calculated rejections of specialty chemicals (open symbols) of membrane N0265 in comparison to experimentally determined rejections (filled symbols) in THF, n-heptane and ethanol

6.4 Conclusion

Currently, ceramic membranes do not keep the promise of several advantages over polymeric membranes. Permeate fluxes of narrow-pore ceramic membranes with acceptable rejections of molecules in the range between 200 and 600 g/mol are in the same range as polymeric membranes or even lower. Contrary to widespread expectations, even the rejection of ceramic membranes depends substantially on the specific solvent just like the polymeric OSN membranes. This dependency and the influencing factors should be further investigated in the future in order

to enable industrial application for ceramic OSN membranes. The reason for the dependence on the solvent remains unclear, but affinity effects seem to have a higher impact than properties typically influencing pore flow. Further investigations are necessary to clarify this phenomenon. An application of ceramic membranes in a multi-purpose production environment is thus not (yet) conceivable at this point in time.

Permporometry was identified as a suitable and helpful tool for quality control of the membrane. It might be a useful tool for the customer as well as it allows for the identification of a good OSN membrane (in THF). Based on the permporometry measurements substantial requirements of a ceramic membrane for organic solvent nanofiltration were identified: One the one hand, pores have to be small enough to retain the molecules, but big enough to enable solvent permeation (mean pore size >0.5 nm in permporometry). The smaller the pores, the more difficult is the prevention of permeation through defect pores. Elimination of defect pores is therefore the most important target for the development of tighter ceramic OSN membranes besides the reduction of the pore size.

A transport model based on the original aqueous nanofiltration model of Bowen and Welfoot [5] was developed which is able to predict rejections of ceramic OSN membranes. The rejections of polystyrenes as well as of specialty chemicals in THF could be very well predicted without any fitting parameters in the model. Membrane parameters necessary for the model were given by the manufacturer or obtained by permporometry measurements (conducted by the manufacturer). However, the effect of defect pores cannot be reflected by the model. Nevertheless, rejections of small polystyrenes can be represented very well. Since the focus of an OSN membrane is the rejection of molecules smaller than 1000 g/mol, this is adequate for process simulation within this molecular range. A further restriction of the model is its applicability only for suitable solvents so far. The model fails in terms of the description of various solvents as n-heptane or ethanol, because unknown interaction effects occur here. The dependencies and the influencing factors should be further investigated in future in order to modify the model regarding rejection prediction for a wide range of solvents. The identification of such parameters would allow the development of an heuristic for membrane selection of ceramic membranes and thus an equalization of ceramic and polymeric membranes concerning their application in process development.

Moreover, the calculated fluxes obtained with the proposed model are overestimated by a factor of 10-15. By fitting porosity and tortuosity to experimentally determined fluxes this gap can be easily closed without any effect on the rejection curve because these parameter do only affect

the solvent flux. The clarification of the effects influencing the permeance reduction has to be a focus in further investigations anyway. Nevertheless, the proposed model offers a solid basis for further development and expansion to different solvents.

7 Refined potential assessment

In this chapter the approach to estimate the potential of OSN in a multi-purpose environment presented in chapter 4 is refined based on the results and the knowledge gained from chapter 5 and 6.

7.1 Technically realizable potential

The next level of detail in the assessment of the potential of OSN (c.f. Figure 4.1) considers technical limitations or restrictions regarding an implementation within a multi-purpose production of specialty chemicals. With the help of the insights gained in the previous chapters, it is now possible to refine the assumptions made for the membrane performance in calculation of the theoretical potential in chapter 4.2.

The following aspects will be revised in this chapter to estimate the technically realizable potential:

- **Maximum solute concentration in the retentate**:
  The maximum retentate concentration $w_{R,max}$ influences the degree of concentration by the OSN process and thus the process time. Consequently, this parameter affects every term of the potential (c.f. equation 4.1).

- **Rejection**:
  In chapter 4.2 this parameter emerged as the most important factor regarding the potential of OSN within a specialty chemical production environment. A general rejection of 90 % was assumed in the theoretical potential as no adequate short-cut models were available to estimate it. Based on the insights gained in chapter 5 and 6, which allow for a pre-estimation of the expected rejection, it now becomes possible to fine tune the potential.

- **Feasibility of the process**:
  Last but not least, the feasibility of the processes has to be ensured in terms of suitable membranes, requirements for the OSN plant, technical limitations, etc.

In order to define the maximum retentate concentration, the solubility of the substances in the respective solvents has to be taken into account. To prevent crystallization in the filtration process, 90% of the solubility limit is taken as $w_{R,max}$. Though crystallization will not start at the solubility limit but will need a certain amount of oversaturation, it has to be kept in mind that a safety buffer must be used. This is because of concentration polarization effects which cause higher retentate concentrations at the membrane surface than in the bulk solution. Some solubility data are taken from an internal solubility database of Merck KGaA. If no solubility data were available, they were estimated from similar products or solvents.

With the help of the rejection rules (chapter 5.5.1) and the developed heuristic (chapter 5.5.2), the assumed rejection of 90% in each process in the calculation of the theoretical potential (c.f. chapter 4.2) could be revised. Ceramic membranes are not considered in this estimate because the influence of the solvent is not sufficiently understood and rejections are currently lower than those of polymeric membranes. In Table C.1, C.2 and C.3 the products, their solubility parameters and the solubility parameters of the solvents as well as the estimated rejections, which are used for the assessment of the technical potential, are given. To verify the suitability of the estimation process of rejection, several products were experimentally tested in real production solutions to incorporate all additional substances and their potential effects on the membrane performance. The comparison between the estimated and the experimentally determined rejection values is presented in Table 7.1. In general, the experimental results prove the recommendation of the membrane type in the heuristic and the measured rejections correspond very well to the estimated values.

After these refinements to some of the parameters necessary for the calculation of the potential, the processes of interest are scrutinized with regard to the practicability of a separation by OSN, special requirements to the plants and the membranes because of their use for specialty chemicals as well as technical limitations and demands due to the implementation in a multi-purpose environment. First of all, the different processes (i.e. the solvents involved therein) which are taken into account for the potential assessment were proven in terms of their compatibility with existing OSN membranes. For some solvents there is still no suitable membrane (e.g. in terms of stability) commercially available. Those processes were excluded from the calculation of the

Table 7.1: Comparison between the estimated rejection and experimental results for several typical production solutions of specialty chemicals (same class as used for the development of the heuristic)

		Estimated		Experimental	
Product	Solvent	Membrane type	R [%]	$R_{hydrophobic}$ [%]	$R_{hydrophilic}$ [%]
P1	THF/n-hexane	hydrophobic	80	66	
P2	THF/n-hexane	hydrophobic	85	79	3
P4	THF/n-hexane	hydrophobic	85	86	41
P14	THF/n-hexane	hydrophobic	50	31	
P20	ethyl acetate/ methanol	hydrophilic	90		88
P27	toluene/ethanol	hydrophilic	90	37	88
P31	ethyl acetate	hydrophilic	85		95

potential. In the scope of this work, the processes in dichloromethane (DCM) are affected in particular.

Technical requirements to the membrane:

Due to the use in a multi-purpose environment, the membrane is exposed to frequent solvent and pressure changes. In the present case, six main solvents are used in the relevant process steps and another six solvents in mixtures with them (c.f. Table C.1, C.2 and C.3). Regarding the practical handling of such solvent exchanges, present data in literature is marginal. The stability of the membrane material during solvent exchanges was thus experimentally-confirmed in this work even with a solvent that causes negative rejections for the specialty chemicals. In Figure 7.1 the rejections of a new PDMS membrane are given in THF and ethanol. In contrast, the rejections of membranes are shown which underwent a solvent exchange from the respective other solvent e.g. firstly ethanol, then THF. As can be clearly seen, there is no detectable difference and thus, separation performances induced by the solvents are reversible. This also proves that negative rejections are not a result of a damage to the membranes. In conclusion, solvent exchanges should not pose a problem for the integration of OSN in a multi-purpose production.

Moreover, an easy clean-up of the membranes is essential due to the high demand of purity for the affected products. Extractables from the membrane may not exceed ppb-levels (some even lower) to secure the performance of the specialty chemical products in their respective

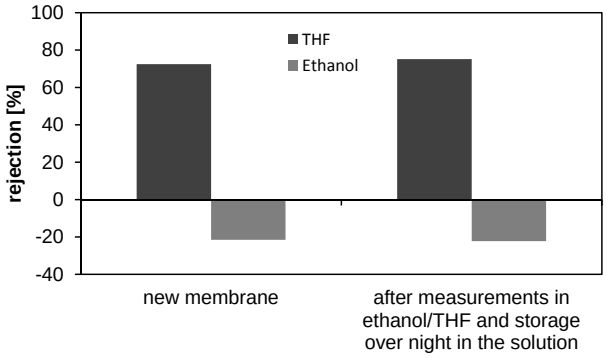

Figure 7.1: Rejections of solute B in THF and ethanol measured with a new membrane (GMT-oNF-2) in comparison with the rejections measured with a membrane which was used in the respective other solvent before

applications. These issues have to be investigated and appropriate cleaning and flushing procedures have to be defined. The general possibility to remove and reduce the extractables to the specified limit has been proven elsewhere [178].

Technical requirements to the plant:

As a basic principle, a multi-purpose filtration plant has to be easy to handle in terms of its weight and dimension, since the plant has to be movable between several STRs within the whole facility. This requires a very compact, lightweight construction with an even weight distribution. Moreover, the filtration plant has to be integrated in the process control system of the production site and needs a connection to every eligible tank reactor. The production site is classified as hazardous (Zone 2 Ex T4 II b), therefore, every device of the plant, like pumps, valves, control elements, etc. demands an ATEX certification for use in zone 2. Furthermore, the plant has to be naturally easy to clean as well as dead volume zones have to be minimized to reduce the risk of contamination by other products.

Another issue to be resolved is the fact that the OSN separation unit has to be able to handle different membrane types because no one available membrane is capable to deal with every solvent in the relevant processes. This could be either pursued by the design of two identical plants which are dedicated for one membrane type. The other possibility would be to design interchangeable membrane modules with good accessibility and safe and contamination-free removal process. However, this requires the storage capacity for the membrane modules and their housings.

Except for the exclusion of processes in DCM, there are no further limitations in the imple-

mentation of OSN in the specialty chemicals production based on the aforementioned technical requirements. With the above refinements, the potential was recalculated based on equation 4.1 and the limitations for considering in the assessment according to equation 4.10. The evaluation of the technically realizable potential results in only five economic processes with an overall potential of 5.13mṀU/a. In Figure 7.2 the single potential of these processes is shown and split in the individual terms contributing to the potential. The technically realizable potential is only about 30$\dot{\%}$ of the theoretical potential. An implementation of these OSN processes would free up 4000 production hours of a stirred tank reactor. This might be a further benefit when production capacities are limited and new equipment is needed.

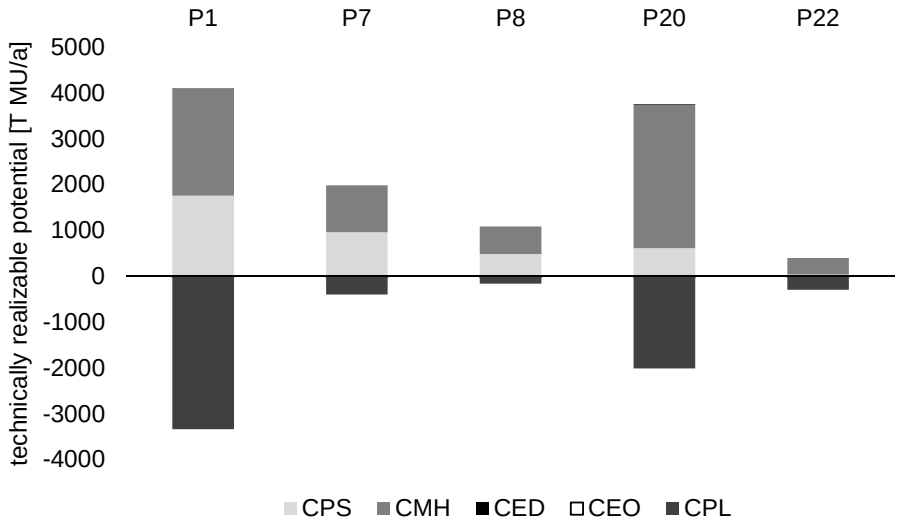

Figure 7.2: Distribution of the different costs on the technical potential (according to equation 4.1) of the realizable five products (costs due to process shortening C_{PS}, costs due to reduction of machine hours C_{MH}, costs for energy demand of distillation C_{ED}, costs for energy demand of OSN C_{EO}, costs due to product losses C_{PL})

This dramatic decrease in potential is mainly caused by the more realistic rejections used for the calculation. Figure 4.4 already emphasized the enormous impact of the rejection on the theoretical potential of an application of OSN in the multi-purpose environment. However, as the potential is strongly dependent on the rejection, this also means that more processes may become economical with the development of new tighter membranes. Especially applications in nonpolar solvents would be of interest for further membrane research.

7.2 Economically realizable potential

To evaluate the economic efficiency of an implementation of OSN in a multi-purpose process environment, some financial key figures will be used to assess the economically realizable potential of an implementation of an OSN plant for product solution concentration in a multi-purpose environment. These are the return on investment *ROI* and the payback period t_A. Return on investment describes the ratio between the profit and the total capital. To evaluate a single investment, it is common to consider the benefit due to the investment in relation to the investment costs I. In the present study the technical potential Pot_{te} accounts for the potential benefit.

$$ROI = \frac{Pot_{te}}{I} \tag{7.1}$$

The capital costs were roughly estimated on the basis of the technical requirements (c.f. chapter 7.1) and includes the purchasing price of the membrane plant, the technical installation (labor costs and infrastructure) and the integration into the process control system. Here, the return flow is 22 %/a.

The payback period t_A depicts the period of time to recoup the investment costs. An useful economic life t_{UEL} of the OSN plant of ten years is assumed. After that time no residual value *RV* of the plant exists. A linear approach was used for the calculation of the payback period because constant sales volumes and constant process conditions are assumed.

$$t_A = \frac{I - RV}{Pr + C_A} \tag{7.2}$$

The profit Pr gained by the new investment is the technical potential of the implementation of an OSN plant reduced by the amortization costs C_A, the weighted average cost of capital and the operating costs C_{OP}. The operating costs contain an annual exchange of the modules, occupancy costs, costs for an annual exchange of the seals and for the exchange of the oil of the pumps.

$$Pr = Pot_{te} - C_A - \frac{I + RV}{2} \cdot wacc - C_{OP} \tag{7.3}$$

To calculate the amortization costs, a linear depreciation is applied.

$$C_A = \frac{I - RV}{t_{UEL}} \tag{7.4}$$

To visualize the calculations, a break-even analysis based on these assumptions is presented in Figure 7.3.

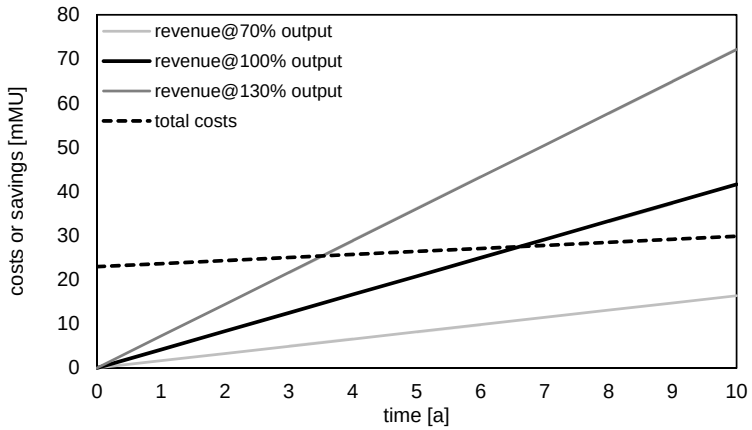

Figure 7.3: Break-even analysis for different production outputs of a two-stage multi-purpose production plant for specialty chemicals

The revenue is presented here by the technical potential reduced by the imputed interests. The total costs are composed of the capital costs and the operating costs of the membrane plant. The break-even-point (BEP) is reached after 6.6 years assuming a constant production output. A production increase and a decrease of 30 % are also incorporated into diagram and show the drastic impact of the output on the BEP (3.5 years and 24 years, respectively). With a typical lifetime cycle of the investigated specialty chemical class of five to ten years, a payback period of two years is usually considered as a positive investment option. An implementation of a multi-purpose OSN plant is thus currently not of high potential. However, when contemplating a three-stage OSN plant (see Figure 7.4), the BEP declines drastically because product losses diminish.

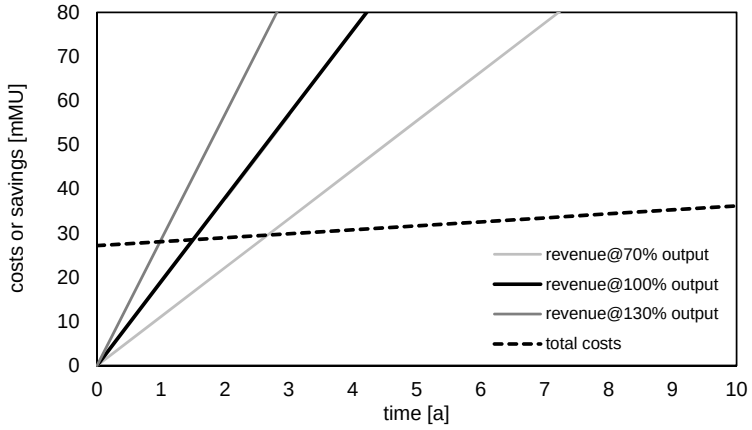

Figure 7.4: Break-even analysis for different production outputs of a three-stage multi-purpose production plant for specialty chemicals

Furthermore, the amount of economic processes which come into consideration in the assessment increases from five to fourteen. Increasing the number of membrane stages, however,

implies an increase of the plant volume as well which should be kept to a minimum in a production environment with very low product volumes and high product values.

As already mentioned, it has also to be kept in mind that an implementation of OSN accomplishes new facility capacity besides the savings on the considered products. This might offer further possibilities for benefits due to higher sales volumes or larger capacity for new products. This potential assessment only includes the potential by current state-of-the art membranes, but the potential might change drastically with new commercialized membranes which enables higher rejections especially in non-polar solvents. Furthermore, only concentration processes were investigated within the scope of this thesis because distillation emerged as a time-consuming production step and the most frequent downstream process. The potential assessment for an application of OSN for purification processes might additionally offer a high potential in a multi-purpose production environment and should be further considered in future.

8 Conclusion and Outlook

The objective of this thesis was the evaluation of the applicability of organic solvent nanofiltration in a multi-purpose process environment in terms of its technical realizability and its economic potential. To assess the potential of a process, performance data of the unit operation are necessary. From a thorough analysis of the literature it became apparent, that due to the young age of this technology and complex interactions between membrane, solvent and solute, neither general mathematical methods nor short-cut models for the determination of the membrane performance parameters exist. Currently, feasibilities of OSN processes have to be verified by experimental measurements. However, targeting an application of an OSN plant in a multi-purpose production, the screening effort for a high amount of different products which are necessary to guarantee a high utilization of the plant is not viable under the consideration of the expenditure of time and the risk to fail. To address this problem, this work was also focussed on improving the understanding of the underlying transport phenomena in OSN and thus the predictability of processes for polymeric as well as ceramic OSN membranes since these are essential for an assessment of potential in a multi product plant.

To identify the most promising application of OSN in a multi-purpose production first, the most typical production steps and downstream operations within a typical production facility were compiled. Distillation for product concentration or solvent exchange emerged as the most frequent process step. A general procedure for the assessment of the economic benefit of OSN was developed thus based on the application of OSN in concentration steps. This general approach was applied with fixed values for the unknown membrane performance parameters. Under these assumptions, an integration of OSN was profitable only for 11 of the 75 considered distillation steps. In a sensitivity analysis several influencing parameters were varied to consider e.g. uncertainties in the estimation of parameters, changes over the entire useful life of the plant, etc. Among the varied parameters, rejection turned out as the most influential parameter. An increasing rejection significantly increased the number of economic processes and thus the potential of

an application of OSN whereas the potential stagnates with increasing permeate fluxes. Based on the decisive importance of rejection, the approaches to investigate the separation behavior of OSN membranes were predominantly focussed on rejection.

To simplify process development and to enable a rough estimate of the performance of polymeric OSN membranes, simple rules for a rough prediction of the expected rejection of a specialty chemicals class had to be identified. For this purpose, a comprehensive study on the performance parameters of polymeric membranes (particularly rejection) was conducted to investigate the influence of the solvents and the impact of the membrane material. A specialty chemicals class, which is usually produced in multi-purpose facilities and which possesses different molecular sizes and diverse functional groups by keeping an unchanged core structure, was selected. To span the three dimensional space of interactions between membrane, solvent and solute over a wide range, solvents of different properties and different membrane materials were investigated. The affinity between the components reflected by the Hildebrand solubility parameters was identified as the most crucial factor determining the membrane performance. This observation was verified by solvents with similar solubility parameters but completely different molecular structures. However, the solubility parameter could not entirely represent all effects on the rejection of the solute. The effect of different functional groups of the solutes was therefore examined by a Design of Experiments and a direct comparison between two solutes which only differ in their functional groups. A positive effect of polar functional groups on the rejection with hydrophobic membranes and vice versa was observed. Subsequently, the findings were verified with differing solvents of similar solubility parameters, membranes of the same material but higher cut-offs and literature data in matters of diverse solutes. In addition, the separation behavior in solvent mixtures was investigated. Overall, the solvent emerged as the most influential factor regarding the solute rejection provoking even differing effects of the solute properties (as molecular weight) and the functional groups on the separation behavior. Besides the collection of rules to roughly predict rejection, these results were also used to address the membrane selection hurdle in specialty chemicals industry: An heuristic to identify the most suitable membranes for a given separation problem was developed. Such an heuristic based on easily accessible solute and solvent properties allows for a fast identification of a suitable membrane which is essential for the high amount of solutes which have to be screened. Furthermore, compared to detailed transport modeling, this approach is also viable if no relevant property parameter is known which is usually the case for most of the products produced in multi-purpose plants. This development drives the decision whether there is a suitable membrane for a given

separation problem even prior to any experimental investigation. It also already gives a hint whether it is economically worthwhile to develop an OSN process which finally yields a signification acceleration of the total development process. Moreover, the assessment of the potential of OSN becomes more realistic as predictability of the membrane performance has been significantly improved. This reduces the risk of failure during the process development and the economic risk of an implementation in production.

Although the solubility parameter of the compounds emerged as a huge help in the prediction of membrane performance, several effects remained which could not be represented by the solubility parameters. To predict these data more precisely, further effort should be put into detailed mass transport description. For solutes with poor availability of material properties, such as the investigated specialty chemicals, empiric models based on a comprehensive data base might be an option to predict membrane performance mathematically and to take further aspects into account. Future work should also focus on the expansion of the prediction of membrane performance parameters and of the heuristic for membrane selection to other material classes and further polymeric membrane materials as well as ceramic membranes. To develop the heuristic into a generalized tool for universal use in process industry, particularly the range of solutes has to be spread significantly considering e.g. different solute geometries and further functional groups to represent typical products of each industrial sector. Besides, the generated heuristic rules consider only the rejection of the solutes. Depending on the specific processes the permeate flux could be an important process factor as well and has also to be taken into account for the identification of the best membrane.

Since ceramic membranes promise decisive advantages like higher chemical stability, no swelling and a marginal solvent dependency for an application in a multi-purpose environment, performance data of ceramic membranes were required as well to gain comparative data against polymeric membranes. However, due to the early stage development of ceramic OSN membranes, the approach here was more focussed on a fundamental understanding of the transport behavior. By investigating the separation of new membranes with tighter selective layers, which were developed in parallel to this work, quality parameters of ceramic membranes for OSN could also be defined. Low mean pore sizes (about 0.6 nm) and especially a very low amount of defect pores (relative permeance at pore sizes > 5 nm) are required to come to low molecular weight cut-offs. Those parameters are most easily accessible with the help of permporometry measurements. Surprisingly, even for ceramic membranes differences in rejections of solutes

with similar molecular weights could be detected in the experiments as well as an influence of the used solvent on the rejection. Furthermore, a history effect depending on the previously used solvent was determined. This combination made it difficult to allocate the root-cause of the observations to one of these effects. Especially in terms of an application of these membranes in a multi-purpose environment, a comprehensive study on the background of the influence of solvents on the separation performance as well as on the history effects induced by different solvents is necessary to keep pace with polymeric membranes. As a prerequisite, membranes with secured, defined pore size distributions and without defect pores are required.

Up to now data about the transport through ceramic membranes in organic solvents was marginal. To improve the predictability of ceramic membrane performance a first approach to describe the transport was developed in this work. Based on a model originally developed for aqueous nanofiltration [5], a transport model for ceramic OSN membranes was generated which was able to predict rejections of polystyrenes as well as of specialty chemicals in THF very well. Even a variation of process parameters such as pressure, temperature and feed velocity was in very good accordance with the model. Required membrane parameters were provided by the manufacturer or obtained by the permporometry measurements. Although the model was not able to reflect the effect of defect pores and the extreme dependency of the solvent on the rejection, it offers a solid basis for evolution as it is simply extendible e.g. by a bimodal pore size distribution to include the defect pores. Future work should intensively focus on the understanding of the transport and the description of the effects of different solvents on the transport mechanism to generate a universally applicable transport model. These investigations should also address the improvement in description of permeate fluxes. Summarizing these results, ceramic membranes are not yet suitable for an application in an multi-purpose process environment at the current state of the art as there are still too many uncertainties e.g. in terms of reproducibility, unknown solvent effects, low fluxes.

Overall, the achievements of this thesis significantly improve the understanding of the separation performance of OSN membranes and the industrial relevance of this technology. The heuristic for membrane selection was verified by real process solutions of the production facility used for the assessment of the economic potential. Furthermore, the knowledge of the applicability of ceramic membranes and their transport behavior could be improved. Thus, this work is an important step to pave the way for OSN to become a standard unit operation in process engineering.

The applicability of OSN was proven in terms of its compatibility to a flexible, interchangeable production equipment and other technical requirements in a multi-purpose process environment. Several technical aspects important for an integration in a multi-purpose production as solvent and pressure changes and plant design were considered and incorporated in the potential assessment. Finally, by means of the insights gained in this work, the first approach for the assessment of the potential of OSN in a multi-purpose production environment could be concretized. This refined economic potential turned out at only a third of the theoretical potential. In this case study, the pay-back period of an OSN plant would thus be higher than 5 years and requires a long run-time which cannot be ensured in case of specialty chemicals. Increasing the membrane stages of the considered plant from two to three stages would significantly increase the potential and more processes would become feasible. However, this would provoke higher plant volume which might be a problem for products with low production volumes. Enhancement of the membranes regarding their rejection capacities especially in very nonpolar solvents such as n-heptane would increase the potential as well. Furthermore, this potential assessment covers only the implementation of OSN to support and shorten concentration steps. An expansion of the assessment to purification tasks or hybrid processes should be pursued to fully exploit the potential of this technology in a multi-purpose process environment in specialty chemicals industry.

References

[1] Tarleton, E. S.; Robinson, J. P.; Millington, C. R.; Nijmeijer, A.: Non-aqueous nanofiltration: Solute rejection in low-polarity binary systems. *Journal of Membrane Science 252*, 1-2 (**2005**), 123–131.

[2] Bowen, W. R.; Welfoot, J. S.: Modelling of membrane nanofiltration-pore size distribution effects. *Chemical Engineering Science 57*, 8 (**2002**), 1393–1407.

[3] Machado, D. R.; Hasson, D.; Semiat, R.: Effect of solvent properties on permeate flow through nanofiltration membranes: Part II. transport model. *Journal of Membrane Science 166*, 1 (**2000**), 63–69.

[4] Bhanushali, D.; Kloos, S.; Kurth, C.; Bhattacharyya, D.: Performance of solvent-resistant membranes for non-aqueous systems: solvent permeation results and modeling. *Journal of Membrane Science 189*, 1 (**2001**), 1–21.

[5] Bowen, W. R.; Welfoot, J. S.: Modelling the performance of membrane nanofiltration - critical assessment and model development. *Chemical Engineering Science 57*, 7 (**2002**), 1121–1137.

[6] Malanowski, N.; Brandt, J. C.: Innovations- und Effizienzsprünge in der chemischen Industrie? Wirkungen und Herausforderungen von Industrie 4.0 und Co. *Tech. Rep.*, VDI Technologiezentrum GmbH, **2014**.

[7] Achema Trendberichte: Chem. Ing. Tech. 5/2009. *Chemie Ingenieur Technik 81*, 5 (**2009**), 530–539.

[8] The German Chemical Industry in 2030 - Short Version. *Tech. Rep.*, Verband der chemischen Industrie e.V., **2012**. www.vci.de.

[9] Geipel-Kern, A.: Diese Mega-Trends zur Prozessindustrie sollten Sie kennen. www.process.vogel.de, **2012**.

[10] Mulder, M.: *Basic Principles of Membrane Technology*. Kluwer Academic Publishers, **1996**.

[11] Boam, A.; Nozari, A.: Fine chemical: OSN - a lower energy alternative. *Filtration & Separation 43*, 3 (**2006**), 46–48.

[12] White, L. S.; Wildemuth, C. R.: Aromatics enrichment in refinery streams using hyperfiltration. *Industrial and Engineering Chemistry Research 45*, 26 (**2006**), 9136–9143.

[13] Rundquist, E. M.; Pink, C. J.; Livingston, A. G.: Organic solvent nanofiltration: a potential alternative to distillation for solvent recovery from crystallisation mother liquors. *Green Chemistry 14* (**2012**), 2197–2205.

[14] Rundquist, E.; Pink, C.; Vilminot, E.; Livingston, A.: Facilitating the use of countercurrent chromatography in pharmaceutical purification through use of organic solvent nanofiltration. *Journal of Chromatography A 1229* (**2012**), 156–163.

[15] Darvishmanesh, S.; Firoozpour, L.; Vanneste, J.; Luis, P.; Degrève, J.; Van der Bruggen, B.: Performance of solvent resistant nanofiltration membranes for purification of residual solvent in the pharmaceutical industry: experiments and simulation. *Green Chemistry 13* (**2011**), 3476–3483.

[16] Priske, M.; Wiese, K. D.; Drews, A.; Kraume, M.; Baumgarten, G.: Reaction integrated separation of homogenous catalysts in the hydroformylation of higher olefins by means of organophilic nanofiltration. *Journal of Membrane Science 360*, 1-2 (**2010**), 77–83.

[17] Nair, D.; Scarpello, J. T.; White, L. S.; Freitas Dos Santos, L. M.; Vankelecom, I. F. J.; Livingston, A. G.: Semi-continuous nanofiltration-coupled heck reactions as a new approach to improve productivity of homogeneous catalysts. *Tetrahedron Letters 42*, 46 (**2001**), 8219–8222.

[18] Nair, D.; Luthra, S. S.; Scarpello, J. T.; White, L. S.; Freitas dos Santos, L. M.; Livingston, A. G.: Homogeneous catalyst separation and re-use through nanofiltration of organic solvents. *Desalination 147*, 1-3 (**2002**), 301–306.

[19] Scarpello, J. T.; Nair, D.; Freitas dos Santos, L. M.; White, L. S.; Livingston, A. G.: The separation of homogeneous organometallic catalysts using solvent resistant nanofiltration. *Journal of Membrane Science 203*, 1-2 (**2002**), 71–85.

[20] Rauch, J.: *Mehrproduktanlagen*. Wiley VCH Verlag GmbH, **1998**.

[21] Lüneburg, W.; Zahn, W.: Das Design von Mehrprodukt- und Mehrzweckanlagen unter dem Einfluss der Anforderung nach Flexibilität. Presentation at Achema, **2003**.

[22] Kraume, M.: *Transportvorgänge in der Verfahrenstechnik: Grundlagen und apparative Umsetzungen*. Springer-Verlag Berlin Heidelberg, **2013**.

[23] Melin, T.; Rautenbach, R.: *Membranverfahren: Grundlagen der Modul- und Anlagenauslegung*. Springer-Verlag Berlin Heidelberg, **2010**.

[24] Vandezande, P.; Gevers, L. E. M.; Vankelecom, I. F. J.: Solvent resistant nanofiltration: separating on a molecular level. *Chemical Society Reviews 37*, 2 (**2008**), 365–405.

[25] Peshev, D.; Peeva, L. G.; Peev, G.; Baptista, I. I. R.; Boam, A. T.: Application of organic solvent nanofiltration for concentration of antioxidant extracts of rosemary (rosmarinus officiallis L.). *Chemical Engineering Research and Design 89*, 3 (**2011**), 318–327.

[26] Geens, J.; De Witte, B.; Van der Bruggen, B.: Removal of API's (active pharmaceutical ingredients) from organic solvents by nanofiltration. *Separation Science and Technology 42*, 11 (**2007**), 2435–2449.

[27] Cano-Odena, A.; Vandezande, P.; Fournier, D.; Van Camp, W.; Du Prez, F. E.; Vankelecom, I. F. J.: Solvent-resistant nanofiltration for product purification and catalyst recovery in click chemistry reactions. *Chemistry - A European Journal 16*, 3 (**2010**), 1061–1067.

[28] Othman, R.; Mohammad, A. W.; Ismail, M.; Salimon, J.: Application of polymeric solvent resistant nanofiltration membranes for biodiesel production. *Journal of Membrane Science 348*, 1-2 (**2010**), 287–297.

[29] Han, S.; Wong, H. T.; Livingston, A. G.: Application of organic solvent nanofiltration to separation of ionic liquids and products from ionic liquid mediated reactions. *Chemical Engineering Research and Design 83*, 3 A (**2005**), 309–316.

[30] Werhan, H.; Farshori, A.; Rudolf von Rohr, P.: Separation of lignin oxidation products by organic solvent nanofiltration. *Journal of Membrane Science 423-424* (**2012**), 404–412.

[31] Teixeira, A.; Santos, J.; Crespo, J.: Solvent resistant diananofiltration for production of steryl esters enriched extracts. *Separation and Purification Technology 135* (**2014**), 243–251.

[32] Székely, G.; Bandarra, J.; Heggie, W.; Sellergren, B.; Ferreira, F. C.: Organic solvent nanofiltration: a platform for removal of genotoxins from active pharmaceutical ingredients. *Journal of Membrane Science 381*, 1 (**2011**), 21–33.

[33] Lin, J. C. T.; Livingston, A. G.: Nanofiltration membrane cascade for continuous solvent exchange. *Chemical Engineering Science 62*, 10 (**2007**), 2728–2736.

[34] Livingston, A.; Peeva, L.; Han, S.; Nair, D.; Luthra, S. S.; White, L. S.; Freitas Dos Santos, L. M.: Membrane separation in green chemical processing: Solvent nanofiltration in liquid phase organic synthesis reactions. *Annals of the New York Academy of Sciences 984* (**2003**), 123–141.

[35] Ferguson, S.; Ortner, F.; Quon, J.; Peeva, L.; Livingston, A.; Trout, B. L.; Myerson, A. S.: Use of continuous msmpr crystallization with integrated nanofiltration membrane recycle for enhanced yield and purity in api crystallization. *Crystal Growth & Design 14*, 2 (**2013**), 617–627.

[36] Micovic, J.; Werth, K.; Lutze, P.: Hybrid separations combining distillation and organic solvent nanofiltration for separation of wide boiling mixtures. *Chemical Engineering Research and Design 92*, 11 (**2014**), 2131 – 2147.

[37] Micovic, J.: *Design of energy-efficient hybrid separations combining distillation with organic solvent nanofiltration and melt crystallisation*. Ph.D. thesis, Technische Universität Dortmund, **2014**.

[38] Werth, K.; Neumann, K.; Skiborowski, M.: Computer-aided process analysis of an integrated biodiesel process incorporating reactive distillation and organic solvent nanofiltration. In *12th International Symposium on Process Systems Engineering and 25th European Symposium on Computer Aided Process Engineering*, *Computer Aided Chemical Engineering*, vol. 37, edited by Krist V. Gernaey, J. K. H.; Gani, R., Elsevier, **2015**, pp. 1277–1282.

[39] Peeva, L. G.; Sairam, M.; Livingston, A. G.: *Nanofiltration Operations in Nonaqueous Systems*. No. 1 in Comprehensive Membrane Science and Engineering, Elsevier Science, **2010**.

[40] Vankelecom, I. F. J.; De Smet, K.; Gevers, L. E. M.; Livingston, A. G.; Nair, D.; Aerts, S.; Kuypers, S.; Jacobs, P. A.: Physico-chemical interpretation of the SRNF transport mechanism for solvents through dense silicone membranes. *Journal of Membrane Science 231*, 1-2 (**2004**), 99–108.

[41] Ebert, K.; Koll, J.; Dijkstra, M. F. J.; Eggers, M.: Fundamental studies on the performance of a hydrophobic solvent stable membrane in non-aqueous solutions. *Journal of Membrane Science 285*, 1-2 (**2006**), 75–80.

[42] Evonik Industries. duramem.evonik.com, **2013**. (accessed Nov 5, 2013).

[43] Jimenez Solomon, M. F.; Bhole, Y.; Livingston, A. G.: High flux membranes for organic solvent nanofiltration (OSN) - interfacial polymerization with solvent activation. *Journal of Membrane Science 423-424*, 0 (**2012**), 371–382.

[44] White, L. S.: Transport properties of a polyimide solvent resistant nanofiltration membrane. *Journal of Membrane Science 205*, 1-2 (**2002**), 191–202.

[45] See Toh, Y. H.; Lim, F. W.; Livingston, A. G.: Polymeric membranes for nanofiltration in polar aprotic solvents. *Journal of Membrane Science 301*, 1-2 (**2007**), 3–10.

[46] Behnke, S.; Ulbricht, M.: Thin-film composite membranes for organophilic nanofiltration based on photo-cross-linkable polyimide. *Reactive and Functional Polymers 86* (**2015**), 233–242.

[47] Vanherck, K.; Vandezande, P.; Aldea, S. O.; Vankelecom, I. F. J.: Cross-linked polyimide membranes for solvent resistant nanofiltration in aprotic solvents. *Journal of Membrane Science 320*, 1-2 (**2008**), 468–476.

[48] Hendrix, K.; Vanherck, K.; Vankelecom, I. F. J.: Optimization of solvent resistant nanofiltration membranes prepared by the in-situ diamine crosslinking method. *Journal of Membrane Science 421-422*, 0 (**2012**), 15–24.

[49] Volkov, A. V.; Parashchuk, V. V.; Stamatialis, D. F.; Khotimsky, V. S.; Volkov, V. V.; Wessling, M.: High permeable PTMSP/PAN composite membranes for solvent nanofiltration. *Journal of Membrane Science 333*, 1-2 (**2009**), 88–93.

[50] Fritsch, D.; Merten, P.; Heinrich, K.; Lazar, M.; Priske, M.: High performance organic solvent nanofiltration membranes: Development and thorough testing of thin film composite membranes made of polymers of intrinsic microporosity (PIMs). *Journal of Membrane Science 401-402* (**2012**), 222–231.

[51] Darvishmanesh, S.; Jansen, J. C.; Tasselli, F.; Tocci, E.; Luis, P.; Degrève, J.; Drioli, E.; Van der Bruggen, B.: Novel polyphenylsulfone membrane for potential use in solvent nanofiltration. *Journal of Membrane Science 379*, 1-2 (**2011**), 60–68.

[52] Holda, A. K.; Roeck, M. D.; Hendrix, K.; Vankelecom, I. F.: The influence of polymer purity and molecular weight on the synthesis of integrally skinned polysulfone membranes. *Journal of Membrane Science 446* (**2013**), 113–120.

[53] Holda, A. K.; Vankelecom, I. F.: Integrally skinned PSf-based SRNF-membranes prepared via phase inversion - Part a: Influence of high molecular weight additives. *Journal of Membrane Science 450* (**2014**), 512–521.

[54] Holda, A. K.; Vankelecom, I. F.: Integrally skinned PSf-based SRNF-membranes prepared via phase inversion - Part b: Influence of low molecular weight additives. *Journal of Membrane Science 450* (**2014**), 499–511.

[55] Loh, X. X.; Sairam, M.; Bismarck, A.; Steinke, J. H. G.; Livingston, A. G.; Li, K.: Crosslinked integrally skinned asymmetric polyaniline membranes for use in organic solvents. *Journal of Membrane Science 326*, 2 (**2009**), 635–642.

[56] Sairam, M.; Loh, X. X.; Bhole, Y.; Sereewatthanawut, I.; Li, K.; Bismarck, A.; Steinke, J. H. G.; Livingston, A. G.: Spiral-wound polyaniline membrane modules for organic solvent nanofiltration (OSN). *Journal of Membrane Science 349*, 1-2 (**2010**), 123–129.

[57] Pérez-Manríquez, L.; Aburabie, J.; Neelakanda, P.; Peinemann, K.-V.: Cross-linked PAN-based thin-film composite membranes for non-aqueous nanofiltration. *Reactive and Functional Polymers 86* (**2015**), 243–247.

[58] da Silva Burgal, J.; Peeva, L. G.; Kumbharkar, S.; Livingston, A.: Organic solvent resistant poly(ether-ether-ketone) nanofiltration membranes. *Journal of Membrane Science 479* (**2015**), 105–116.

[59] Valtcheva, I. B.; Kumbharkar, S. C.; Kim, J. F.; Bhole, Y.; Livingston, A. G.: Beyond polyimide: Crosslinked polybenzimidazole membranes for organic solvent nanofiltration (OSN) in harsh environments. *Journal of Membrane Science 457* (**2014**), 62–72.

[60] Valtcheva, I. B.; Marchetti, P.; Livingston, A. G.: Crosslinked polybenzimidazole membranes for organic solvent nanofiltration (OSN): Analysis of crosslinking reaction mechanism and effects of reaction parameters. *Journal of Membrane Science 493* (**2015**), 568–579.

[61] Székely, G.; Valtcheva, I. B.; Kim, J. F.; Livingston, A. G.: Molecularly imprinted organic solvent nanofiltration membranes - Revealing molecular recognition and solute rejection behaviour. *Reactive and Functional Polymers 86* (**2015**), 215–224.

[62] Darvishmanesh, S.; Degrève, J.; Van der Bruggen, B.: Comparison of pressure driven transport of ethanol/n-hexane mixtures through dense and microporous membranes. *Chemical Engineering Science 64*, 17 (**2009**), 3914–3927.

[63] Darvishmanesh, S.; Degrève, J.; Bruggen, B. V. D.: Performance of solvent-pretreated polyimide nanofiltration membranes for separation of dissolved dyes from toluene. *Industrial and Engineering Chemistry Research 49*, 19 (**2010**), 9330–9338.

[64] Santos, J. L. C.; Hidalgo, A. M.; Oliveira, R.; Velizarov, S.; Crespo, J. G.: Analysis of solvent flux through nanofiltration membranes by mechanistic, chemometric and hybrid modelling. *Journal of Membrane Science 300*, 1-2 (**2007**), 191–204.

[65] Silva, P.; Han, S.; Livingston, A. G.: Solvent transport in organic solvent nanofiltration membranes. *Journal of Membrane Science 262*, 1-2 (**2005**), 49–59.

[66] Silva, P.; Peeva, L. G.; Livingston, A. G.: Organic solvent nanofiltration (OSN) with spiral-wound membrane elements - Highly rejected solute system. *Journal of Membrane Science 349*, 1-2 (**2010**), 167–174.

[67] Zhao, Y.; Yuan, Q.: A comparison of nanofiltration with aqueous and organic solvents. *Journal of Membrane Science 279*, 1-2 (**2006**), 453–458.

[68] Schmidt, P.; Köse, T.; Lutze, P.: Characterisation of organic solvent nanofiltration membranes in multi-component mixtures: Membrane rejection maps and membrane selectivity maps for conceptual process design. *Journal of Membrane Science 429* (**2013**), 103–120.

[69] Hesse, L.; Mićović, J.; Schmidt, P.; Górak, A.; Sadowski, G.: Modelling of organic-solvent flux through a polyimide membrane. *Journal of Membrane Science 428*, 0 (**2013**), 554–561.

[70] Darvishmanesh, S.; Vanneste, J.; Tocci, E.; Jansen, J.; Tasseli, F.; Degrève, J.; Drioli, E.; Van Der Bruggen, B.: Physicochemical characterization of solute retention in solvent resistant nanofiltration: The effect of solute size, polarity, dipole moment, and solubility parameter. *Journal of Physical Chemistry B 115*, 49 (**2011**), 14507–14517.

[71] Cuperus, F. P.: Recovery of organic solvents and valuable components by membrane separation. *Chemie Ingenieur Technik 77*, 8 (**2005**), 1000–1001.

[72] GMT Membrantechnik GmbH. www.gmtmem.com, **2013**. (accessed Nov 14, 2013).

[73] Benfer, S.; Popp, U.; Richter, H.; Siewert, C.; Tomandl, G.: Development and characterization of ceramic nanofiltration membranes. *Separation and Purification Technology 22-23* (**2001**), 231–237.

[74] Puhlfürß, P.; Voigt, A.; Weber, R.; Morbé, M.: Microporous TiO2 membranes with a cut off <500 Da. *Journal of Membrane Science 174*, 1 (**2000**), 123–133.

[75] Tsuru, T.; Sudoh, T.; Yoshioka, T.; Asaeda, M.: Nanofiltration in non-aqueous solutions by porous silica-zirconia membranes. *Journal of Membrane Science 185*, 2 (**2001**), 253–261.

[76] Tsuru, T.; Wada, S. I.; Izumi, S.; Asaeda, M.: Silica-zirconia membranes for nanofiltration. *Journal of Membrane Science 149*, 1 (**1998**), 127–135.

[77] Van Gestel, T.; Kruidhof, H.; Blank, D. H. A.; Bouwmeester, H. J. M.: ZrO2 and TiO2 membranes for nanofiltration and pervaporation. Part 1. Preparation and characterization of a corrosion-resistant ZrO2 nanofiltration membrane with a MWCO <300. *Journal of Membrane Science 284*, 1-2 (**2006**), 128–136.

[78] Van Gestel, T.; Vandecasteele, C.; Buekenhoudt, A.; Dotremont, C.; Luyten, J.; Leysen, R.; Van der Bruggen, B.; Maes, G.: Alumina and titania multilayer membranes for nanofiltration: Preparation, characterization and chemical stability. *Journal of Membrane Science 207*, 1 (**2002**), 73–89.

[79] Voigt, I.: personal communication, **2011**.

[80] Inopor Rauschert. www.inopor.com, **2013**. (accesses Dez 04, 2013).

[81] Whu, J. A.; Baltzis, B. C.; Sirkar, K. K.: Nanofiltration studies of larger organic microsolutes in methanol solutions. *Journal of Membrane Science 170*, 2 (**2000**), 159–172.

[82] Yang, X. J.; Livingston, A. G.; Freitas Dos Santos, L.: Experimental observations of nanofiltration with organic solvents. *Journal of Membrane Science 190*, 1 (**2001**), 45–55.

[83] Voigt, I.; Fischer, G.; Puhlfürß, P.; Schleifenheimer, M.; Stahn, M.: TiO2-NF-membranes on capillary supports. *Separation and Purification Technology 32*, 1-3 (**2003**), 87–91.

[84] See Toh, Y. H.; Loh, X. X.; Li, K.; Bismarck, A.; Livingston, A. G.: In search of a standard method for the characterisation of organic solvent nanofiltration membranes. *Journal of Membrane Science 291*, 1-2 (**2007**), 120–125.

[85] Basu, S.; Maes, M.; Cano-Odena, A.; Alaerts, L.; De Vos, D. E.; Vankelecom, I. F. J.: Solvent resistant nanofiltration (SRNF) membranes based on metal-organic frameworks. *Journal of Membrane Science 344*, 1-2 (**2009**), 190–198.

[86] Darvishmanesh, S.; Tasselli, F.; Jansen, J. C.; Tocci, E.; Bazzarelli, F.; Bernardo, P.; Luis, P.; Degrève, J.; Drioli, E.; Van der Bruggen, B.: Preparation of solvent stable polyphenylsulfone hollow fiber nanofiltration membranes. *Journal of Membrane Science 384*, 1-2 (**2011**), 89–96.

[87] Kosaraju, P. B.; Sirkar, K. K.: Interfacially polymerized thin film composite membranes on microporous polypropylene supports for solvent-resistant nanofiltration. *Journal of Membrane Science 321*, 2 (**2008**), 155–161.

[88] Peyravi, M.; Rahimpour, A.; Jahanshahi, M.: Thin film composite membranes with modified polysulfone supports for organic solvent nanofiltration. *Journal of Membrane Science 423-424* (**2012**), 225–237.

[89] Tsuru, T.; Nakasuji, T.; Oka, M.; Kanezashi, M.; Yoshioka, T.: Preparation of hydrophobic nanoporous methylated SiO2 membranes and application to nanofiltration of hexane solutions. *Journal of Membrane Science 384*, 1-2 (**2011**), 149–156.

[90] Dijkstra, M. F. J.; Bach, S.; Ebert, K.: A transport model for organophilic nanofiltration. *Journal of Membrane Science 286*, 1-2 (**2006**), 60–68.

[91] Dobrak-Van Berlo, A.; Vankelecom, I. F. J.; Van der Bruggen, B.: Parameters determining transport mechanisms through unfilled and silicalite filled PDMS-based membranes and dense PI membranes in solvent resistant nanofiltration: Comparison with pervaporation. *Journal of Membrane Science 374*, 1-2 (**2011**), 138–149.

[92] Kedem, O.; Katchalsky, A.: Thermodynamic analysis of the permeability of biological membranes to non-electrolytes. *BBA - Biochimica et Biophysica Acta 27*, C (**1958**), 229–246.

[93] Spiegler, K. S.; Kedem, O.: Thermodynamics of hyperfiltration (reverse osmosis): criteria for efficient membranes. *Desalination 1*, 4 (**1966**), 311–326.

[94] Wijmans, J. G.; Baker, R. W.: The solution-diffusion model: A review. *Journal of Membrane Science 107*, 1-2 (**1995**), 1–21.

[95] Combe, C.; Guizard, C.; Aimar, P.; Sanchez, V.: Experimental determination of four characteristics used to predict the retention of a ceramic nanofiltration membrane. *Journal of Membrane Science 129*, 2 (**1997**), 147–160.

[96] Niemi, H.; Palosaari, S.: Flowsheet simulation of ultrafiltration and reverse osmosis processes. *Journal of Membrane Science 91*, 1-2 (**1994**), 111–124.

[97] Matsuura, T.; Sourirajan, S.: Reverse osmosis transport through capillary pores under the influence of surface forces. *Industrial & Engineering Chemistry Process Design and Development 20*, 2 (**1981**), 273–282.

[98] Ferry, J. D.: Statistical evaluation of sieve constants in ultrafiltration. *The Journal of General Physiology 20*, 1 (**1936**), 95–104.

[99] Bowen, W. R.; Mohammad, A. W.: Characterization and prediction of nanofiltration membrane performance - a general assessment. *Chemical Engineering Research and Design 76*, 8 (**1998**), 885–893.

[100] Israelachvili, J.: Measurement of the viscosity of liquids in very thin films. *Journal of Colloid and Interface Science 110*, 1 (**1986**), 263–271.

[101] Belfort, G.; Scherfig, J.; Seevers, D.: Nuclear magnetic resonance relaxation studies of adsorbed water on porous glass of varying pore size. *Journal of Colloid And Interface Science 47*, 1 (**1974**), 106–116.

[102] Israelachvili, J.; McGuiggan, P.; Gee, M.; Homola, A.; Robbins, M.; Thompson, P.: Liquid dynamics in molecularly thin films. *Journal of Physics: Condensed Matter 2*, S (**1990**), SA89.

[103] Churaev, N.: Thin liquid layers. *Colloid journal of the Russian Academy of Sciences 58*, 6 (**1996**), 681–693.

[104] Dias, C. R.; Rosa, M. J.; de Pinho, M. N.: Structure of water in asymmetric cellulose ester membranes - and ATR-FTIR study. *Journal of membrane science 138*, 2 (**1998**), 259–267.

[105] Lonsdale, H. K.; Merten, U.; Riley, R. L.: Transport properties of cellulose acetate osmotic membranes. *Journal of Applied Polymer Science 9*, 4 (**1965**), 1341–1362.

[106] Mason, E. A.; Lonsdale, H. K.: Statistical-mechanical theory of membrane transport. *Journal of Membrane Science 51*, 1-2 (**1990**), 1–81.

[107] Paul, D. R.: Reformulation of the solution-diffusion theory of reverse osmosis. *Journal of Membrane Science 241*, 2 (**2004**), 371–386.

[108] Peeva, L. G.; Gibbins, E.; Luthra, S. S.; White, L. S.; Stateva, R. P.; Livingston, A. G.: Effect of concentration polarisation and osmotic pressure on flux in organic solvent nanofiltration. *Journal of Membrane Science 236*, 1-2 (**2004**), 121–136.

[109] Stafie, N.; Stamatialis, D. F.; Wessling, M.: Insight into the transport of hexane-solute systems through tailor-made composite membranes. *Journal of Membrane Science 228*, 1 (**2004**), 103–116.

[110] Robinson, J. P.; Tarleton, E. S.; Millington, C. R.; Nijmeijer, A.: Solvent flux through dense polymeric nanofiltration membranes. *Journal of Membrane Science 230*, 1-2 (**2004**), 29–37.

[111] Hesse, L.; Sadowski, G.: Modeling liquid-liquid equilibria of polyimide solutions. *Industrial & Engineering Chemistry Research 51*, 1 (**2011**), 539–546.

[112] Hesse, L.; Naeem, S.; Sadowski, G.: VOC sorption in glassy polyimides-measurements and modeling. *Journal of Membrane Science 415-416* (**2012**), 596–607.

[113] Postel, S.; Wessel, S.; Keil, T.; Eiselt, P.; Wessling, M.: Multicomponent mass transport in organic solvent nanofiltration with solvent mixtures. *Journal of Membrane Science 466* (**2014**), 361 – 369.

[114] Marchetti, P.; Livingston, A. G.: Predictive membrane transport models for organic solvent nanofiltration: How complex do we need to be? *Journal of Membrane Science 476* (**2015**), 530–553.

[115] Mehdizadeh, H.; Dickson, J.: Theoretical modification of the surface force-pore flow model for reverse osmosis transport. *Journal of Membrane Science 42*, 1 (**1989**), 119–145.

[116] Yaroshchuk, A. E.: Solution-diffusion-imperfection model revised. *Journal of Membrane Science 101*, 1-2 (**1995**), 83–87.

[117] Sherwood, T. K.; Brian, P. L. T.; Fisher, R. E.: Desalination by reverse osmosis. *Industrial & Engineering Chemistry Fundamentals 6*, 1 (**1967**), 2–12.

[118] Tsarkov, S.; Khotimskiy, V.; Budd, P. M.; Volkov, V.; Kukushkina, J.; Volkov, A.: Solvent nanofiltration through high permeability glassy polymers: Effect of polymer and solute nature. *Journal of Membrane Science 423* (**2012**), 65–72.

[119] Postel, S.; Spalding, G.; Chirnside, M.; Wessling, M.: On negative retentions in organic solvent nanofiltration. *Journal of Membrane Science 447* (**2013**), 57 – 65.

[120] Van der Bruggen, B.; Mänttäri, M.; Nyström, M.: Drawbacks of applying nanofiltration and how to avoid them: A review. *Separation and Purification Technology 63*, 2 (**2008**), 251–263.

[121] Darvishmanesh, S.; Buekenhoudt, A.; Degrève, J.; Van der Bruggen, B.: General model for prediction of solvent permeation through organic and inorganic solvent resistant nanofiltration membranes. *Journal of Membrane Science 334*, 1-2 (**2009**), 43–49.

[122] Geens, J.; Van Der Bruggen, B.; Vandecasteele, C.: Transport model for solvent permeation through nanofiltration membranes. *Separation and Purification Technology 48*, 3 (**2006**), 255–263.

[123] Darvishmanesh, S.; Buekenhoudt, A.; Degrève, J.; Van der Bruggen, B.: Coupled series-parallel resistance model for transport of solvent through inorganic nanofiltration membranes. *Separation and Purification Technology 70*, 1 (**2009**), 46–52.

[124] Marchetti, P.; Butté, A.; Livingston, A. G.: An improved phenomenological model for prediction of solvent permeation through ceramic NF and UF membranes. *Journal of Membrane Science 415-416* (**2012**), 444–458.

[125] Buekenhoudt, A.; Bisignano, F.; Luca, G. D.; Vandezande, P.; Wouters, M.; Verhulst, K.: Unravelling the solvent flux behaviour of ceramic nanofiltration and ultrafiltration membranes. *Journal of Membrane Science 439*, 0 (**2013**), 36–47.

[126] Van Der Bruggen, B.; Schaep, J.; Wilms, D.; Vandecasteele, C.: A comparison of models to describe the maximal retention of organic molecules in nanofiltration. *Separation Science and Technology 35*, 2 (**1999**), 169–182.

[127] Geens, J.; Boussu, K.; Vandecasteele, C.; Van der Bruggen, B.: Modelling of solute transport in non-aqueous nanofiltration. *Journal of Membrane Science 281*, 1-2 (**2006**), 139–148.

[128] Nakao, S.-I.; Kimura, S.: Models of membrane transport phenomena and their applications for ultrafiltration data. *Journal of Chemical Engineering of Japan 15*, 3 (**1982**), 200–205.

[129] Wang, X.-L.; Tsuru, T.; Nakao, S.-I.; Kimura, S.: The electrostatic and steric-hindrance model for the transport of charged solutes through nanofiltration membranes. *Journal of Membrane Science 135*, 1 (**1997**), 19–32.

[130] Verniory, A.; Du Bois, R.; Decoodt, P.; Gassee, J. P.; Lambert, P. P.: Measurement of the permeability of biological membranes. Application to the glomerular wall. *The Journal of General Physiology 62*, 4 (**1973**), 489–507.

[131] Gibbins, E.; D' Antonio, M.; Nair, D.; White, L. S.; Freitas dos Santos, L. M.; Vankelecom, I. F. J.; Livingston, A. G.: Observations on solvent flux and solute rejection across solvent resistant nanofiltration membranes. *Desalination 147*, 1-3 (**2002**), 307–313.

[132] Bhanushali, D.; Kloos, S.; Bhattacharyya, D.: Solute transport in solvent-resistant nanofiltration membranes for non-aqueous systems: Experimental results and the role of solute-solvent coupling. *Journal of Membrane Science 208*, 1-2 (**2002**), 343–359.

[133] Geens, J.; Hillen, A.; Bettens, B.; Van der Bruggen, B.; Vandecasteele, C.: Solute transport in non-aqueous nanofiltration: Effect of membrane material. *Journal of Chemical Technology and Biotechnology 80*, 12 (**2005**), 1371–1377.

[134] Gevers, L. E. M.; Meyen, G.; De Smet, K.; Van De Velde, P.; Du Prez, F.; Vankelecom, I. F. J.; Jacobs, P. A.: Physico-chemical interpretation of the SRNF transport mechanism for solutes through dense silicone membranes. *Journal of Membrane Science 274*, 1-2 (**2006**), 173–182.

[135] Zheng, F.; Li, C.; Yuan, Q.; Vriesekoop, F.: Influence of molecular shape on the retention of small molecules by solvent resistant nanofiltration (SRNF) membranes: A suitable molecular size parameter. *Journal of Membrane Science 318*, 1-2 (**2008**), 114–122.

[136] Tarleton, E. S.; Robinson, J. P.; Salman, M.: Solvent-induced swelling of membranes - Measurements and influence in nanofiltration. *Journal of Membrane Science 280*, 1-2 (**2006**), 442–451.

[137] Darvishmanesh, S.; Degrève, J.; Van Der Bruggen, B.: Mechanisms of solute rejection in solvent resistant nanofiltration: The effect of solvent on solute rejection. *Physical Chemistry Chemical Physics 12*, 40 (**2010**), 13333–13342.

[138] Burke, J.: *Solubility Parameters: Theory and Application*. The Oakland Museum of California, **1984**.

[139] Van Krevelen, D.; Nijenhuis, K.: *Properties of polymers: their correlation with chemical structure; their numerical estimation and prediction from additive group contributions*. Elsevier, **2009**.

[140] Favre, E.: Swelling of crosslinked polydimethylsiloxane networks by pure solvents: Influence of temperature. *European Polymer Journal 32*, 10 (**1996**), 1183–1188.

[141] Hansen, C. M.: *The three dimensional solubility parameter and solvent diffusion coefficient*. Ph.D. thesis, Danish Technical Press, Copenhagen, **1967**.

[142] Hoy, K. L.: *The Hoy tables of solubility parameters*. Union Carbide Corporation, Solvents & Coatings Materials, Research & Development Department, **1985**.

[143] Hoy, K. L.: Solubility parameter as a design parameter for water-borne polymers and coatings. *Journal of Coated Fabrics* , 19, July (**1989**), 53–67.

[144] Postel, S.; Schneider, C.; Wessling, M.: Solvent dependent solute solubility governs retention in silicone based organic solvent nanofiltration. *Journal of Membrane Science 497* (**2016**), 47–54.

[145] Marchetti, P.; Butté, A.; Livingston, A. G.: NF in organic solvent/water mixtures: Role of preferential solvation. *Journal of Membrane Science 444* (**2013**), 101–115.

[146] Hosseinabadi, S. R.; Wyns, K.; Buekenhoudt, A.; der Bruggen, B. V.; Ormerod, D.: Performance of grignard functionalized ceramic nanofiltration membranes. *Separation and Purification Technology 147* (**2015**), 320–328.

[147] Hosseinabadi, S. R.; Wyns, K.; Meynen, V.; Carleer, R.; Adriaensens, P.; Buekenhoudt, A.; der Bruggen, B. V.: Organic solvent nanofiltration with grignard functionalised ceramic nanofiltration membranes. *Journal of Membrane Science 454* (**2014**), 496–504.

[148] White, L. S.: Development of large-scale applications in organic solvent nanofiltration and pervaporation for chemical and refining processes. *Journal of Membrane Science 286*, 1-2 (**2006**), 26–35.

[149] Schmalz, D.: *Eine systematische Potentialbewertung für die Einführung neuer Technologien in der Prozessindustrie am Beispiel der Mikroreaktionstechnik*. Ph.D. thesis, Technische Universität Clausthal, **2006**.

[150] DuraMem Membrane Flat Sheet - Instructions for use. Evonik Industries, **2011**.

[151] Membrane data sheet GMT-oNF-1. BORSIG Membrane Technology GmbH, **2011**.

[152] Membrane data sheet GMT-oNF-2. BORSIG Membrane Technology GmbH, **2011**.

[153] Tarleton, E. S.; Robinson, J. P.; Smith, S. J.; Na, J. J. W.: New experimental measurements of solvent induced swelling in nanofiltration membranes. *Journal of Membrane Science 261*, 1-2 (**2005**), 129–135.

[154] Lee, J. N.; Park, C.; Whitesides, G. M.: Solvent compatibility of poly(dimethylsiloxane)-based microfluidic devices. *Analytical Chemistry 75*, 23 (**2003**), 6544–6554.

[155] Mohammadi, T.; Aroujalian, A.; Bakhshi, A.: Pervaporation of dilute alcoholic mixtures using PDMS membrane. *Chemical Engineering Science 60*, 7 (**2005**), 1875–1880.

[156] Kreis, P.: personal communication, **2012**.

[157] Zeidler, S.; Kätzel, U.; Kreis, P.: Systematic investigation on the influence of solutes on the separation behavior of a PDMS membrane in organic solvent nanofiltration. *Journal of Membrane Science 429* (**2013**), 295–303.

[158] Fedors, R. F.: A method for estimating both the solubility parameters and molar volumes of liquids. *Polymer Engineering & Science 14*, 6 (**1974**), 472–472.

[159] Small, P. A.: Some factors affecting the solubility of polymers. *Journal of Applied Chemistry 3*, 2 (**1953**), 71–80.

[160] Hoy, K. L.: New values of the solubility parameters from vapor pressure data. *Journal of paint technology 42*, 541.

[161] Stefanis, E.; Constantinou, L.; Panayiotou, C.: A group-contribution method for predicting pure component properties of biochemical and safety interest. *Industrial & Engineering Chemistry Research 43*, 19 (**2004**), 6253–6261.

[162] Daubert, T. E.; Danner, R. P.; Sibul, H.; Stebbins, C.: *Physical and thermodynamic properties of pure chemicals: data compilation*. Hemisphere Publishing Corporation New York, **1989**.

[163] Zhao, Y.; Truhlar, D. G.: The M06 suite of density functionals for main group thermochemistry, thermochemical kinetics, noncovalent interactions, excited states, and transition elements: two new functionals and systematic testing of four M06-class functionals and 12 other functionals. *Theoretical Chemistry Accounts 120*, 1-3 (**2008**), 215–241.

[164] Smallwood, I. M.: *Handbook of Organic Solvent Properties*. Butterworth-Heinemann, Oxford, **1996**.

[165] Stamatialis, D. F.; Stafie, N.; Buadu, K.; Hempenius, M.; Wessling, M.: Observations on the permeation performance of solvent resistant nanofiltration membranes. *Journal of Membrane Science 279*, 1-2 (**2006**), 424–433.

[166] Tarleton, E. S.; Robinson, J. P.; Low, J. S.: Nanofiltration: A technology for selective solute removal from fuels and solvents. *Chemical Engineering Research and Design 87*, 3 (**2009**), 271–279.

[167] Soravia, S.; Orth, A.: *Design of Experiments*. Wiley-VCH Verlag GmbH & Co. KGaA, **2000**.

[168] Eriksson, L.: *Design of Experiments: Principles and Applications*. Umetrics Academy, **2008**.

[169] Barton, A.: *CRC handbook of solubility parameters and other cohesion parameters*. CRC Press, **1991**.

[170] Schmidt, P.; Bednarza, E. L.; Lutze, P.; Górak, A.: Characterisation of organic solvent nanofiltration membranes in multi-component mixtures: Process design workflow for utilising targeted solvent modifications. *Chemical Engineering Science 115* (**2014**), 115 – 126.

[171] Soroko, I.; Lopes, M. P.; Livingston, A.: The effect of membrane formation parameters on performance of polyimide membranes for organic solvent nanofiltration (OSN): Part A. Effect of polymer/solvent/non-solvent system choice. *Journal of Membrane Science 381*, 1-2 (**2011**), 152–162.

[172] Soltane, H. B.; Roizard, D.; Favre, E.: Study of the rejection of various solutes in OSN by a composite polydimethylsiloxane membrane: Investigation of the role of solute affinity. *Separation and Purification Technology 161* (**2016**), 193–201.

[173] Zeidler, S.; Puhlfürß, P.; Kätzel, U.; Voigt, I.: Preparation and characterization of new low MWCO ceramic nanofiltration membranes for organic solvents. *Journal of Membrane Science 470* (**2014**), 421–430.

[174] Tsuru, T.; Hino, T.; Yoshioka, T.; Asaeda, M.: Permporometry characterization of microporous ceramic membranes. *Journal of Membrane Science 186*, 2 (**2001**), 257–265.

[175] Cuperus, F. P.; Bargeman, D.; Smolders, C. A.: Permporometry: the determination of the size distribution of active pores in UF membranes. *Journal of Membrane Science 71*, 1-2 (**1992**), 57–67.

[176] Baerns, M.; Behr, A.; Brehm, A.; Gmehling, J.; Hofmann, H.; Onken, U.; Renken, A.: *Technische Chemie*. Wiley-VCH Verlag GmbH & Co. KGaA Weinheim, **2006**.

[177] Van der Bruggen, B.; Vandecasteele, C.: Modelling of the retention of uncharged molecules with nanofiltration. *Water Research 36*, 5 (**2002**), 1360–1368.

[178] Kätzel, U.; Druwe, S.: personal communication, **2013**.

List of Figures

2.1 Characteristics of different chemical industries 4
2.2 Modular multi-purpose plant [20] 6
2.3 Multi-purpose plant with mobile transfer containers [21] 7
2.4 Overview pressure driven membrane processes [22] 8
2.5 Principle of a membrane process [23] 9
2.6 Different operating modes in membrane processes adapted from Mulder [10] left: dead-end mode right: cross-flow mode 10
2.7 Concentration polarization: concentration gradient at equilibrium according to Mulder [10] 12
2.8 The two types of polymeric nanofiltration membranes left: integrally skinned membranes right: thin film composite membrane [24] 14
2.9 Sliced spiral wound module 17
2.10 Structure of a ceramic nanofiltration membrane 18
2.11 Different geometries of ceramic membrane modules 19
2.12 Gradient profiles of the chemical potential, the pressure and the activity assumed for the pore-flow and the solution-diffusion model adapated from Wijmans and Baker [94] 22
2.13 Possible pore structures adapted from Mulder[10] 23

3.1 Three-dimensional interaction space of OSN 35

4.1 Assessment of technological potential of OSN adapted from [149] 39
4.2 Distribution of different downstream process steps sorted according to their number in an exemplary multi-purpose production facility 39
4.3 Percentage of the costs contributing to the theoretical potential using the example of two selected products manufactured in the multi-purpose facility 43

4.4 Influence of rejection of a membrane on the theoretical potential of a two-stage OSN plant in a multi-purpose environment (flux is fixed at 30 l/m^{2}h) and the number of economic processes (black numbers) as well as the minimal number of processes that amount to 90 % of the possible savings (white numbers) . . . 44
4.5 Influence of flux of a membrane on the theoretical potential of a two-stage OSN plant in a multi-purpose environment (rejection is fixed at 0.9) and the number of economic processes (black numbers) as well as the minimal number of processes that amount to 90 % of the possible savings (white numbers) 44
4.6 Sensitivity of different factors on the theoretical potential $Pot_{th,total}$ 45

5.1 Comparison between the rejections measured with a mixture of the solutes and the single molecule (here GMT-oNF-2 in THF) 49
5.2 Schematical set-up of the experiments with the polymeric membranes 53
5.3 Rectangular membrane module 54
5.4 METCell 4" radial membrane module 54
5.5 Pure solvent flux measurement with a membrane housed in the rectangular cell measured at 30 bar, room temperature and 1 l/min feed-flow in a long-term experiment. a) GMT-oNF-2 b) DuraMem® 200 55
5.6 Rejection course of one solute in the three solvents THF, n-heptane and ethanol as a function of the time for both membranes 55
5.7 Pure solvent flux through the membranes as a function of the solubility parameter of the solvent and the solubility parameter of the membrane polymer (dashed line) a) GMT-oNF-2 b) DuraMem® 200 58
5.8 Pure solvent flux through the membranes as a function of the inverse viscosity of the solvent a) GMT-oNF-2 b) DuraMem® 200 59
5.9 Pure solvent fluxes of ethanol, n-heptane and THF as a function of their inverse viscosity a) GMT-oNF-2 b) DuraMem® 200 60

5.10 Rejections of specialty chemicals in ethanol, THF and n-heptane vs. their molecular weight. Values taken after 180 min at 30 bar transmembrane pressure. a) GMT-oNF-2 membrane, star symbols the separation characterization given by the manufacturer determined by rejection measurements of alkanes in toluene. b) DuraMem 200 membrane, dotted line symbols the MWCO given by the manufacturer determined by rejection measurements of styrene oligomers in acetone. 62
5.11 Rejection in dependence of the maximum width of the solutes determined by force field calculations a) GMT-oNF-2 b) DuraMem® 200 66
5.12 Rejection in dependence of the dipole moment of the solutes calculated by density functional theory (DFT) a) GMT-oNF-2 b) DuraMem® 200 67
5.13 Rejection in dependence of the solubility parameters of the solutes calculated by the method of Stefanis [161] and the solubility parameters of the membrane (dashed line) and THF (solid line) a) GMT-oNF-2 b) DuraMem® 200 67
5.14 Rejection in dependence of the solubility parameters of the solutes calculated by the method of Stefanis [161] and the solubility parameters of the membrane (dashed line) and n-heptane (solid line) a) GMT-oNF-2 b) DuraMem® 200 . . . 68
5.15 Rejection in dependence of the solubility parameters of the solutes calculated by the method of Stefanis [161] and the solubility parameters of the membrane (dashed line) and ethanol (solid line) a) GMT-oNF-2 b) DuraMem® 200 69
5.16 Example for the notation of the functional groups 70
5.17 Functional groups influencing the rejection of the GMT-oNF-2 in different solvents 71
5.18 Functional groups influencing the rejection of the DuraMem® 200 in different solvents 72
5.19 Rejection of two molecules which differ only in their left side chain length ($R_G > R_K$) a) GMT-oNF-2 b) DuraMem® 200 74
5.20 Rejection of two molecules which differ only in their endgroup (G: nonpolar; J: polar) a) GMT-oNF-2 b) DuraMem® 200 75
5.21 Rejection of two molecules which differ only in their endcore (E: cyclohexane; B: benzene) a) GMT-oNF-2 b) DuraMem® 200 76
5.22 Rejection of two molecules which differ only in the fluor substituent (G: no fluorination; H: fluorination) a) GMT-oNF-2 b) DuraMem® 200 76

5.23 Rejection progression of specialty chemicals (squares: 2-core solutes; circles: 3-core solutes; triangles: 4-core solutes) in a mixture of ethanol and THF of different composition a) GMT-oNF-2 b) DuraMem® 200 77
5.24 Rejection progression of specialty chemicals (squares: 2-core solutes; circles: 3-core solutes; triangles: 4-core solutes) in a mixture of THF and heptane of different composition a) GMT-oNF-2 b) DuraMem® 200 78
5.25 Rejection progression of specialty chemicals (squares: 2-core solutes; circles: 3-core solutes; triangles: 4-core solutes) in a mixture of heptane and ethanol of different composition a) GMT-oNF-2 b) DuraMem® 200 79
5.26 Rejection of substances B and F (symbols) in solvent mixture of a solvent with high rejections and a solvent with a high affinity to the membrane. Additionally, the solubility parameter (lines) of the solutes B and F, the membranes (Mem) and the solvent mixture (SM) are given. a) GMT-oNF-2 in n-heptane/THF b) DuraMem® 200 in THF/ethanol 80
5.27 Rejection of substances B and F (symbols) in solvent mixture of a solvent with high rejections and a solvent causing negative rejections. Additionally, the solubility parameter (lines) of the solutes B and F, the membranes (Mem) and the solvent mixture (SM) are given. a) GMT-oNF-2 in THF/ethanol b) DuraMem® 200 in THF/n-heptane 81
5.28 Rejection of substances B and F (symbols) in mixture of n-heptane and ethanol. Additionally, the solubility parameter (lines) of the solutes B and F, the membranes (Mem) and the solvent mixture (SM) are given. a) GMT-oNF-2 b) DuraMem® 200 82
5.29 Rejections of specialty chemicals in ethanol, THF and n-heptane vs. their molecular weight. Values taken after 180 min at 30 bar transmembrane pressure. a) GMT-oNF-1 b) DuraMem® 300 84
5.30 Rejections of GMT-oNF-1 in n-heptane subdivided in the specialty chemicals with polar endgroups (filled square) and without (unfilled square) 85

5.31 Rejections of the substances in ethyl acetate, MTBE and isopropyl alcohol and DMSO, respectively vs. their molecular weight. Values taken after 3 h at 30 bar transmembrane pressure. a) GMT-oNF-2 membrane, star symbols the separation characterization given by the manufacturer determined by rejection measurements of alkanes in toluene. b) DuraMem 200 membrane, dotted line symbols the MWCO given by the manufacturer determined by rejection measurements of styrene oligomers in acetone. 87
5.32 Rejections of the substances in dependence of the solubility parameters of the solutes calculated by the method of Stefanis [161] and the solubility parameters of the membrane (dashed line) and ethyl acetate (solid line) a) GMT-oNF-2 b) DuraMem® 200 87
5.33 Rejection in dependence of the solubility parameters of the solutes calculated by the method of Stefanis [161] and the solubility parameters of the membrane (dashed line) and MTBE (solid line) a) GMT-oNF-2 b) DuraMem® 200 88
5.34 Rejection in dependence of the solubility parameters of the solutes calculated by the method of Stefanis [161] and the solubility parameters of the membrane (dashed line) and the solvent (solid line) a) GMT-oNF-2 measured in IPA b) DuraMem® 200 (T2) measured in DMSO 89
5.35 Functional groups influencing the rejection of the GMT-oNF-2 in varying solvents to validate the results of chapter 5.3.2 90
5.36 Functional groups influencing the rejection of the DuraMem® 200 in varying solvents to validate the results of chapter 5.3.2 91
5.37 Rejections of a silicone acrylate composite membrane in methanol as a function of the solubility parameter of the solutes calculated by the method of Stefanis[161]. Data taken from Postel et al. [119] 93
5.38 Rejections in different solvents in dependence of the solubility parameter of the solutes calculated by the method of Fedors [158]. Data taken from Darvishmanesh et al. [137] 94
5.39 Rejections in dependence of the solubility parameter of the solutes calculated by the method of Van Krevelen [139] for high permeability glassy polymers in ethanol. Data taken from Tsarkov et al. [118] 95

5.40 Rejections in dependence of the solubility parameter of the solutes for a PDMS membrane (PERVAP™ 4060)(symbolized by the dotted line) in toluene, DMC and ethanol. Data taken from Soltane et al. [172] 96
5.41 Heuristic for membrane selection 100

6.1 Permporometry measurement using the example of membrane N0328 (data kindly provided by Fraunhofer IKTS) 104
6.2 Multi-purpose cross-flow membrane plant 105
6.3 Lab scale ceramic module housing 106
6.4 Pure solvent flux measurement measured at 20 bar and 20°C in a long-term experiment. a) type 1 b) type 4 106
6.5 Pure solvent fluxes of n-heptane, ethanol and THF a) commercially available hydrophobized membrane b) newly developed hydrophobic membrane 107
6.6 Characterization of a new membrane (N0354) a) Permporometry measurement by use of cyclohexane as condensable vapor (data kindly provided by Fraunhofer IKTS) b) rejection curve determined with polystyrenes in THF at 20 bar 108
6.7 Characterization of a new membrane (N0353) a) Permporometry measurement by use of cyclohexane as condensable vapor (data kindly provided by Fraunhofer IKTS) b) rejection curve determined with polystyrenes in THF at 20 bar 109
6.8 Characterization of a new membrane type 4 (N0426) for aqueous nanofiltration a) Permporometry measurement by use of cyclohexane as condensable vapor (data kindly provided by Fraunhofer IKTS) b) rejection curve determined with polyethylene glycol in water at 10 bar (data kindly provided by Fraunhofer IKTS) 109
6.9 Characterization of a new membrane (N0157) hydrophobized by a phenolic resin a) Permporometry measurement by use of cyclohexane as condensable vapor (data kindly provided by Fraunhofer IKTS) b) rejection curve determined with polystyrenes in THF at 20 bar 110
6.10 Characterization of a new membrane (N0328) hydrophobized by DEA a) Permporometry measurement by use of cyclohexane as condensable vapor (data kindly provided by Fraunhofer IKTS) b) rejection curve determined with polystyrenes in THF at 20 bar 111

6.11 Maximum rejection of a membrane measured with polystyrenes in THF as a function of the ratio of dry nitrogen permeance and the permeance at a pore size of 5 nm (representing the number of defect pores in the membrane) 112
6.12 Rejection curves of the DEA membrane (N0265) determined with polystyrene in n-heptane, ethanol and THF 113
6.13 Rejection measurements of membranes containing DEA in THF. One membrane was characterized with permporometry prior to the rejection measurements (N0403), the other two membranes were measured untreated (N0406, N0407) 114
6.14 Rejection measurements of membranes containing DEA in ethanol. One membrane was characterized with permporometry prior to the rejection measurements (N0405), the other two membranes were measured untreated (N0410, N0411) 114
6.15 Rejection measurements of membranes containing DEA in n-heptane. One membrane was characterized with permporometry prior to the rejection measurements (N0404), the other two membranes were measured untreated (N0408, N0409) 115
6.16 Rejection curves of the DEA membrane (N0328) determined with polystyrene in THF, MTBE, toluene and ethyl acetate 116
6.17 Rejections of specialty chemicals in ethanol, THF and n-heptane vs. their molecular weight. a) N0265 (Values taken after 180 min at 30 bar transmembrane pressure) b) N0346 (Values taken after 60 min at 20 bar transmembrane pressure) 118
6.18 Model structure of the ACM simulation for mass transport through ceramic OSN membranes 120
6.19 Simulation results of rejection of polystyrene in THF with different standard deviations of the pore size distribution (σ_p =0; 0.1; 0.2; 0.5) and the experimental results a) N0328 ($r_p = 0.3$) b) N0330 ($r_p = 0.43$) 124
6.20 Simulation results of rejection of polystyrene in THF with different standard deviations of the pore size distribution (σ_p =0; 0.1; 0.2; 0.5) and the experimental results a) N0157 ($r_p = 0.78$) b) N0265 ($r_p = 0.55$) 124
6.21 Influence of $r_{max}(= x \cdot r_p)$ on calculated rejections of polystyrene in THF (exemplarily shown for membrane N0328 with σ_p =0.15) 126

6.22 Improvement of calculated rejections of polystyrene in THF by enlargement of the maximum pore size r_{max} (exemplarily shown for membrane N0288) 127
6.23 Influence of transmembrane pressure on the calculated (lines) (σ_p =0.1) and experimentally determined rejections of polystyrenes (symbols) in THF at 20 °C, 6 l/min of membrane N0328 128
6.24 Influence of a) temperature at 6 l/min b) feed velocity at 20 °C on the calculated (lines) (σ_p =0.1) and experimentally determined rejections of polystyrenes (symbols) in THF at 20 bar of membrane N0328 128
6.25 Calculated rejections (lines) of membrane N0265 in comparison to experimentally determined rejections of polystyrene in THF, n-heptane and ethanol (symbols) 129
6.26 Calculated rejections of specialty chemicals (open symbols) of membrane N0265 in comparison to experimentally determined rejections (filled symbols) in THF, n-heptane and ethanol 130

7.1 Rejections of solute B in THF and ethanol measured with a new membrane (GMT-oNF-2) in comparison with the rejections measured with a membrane which was used in the respective other solvent before 136
7.2 Distribution of the different costs on the technical potential (according to equation 4.1) of the realizable five products (costs due to process shortening C_{PS}, costs due to reduction of machine hours C_{MH}, costs for energy demand of distillation C_{ED}, costs for energy demand of OSN C_{EO}, costs due to product losses C_{PL}) 137
7.3 Break-even analysis for different production outputs of a two-stage multi-purpose production plant for specialty chemicals 139
7.4 Break-even analysis for different production outputs of a three-stage multi-purpose production plant for specialty chemicals 139

A.1 Pure solvent flux through the GMT-oNF-2 membrane as a function of the a) Polarity according to Smallwood [164] b) Dielectric constant of the solvents . . 175
A.2 Rejections and the averaged permeate fluxes in l/m^2 h of the DuraMem® 200 at the end of this work 175
A.3 Rejection of two molecules which differ only in their left side chain length ($R_G > R_K$) a) GMT-oNF-2 b) DuraMem® 200 177

A.4 Rejection of two molecules which differ only in their endgroup (G: nonpolar; J: polar) a) GMT-oNF-2 b) DuraMem® 200 177
A.5 Rejection of two molecules which differ only in their endcore (E: cyclohexane; B: benzene) a) GMT-oNF-2 b) DuraMem® 200 177
A.6 Rejection of two molecules which differ only in the fluor substituent (G: no fluorination; H: fluorination) a) GMT-oNF-2 b) DuraMem® 200 178

B.1 Permporometry measurement by use of cyclohexane as condensable vapor (data kindly provided by Fraunhofer IKTS) of type 2 membranes. a) N0265 b) N0328 c) N0330 d) N0353 e) N0353 186
B.2 Permporometry measurement by use of cyclohexane as condensable vapor (data kindly provided by Fraunhofer IKTS) of type 2 membranes. a) N0157 b) N0288 186
B.3 Permporometry measurement by use of cyclohexane as condensable vapor (data kindly provided by Fraunhofer IKTS) of type 4 membranes. a) N0346 b) N0426 187
B.4 Permporometry measurement by use of cyclohexane as condensable vapor (data kindly provided by Fraunhofer IKTS) of the membranes which were used for the comparison of the performance with and without precharacterization by permporometry. a) Membrane (N0403) characterized with THF c.f. Figure 6.13 b) Membrane (N0404) characterized in n-heptane c.f. Figure 6.15 c) Membrane (N0405) characterized in ethanol c.f. Figure 6.14 187

List of Tables

2.1 Typical polymers used for preparation of OSN membranes 16
2.2 Commercially available ceramic membranes in the nanofiltration range 19
2.3 Comparison between polymeric and ceramic membranes 20

4.1 Assumptions for the parameters necessary for the assessment of the theoretical potential 42

5.1 Commercially available polymeric membranes used in this work 47
5.2 Characterization of the GMT membranes given by the manufacturer [151, 152] 48
5.3 Specialty chemicals used for membrane characterization 50
5.4 Classification of the molecules of Table 5.3 in the two groups and their GC retention times 51
5.5 Substances of similar chemical structure to validate the calculation methods for the solubility parameter by means of the experimental values [162] 52
5.6 Pure solvent flux measured at 30 bar and 25±3 °C 57
5.7 Partial fluxes of the solutes in THF, n-heptane and ethanol 64
5.8 Functional groups used as factors in the DoE 70
5.9 Solubility parameters of the solvent mixtures 79
5.10 Predominating transport mechanism in dependency of the respective solvent and membrane type 99

6.1 Ceramic membranes 103
6.2 Permeate fluxes of THF, ethanol and n-heptane of type 2 membranes with and without precharacterization 116
6.3 Order of THF, MTBE, toluene and ethyl acetate in terms of different solvent properties 117

6.4 Permeate fluxes determined for membrane N0328 in the chronological order of the experiments . . . 118
6.5 Ceramic membranes used for the verification of the rejection modeling . . . 123
6.6 Calculated and measured permeate fluxes in $\left[\mathrm{l/m^2h}\right]$ . . . 126

7.1 Comparison between the estimated rejection and experimental results for several typical production solutions of specialty chemicals (same class as used for the development of the heuristic) . . . 135

A.1 Properties of the specialty chemicals . . . 176
A.2 Solvent grades used in the experiments . . . 178
A.3 Solvent properties taken from Smallwood [164] . . . 179
A.4 Rejection in [%] of the chemicals in THF, n-heptane and ethanol . . . 180
A.5 Permeate fluxes in THF, n-heptane and ethanol . . . 181
A.6 Permeate fluxes of the membranes with higher MWCOs (GMT-oNF-1 and DuraMem® 300) . . . 181
A.7 Rejection in [%] of the chemicals in ethyl acetate, MTBE and DMSO and isopropyl alcohol, respectively . . . 182
A.8 Permeate fluxes in ethyl acetate, MTBE and isopropyl alcohol (GMT-oNF-2) or DMSO (DuraMem® 200) . . . 182
A.9 Permeate fluxes of the pure solvents and their mixtures in the rejection measurements . . . 183
A.10 Comparison of solubility parameters of the solutes used by Postel et al. [119] . . . 183
A.11 Rejections of the PDMS membrane PERVAP™ 4060 measured by Soltane et al. [172]. Values written in italic type are estimated from the diagrams. . . . 184

B.1 Pore radius and defect pores of the membranes used in this work . . . 185
B.2 Calculated properties of the polystyrenes . . . 188

C.1 Properties of the product solutions, the membrane types proposed by the heuristic and the estimated rejections - Part I . . . 190
C.2 Properties of the product solutions, the membrane types proposed by the heuristic and the estimated rejections - Part II . . . 191
C.3 Properties of the product solutions, the membrane types proposed by the heuristic and the estimated rejections - Part III . . . 192

A Additional information concerning the investigations on polymeric membranes

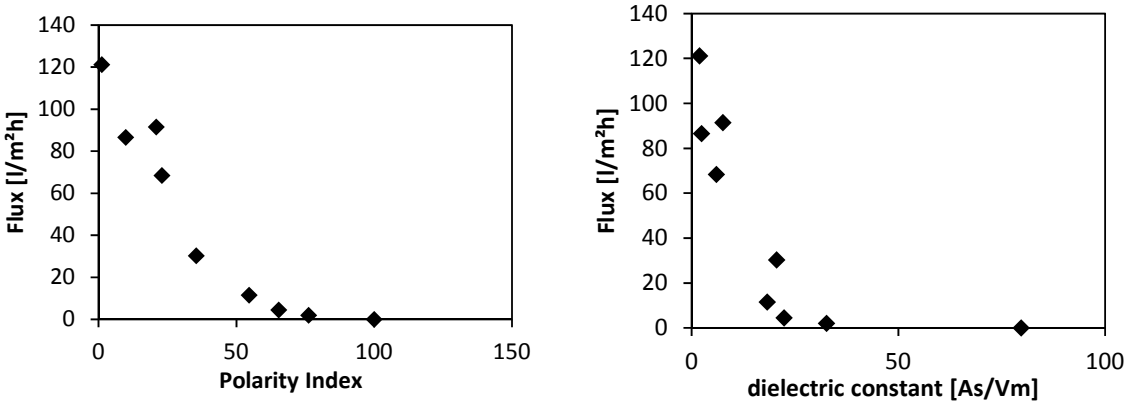

(a) (b)

Figure A.1: Pure solvent flux through the GMT-oNF-2 membrane as a function of the a) Polarity according to Smallwood [164] b) Dielectric constant of the solvents

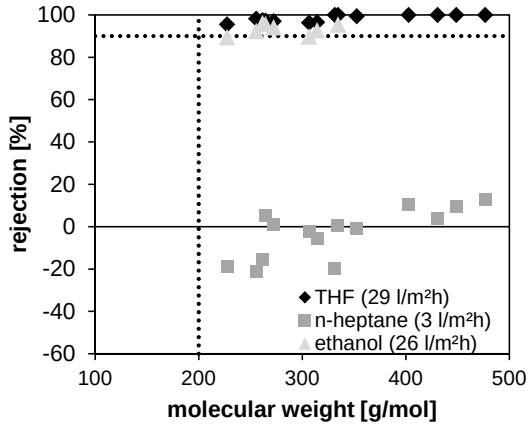

Figure A.2: Rejections and the averaged permeate fluxes in $l/m^2\,h$ of the DuraMem® 200 at the end of this work

Table A.1: Properties of the specialty chemicals

Name	Melting point	Length	$Width_{max}$	$Width_{mid}$	Dipole moment	log P	Solubility parameter	Density
Unit	[°C]	[Å]	[Å]	[Å]	[D]	[-]	$[(J/cm^3)^{1/2}]$	$[g/cm^3]$
A	45	16.93	7.26	5.52	5.55	5.02	21.08	1.06
B	31	19.36	7.75	5.54	5.59	5.96	20.88	
C	3	17.37	7.29	5.53	0.09	6.75	16.49	
D	−8	20.87	7.67	5.50	0.10	8.16	16.16	
E	67	19.26	8.01	5.70	4.59	6.42	19.63	
F	−5	19.39	7.95	5.81	0.10	8.46	14.63	0.89
G	39	23.76	7.90	5.74	0.16	9.65	16.80	1.05
H	27	23.77	7.97	5.77	1.41	9.69	16.52	
I	66	19.85	7.82	5.67	3.14	8.05	16.97	1.19
J	96	23.57	7.79	5.68	6.14	7.92	21.36	
K	66	21.37	7.70	5.68	0.15	8.71	17.01	
L	64	29.59	7.81	5.66	0.03	12.64	15.69	1.05
M	158	27.17	7.59	5.63	0.03	11.70	15.92	
N	86	29.59	7.93	5.67	1.19	12.69	15.41	
O	85	32.00	7.87	5.69	1.27	13.63	15.19	

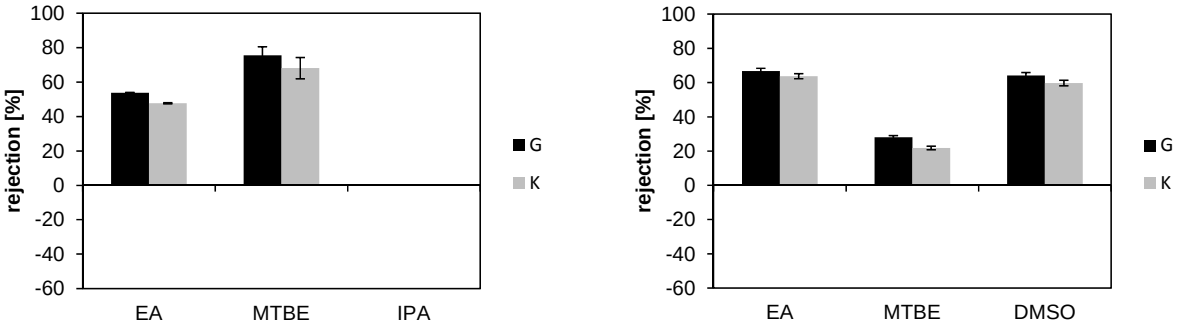

(a) (b)

Figure A.3: Rejection of two molecules which differ only in their left side chain length ($R_G > R_K$) a) GMT-oNF-2 b) DuraMem® 200

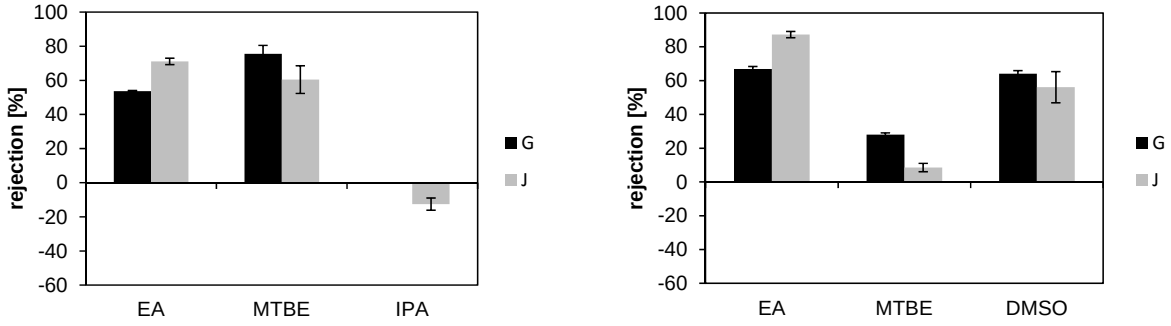

(a) (b)

Figure A.4: Rejection of two molecules which differ only in their endgroup (G: nonpolar; J: polar) a) GMT-oNF-2 b) DuraMem® 200

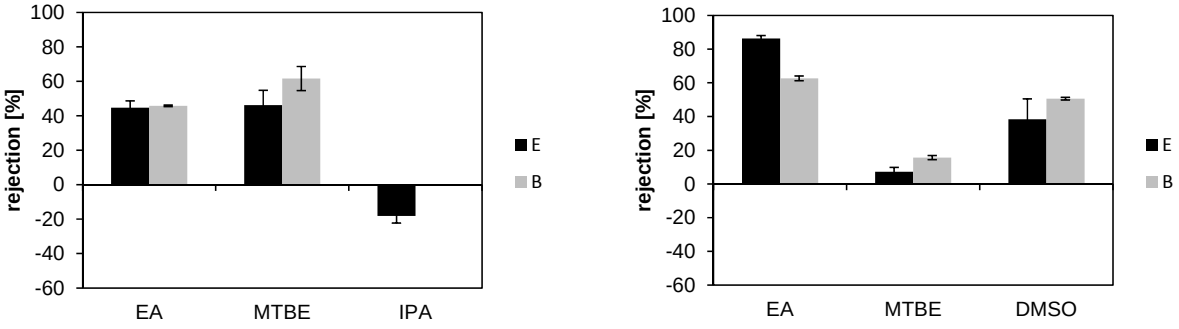

(a) (b)

Figure A.5: Rejection of two molecules which differ only in their endcore (E: cyclohexane; B: benzene) a) GMT-oNF-2 b) DuraMem® 200

Table A.2: Solvent grades used in the experiments

Name	Supplier	Purity grade
THF	Merck KGaA	Emplura® ($\geq$ 99%)
n-Heptane	Merck KGaA	Emplura® ($\geq$ 99%)
Ethanol	Merck KGaA	Emplura® ($\geq$ 99.5%) absolute, undenatured
Methanol	Merck KGaA	Emplura® ($\geq$ 99.5%)
Ethyl acetate	Merck KGaA	Emplura® ($\geq$ 99.5%)
Toluene	Merck KGaA	Emplura® ($\geq$ 99%)
Isopropyl alcohol	Merck KGaA	Emplura® ($\geq$ 99.5%)
Acetone	Merck KGaA	Emplura® ($\geq$ 99%)
DMSO	Merck KGaA	Emplura® ($\geq$ 98%)
MTBE	Merck KGaA	Emplura® ($\geq$ 99%)

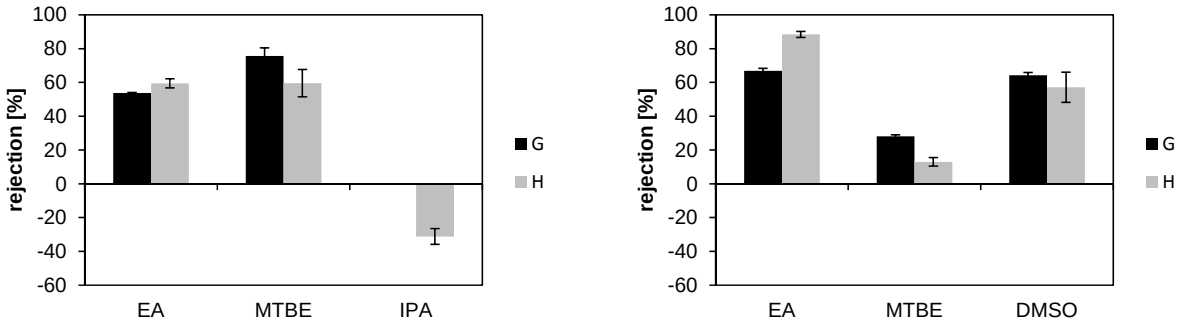

(a) (b)

Figure A.6: Rejection of two molecules which differ only in the fluor substituent (G: no fluorination; H: fluorination) a) GMT-oNF-2 b) DuraMem® 200

Table A.3: Solvent properties taken from Smallwood [164]

Solvent Unit	Molecular weight [g/mol]	Density [g/ml]	Molar volume [m^3/mol]	Viscosity [mPas]	Surface Tension [dyn/cm]	Dielectric constant [As/Vm]	Dipole moment [D]	Polarity [-]	Solubility parameter [$(J/cm^3)^{1/2}$]
THF	72	0.888	81.1	0.55	28.0	7.6	1.75	21.0	18.6
n-Heptane	100	0.664	147.5	0.41	19.3	1.9	0	1.2	15.3
Ethanol	46	0.789	58.7	1.08	22.3	22.4	1.70	65.4	27.4
Methanol	32	0.792	40.4	0.60	22.6	32.6	1.70	76.2	29.7
Ethyl acetate	88	0.895	98.5	0.46	24.0	6.0	1.70	23.0	18.6
Toluene	92	0.867	106.9	0.59	28.5	2.4	0.40	9.9	18.2
Isopropyl alcohol	60	0.786	76.9	2.00	21.7	18.3	1.66	54.6	23.5
Acetone	58	0.790	73.4	0.33	23.3	20.6	2.90	35.5	20.5
DMSO	78	1.101	71.3	2.00	43.7	46.6	3.96	44.4	26.6
MTBE	88	0.741	119.0	0.35	18.3	4.5	1.20	14.8	15.1
Water	18	0.998	18.0	0.89	72.8	79.7	1.87	100.0	47.9

Table A.4: Rejection in [%] of the chemicals in THF, n-heptane and ethanol

Name	MW [g/mol]	GMT-oNF-2 Rejection [%] in			DuraMem® 200 Rejection [%] in		
		THF	n-heptane	ethanol	THF	n-heptane	ethanol
A	227	64	21	−17	78	−31	75
B	255	72	26	−22	80	−27	65
C	230						
D	272	72	54	−42	82	9	30
E	261	72	38	−12	57	−20	54
F	265	55	54	−41	77	8	84
G	335	82	65	−35	85	−1	75
H	353	87	72	−41	80	−1	
I	314	83	42	−27	84	−5	70
J	332	90	54	−17	82	−22	75
K	307	78	56	−31	84	−3	60
L	431	87	75				
M	403	89	78		79	9	
N	449	95		−44			79
O	477	96	79		88	16	

Table A.5: Permeate fluxes in THF, n-heptane and ethanol

	GMT-oNF-2			DuraMem® 200		
Name	THF [l/m²h]	n-heptane [l/m²h]	ethanol [l/m²h]	THF [l/m²h]	n-heptane [l/m²h]	ethanol [l/m²h]
A	133	137	5	79	24	34
B	84	83	4	76	55	47
D	121	141	6	69	114	39
E	151	98	6	88	61	61
F	89	137	7	81	148	44
G	141	132	6	74	59	52
H	105	121	6	72	51	
I	128	102	4	65	181	48
J	131	126	6	73	112	51
K	135	91	9	67	97	48
L	146	154				
M	139	130		69	53	
N	83		7			51
O	131	131		51	76	

Table A.6: Permeate fluxes of the membranes with higher MWCOs (GMT-oNF-1 and DuraMem® 300)

Membrane	THF [l/m²h]	n-heptane [l/m²h]	ethanol [l/m²h]
GMT-oNF-1	104	95	8
DuraMem® 300	127	190	90

Table A.7: Rejection in [%] of the chemicals in ethyl acetate, MTBE and DMSO and isopropyl alcohol, respectively

Name	MW [g/mol]	GMT-oNF-2 Rejection [%] in			DuraMem® 200 Rejection [%] in		
		ethyl acetate	MTBE	isopropyl alcohol	ethyl acetate	MTBE	DMSO
A	227	41	38	−18	73	3	34
B	255	46	57		70	18	51
C	230	19	31	−30		7	30
D	272	28	47	−35	77	13	40
E	261	44	50	−18	77	10	44
F	265	0	44		70	27	
G	335	54	73	−31	72	30	66
H	353	59	64		78	16	62
I	314	50	63		72	25	62
J	332	70	66	−13	77	11	61
K	307	48	64		71	24	61
L	431	70	76		80	22	
M	403	65	84		74	41	
N	449	73	89		75	50	
O	477	77	92		76	54	

Table A.8: Permeate fluxes in ethyl acetate, MTBE and isopropyl alcohol (GMT-oNF-2) or DMSO (DuraMem® 200)

Membrane	ethyl acetate [l/m^{2}h]	MTBE [l/m^{2}h]	IPA / DMSO [l/m^{2}h]
GMT-oNF-2	71	96	7
DuraMem® 200	19	16	6

Table A.9: Permeate fluxes of the pure solvents and their mixtures in the rejection measurements

	Permeate flux of GMT-oNF-2 [l/m²h]					Permeate flux of DuraMem® 200 [l/m²h]				
Molar ratio	0:1	1:3	1:1	3:1	1:0	0:1	1:3	1:1	3:1	1:0
Ethanol/ THF	84	110	52	34	4	39	62	49	44	27
THF/ n-heptane	104	147	84	166	84	27	10	26	20	39
n-heptane/ ethanol	4	61	60	143	104	27	13	16	15	27

Table A.10: Comparison of solubility parameters of the solutes used by Postel et al. [119]

Name	Formula	Solubility Parameter $\left(J/cm^3\right)^{1/2}$		
		Postel [119]	Stefanis [161]	Fedors [158]
n-Alkanes				
Decane	$C_{10}H_{22}$	15.8	15.9	15.8
Dodecane	$C_{12}H_{26}$	16.1	15.7	16.1
Tetradecane	$C_{14}H_{30}$	16.3	15.4	16.2
Hexadecane	$C_{16}H_{34}$	16.5	15.2	16.4
Octadecane	$C_{18}H_{38}$	16.7	15.0	16.5
Docosane	$C_{22}H_{46}$	16.7	14.6	16.7
Tetracosane	$C_{24}H_{50}$	16.7	14.3	16.7
Octacosane	$C_{28}H_{58}$	16.7	13.9	16.8
Polystyrenes	$[C_8H_8]_n$	18.7		
Polyethylene glycols				
	$HO[C_2H_4O]_4H$	23.7	28.6	26.1
	$HO[C_2H_4O]_{13}H$	20.5	33.7	21.7
Carboxylic acids				
Myristic acid	$C_{13}H_{27}COOH$	17.5	20.0	18.9
Stearic acid	$C_{17}H_{35}COOH$	16.6	19.6	18.7
Docosanic acid	$C_{21}H_{43}COOH$	15.9	19.2	18.5

Table A.11: Rejections of the PDMS membrane PERVAP™ 4060 measured by Soltane et al. [172]. Values written in italic type are estimated from the diagrams.

Name	MW	Solubility parameter	Rejection [%] in		
	[g/mol]	$[(J/cm^3)^{1/2}]$	toluene	DMC	ethanol
Sudan Blue	350.4	21.02	36	*20*	*-10*
CI Disperse Red 82	439.0	21.9	56	*64*	*29*
Alphazurine FG	792.9	35.3	99	78	90
n-tetracosane	338.7	16.4	40		
n-triacontane	422.8	16.6	60		
n-pentacontane	703.3	16.8	100		

B Additional information concerning the investigations on ceramic membranes

Table B.1: Pore radius and defect pores of the membranes used in this work

Name	Nominal pore radius [nm]	rel. permeance at 5 nm [%]
N0157	0.775	1
N0265	0.550	6
N0288	0.350	8
N0328	0.300	2
N0330	0.425	5
N0346	0.600	5
N0353	0.425	5
N0354	0.425	2
N0403	0.503	6
N0404	0.503	6
N0405	0.600	8
N0426	0.550	5

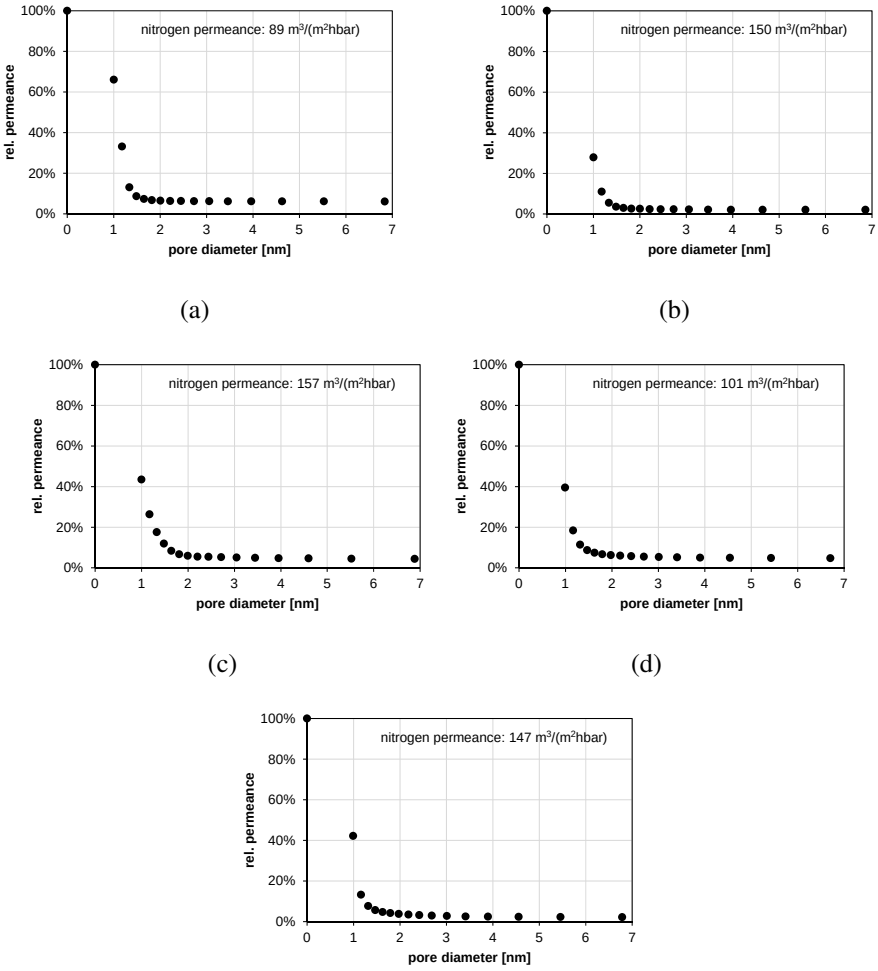

(a) (b)

(c) (d)

(e)

Figure B.1: Permporometry measurement by use of cyclohexane as condensable vapor (data kindly provided by Fraunhofer IKTS) of type 2 membranes.
a) N0265 b) N0328 c) N0330 d) N0353 e) N0353

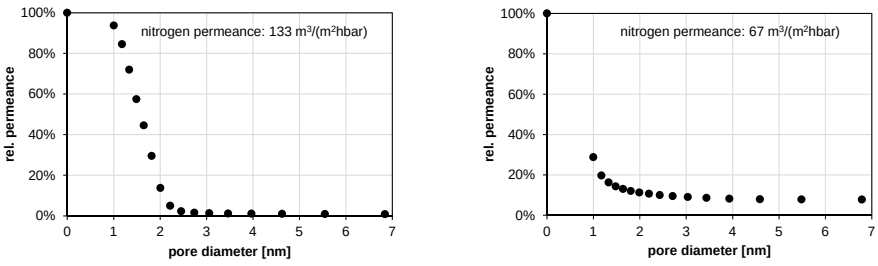

(a) (b)

Figure B.2: Permporometry measurement by use of cyclohexane as condensable vapor (data kindly provided by Fraunhofer IKTS) of type 2 membranes.
a) N0157 b) N0288

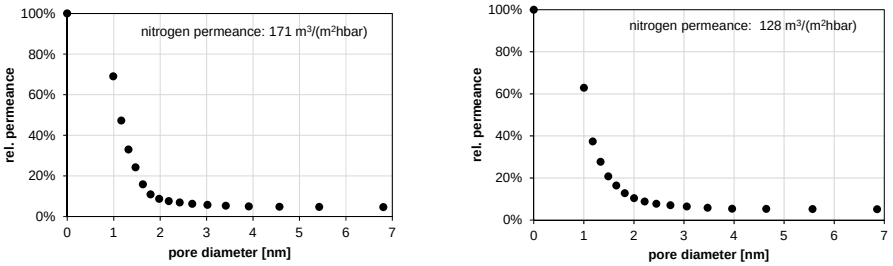

(a) (b)

Figure B.3: Permporometry measurement by use of cyclohexane as condensable vapor (data kindly provided by Fraunhofer IKTS) of type 4 membranes.
a) N0346 b) N0426

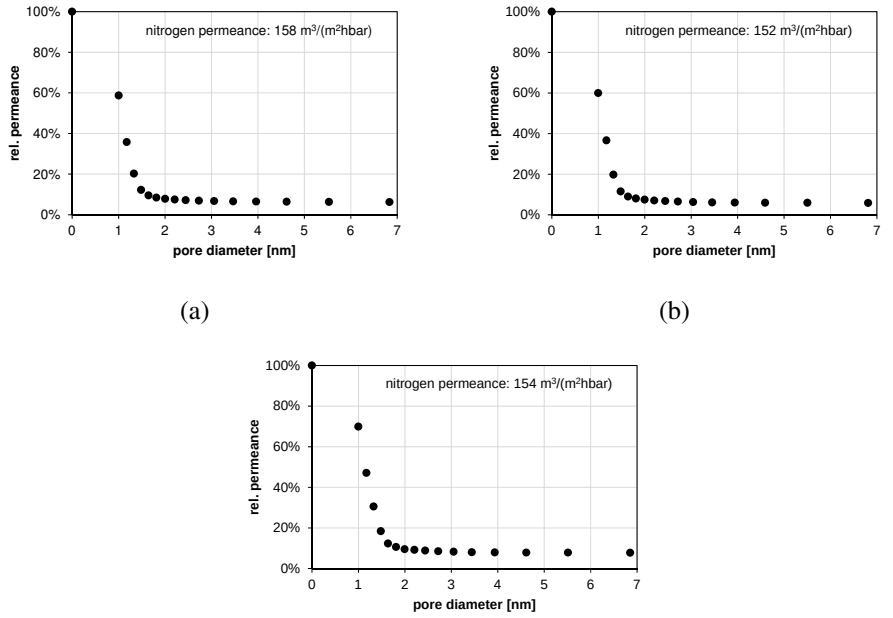

(a) (b)

(c)

Figure B.4: Permporometry measurement by use of cyclohexane as condensable vapor (data kindly provided by Fraunhofer IKTS) of the membranes which were used for the comparison of the performance with and without precharacterization by permporometry.
a) Membrane (N0403) characterized with THF c.f. Figure 6.13
b) Membrane (N0404) characterized in n-heptane c.f. Figure 6.15
c) Membrane (N0405) characterized in ethanol c.f. Figure 6.14

Table B.2: Calculated properties of the polystyrenes

PS	M_s	ρ_s	υ_s	D_{THF}	r_{s_THF}	D_{EtOH}	r_{s_EtOH}	D_{hept}	r_{s_hept}
	$[\frac{kg}{kmol}]$	$[\frac{kg}{m^3}]$	$[\frac{m^3}{kmol}]$	$[10^{-9}\frac{m^2}{s}]$	[nm]	$[10^{-9}\frac{m^2}{s}]$	[nm]	$[10^{-9}\frac{m^2}{s}]$	[nm]
1	210	1815	0.21	1.66	0.27	0.57	0.28	2.14	0.23
2	314	2713	0.29	1.35	0.33	0.46	0.33	1.74	0.28
3	419	3612	0.38	1.15	0.37	0.39	0.38	1.49	0.31
4	522	4510	0.47	1.02	0.41	0.35	0.42	1.32	0.35
5	627	5409	0.55	0.92	0.44	0.31	0.45	1.19	0.37
6	1873	7714	1.55	0.50	0.71	0.17	0.73	0.64	0.60
7	6039	24876	5.01	0.25	1.19	0.08	1.21	0.32	1.01

C Additional information concerning the potential assessment

Table C.1: Properties of the product solutions, the membrane types proposed by the heuristic and the estimated rejections - Part I

Product	Molecular weight [g/mol]	Solubility Parameter $[(J/cm^3)^{1/2}]$	Polar end-group	Solvent	Solubility Parameter $[(J/cm^3)^{1/2}]$	2.Solvent	Solubility Parameter $[(J/cm^3)^{1/2}]$	Membrane type	Rejection
P1	202	29.4*	yes	THF	18.6	Hexane	14.1	hydrophobic	80
P2	244	27.6*	yes	THF	18.6	Hexane	14.1	hydrophobic	85
P3	258	26.9*	yes	THF	18.6	Hexane	14.1	hydrophobic	85
P4	272	26.3*	yes	THF	18.6	Hexane	14.1	hydrophobic	85
P5	200	18.3	F	THF	18.6	Toluene	18.2	hydrophilic	80
P5	200	18.3	F	Heptane	15.3	Isopropyl alcohol	23.5	hydrophilic	40
P5	200	18.3	F	Heptane	15.3			hydrophobic	30
P6	214	18.2	F	THF	18.6	Toluene	18.2	hydrophilic	80
P6	214	18.2	F	Heptane	15.3	Isopropyl alcohol	23.5	hydrophilic	40
P6	214	18.2	F	Heptane	15.3			hydrophobic	30
P7	344	17.3	no	Toluene	18.2	Ethanol	27.4	hydrophilic	95
P7	344	17.3	no	Toluene	18.2			both	95
P8	358	17.2	no	Toluene	18.2			both	95
P8	358	17.2	no	Toluene	18.2	Ethanol	27.4	hydrophilic	95
P8	358	17.2	no	Heptane	15.3			hydrophobic	70
P9	363	16.5	no	THF	18.6	Hexane	14.1	hydrophobic	60
P10	377	16.4	no	THF	18.6	Hexane	14.1	hydrophobic	60
P11	377	16.4	no	THF	18.6	Hexane	14.1	hydrophobic	60
P12	391	16.3	no	THF	18.6	Hexane	14.1	hydrophobic	60
P13	318	16.3	no	THF	18.6	Hexane	14.1	hydrophobic	50

*Solubility parameter calculated according to the method of Fedors [158]

Table C.2: Properties of the product solutions, the membrane types proposed by the heuristic and the estimated rejections - Part II

Product	Molecular weight [g/mol]	Solubility Parameter $[(J/cm^3)^{1/2}]$	Polar end-group	Solvent	Solubility Parameter $[(J/cm^3)^{1/2}]$	2.Solvent	Solubility Parameter $[(J/cm^3)^{1/2}]$	Membrane type	Rejection
P14	332	16.2	no	THF	18.6	Hexane	14.1	hydrophobic	50
P14	332	16.2	no	Ethanol	27.4	THF	18.6	hydrophilic	90
P15	363	16.5	no	Heptane	15.3			hybrophobic	70
P16	280	17.3	no	THF	18.6	Hexane	14.1	hydrophobic	60
P16	280	17.3	no	Ethanol	27.4			hydrophilic	80
P16	280	17.3	no	Toluene	18.2	Ethanol	27.4	hydrophilic	85
P17	308	17.1	no	THF	18.6	Hexane	14.1	hydrophobic	60
P17	308	17.1	no	Ethanol	27.4			hydrophilic	80
P17	308	17.1	no	Toluene	18.2	Ethanol	27.4	hydrophilic	85
P18	308	17.1	no	THF	18.6	Hexane	14.1	hydrophobic	60
P18	308	17.1	no	Ethanol	27.4			hydrophilic	80
P18	308	17.1	no	Toluene	18.2	Ethanol	27.4	hydrophilic	85
P19	336	16.9	no	THF	18.6	Hexane	14.1	hydrophobic	60
P19	336	16.9	no	Ethanol	27.4			hydrophilic	80
P19	336	16.9	no	Toluene	18.2	Ethanol	27.4	hydrophilic	85
P20	234	14.8	no	Ethyl acetate	18.6	Methanol	29.7	hydrophilic	90
P20	234	14.8	no	Ethyl acetate	18.6			hydrophilic	85
P21	236	14.9	no	Heptane	15.3			hydrophobic	30
P21	236	14.9	no	DCM	19.8			hydrophilic	50
P22	366	17.0	yes	Toluene	18.2	THF	18.6	hydrophobic	90
P22	366	17.0	yes	Toluene	18.2			hydrophobic	90

*Solubility parameter calculated according to the method of Fedors [158]

Table C.3: Properties of the product solutions, the membrane types proposed by the heuristic and the estimated rejections - Part III

Product	Molecular weight [g/mol]	Solubility Parameter $[(J/cm^3)^{1/2}]$	Polar end-group	Solvent	Solubility Parameter $[(J/cm^3)^{1/2}]$	2.Solvent	Solubility Parameter $[(J/cm^3)^{1/2}]$	Membrane type	Rejection [%]
P23	368	16.4	yes	Toluene	18.2			hydrophobic	90
P23	368	16.4	yes	Heptane	15.3			hydrophobic	80
P24	264	24.9*	yes	THF	18.6			hydrophilic	80
P24	264	24.9*	yes	THF	18.6	Water	47.1	hydrophilic	70
P25	346	23.4*	yes	THF	18.6			hydrophilic	90
P25	346	23.4*	yes	Heptan	15.3	THF	18.6	hydrophobic	80
P26	302	15.9	F	THF	18.6	NMP	22.5	hydrophilic	90
P26	302	15.9	F	Heptane	15.3			hydrophobic	50
P27	336	18.0	no	Toluene	18.2	Ethanol	27.4	hydrophilic	90
P27	336	18.0	no	Heptane	15.3			hydrophobic	70
P28	350	17.9	no	Heptane	15.3			hydrophobic	70
P29	344	17.9	F	THF	18.6			both	90
P29	344	17.9	F	Heptane	15.3			hydrophobic	70
P30	344	17.9	F	Heptane	15.3	Methanol	29.7	hydrophobic	60
P31	236	14.9	no	Heptane	15.3			hydrophobic	30
P31	236	14.9	no	Ethyl acetate	18.6			hydrophilic	85
P32	292	18.3	yes	DCM	19.8	THF	18.6	hydrophilic	85
P32	292	18.3	yes	Heptane	15.3	DCM	19.8	hydrophobic	60
P33	324	15.5	F	Heptane	15.3			hydrophobic	70
P34	350	16.4	F	Heptane	15.3			hydrophobic	70
P35	234	14.8	no	Ethyl acetate	18.6			hydrophilic	85

*Solubility parameter calculated according to the method of Fedors [158]

Publications

Journal Articles

Zeidler, S.; Kätzel, U; Kreis, P.: Systematic investigation on the influence of solutes on the separation behavior of a PDMS membrane in organic solvent nanofiltration. *Journal of Membrane Science 429* (2013), 295-303

Zeidler, S.; Puhlfürß, P.; Kätzel, U; Voigt, I.: Preparation and characterization of new low MWCO ceramic nanofiltration membranes for organic solvents. *Journal of Membrane Science 470* (2014), 421-430

Zeidler, S.; Kätzel, U., Schmalz, D.: Potenziale und Herausforderungen in der Implementierung der organophilen Nanofiltration in der Spezialchemie. *Chemie Ingenieur Technik 86* (2014), 594-601

Blumenschein, S.; Böcking, A.; Kätzel, U.; Postel, S.; Wessling, M.: Rejection modeling of membranes in organic solvent nanofiltration. *Journal of Membrane Science 510* (2016), 191-200

Blumenschein, S.; Kätzel, U.: An heuristic-based selection process for organic solvent nanofiltration membranes. *Separation and Purification Technology 183* (2017), 83-95

Conference Proceedings

Zeidler, S.; Kätzel, U.; Kreis, P.: A Heuristic Approach for Membrane Selection in Organic Solvent Nanofiltration. *Procedia Engineering 44* (2012), 1646-1648

Zeidler, S.; Kätzel, U.; Puhlfürß, P.; Voigt, I.: New Ceramic Membranes for Organic Solvent Nanofiltration with a Molecular Weight Cut-Off < 500 Da. *Procedia Engineering 44* (2012), 646-648

Oral Presentations

Kätzel, U.; Zeidler, S.: OSN process development for specialty chemicals production at Merck

KGaA. *3th International Conference on Organic Solvent Nanofiltration* (2010), London, United Kingdom

Kätzel, U.; Zeidler, S.: Organophile Nanofiltration: Prozessintensivierung im Downstream von Spezialchemikalien. *ChemPharm Symposium*(2011), Darmstadt, Germany

Zeidler, S.; Kätzel, U.; Mäussler, L.; Kreis, P.; Górak, A.: Investigation of the separation behaviour of a material class of linear organic molecules in organic solvent nanofiltration with special focus on the influence of their functional groups. *International congress on membranes and membrane processes* (2011), Amsterdam, The Netherlands

Zeidler, S.; Kätzel, U.; Kreis, P.: First steps to a heuristic for membrane selection in organic solvent nanofiltration. *Nemopur Workshop* (2012), Cetraro, Italy

Zeidler, S.; Kätzel, U.; Kreis, P.: Practical aspects in applying organic solvent nanofiltration in specialty chemicals production. *ACHEMA* (2012), Frankfurt, Germany

Zeidler, S.; Kätzel, U.; Puhlfürß, P.; Voigt, I.: New Ceramic Membranes for Organic Solvent Nanofiltration with a Molecular Weight Cut-Off < 500 Da. *EuroMembrane* (2012), London, United Kingdom

Zeidler, S.; Kätzel, U.; Kreis, P.; Górak, A.: A heuristic for membrane selection in organic solvent nanofiltration. *4th International Conference on Organic Solvent Nanofiltration* (2013), Aachen, Germany

Zeidler, S.; Kätzel, U.; Kreis, P.; Górak, A.: Simplified membrane selection for organic solvent nanofiltration using a heuristic. *International congress on membranes and membrane processes* (2014), Suzhou, China

Blumenschein, S.; Kätzel, U.; Druwe, S.: The first of its kind OSN plant in a specialty chemicals company. *5th International Conference on Organic Solvent Nanofiltration* (2015), Antwerp, Belgium

Druwe, S.; Kätzel, U.; Blumenschein, S.: OSN Design Tool - Development of a software based tool for the process and plant design for different applications. *5th International Conference on Organic Solvent Nanofiltration* (2015), Antwerp, Belgium

Thiermeyer, Y.; Blumenschein, S.: Erweiterung einer Heuristik zur organophilen Nanofiltration. *Presentation at Jahrestreffen der ProcessNet-Fachgruppen Mechanische Flüssigkeitsabtrennung und Membrantechnik* (2016), Kassel, Germany

Poster Presentations

Zeidler, S.; Kätzel, U.; Kreis, P.: A Heuristic Approach for Membrane Selection in Organic

Solvent Nanofiltration. *EuroMembrane* (2012), London, United Kingdom

Thiermeyer, Y.; Blumenschein, S.: Development of a standardized OSN membrane testing methodology. *5th International Conference on Organic Solvent Nanofiltration* (2015), Antwerp, Belgium

Supervised Theses

Belegarbeiten

Jessica Behnke, Charakterisierung einer hydrophilen Nanofiltrationsmembran zum Einsatz in der Produktion von Spezialchemikalien, Technische Universität Dresden (2012)

Diplomarbeiten

Axel Böcking, Theoretische Beschreibung des Stofftransports in der organophilen Nanofiltration, RWTH Aachen (2012)

Masterarbeiten

Lorenz Mäussler, Untersuchungen zum Einfluss verschiedener Produkteigenschaften von linearen, organischen Molekülen auf das Trennverhalten der organophilen Nanofiltration, RWTH Aachen (2011)

Sebastian Druwe, Entwicklung eines softwarebasierten Tools zur Dimensionierung von Anlagen für verschiedene Anwendungen der organophilen Nanofiltration, Provadis School of International Management and Technology (2015)

Curriculum Vitae

_____Stefanie Blumenschein (nee Zeidler)

Born on 29 October 1983 in Seeheim-Jugenheim, Germany

_____Education

10/2003 - 07/2010	Study of Chemical Engineering at Karlsruhe Institute of Technology, Karlsruhe, Germany (Degree: Dipl. Ing.)
08/1994 - 06/2003	High School, Liebfrauenschule Bensheim, Germany

_____Work Experience

since 04/2013	Development Engineer at Merck KGaA, Darmstadt, Germany
08/2010 - 03/2013	Scientific Assistant at Merck KGaA, Darmstadt, Germany in cooperation with the Laboratory of Fluid Separations of Prof. Dr.-Ing. Andrzej Górak, TU Dortmund University, Dortmund, Germany
05/2009 - 12/2009	Internship at Merck KGaA, Darmstadt, Germany
03/2009	Student Assistant at Institute of Process Engineering in Life Science - Food Process Engineering, Karlsruhe Institute of Technology, Karlsruhe, Germany